DISSERTATION

IMPROVED ASSESSMENT OF NITROGEN AND PHOSPHORUS FATE AND

TRANSPORT FOR INTENSIVELY MANAGED IRRIGATED STREAM-AQUIFER

SYSTEMS

Submitted by

Xiaolu Wei

Department of Civil and Environmental Engineering

In partial fulfillment of the requirements

For the Degree of Doctor of Philosophy

Colorado State University

Fort Collins, Colorado

Fall 2019

Doctoral Committee:

    Advisor: Ryan T. Bailey

    Mazdak Arabi
    Timothy K. Gates
    Timothy Covino

ABSTRACT

IMPROVED ASSESSMENT OF NITROGEN AND PHOSPHORUS FATE AND

TRANSPORT FOR INTENSIVELY MANAGED IRRIGATED STREAM-AQUIFER

SYSTEMS

Nitrogen (N) and Phosphorus (P) are essential elements for animal nutrition and plant growth. However, over the previous decades, excessive loading of fertilizers in agricultural activities has led to elevated concentrations of N and P contaminations in surface waters and groundwater worldwide and associated eutrophication. Therefore, precisely understanding and representation of water movement and fate and transport of N and P within a complex dynamic groundwater-surface water system affected by agricultural practices is of essential importance for sustaining ecological health of the stream-aquifer environment while maintaining high agricultural productivity. Modeling tools often are used to assess N and P contamination and evaluate the impact of management practices. Such models include land surface-based watershed models such SWAT, and aquifer-based models that simulate spatially-distributed groundwater flow. However, SWAT simulates groundwater flow in a simplistic fashion and therefore is not suited for watersheds with complex groundwater flow patterns and groundwater-surface interactions, whereas groundwater models do not simulate land surface processes.

This dissertation establishes the modeling capacity for assessing the movement, transformation, and storage of nitrate (NO_3) and soluble P in intensively managed irrigated stream-aquifer systems. This is accomplished by (1) developing a method to apply the SWAT model to such a system, and includes: designating each cultivated field as an individual hydrologic response unit (HRU), crop rotations to simulate the impact of changing crop types for each cultivated field, including N and P mass in irrigation water, and seepage from earthen irrigation canals into the aquifer; (2) simulating land surface hydrology, groundwater flow, and groundwater-surface water interactions in the system using the coupled flow

model SWAT-MODFLOW, with the enhanced capability of linkage between SWAT groundwater irrigation HRUs and MODFLOW pumping cells, and the use of MODFLOW's EVT package to simulate groundwater evapotranspiration; and (3) linking RT3D, a widely used groundwater reactive solute transport model, to SWAT-MODFLOW to credibly represent of NO_3-N and soluble P fate and transport processes in irrigated agroecosystems to evaluate best management practices for nutrient contamination. This last phase will also address the uncertainty in system output (in-stream nutrient loads and concentrations, groundwater nutrient concentrations model predictions).

Each modeling phase is applied to a 734 km^2 study region in the Lower Arkansas River Valley (LARV), an alluvial valley in Colorado, USA, which has been intensively irrigated for over 130 years and is threatened by shallow water tables and nutrient contamination. Multiple best management practices (BMPs) are investigated to analyze the effectiveness in reducing NO_3-N and soluble P contamination in the LARV. These strategies are related to irrigation management, nutrient management, water conveyance efficiency, and tillage operations. The most effective individual BMP in most areas is to decrease fertilizer by 30%, resulting in average NO_3-N and soluble P concentrations within the region could be reduced by 14% and 9%, respectively. This individual BMP could lower the average NO_3-N concentrations by 19% and soluble P concentrations by 2%. Combinations of using 30% irrigation reduction, 30% fertilization reduction, 60% canal seepage, and conservation tillage are predicted to have the greatest overall impact that can not only provide a decrease of groundwater concentration in NO_3-N up to 41% and soluble P concentration up to 8%, but also reduce the median of the in-stream NO_3-N and soluble P to meet the Colorado interim standard. As nutrient conditions within the Lower Arkansas River Valley are typical of those in many other intensively irrigated regions, the results of this dissertation and the developed modeling tools can be applied to other watersheds worldwide.

ACKNOWLEDGEMENTS

TABLE OF CONTENTS

LIST OF TABLES

LIST OF FIGURES

xi

CHAPTER 1. INTRODUCTION AND LITERATURE REVIEW

1.1 THE NITROGEN AND PHOSPHORUS PROBLEMS

Nitrogen (N) and phosphorus (P) are essential nutrients for crop growth, but excess use of fertilizers in agricultural activities has led to elevated of N and P concentrations in surface waters and groundwater systems worldwide (Heathwaite et al., 2000; Kato et al., 2009; Bouraima et al., 2016; Jang et al., 2017). The most common impact of elevated N and P in fresh water is eutrophication, which accounts for almost one half of the impaired lake area and 60% of impaired river reaches within the United States, and is the most widespread contaminant issue of U.S. estuaries (Carpenter et al., 1998). Eutrophication related water quality contamination can result in very substantial negative effects on drinking water supply, social economics, and aquatic ecosystems (Monteagudo et al., 2012; Smith, 2003)

Nitrate (NO_3) has been one of the dominant forms of increased N loading since the 1970s (Vitousek et al., 1997). NO_3 pollution poses a direct health threat to humans, livestock, and other organisms. NO_3 in water at high concentrations is confirmed to relate with methemoglobinemia in infants (Elser et al., 1990), increased hypertension (Capes et al., 2000), and certain cancers including stomach cancer (Hill et al., 1973) and non-Hodgkin's lymphoma (Weisenburger, 1991). The presence of NO_3 in groundwater systems also can contribute to the oxidative dissolution and inhibition of chemical reduction of other dissolved environmental pollutants, such as selenite (SeO_4) and sulfate (SeO_4) (e.g. Wright, 1999; Bailey et al., 2012). As such, the U.S. Environmental Protection Agency (US EPA) has established a maximum contaminant level (MCL) of 10 mg/L NO_3-N (US EPA, 2015). NO_3 is very mobile in soil water and groundwater systems. Under rainfall or irrigated conditions, high levels of soluble NO_3 can occur in groundwater due to leaching through the soil profile (Randall and Iragavarapu, 1995). NO_3 then is transported through the saturated zone according to advection-dispersion processes and finally delivered to streams and rivers via groundwater discharge (Duff and Triska, 2000).

Phosphorus in water, in contrast, is not considered to be directly toxic to human and animals (Amdur et al., 1993), but it is the limiting nutrient in freshwaters and can cause eutrophication at concentrations as

low as 0.02 mg L^{-1} (Correll, 1998). Soil erosions in surface runoff pathways are generally considered to be the primary contributing factor to P flux from agricultural fields (Sharpley et al., 1992), where in-stream P concentrations increase with discharge (Doody et al., 2006). Other studies have proposed that P flux may also be related to leaching processes since it can be attached at the mineral surface through soil-P sorption (Lookman et al., 1996), and transfer pathways such as rapid percolation in preferential flow paths (Kilroy and Coxon, 2005). These processes may increase the concentrations of soluble P in groundwater. Being aware of problems caused by N and P, approaches to assess the contamination, fate, and reactive transport at the regional level are needed to investigate remediation strategies under best management practices (BMPs). This requires knowledge of understanding the hydrological processes and chemical mobilization. Intensively managed irrigation systems in semi-arid regions in the United States are human-impacted agro-ecosystem wherein cultivated fields, river diversion points, and artificial canals are spatially distributed (Figure 1). It relies on both surface water irrigation (through canal diversion) and groundwater irrigation (through pumping wells) to sustain agricultural practices. This system has strong connection between the aquifer and the stream network, with seepage from the stream to the aquifer or groundwater discharge from the aquifer to the stream depending on seasonal hydrologic conditions. Groundwater discharge to streams is a substantial feature of water and nutrient mass flow to surface water bodies and groundwater flow paths are non-uniform due to spatial variability in hydrologic parameters such as hydraulic conductivity and porosity.

For many irrigated agricultural systems, irrigation return flow can be the major source of pollution for surface water bodies (Barros et al., 2012; Morway et al., 2013). Reactive transport of N and P species in the aquifer system has a strong influence on the storage of N and P within the interior of the watershed, and greatly affects the timing and amount of N and P mass loading to surface water. The concentrations of the species in groundwater, which strongly affects the amount of N and P mass loaded to streams, is influenced by the hydrogeological setting and the thickness of the soil profile. The other key components affecting NO$_3$-N fate and transport including denitrification and irrigation water chemistry. Heterotrophic denitrification is a particularly important processes for chemical reaction that affects nitrate in the aquifer

(Korom, 1992). Autotrophic denitrification is a microbially-mediated denitrification process with pyrite (FeS_2) acting as the primary electron (e^-) donor (Frind et al., 1990; Juncher Jørgensen et al., 2009), and has been observed in aquifers all over the world (Puckett and Cowdery, 2002; Wriedt and Rode, 2006) and even proposed as a means of remediating NO_3 contamination in groundwater systems (Pauwels et al., 2002).

Diverted canal water and pumped groundwater contain N and P mass, and hence applied irrigation water is an additional source of N and P mass to the soil profile. N and P mass in the river water are apportioned throughout the region based on the location of irrigation as well as the rate and amount of application. This contributes, in conjunction with fertilizer application, to the spatial variability in N and P mass accumulation in the soil profile and significant heterogeneity in aqueous chemistry in shallow aquifers underlying irrigated, cultivated fields (Kelly, 1997). Furthermore, irrigation chemistry can change significantly if pumped groundwater is used for irrigation water, due to the typically much higher concentration of NO_3 in groundwater than in surface water (McMahon and Böhlke, 1996), with the difference due to mixing between surface and groundwater systems.

1.2 APPROACHES FOR ASSESSING NUTRIENT TRANPORTATION AND REMEDIATIONS

Traditionally, field experiments can provide direct evidence of human influence on realistic processes in managed watersheds (Luo et al., 2008; Wang et al., 2005). In the case of intensively irrigated systems, continuous monitoring of drainage water, groundwater levels, streamflow, groundwater return flow, and N and P concentrations in river and groundwater can assist in understanding watershed hydrologic and pollutants dynamics (Dechmi et al., 2012). Monitoring studies permit the identification of the actual trophic status of waters and the assessment of the effectiveness of post-implementation of best management practice (BMPs). However, uncertainties/errors associated with every individual measurement due to limitations in equipment and methodology, and it is quite difficult to associate the environmental improvements to specific BMPs, unless extensive sampling points are available. In addition, using field experiments as the sole method associated with understanding nutrient contamination

is difficult and resource-intensive, especially if they are applied over the large scales for a sequence of years (Santhi et al., 2006). Interactions between the groundwater-surface water cannot be effectively identified either through regional scale monitoring projects.

Due to the complex dynamics of N and P fate and transport processes, the numerical simulation tools is an appealing approach to understand the relate system changes (agriculture management, land use) to system responses (streamflow, nutrient concentration, soil, groundwater, and groundwater-surface water interactions) (Almendinger and Ulrich, 2017; Liu et al., 2019), and to find solutions through BMPs. Deterministic models can be classified into following categories that commonly used in nutrient transport and contaminant remediation studies in watersheds:1) lumped or distributed models, 2) continuous or event-based models, and 3) empirical or physically-based models. Among all different combinations of model types, the continuous physically-based, spatially distributed models are ideal to analyzing long-term effects of hydrological changes and the effectiveness of watershed management practices, especially agricultural practices (Bouraoui and Dillaha, 1996). Previous studies reported the frequently used watershed-scale hydrological and water quality models include HSPF (Bicknell et al., 1993), ANSWERS-continuous (Bouraoui and Dillaha, 2000), MIKE SHE (Refsgaard, 1997), ParFLOW (Kollet and Maxwell, 2008), and SWAT (Arnold et al., 1998). HSPF is an empirical semi-distributed model, which limits its capability of simulating impact of BMPs in different fields within a subwatershed on hydrology and water quality. ANSWERS-Continuous does not have channel erosion and sediment transport routines, which may cause difficulties in evaluating in-stream nutrient transport, especially for P. MIKE-SHE is a physically based, comprehensive, and distributed model, suitable for simulating water, sediment, and water quality in surface and groundwater systems. However, the source code is not available for public use, and the difficulty in obtaining sediment information and extensive requirement of input parameters are known to be limiting factors in application of MIKE-SHE (Borah and Bera, 2003). ParFlow, a recently developed fully integrated hydrological model, is a continental scale model that using Richards' Equation to solve variably saturated 3-D groundwater flow. Thus, the main disadvantage over the complex physically based ParFlow is that it is much more computationally heavy requiring for more

comprehensive model evaluations and uncertainty assessments. SWAT, the most frequently use of these, is performed satisfactorily in simulating flow, sediment, and nutrient transport, and can investigate various land and water management practices and the impacts on water and nutrient in regional scale watersheds over long periods of time (Lam et al., 2011; Liu et al., 2013). However, the use of SWAT in those groundwater dominant regions is problematic due to the lumped, semi-distributed representation of groundwater flow to streams (Chu and Shirmohammadi, 2004; Gassman et al., 2007).

Another subset of models, attempting to provide more accuracy in terms of subsurface flow pathways and aquifer heterogeneity, has modified existing groundwater solute reactive transport models such as RT3D (Clement, 1999) and MT3D (Zheng and Wang, 1999) to include chemical kinetics (Bailey and Ahmadi, 2014; Shultz et al., 2018) at the regional scale, with the three-dimensional groundwater flow model MODFLOW (Harbaugh, 2005). In attempts to account for the main hydrological processes in both the land surface system and the groundwater system, some studies in the past two decades have linked SWAT with MODFLOW at varying levels of complexity (Sophocleous and Perkins, 2000; Conan et al., 2003; Kim et al., 2008; Guzman et al., 2015). Most recently, Bailey et al (2016) provided an enhanced SWAT-MODFLOW modeling framework which uses an internal mapping scheme to pass simulated data between SWAT Hydrologic Response Units (HRUs) and MODFLOW finite difference grid cells on a time step defined by the model user. The modeling system also allows the SWAT and MODFLOW models to be of difference spatial extents. To incorporate nutrient fate and transport, three specific studies have linked MT3D to SWAT-MODFLOW modeling systems: Conan et al. (2003) for a 12 km^2 catchment in Brittany, France; Galbiati et al. (2006) for the 20 km^2 Bonello watershed in Italy; Narula and Gosain (2013) for the 11,600 km^2 Upper Yamuna watershed in the Ganga River Basin, India; Pulido-Velazquez et al. (2015) for 8400 km^2 Jucar River basin, Spain; and Sullivan et al. (2019). All these modelling framework are targeting on NO_3 with both uniform recharge amount and NO_3 loading specified as input to the models, therefore, accurate timing and amount of water and nutrient leaching out of the soil is not simulated and spatial representation of nutrient concentration in groundwater cannot be produced. In addition, each modeling systems, consisted of the three separate models (SWAT, MODFLOW, MT3D)

that are loosely coupled, i.e. outputs from one model are provided as inputs to another model, with direct model integration not performed. Each study also used month-averaged rates and loads from SWAT to input into MODFLOW. To our best knowledge, no study has developed a comprehensive tool for assessing the effectiveness of selected BMPs to reduce both N and P, and to demonstrate the applicability of the system by considering spatially and temporally changing land management practices in the high degree of human intervention stream-aquifer system.

1.3 GOAL AND OBJECTIVES

The overall objective of this dissertation is to establish a numerical model capable of providing a fully-integrated surface-subsurface watershed model that simulates water, sediment, and the fate and transport of N and P species in a semi-arid irrigated system with complex groundwater-surface water interactions.

(1) Development of a methodology to enhance the capability of the SWAT model in intensively managed irrigated stream-aquifer systems.

(2) Improve understanding of the spatio-temporal patterns of groundwater-surface water interactions and nutrient fate and transport in a semi-arid irrigated stream-aquifer system. This will be accomplished by developing and applying a SWAT-MODFLOW model and a SWAT-MODFLOW-RT3D model to an intensively-irrigated semi-arid watershed.

(3) Application of the developed SWAT-MODFLOW-RT3D model to a regional-scale, intensively irrigated stream-aquifer system. Selected best management practices (BMPs) will be analyzed for N and P contamination in surface and groundwater in highly-managed irrigation watershed.

The results of these research objectives are organized in the remaining chapters, with each chapter building on results of the previous chapter: Chapter 2 presents a new method to apply SWAT in the intensively irrigation stream-aquifer system; Chapter 3 outlines the updated version of SWAT-MODFLOW model to handle groundwater irrigation and groundwater evaporation that can be used to assess the groundwater and surface water hydrological processes and quantify the effects of decreasing irrigation on hydrologic responses and food production; Chapter 4 outlines the development and

6

calibration of SWAT-MODFLOW-RT3D to simulate N and P fate and transport in intensively managed irrigated watershed. Selected BMPs are investigated using the calibrated integrated model in this chapter; Chapter 5 quantifying the sensitivity and uncertainty of the coupled SWAT-MODFLOW-RT3D model; and the final chapter of this dissertation (Chapter 6) summarizes major conclusions, and offers directions for future work. The Appendix includes a published journal article that presents the development and application of SWAT-MODFLOW-RT3D to simulate nitrate (NO_3) fate and transport in the Klamath River Basin, Oregon. Although it was not used in the same study area of LARV, it is included here as a demonstration of potential use of the model for regional-scale watersheds.

- Wei, X., Bailey, R.T., Records, R.M., Wible, T.C. and Arabi, M., 2018. Comprehensive simulation of nitrate transport in coupled surface-subsurface hydrologic systems using the linked SWAT-MODFLOW-RT3D model. *Environmental Modelling & Software*. https://doi.org/10.1016/j.envsoft.2018.06.012
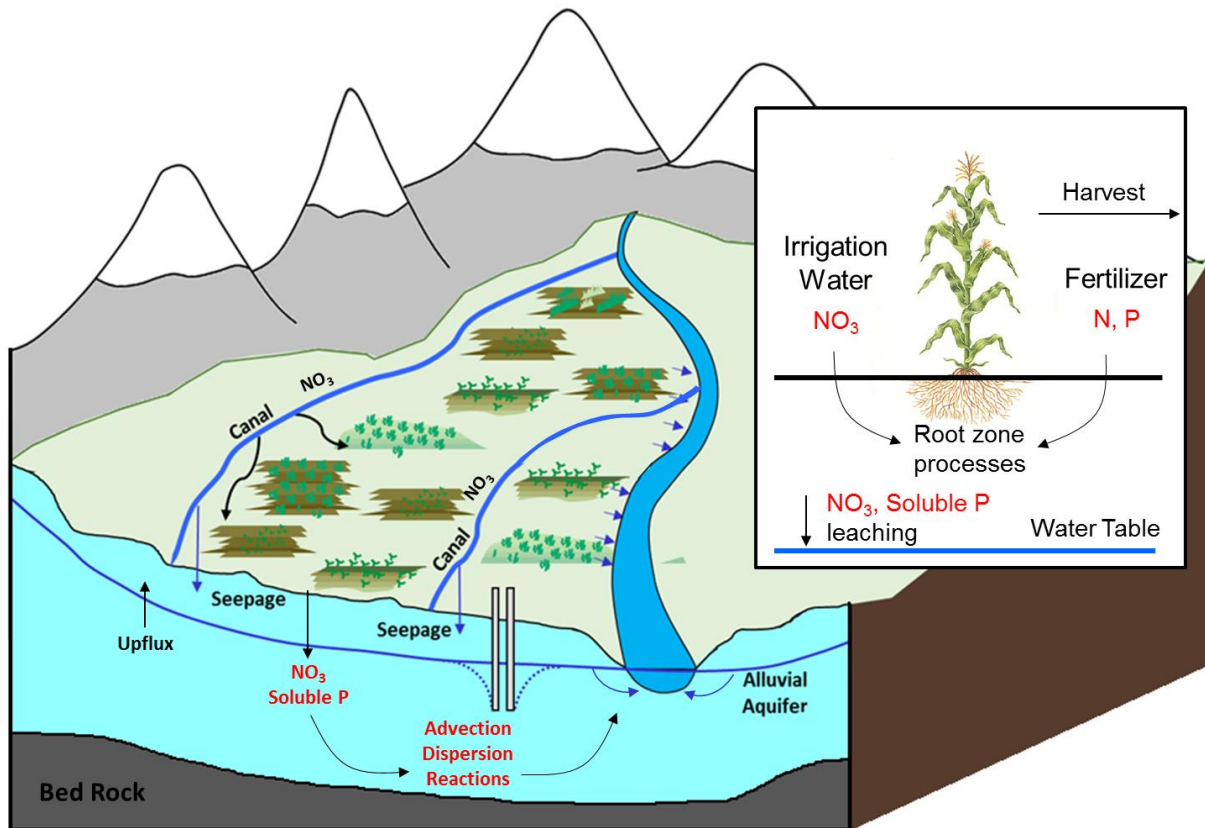
Figure 1. Conceptual scheme of fate and transport of NO_3 and soluble P in an irrigated stream-aquifer system subject to agricultural activities (e.g. surface and groundwater irrigation, and fertilizer loading)

REFERENCES

Almasri, M.N., Kaluarachchi, J.J., 2007. Modeling nitrate contamination of groundwater in agricultural watersheds. Journal of Hydrology 343, 211–229. https://doi.org/10.1016/j.jhydrol.2007.06.016

Almendinger, J.E., Ulrich, J.S., 2017. Use of SWAT to Estimate Spatial Scaling of Phosphorus Export Coefficients and Load Reductions Due to Agricultural BMPS. JAWRA Journal of the American Water Resources Association 53, 547–561. https://doi.org/10.1111/1752-1688.12523

Amdur, M.O., Doull, J., Klaassen, C.D., 1993. Casarett and Doull's Toxicology: The Basic Science of Poisons, 4th Edition. Journal of Occupational and Environmental Medicine 35, 76.

Arnold, J.G., Srinivasan, R., Muttiah, R.S., Williams, J.R., 1998. Large Area Hydrologic Modeling and Assessment Part I: Model Development1. JAWRA Journal of the American Water Resources Association 34, 73–89. https://doi.org/10.1111/j.1752-1688.1998.tb05961.x

Bailey, R.T., Ahmadi, M., 2014. Spatial and temporal variability of in-stream water quality parameter influence on dissolved oxygen and nitrate within a regional stream network. Ecological Modelling 277, 87–96. https://doi.org/10.1016/j.ecolmodel.2014.01.015

Bailey, R.T., Wible, T.C., Arabi, M., Records, R.M., Ditty, J., 2016. Assessing regional-scale spatio-temporal patterns of groundwater–surface water interactions using a coupled SWAT-MODFLOW model. Hydrological Processes 30, 4420–4433. https://doi.org/10.1002/hyp.10933

Barros, R., Isidoro, D., Aragüés, R., 2012. Three study decades on irrigation performance and salt concentrations and loads in the irrigation return flows of La Violada irrigation district (Spain). Agriculture, Ecosystems & Environment 151, 44–52. https://doi.org/10.1016/j.agee.2012.02.003

Bicknell, B.R., Imhoff, J.C., Kittle Jr, J.L., Donigian Jr, A.S., Johanson, R.C., 1993. Hydrologic simulation program-FORTRAN (HSPF): User's Manual for Release 10.

Borah, K.K., Bera, M., 2003. WATERSHED-SCALE HYDROLOGIC AND NONPOINT-SOURCE POLLUTION MODELS: REVIEW OF MATHEMATICAL BASES. Transactions of the ASAE 46, 1553–1566. https://doi.org/10.13031/2013.15644

Bouraima, A.-K., He, B., Tian, T., 2016. Runoff, nitrogen (N) and phosphorus (P) losses from purple slope cropland soil under rating fertilization in Three Gorges Region. Environ Sci Pollut Res 23, 4541–4550. https://doi.org/10.1007/s11356-015-5488-1

Bouraoui, F., Dillaha, T.A., 2000. ANSWERS-2000: Non-Point-Source Nutrient Planning Model. Journal of Environmental Engineering 126, 1045–1055. https://doi.org/10.1061/(ASCE)0733-9372(2000)126:11(1045)

Bouraoui, F., Dillaha, T.A., 1996. ANSWERS-2000: Runoff and Sediment Transport Model. Journal of Environmental Engineering 122, 493–502. https://doi.org/10.1061/(ASCE)0733-9372(1996)122:6(493)

Capes, S.E., Hunt, D., Malmberg, K., Gerstein, H.C., 2000. Stress hyperglycaemia and increased risk of death after myocardial infarction in patients with and without diabetes: a systematic overview. The Lancet 355, 773–778. https://doi.org/10.1016/S0140-6736(99)08415-9

Carpenter, S.R., Caraco, N.F., Correll, D.L., Howarth, R.W., Sharpley, A.N., Smith, V.H., 1998. Nonpoint Pollution of Surface Waters with Phosphorus and Nitrogen. Ecological Applications 8, 559–568. https://doi.org/10.1890/1051-0761(1998)008[0559:NPOSWW]2.0.CO;2

Chu, T.W., Shirmohammadi, A., 2004. Evaluation of the SWAT model's hydrology component in the piedmont physiographic region of Maryland. Transactions of the ASAE 47, 1057.

Clement, T.P., 1999. A Modular Computer Code for Simulating Reactive Multi-Species Transport in 3-Dimensional Groundwater Systems (No. PNNL-11720; EW4010). Pacific Northwest National Lab., Richland, WA (US). https://doi.org/10.2172/8022

Conan, C., Bouraoui, F., Turpin, N., de Marsily, G., Bidoglio, G., 2003. Modeling Flow and Nitrate Fate at Catchment Scale in Brittany (France). Journal of Environmental Quality 32, 2026–2032. https://doi.org/10.2134/jeq2003.2026

Correll, D.L., 1998. The Role of Phosphorus in the Eutrophication of Receiving Waters: A Review. Journal of Environmental Quality 27, 261–266. https://doi.org/10.2134/jeq1998.00472425002700020004x

Dechmi, F., Burguete, J., Skhiri, A., 2012. SWAT application in intensive irrigation systems: Model

    modification, calibration and validation. Journal of Hydrology 470–471, 227–238.

    https://doi.org/10.1016/j.jhydrol.2012.08.055

Doody, D., Moles, R., Tunney, H., Kurz, I., Bourke, D., Daly, K., O'Regan, B., 2006. Impact of flow path

    length and flow rate on phosphorus loss in simulated overland flow from a humic gleysol grassland

    soil. Science of The Total Environment 372, 247–255. https://doi.org/10.1016/j.scitotenv.2006.08.029

Duff, J.H., Triska, F.J., 2000. Nitrogen biogeochemistry and surface-subsurface exchange in streams 197–

    220. https://doi.org/10.1016/B978-012389845-6/50009-0

Elser, J.J., Marzolf, E.R., Goldman, C.R., 1990. Phosphorus and Nitrogen Limitation of Phytoplankton

    Growth in the Freshwaters of North America: A Review and Critique of Experimental Enrichments.

    Can. J. Fish. Aquat. Sci. 47, 1468–1477. https://doi.org/10.1139/f90-165

Frind, E.O., Duynisveld, W.H.M., Strebel, O., Boettcher, J., 1990. Modeling of multicomponent transport

    with microbial transformation in groundwater: The Fuhrberg Case. Water Resources Research 26,

    1707–1719. https://doi.org/10.1029/WR026i008p01707

Galbiati, L., Bouraoui, F., Elorza, F.J., Bidoglio, G., 2006. Modeling diffuse pollution loading into a

    Mediterranean lagoon: Development and application of an integrated surface–subsurface model tool.

    Ecological Modelling, Special Issue on Southern European Coastal Lagoons 193, 4–18.

    https://doi.org/10.1016/j.ecolmodel.2005.07.036

Gassman, P.W., Reyes, M.R., Green, C.H., Arnold, J.G., 2007. The soil and water assessment tool:

    historical development, applications, and future research directions. Transactions of the ASABE 50,

    1211–1250.

Guzman, J.A., Moriasi, D.N., Gowda, P.H., Steiner, J.L., Starks, P.J., Arnold, J.G., Srinivasan, R., 2015.

    A model integration framework for linking SWAT and MODFLOW. Environmental Modelling &

    Software 73, 103–116. https://doi.org/10.1016/j.envsoft.2015.08.011

Heathwaite, L., Sharpley, A., Gburek, W., 2000. A Conceptual Approach for Integrating Phosphorus and Nitrogen Management at Watershed Scales. Journal of Environmental Quality 29, 158–166. https://doi.org/10.2134/jeq2000.00472425002900010020x

Hill, M.J., Hawksworth, G., Tattersall, G., 1973. Bacteria, Nitrosamines and Cancer of the Stomach. Br J Cancer 28, 562–567. https://doi.org/10.1038/bjc.1973.186

Jang, S.S., Ahn, S.R., Kim, S.J., 2017. Evaluation of executable best management practices in Haean highland agricultural catchment of South Korea using SWAT. Agricultural Water Management, Agricultural water and nonpoint source pollution management at a watershed scale Part II Overseen by: Dr. Brent Clothier 180, 224–234. https://doi.org/10.1016/j.agwat.2016.06.008

Juncher Jørgensen, C., Jacobsen, O.S., Elberling, B., Aamand, J., 2009. Microbial Oxidation of Pyrite Coupled to Nitrate Reduction in Anoxic Groundwater Sediment. Environ. Sci. Technol. 43, 4851–4857. https://doi.org/10.1021/es803417s

Kato, T., Kuroda, H., Nakasone, H., 2009. Runoff characteristics of nutrients from an agricultural watershed with intensive livestock production. Journal of Hydrology 368, 79–87. https://doi.org/10.1016/j.jhydrol.2009.01.028

Kelly, W.R., 1997. Heterogeneities in ground-water geochemistry in a sand aquifer beneath an irrigated field. Journal of Hydrology 198, 154–176. https://doi.org/10.1016/S0022-1694(96)03316-1

Kilroy, G., Coxon, C., 2005. Temporal variability of phosphorus fractions in Irish karst springs. Env Geol 47, 421–430. https://doi.org/10.1007/s00254-004-1171-4

Kim, N.W., Chung, I.M., Won, Y.S., Arnold, J.G., 2008. Development and application of the integrated SWAT–MODFLOW model. Journal of Hydrology 356, 1–16. https://doi.org/10.1016/j.jhydrol.2008.02.024

Kollet, S.J., Maxwell, R.M., 2008. Capturing the influence of groundwater dynamics on land surface processes using an integrated, distributed watershed model. Water Resources Research 44. https://doi.org/10.1029/2007WR006004

Lam, Q.D., Schmalz, B., Fohrer, N., 2011. The impact of agricultural Best Management Practices on water quality in a North German lowland catchment. Environ Monit Assess 183, 351–379. https://doi.org/10.1007/s10661-011-1926-9

Liu, R., Zhang, P., Wang, X., Chen, Y., Shen, Z., 2013. Assessment of effects of best management practices on agricultural non-point source pollution in Xiangxi River watershed. Agricultural Water Management 117, 9–18. https://doi.org/10.1016/j.agwat.2012.10.018

Liu, Y., Wang, R., Guo, T., Engel, B.A., Flanagan, D.C., Lee, J.G., Li, S., Pijanowski, B.C., Collingsworth, P.D., Wallace, C.W., 2019. Evaluating efficiencies and cost-effectiveness of best management practices in improving agricultural water quality using integrated SWAT and cost evaluation tool. Journal of Hydrology 577, 123965. https://doi.org/10.1016/j.jhydrol.2019.123965

Lookman, R., Geerts, H., Grobet, P., Merckx, R., Vlassak, K., 1996. Phosphate speciation in excessively fertilized soil: a 31P and 27Al MAS NMR spectroscopy study. European Journal of Soil Science 47, 125–130. https://doi.org/10.1111/j.1365-2389.1996.tb01379.x

Luo, Y., He, C., Sophocleous, M., Yin, Z., Hongrui, R., Ouyang, Z., 2008. Assessment of crop growth and soil water modules in SWAT2000 using extensive field experiment data in an irrigation district of the Yellow River Basin. Journal of Hydrology 352, 139–156. https://doi.org/10.1016/j.jhydrol.2008.01.003

McMahon, P.B., Böhlke, J.K., 1996. Denitrification and mixing in a stream—aquifer system: effects on nitrate loading to surface water. Journal of Hydrology 186, 105–128. https://doi.org/10.1016/S0022-1694(96)03037-5

Monteagudo, L., Moreno, J.L., Picazo, F., 2012. River eutrophication: Irrigated vs. non-irrigated agriculture through different spatial scales. Water Research 46, 2759–2771. https://doi.org/10.1016/j.watres.2012.02.035

Morway, E.D., Gates, T.K., Niswonger, R.G., 2013. Appraising options to reduce shallow groundwater tables and enhance flow conditions over regional scales in an irrigated alluvial aquifer system. Journal of Hydrology 495, 216–237. https://doi.org/10.1016/j.jhydrol.2013.04.047

Narula, K.K., Gosain, A.K., 2013. Modeling hydrology, groundwater recharge and non-point nitrate loadings in the Himalayan Upper Yamuna basin. Science of The Total Environment, Changing water resources availability in Northern India with respect to Himalayan glacier retreat and changing monsoon patterns: consequences and adaptation 468–469, S102–S116. https://doi.org/10.1016/j.scitotenv.2013.01.022

Pauwels, H., Tercier-Waeber, M.-L., Arenas, M., Castroviejo, R., Deschamps, Y., Lassin, A., Graziottin, F., Elorza, F.-J., 2002. Chemical characteristics of groundwater around two massive sulphide deposits in an area of previous mining contamination, Iberian Pyrite Belt, Spain. Journal of Geochemical Exploration 75, 17–41. https://doi.org/10.1016/S0375-6742(01)00198-4

Puckett, L.J., Cowdery, T.K., 2002. Transport and Fate of Nitrate in a Glacial Outwash Aquifer in Relation to Ground Water Age, Land Use Practices, and Redox Processes. Journal of Environmental Quality 31, 782–796. https://doi.org/10.2134/jeq2002.7820

Pulido-Velazquez, M., Peña-Haro, S., García-Prats, A., Mocholi-Almudever, A.F., Henriquez-Dole, L., Macian-Sorribes, H., Lopez-Nicolas, A., 2015. Integrated assessment of the impact of climate and land use changes on groundwater quantity and quality in the Mancha Oriental system (Spain). Hydrology and Earth System Sciences 19, 1677–1693. https://doi.org/10.5194/hess-19-1677-2015

Randall, G.W., Iragavarapu, T.K., 1995. Impact of Long-Term Tillage Systems for Continuous Corn on Nitrate Leaching to Tile Drainage. Journal of Environmental Quality 24, 360–366. https://doi.org/10.2134/jeq1995.00472425002400020020x

Refsgaard, J.C., 1997. Parameterisation, calibration and validation of distributed hydrological models. Journal of Hydrology 198, 69–97. https://doi.org/10.1016/S0022-1694(96)03329-X

Santhi, C., Srinivasan, R., Arnold, J.G., Williams, J.R., 2006. A modeling approach to evaluate the impacts of water quality management plans implemented in a watershed in Texas. Environmental Modelling & Software 21, 1141–1157. https://doi.org/10.1016/j.envsoft.2005.05.013

Sharpley, A.N., Smith, S.J., Jones, O.R., Berg, W.A., Coleman, G.A., 1992. The Transport of

    Bioavailable Phosphorus in Agricultural Runoff. Journal of Environmental Quality 21, 30–35.

    https://doi.org/10.2134/jeq1992.00472425002100010003x

Shultz, C.D., Bailey, R.T., Gates, T.K., Heesemann, B.E., Morway, E.D., 2018. Simulating selenium and

    nitrogen fate and transport in coupled stream-aquifer systems of irrigated regions. Journal of

    Hydrology 560, 512–529. https://doi.org/10.1016/j.jhydrol.2018.02.027

Smith, V.H., 2003. Eutrophication of freshwater and coastal marine ecosystems a global problem.

    Environ Sci & Pollut Res 10, 126–139. https://doi.org/10.1065/espr2002.12.142

Sophocleous, M., Perkins, S.P., 2000. Methodology and application of combined watershed and ground-

    water models in Kansas. Journal of Hydrology 236, 185–201. https://doi.org/10.1016/S0022-

    1694(00)00293-6

Sullivan, T.P., Gao, Y., Reimann, T., 2019. Nitrate transport in a karst aquifer: Numerical model

    development and source evaluation. Journal of Hydrology 573, 432–448.

    https://doi.org/10.1016/j.jhydrol.2019.03.078

US EPA, O., 2015. National Primary Drinking Water Regulations [WWW Document]. US EPA. URL

    https://www.epa.gov/ground-water-and-drinking-water/national-primary-drinking-water-regulations

    (accessed 8.28.19).

Vitousek, P.M., Aber, J.D., Howarth, R.W., Likens, G.E., Matson, P.A., Schindler, D.W., Schlesinger,

    W.H., Tilman, D.G., 1997. Human Alteration of the Global Nitrogen Cycle: Sources and

    Consequences. Ecological Applications 7, 737–750. https://doi.org/10.1890/1051-

    0761(1997)007[0737:HAOTGN]2.0.CO;2

Wang, W.-Y., Luo, W., Wang, Z.-R., 2005. Surge flow irrigation with sediment-laden water in

    northwestern China. Agricultural Water Management 75, 1–9.

    https://doi.org/10.1016/j.agwat.2004.12.009

Weisenburger, D.D., 1991. Potential Health Consequences of Ground-Water Contamination by Nitrates in Nebraska, in: Bogárdi, I., Kuzelka, R.D., Ennenga, W.G. (Eds.), Nitrate Contamination, NATO ASI Series. Springer Berlin Heidelberg, pp. 309–315.

Wriedt, G., Rode, M., 2006. Modelling nitrate transport and turnover in a lowland catchment system. Journal of Hydrology, Measurement and Parameterization of Rainfall Microstructure 328, 157–176. https://doi.org/10.1016/j.jhydrol.2005.12.017

Zheng, C., Wang, P.P., 1999. MT3DMS: A Modular Three-Dimensional Multispecies Transport Model for Simulation of Advection, Dispersion, and Chemical Reactions of Contaminants in Groundwater Systems; Documentation and User's Guide. ALABAMA UNIV UNIVERSITY.

CHAPTER 2. USING THE SWAT MODEL IN INTENSIVELY MANAGED IRRIGATED WATERSHEDS: MODEL MODIFICATION AND APPLICATION[1]

2.1. SUMMARY

The Soil Water and Assessment Tool (SWAT) is a well-established modeling tool for simulating hydrologic processes in watershed systems. However, SWAT often does not perform well in highly-managed watersheds with intensive irrigation due to management practices and associated hydrologic processes (e.g. canal seepage) not included in the modeling code. In this study, we present a method to apply SWAT to managed irrigated watersheds, which includes: designating each cultivated field as a hydrologic response unit (HRU) and including recorded crop rotations; applying scheduled irrigation according to water rights; and simulating seepage from earthen irrigation canals, with the latter requiring a minor modification to the SWAT code. SWAT's auto-irrigation function is also used as a comparison. Methodology was applied to a 732 km^2 watershed in the Lower Arkansas River Valley (southeastern Colorado), a semi-arid region that has been intensively irrigated for over 100 years. The model was tested against monthly stream discharge at 5 stream gauging stations in the Arkansas River and its tributaries during the 2001 to 2007 period. Results demonstrate the necessity of including human management features, particularly canal seepage, to capture in-stream flows in the river and the tributaries. The scheduled irrigation approach has a significant better performance in the smaller highly agricultural tributaries while the auto-irrigation functionality had a slightly but not significant better performance at the outlet of the whole watershed. The methods presented herein can be applied to other semi-arid irrigated regions.

2.2. INTRODUCTION

Intensively managed irrigation systems are human-impacted agro-ecosystem wherein cultivated fields, river diversion points, and artificial canals are highly distributed spatially. Rainfall is not adequate to supply crop water needs, and hence irrigation water is provided by nearby streams and/or pumped from the underlying aquifer system leading to diminished streamflow and higher regional groundwater levels (Gates et al., 2006). Due to irrigation deep percolation and canal seepage, this irrigation system is facing higher rates of evapotranspiration and net contribution to streamflow from groundwater (baseflow) (Gates et al., 2009; Niemann et al., 2011; Gates et al., 2012). High groundwater levels in semi-arid regions can lead to high soil salinity and result in crop yield decrease, increased groundwater pollution from leaching chemicals, and increased groundwater mass loading of nitrogen and other chemical species to nearby streams (Herczeg et al., 2001; Jolly et al., 2008; Morway and Gates, 2012; Alarcón-Herrera et al., 2013; Morway et al., 2013; Bailey et al., 2014). Methods are required to monitor human-impacted hydrologic processes and identify remediation strategies.

Traditionally, field experiments provided direct evidence of human impact on hydrologic processes in managed watersheds (Wang et al., 2005; Luo et al., 2008). In the case of intensively irrigated systems, continuous monitoring of drainage water, groundwater levels, groundwater return flows, and streamflow can assist in understanding watershed hydrologic dynamics (Dechmi et al., 2012). However, recommendation derived from site-specific field experiments typically cannot be generalized to the regional level or to other watersheds (Santhi et al., 2006). In addition, using field experiments as the sole method to understanding processes is very expensive and time consuming, especially if they are applied over a sequence of years (Santhi et al., 2006). Rather, hydrologic models often are used in combination with field data to capture the major hydrologic processes and relate system changes (land use, climate) to system responses (streamflow, soil moisture, groundwater discharge). Specific modeling codes that capture these processes at the watershed scale include the Hydrological Simulation Program Fortran (HSPF, Bicknell et al., 1993), the Variable Infiltration Capacity model (VIC, Liang et al., 1994, 1996), TOPMODEL (Beven, 1997), the Soil Water Assessment Tool (SWAT, Arnold et al., 1998; Neitsch et al.,

18

2011), MIKE SHE (DHI, 1999), the Annualized Agricultural Nonpoint Source Model (AnnAGNPS, Bingner et al., 2001), CASC2D (Ogden et al., 2002), ParFlow (Kollet and Maxwell, 2006), WAM (SWET, 2006), and the Distributed Hydrology Soil Vegetation Model (DHSVM, Thanapakpawin et al., 2007). Of these, SWAT has been extensively applied to watersheds throughout the world (Borah and Bera, 2003; Gassman et al., 2007). SWAT incorporates agricultural management practices (e.g. planting, irrigation, fertilization, harvest, and tillage), and has been applied successfully in numerous agricultural watersheds for long-term continuous simulations and assessments of runoff, erosion, sediment, and nutrient transport (Santhi et al., 2001; Bouraoui et al., 2005; Gosain et al., 2005). The following provides a short review of SWAT model applications to managed irrigated watersheds.

Bosch et al. (2004) improved SWAT performance in a coastal plain agricultural watershed area, a 22.1 km^2 subwatershed of the Little River in Georgia, by using higher resolution land use, soils, and topographic coverages and indicated additional model refinements to better represent the physical processes of streamflow. Santhi et al. (2005) configured SWAT as a regional planning tool with canal irrigation capability to estimate crop water demand and irrigation water requirement. However, it could not be used to simulate the actual day-to-day water scheduling and distribution, and might become inefficient in daily simulation and could be prohibitive for large watershed. Garg et al. (2012) characterized the hydrologic processes and crop water productivity using the SWAT model in the Upper Bhima basin in India, with the study area of a 46,066 km^2. In their study, depth, frequency, and timing of irrigation were simulated by SWAT's auto-irrigation option. They did not consider water availability in the upstream region and failed to match water allocation with the realistic water rights. Dechmi et al. (2012) modified the SWAT2005 to include the depths of irrigation water in the soil water balance calculation to improve irrigation return flow when the source of irrigation water is outside the modeled watershed boundary. The developed model, SWAT-IRRIG, was applied to an 18.65 km^2 irrigated watershed in Spain to evaluate best management practices (Dechmi and Skhiri, 2013). A scheduled irrigation approach was used by Zheng et al. (2010) and Ahmadzadeh et al. (2016) to consider real irrigation management variables for each irrigation event in a 1,000 km^2 watershed in China and a 12,025

km^2 watershed in Iran, respectively. Xie and Cui (2011) developed a new version of SWAT by incorporating new processes for irrigation and drainage to simulate daily runoff and crop yields in a 1,129 km^2 depression and impounded study area in China. Among these SWAT applications and other studies that described irrigation management in different watersheds, for instance, a 9.73 km^2 agricultural watershed in eastern India (Behera and Panda, 2006), the 10,488 km^2 Big Sunflower River Watershed in north-west Mississippi, United States (Parajuli et al., 2009), and the 2,380 km^2 Guadalupe River Basin in northwest Mexico (Molina-Navarro et al., 2016), irrigation water was specified by field capacity or crop water demand, and actual water allocation rates were not considered. In most studies, detailed scheduled irrigation data and canal irrigation processes (including canal seepage), two key aspects that control hydrologic processes in agricultural watersheds, have not been taken into consideration concurrently. Additional research needs to be conducted to enhance SWAT's capability in intensively irrigated watersheds. The overall objective of this study is to develop a methodology for applying the SWAT model to highly-managed irrigation systems and to evaluate its predictive capabilities in modeling hydrologic processes. Specific features include incorporating water rights into irrigation application scheduling, specifying each cultivated field as a hydrologic response unit (HRU), and the simulation of seepage from earthen canals, with the latter necessitating modification of the SWAT code. Methods are demonstrated for a 732 km^2 irrigated region in the Lower Arkansas River Valley in southeastern Colorado. The ability of the model to capture streamflow in the tributaries of the Arkansas River, which drain water from surrounding irrigated fields and hence are an artificial hydrologic feature of the watershed, is a key aspect of the model. The relative influence of each human management feature (canal diversion, cultivated fields, canal seepage) on streamflow in the Arkansas River and its tributaries also is demonstrated.

2.3. MATERIALS AND METHODS

This section provides a description of the study area and a summary of model construction and application. A model using the basic SWAT code also is developed and calibrated to provide a comparison with the modified SWAT modeling code.

2.3.1 Study Area

The study region is located in the Lower Arkansas River Valley (LARV) in southeastern Colorado (Figure 2). It lies upstream of John Martin Reservoir and extends west of the town of Fowler to the town of Las Animas, a 90.5 km reach of the Arkansas River. The floodplain alluvium consists of moderately permeable, heterogeneous deposits of gravel, sand, silt, and clay. Bedrock, consisting of Cretaceous shale and limestone and located approximately 10-15 m below ground surface, is relatively impermeable (Moore and Wood, 1967). The Arkansas River has a sandy channel and is in good hydraulic connection with the alluvium system (Person and Konikow, 1986; Morway et al., 2013). The most dominant land cover category in the watershed is agriculture (51%), followed by grassland and pasture (41%), urban (6%), water (1%), and bare land (1%). The amount of cultivated crop types and distribution is representative of the Arkansas River valley in Colorado. Figure 3A shows the crop type information for each cultivated field in 2001, provided by the Farm Service Agency located in Rocky Ford, CO. The dominant crop is alfalfa, followed by corn, grass/pasture, wheat, sunflower, melons, beans, oats, onion, and sorghum. The Arkansas River has a snowmelt-derived flow pattern with high flows in the spring and low flows in the fall. There are two large tributaries in the study region: Timpas Creek and Crooked Arroyo (Figure 2C). These two tributaries collect tail water runoff and groundwater return flows from irrigated fields. The mean elevation of the study region is 1293 m. The climate is semi-arid with an average annual precipitation of 376 mm. Two thirds of the annual precipitation occurs between May and September, primarily during brief but intense thunderstorms. The average annual temperature is 13.6 °C, with the monthly average temperature ranging from -12.6 °C in January to 35.9 °C in July.

Because of the semi-arid climate, much of the applied water is lost to evapotranspiration. Crop water requirements in the region are always in excess of the average annual precipitation, and therefore are supplemented with diverted river and pumped groundwater (Morway et al., 2013). The irrigation season

starts late-March to mid-April and ends in late-October, with earthen irrigation canals diverting water from the Arkansas River during March to November. There are 6 main irrigation canals (Rocky Ford Highline, Catlin, Otero, Rocky Ford Ditch, Fort Lyon, and Holbrook) under a system of irrigation districts according to Colorado water law, and 553 pumping wells (Figure 3B), the vast majority of which supply irrigation water to fields. The diversion point in the Arkansas River for four of the canals is shown in Figure 3B. The other two canals (Rocky Ford Highline, Otero) have diversion points upstream of the study region. The collection of fields receiving irrigation water from each canal (i.e. the "command area" of each canal) also is indicated in Figure 3B. Approximately 20% of the Fort Lyon command area is located within the study region, with the remainder in downstream areas. The vast majority of fields are irrigated using flood-irrigation methods with less than 5% irrigated with sprinklers (typically, center pivot sprinklers) or drip lines (Gates et al., 2012; Morway et al., 2013).

2.3.2 Overview of the SWAT model

SWAT (Arnold et al., 1998; Neitsch et al., 2005; Gassman et al., 2007; Neitsch et al., 2011) is a continuous-in-time, hydrologic/water quality model designed to predict the influence of land management practices on water, sediment, and nutrient yields within a single watershed (http://www.brc.tamus.edu/swat). The watershed is divided into sub-basins using topography, with each sub-basin containing one stream. Within each sub-basin, mass balance equations for water, sediment, and nutrients are computed at the level of HRUs and then scaled up to each sub-basin outlet by the area fraction each HRU occupies. HRUs are areal regions that have a unique combination of land use, soil type, and topographic slope, which can be spatially disconnected and do not have a continuous geographic location. The response of each HRU regarding water flow generation, nutrient loading, and sediment yield are routed directly to their respective sub-basin stream, with the sub-basin connectivity used to route to the watershed outlet.

The hydrologic component of SWAT is based on the water balance equation in the soil profile including rainfall, surface runoff, infiltration, evapotranspiration, lateral flow, percolation, and groundwater upflux. In regards to management operations, SWAT can simulate different operations such

as planting, irrigation, harvest and kill, and tillage. These management practices can be scheduled by date or by heat unit (linked to time to maturity by quantifying the heat required for plants). The model has several built-in databases for crops, soils, and tillage. Additional details on model theory, processes, and construction are provided in Neitsch et al. (2011).

2.3.3 Basic SWAT Model Setup

The ArcSWAT interface for SWAT2012 (Winchell et al., 2013) was used to prepare the basic SWAT model (Revision 664) setup of the watershed, which requires a digital elevation model (DEM), a soil map, a land use map, and climate data as input data. The sources and descriptions of the applied data are summarized in Table 1. The topographic parameters (slope, slope length, drainage network) were obtained from a 30-m DEM of the region. A National Hydrography Dataset (NHD) high-resolution stream layer was superimposed on the DEM to improve the hydrographic segmentation and sub-watershed boundary delineation. A point source was imposed in the Arkansas River near Catlin Dam (see Inlet in Figure 3C) to represent daily streamflow from upstream areas. Five streamflow gauging stations are located in the region (Figure 3C) and are used for model testing during the simulation period of January 2001 to September 2007. Three are located along the Arkansas River, one in Timpas Creek, and one in Crooked Arroyo. A 30-m pixel land use map for the year 2001 from the National Agricultural Statistics Service (NASS) and a US Digital General Soil Map (STATSGO) from the National Resources Conservation Service (NRCS) were applied for creating HRUs. A land use over area, soil type over land use, and slope over soil type threshold of 5%, 0%, and 0% were used respectively for defining the HRUs. A total of 72 sub-basins (Figure 3C) and 2,072 HRUs were delineated. Daily historical data related to precipitation, maximum and minimum average daily air temperature, wind speed, relative humidity, and solar radiation from April 1999 to September 2007 were obtained from four weather stations of the Colorado Agricultural Meteorological Network (CoAgMet) (Ley et al., 2009).

2.3.4 Modified SWAT model: Scheduled Irrigation and Canal Seepage

The cultivated field boundaries do not normally conform to HRU boundaries. A method developed in ArcGIS was used to modify the land use, soil, and slope data so that the resulting HRUs conform to the

boundary of the cultivated fields. In this modified HRU definition approach, HRUs represent individual fields. Furthermore, canal seepage processes were represented through an alteration of the SWAT source code, as explained in Section 2.4.2. The overall data flow in the modified SWAT modeling code, including scheduled irrigation, management operations, and canal seepage, is shown in Figure 4 and is described in the following sections.

2.3.4.1 Scheduled Irrigation to Individual Cultivated Fields

HRUs were delineated to match the boundaries of cultivated fields. This approach provides the capability to later modify the management operation parameters, including parameters related to irrigation, according to an irrigation database for each field. The new HRUs are named "Cultivated Field HRU" (CF_HRU). An example of this modification for some of the HRUs is illustrated in Figure 5. In this example, three original HRUs (Figure 5A), as delineated by SWAT, are modified according to field boundaries resulting in 28 CF_HRUs. Creating CF_HRUs requires field boundary data. The method for creating the CF_HRUs is performed as follows:

1.   Overlay the land use layer with the cultivated field polygons; determine the land use type that covers the majority of each polygon area and modify the land use layer so that the area corresponding to each polygon is covered completely with the majority land use. The original SWAT land use types in the un-cultivated regions are not modified.

2.   Overlay the soil layer with the cultivated field polygons; determine the soil type that covers the majority of each polygon area, and modify the soil layer so that the area corresponding to each polygon is covered completely with a majority soil type; then, use unique soil IDs (MUKEYs) to assign a unique ID to each of the cultivated fields. The original soil types in the un-cultivated regions are not modified. The soil ID and properties associated with a particular soil type were modified using the SWAT soil database.

3.   Use a single slope class in ArcSWAT HRU definition.

4.   Overlay these three layers in ArcSWAT to generate the map of CF_HRUs.

This method also accounts for fields located in multiple sub-basins. When a cultivated field is located in two or more adjacent sub-basins (see white lines in Figure 5B), a separate CF_HRU is created for each part of the field within each sub-basin. For this region there are 3,326 cultivated fields, which resulted in 4,275 CF_HRUs. The total number of HRUs is 5,330.

Management operations, such as irrigation applications, plant growth, harvest and kill data, and tillage operations, were specified in the management file for each of the 4,275 CF_HRUs (see Figure 4). In SWAT, the source of irrigation water can be specified as a river reach, reservoir, shallow aquifer, deep aquifer, or a location outside the watershed. In this study, irrigation water is provided either by a river reach (canal irrigation) or by the shallow aquifer (groundwater irrigation) determined based on the available data from the Colorado Division of Water Resources (CDWR). Two canals, the Rocky Ford Highline and the Otero, are treated as unlimited sources since their diversion points are located upstream of the model domain (Figure 3D). The other four canals (Catlin, Rocky Ford Ditch, Fort Lyon, and Holbrook) divert water from the Arkansas River inside the model boundary and thus are treated as a limited source of water. The source of irrigation water for all CF_HRUs in a given canal command area is set to the section of the Arkansas River coinciding with the point of diversion, except for the two canals with diversion points upstream of the model area (Figure 3D).

Diverted volumes of river water for the six irrigation canals and pumping rates for the 553 pumping wells were obtained from the CDWR and used to establish an irrigation schedule for each CF_HRU using the following method: first, pumped groundwater was allocated to fields surrounding each groundwater pump; second, a river water allocation algorithm distributed canal water to the CF_HRUs in each command area based on available water and a hierarchy of crop demand, similar to the method used by Morway et al. (2013) in the development of a groundwater model for the region. Based on information from local growers and extension agents, irrigation is applied according to the following crop priority: (1) onions, (2) peppers and tomatoes, (3) cantaloupe and melons, (4) pumpkins and squash, (5) alfalfa and corn, (6) barley, beans, and oats, (7) sorghum, (8) wheat, and (9) grass/pasture (Morway et al., 2013). CF_HRUs receive irrigation water on a weekly, bi-weekly, or monthly rotation schedule.

25

Information required for each CF_HRU includes the timing of the operation, the specific crop type to be simulated, and the total number of heat units required for land cover to reach maturity. Crop rotation for each CF_HRU was achieved by changing the plant identification number, identified from the SWAT crop database, for each year of the simulation. Heat unit calculation requires mean daily temperature and plant's minimum growth temperature, which can be obtained from the crop data base.

Management operations governing planting, harvesting, and tillage were obtained from research scientists at Colorado State University's Arkansas Valley Research Center in Rocky Ford, CO (Michael Bartolo, personal communication), and are listed for each crop type in Table 2. In regards to alfalfa, grass/pasture, and hay, five years harvest and kill operation were specified so that they can be replanted every five years. Tillage operation was specified as disk plow.

2.3.4.2 Seepage from Earthern Irrigation Canals

The seepage loss from earthen irrigation canals constitutes a substantial part of usable water in many irrigated areas (Swamee et al., 2000). Canal seepage is included in the SWAT model by adding seepage water depths directly to the shallow aquifer of the CF_HRUs bordering the canal. This addition necessitated the modification of the SWAT source code, with the seepage depth (mm) added to the percolation depth (mm) (water exiting the bottom of the HRU soil profile as deep percolation) in SWAT's groundwater module (*gwmod*). This calculation occurs for each day of the irrigation season for each CF_HRU bordering an irrigation canal (Figure 4).

In the study region, total daily seepage volume (m^3/day) for each canal was estimated using a field-estimated canal seepage rate (m^3/(s-km)) multiplied by the canal length (km), with the seepage depths (mm/day) averaged to each canal-adjacent CF_HRU according to its percentage of total adjacent CF_HRU area. The sets of HRUs adjacent to each canal, and hence receiving canal seepage water, are shown in Figure 3D. A total of 874 CF_HRUs were identified, equal to 6% of the total watershed area. Canal lengths and average seepage loss rates are provided in Table 3. Canal lengths vary from 20.4 km to 102.3 km, as provided by CDWR. A set of canal seepage measurements were obtained for the canals using inflow/outflow water balance techniques (Susfalk et al., 2008; Martin and Gates, 2014), resulting in

seepage loss rates varying from 0.012 m^3/(s-km) to 0.04 m^3/(s-km) (see Table 3), with an average seepage

loss rate of 0.029 m^3/(s-km). Values of daily seepage rates for each canal-bordering CF_HRU were

tabulated in a text file and read during each daily time step of the SWAT simulation.

As the total diverted water for each canal is the sum of the irrigation water applied to fields and the

seepage along the length of the canal, these two values were added and compared to the recorded volume

of water diverted from the Arkansas River to check the accuracy of the methodology (see Section 3.1)

2.3.5 Calibration and Validation

The model was calibrated and tested against observed streamflow data. Daily observed streamflow

(m^3/s) were obtained from CDWR for five gauging stations in the study region (Figure 2C): Rocky Ford,

La Junta, and Las Animas along the Arkansas River, Timpas Creek and Crooked Arroyo. Streamflow data

were averaged on a monthly basis. The model was run from April 1999 to December 2007. The first two

years were specified as a "warm up" period to initialize reasonable starting values for system variables.

Automatic calibration was performed using SWAT-CUP (calibration and uncertainty programs), a

public domain program that links SUFI-2 (Sequential Uncertainty Fitting, version 2) to the SWAT model

(Abbaspour et al., 2008). Calibration was performed for 2001 to 2003 using the simulated and observed

streamflow at Rocky Ford, Las Animas, and Timpus Creek stations used simultaneously in the objective

function of the Nash-Sutcliff coefficient (E_{ns}). E_{ns} is selected based on the recommendation by ASCE

(1993) and is commonly used with extensive information on reported values (Moriasi et al., 2007). Servat

and Dezetter (1991) found E_{ns} to be the best objective function for reflecting the overall model

performance as well. 2500 simulations were run in five iterations of 500 simulations, with the parameters

adjusted after each iteration to obtain a "best simulation" with the lowest residual between observed and

simulated values according to the objective function. The calibrated model was then tested for 2004 to

2007. Observed streamflow at the La Junta and Crooked Arroyo stations were used to test the model at

stream locations other than the calibration outlets for 2001 to 2007.

The basic SWAT model developed in Section 2.3 was first run to calibrate and test the model

performance. Based on literature (Bosch et al., 2004; Muleta and Nicklow, 2005; Van Liew et al., 2007;

Kannan et al., 2010; Neitsch et al., 2011; Yuan et al., 2015; Jang et al., 2017), 20 parameters (Table 4) were adjusted to improve model performance. These specific parameters typically are used in the SWAT calibration process for streamflow simulation. The human management features (canal diversion, CF_HRUs creation, and canal seepage) then were added into the calibrated model one at a time to compare and analyze the relative influence of each feature. The versions of the basic SWAT model with different features were not calibrated so that the influence of each feature is not affected by the calibration processes.

Sensitivity analysis, calibration, and validation were performed on the modified SWAT model developed in Section 2.4 that includes all the human management features. Sensitivity analysis was implemented by changing parameters one at a time to determine impact on streamflow. Based on literature review and sensitivity analysis, the parameters CN2, ESCO, CH_K2, CH_N2, SHALLST, GW_DELAY, GWQMN, GW_REVAP, RCHRG_DP, SOL_AWC, SOIL_K and SFTMP (see Table 4 for definitions) were found to be the most influential on streamflow, similar to results of other modeling studies in irrigated regions (Ghaffari et al., 2010; Dechmi and Skhiri, 2013).

The goodness of the calibration and validation results was estimated qualitatively using time series plots at the five stations and quantitatively using three statistical techniques. The first statistic is the coefficient of determination R^2 (Green and van Griensven, 2008):

$$r^2 = \left(\frac{\sum_{i=1}^{n}(Q_{obs,i} - \overline{Q}_{obs})(Q_{sim,i} - \overline{Q}_{sim})}{\sqrt{\sum_{i=1}^{n}(Q_{obs,i} - \overline{Q}_{obs})^2} \sqrt{\sum_{i=1}^{n}(Q_{sim,i} - \overline{Q}_{sim})^2}} \right)^2 \tag{1}$$

where n is the total number of observations, $Q_{sim,i}$ and $Q_{obs,i}$ are the simulated and observed values, respectively, on time step i, and $\overline{Q}_{sim}$ and $\overline{Q}_{obs}$ is the arithmetic mean of the simulated and observed values, respectively. It ranges from 0 to 1, with higher values indicating better correlations. The second is the percent bias (PBIAS) (Gupta et al., 1999), which represents the average tendency of the simulations to be larger or smaller than the observations:

$$PBIAS = \frac{\sum_{i=1}^{n}(Q_{obs,i} - Q_{sim,i})}{\sum_{i=1}^{n}(Q_{obs,i})} \times 100\%$$

(2)

Moriasi et al. (2015) considered watershed model performance to be "Very good" if PBIAS is less than 5%, "Good" if the error is between 5% and 10%, "Satisfactory" if the error is between 10% to 15%, and "Unsatisfactory" if values are equal to or greater than 15%. This standard was adopted in this study. The third statistic is the Nash-Sutcliff coefficient (E_{ns}) (Nash and Sutcliffe, 1970):

$$E_{ns} = 1 - \frac{\sum_{i=1}^{n}(Q_{obs,i} - Q_{sim,i})^2}{\sum_{i=1}^{n}(Q_{obs,i} - \overline{Q}_{obs})^2}$$

(3)

The E_{ns} indicates how well the plot of observed values vs. the simulated values fall along a 1:1 line. It ranges from negative infinity to 1, where a value of 0 indicates the average observed value is as good as the simulated values. Thus, values approaching 1 indicate better model performance. Simulation results are considered to be "Very Good" for E_{ns} values > 0.8, "Good" if the value is between 0.7 and 0.8, "Satisfactory" if the value is between 0.5 and 0.7, and "Unsatisfactory" for value ≤0.5 (Moriasi et al., 2015).

2.3.6 Effect of using Automated Irrigation

Automatic irrigation methods can be used in SWAT to trigger irrigation events based on plant water demand. This option was used with the calibrated parameter set (see Section 2.5) to compare with results from using the scheduled irrigation method, and hence incorporates the CF_HRU boundary method and canal seepage additions. As with the scheduled irrigation method, irrigation water is provided by either the Arkansas River or the shallow aquifer. For plant water demand, a recommended threshold value of 0.9 (Arnold et al., 2012) is specified to trigger crop irrigation. When plant stress occurs, an irrigation event will be triggered and water will be applied according to the available water in the source. If the crop water demand is more than the available amount, the model will apply only the available water to the HRU, and irrigation will be triggered in subsequent days depending on rainfall, soil moisture, and plant stress. The

amount of water applied is set to 80 mm, which is determined based on the diversion records and HRU area. Other variables required for auto-irrigation, e.g. irrigation efficiency and surface runoff ratio, were based on field monitoring of hundreds of surface irrigation events in the region (Gates et al., 2012). Average values for irrigation efficiency 65% (surface irrigation) and 72% (groundwater irrigation), and values for surface runoff ratio are 15% (surface irrigation) and 5% (groundwater) (Gates et al., 2012).

The statistical comparison between the scheduled irrigation SWAT model and automatic irrigation SWAT model for the entire simulation period is quantified through a simple nonparametric bootstrapping method. The bootstrapping method is a statistical method to estimate standard errors by sampling, where the samples are repeatedly replaced (Efron, 1979). In this study, Bootstrapping was used to generate series of E_{ns} goodness of fit (E_{ns} GOF) for the two models. Random samples of size 40 drawn from 80 values in simulated and observed time series were generated. The values of E_{ns} GOF were then computed for each model at Rocky Ford, Timpas Creek, and Las Animas stations. This procedure was repeated 1000 times generating a series of E_{ns} GOFs for each model. A two sample t-test was then used to test the null hypothesis that the two series of E_{ns} GOFs for the two models come from the same distribution. 0.05 significance level was defined by user to compare with the calculated probability (P-value) in order to identify the similarity of the model simulations. Therefore, P-value < 0.05 represents the null hypothesis can be rejected and there is a significant differences between two models.

2.4. RESULTS AND DISCUSSIONS

2.4.1 Influence of Human Management Features

Figure 6 shows a weekly comparison between the measured diversion water and the calculated diversion water (applied irrigation water + canal seepage) for each canal from April 1999 to December 2007. The comparison is excellent for each canal except the Fort Lyon Canal, since approximately 80% of the land irrigated by the canal is downstream of the modeled region. Overall, a good agreement occurs between the two datasets, and therefore we conclude that the canal seepage methodology provides accurate seepage loss rates for the study region.

Results are first shown to elucidate the relative influence of each human management feature in the irrigated watershed. Figure 7 shows the partitioning of annually averaged inflow to the river network for each model type (basic SWAT, including the Fort Lyon diversion, using CF_HRUs, and including canal seepage). The inflow components include surface runoff, lateral flow, and groundwater discharge from both shallow and deep aquifer units. For all versions, most of the water entering the Arkansas River and its tributaries in the study area is from the aquifer, with lateral flow contributing the lowest portion (less than 1%). Substantial changes in water inflow occurs when including scheduled irrigation and CF_HRUs, with the component of surface runoff from all sources increased from 4.5% to 34.8% due to the applied irrigation water and associated tailwater runoff. Adding canal seepage results in approximately the same magnitude of surface runoff entering the stream, but the groundwater return flows are much higher due to the canal seepage entering the shallow aquifer and adding to groundwater flows. Including canal seepage increased the amount of water diverted from the Arkansas River, which decreases water volume in the river.

Observed and simulated streamflow at the Rocky Ford, Las Animas, and Timpas Creek stations are shown in Figure 8 for each version of the model for the period 2001 to 2003. For the basic SWAT model, a comparison between the observed (black point line) and simulated stream monthly flows (blue line with rectangular point) shows that while the model predicts the general trend in the observed data, there are strong inconsistencies of magnitude between the observed and simulated values, with streamflow over-estimated in the Arkansas River (Figure 8A, 8B) and under-estimated in Timpas Creek (Figure 8C).

After adding a point source to divert water out of Arkansas River to the Fort Lyon Canal (see Figure 3D) , the simulation results improved slightly, with lower streamflow in the Arkansas River due to the Las Animas gauge being downstream of the diversion point, and higher streamflow in the tributary.

(1) HRU boundary modification (i.e. creating CF_HRUs) and (2) assigning irrigation water based on diversion records are major driving factors in decreasing streamflow in the Arkansas River and thereby bringing water onto the landscape and subsequently into the tributaries. Compared with the previous results of the basic SWAT model and the version that added the Fort Lyon Diversion, simulated

streamflows (red line) were decreased at both the Rocky Ford and Las Animas stations (Figure 8A, 8B), and increased at the Timpas Creek station. For the latter, the averaged depths of surface runoff and groundwater flow are 13.4 mm and 24.2, respectively. The timing of the peaks at the Timpas Creek station coincides with the irrigation season from mid-March to early November (Figure 8), indicated that including CF_HRUs and scheduled irrigation captures quite well the temporal patterns of irrigation, runoff, and groundwater return flow.

The last modification includes the impact of canal seepage along the length of each of the six canals. The simulated streamflow (green line) shows the same trend as the CF_HRU version, but with values approaching much more closely the observed vales in Timpas Creek (Figure 8C). Peakflows during the irrigation season are much higher than the other model versions, but still the average simulated streamflow at the Timpas Creek station for the four year period was 0.539 m^3/s, compared to 0.933 m^3/s for the observed streamflow. The simulated average flows for the other model versions at Timpas Creek station ranges from 0.057 to 0.150 m^3/s. Average depths of surface runoff and groundwater flow to Timpas Creek were 49.8 mm and 54.7, respectively. Compared with the CF_HRU versions, the model is overestimating the streamflow both at Rocky Ford and Las Animas stations. The increased flow is not only driven by the streamflow in the tributaries, but also the groundwater return flow that comes from the canal seepage of the aquifer system. The Las Animas station is located close to the outlet of the watershed which is influenced by both of these factors whereas the Rocky Ford only affected only by the groundwater return flow. Therefore, the streamflow simulation at Rocky Ford has a better performance than at the downstream Las Animas station.

Overall, the largest impact on streamflow in the Arkansas River occurred in the CF_HRU and canal seepage versions of the model, with the largest impact on streamflow in Timpas Creek occurred in the canal seepage version. Including canal seepage, and its impacts on groundwater flow to nearby drainage tributaries, is essential for simulating hydrologic processes in irrigated systems.

2.4.2 Results using the Scheduled Irrigation Procedure

This section provides results for the calibrated model that includes canal diversions, CF_HRUs, canal seepage, and scheduled irrigation based on historical diversion records. In general, simulated streamflow follows a similar trend to the observed flow, as seen in Figure 9 for the five gauging stations. Complete goodness-of-fit statistics are given in Table 5. Gray shaded areas on each hydrograph plot indicate the irrigation season (mid-March to mid-November).

Due to the proximity to the watershed inlet, the best fit of observed and simulated streamflow during the calibration period occurs at the Rocky Ford gauging station (Figure 9A), with a "Very Good" E_{ns} value of 0.85. Results for Timpas Creek ($E_{ns} = 0.59$, PBIAS = -5.1 % for the calibration period; $E_{ns} = 0.64$, PBIAS = 7.5% for the validation period) indicate that model is able to capture the timing and magnitude of applied irrigation, canal seepage, and return flows to drainage tributaries. For the Las Animas station which located at the outlet of the watershed, PBIAS is "Satisfactory" with the value of -10.5%. Although the calibrated E_{ns} at outlet is slightly less than 0.5, there is marked improvement as compared to the basic SWAT model (Table 5), with the calculated E_{ns} increased from -1.69 to 0.48. This substantial improvement of the modified model can be seen at the at the Rocky Ford, and Timpas Creek stations as well with E_{ns} values increased from 0.66 to 0.85 (Very Good), and -1.48 to 0.59 (satisfactory), respectively. Based on results presented in Section 3.1, this improvement is due in large part to the inclusion of canal seepage using the modified SWAT code. Of particular note is the capability of the model to represent observed streamflow during the low flow years of 2002 and 2003, for both the Arkansas River and the two tributaries. During these years, annual rainfall depth was 99.2 mm and 162 mm, respectively, compared with the average annual precipitation of 289.7 mm. The model performed well for the La Junta and Crooked Arroyo stations (Figure 9D, 9E), which were not included in the calibration process. Compared with the basic SWAT model, the E_{ns} increased from -0.28 to 0.39 and from -0.19 to 0.36 at La Junta and Crooked Arroyo stations, respectively. PBAIS has a marked improvement at these locations as well.

For the entire simulation period, streamflow in the Arkansas River often is over-estimated during the non-irrigation season (white regions in Figure 9). For example, from October 2001 to January 2002 and

from October 2005 to February 2006 (Figure 9A, 9B, 9D). These high peak flows can be explained by unrecorded water use activities along the Arkansas River, or mis-timing of groundwater return flows to the river, which depends on aquifer properties and groundwater hydraulic gradients that cannot be considered by the SWAT model routines. If the non-irrigation season streamflow discharges are not considered, the E_{ns} values increase to 0.93 (calibration) and 0.88 (validation), 0.89 (calibration) and 0.44 (validation), and 0.41 (validation) for the Rocky Ford, Las Animas, and La Junta stations, respectively.

2.4.3 Results using the Automated Irrigation Procedure

Results using SWAT's auto-irrigation algorithm are shown in Table 5 and Figure 10. No additional calibration was performed. In general, the timing, pattern, and magnitude of streamflow discharge closely follow observed values for all stations. This was further confirmed by acceptable values of model performance evaluation statistics. Based on E_{ns} values, simulations were considered very good at Rocky Ford station (0.88), satisfactory at Las Animas (0.58), Timpas Creek (0.64), and unsatisfactory for La Junta station (0.47) and Crooked Arroyo stations (0.37).

In comparison with the schedule irrigation approach (see Section 3.2) using both goodness-of-fit statistics and visual assessment, results indicate that the auto-irrigation approach is adequate, especially in simulating processes that lead to accurate streamflow predictions in the Arkansas River. This is true even for the 2002-2003 low flow periods, indicating that the SWAT routines are able to limit irrigation water based on the supply in the river. Figure 11 shows comparison of monthly streamflow (m^3/sec) for the Rocky Ford, Las Animas, and Timpas Creek stations for the scheduled irrigation and auto-irrigation approaches. The models compare very well.

For both models, streamflow is over-estimated during the winter months and slightly un-estimated the low flows during February and March at the outlet of the watershed (Las Animas station) (Figure 11B). From the goodness-of-fit statistics (Table 5), the model using the auto-irrigation approach performed similarly to the scheduled irrigation approach. For further comparison, Figure 12 shows the scatter plots of the monthly streamflow observations and two model simulation values. From the linear regression line, the slopes from two models are very similar to each other as well, especially at the Rocky Ford station.

34

The interception from the auto-irrigation version at Rocky Ford is 1.216, which is closer to 0. At the Timpas Creek station, the scheduled irrigation version has higher slope and lower intercept value, indicating the model with scheduled irrigation performs better than the model using auto-irrigation in the tributary.

The bootstrapping and two sample t-test on the E_{ns} distributions showed that, at the 0.05 significance level, the t-test rejects the null hypothesis that the mean and variance of the distributions are equal, demonstrating that the difference between the E_{ns} GOFs of the two models is significant at Rocky Ford and Timpas Creek stations (Table 5). P-value at the Las Animas station is greater than 0.05, indicating there is no significant difference between two models. Since the Las Animas station is located at the outlet of the watershed, the effects of auto and scheduled irrigation has been diminished. However, at the smaller scale with higher percentage of irrigated agriculture, the scheduled irrigation model has a significantly better performance compared to the auto-irrigation model. Further analysis can be seen from the boxplots shown in Figure 13. Figure 13 displays the E_{ns} distributions of the scheduled irrigation and auto-irrigation versions obtained from the bootstrapping. Overall, the boxplots show that interquartile ranges of E_{ns} distributions under auto and scheduled irrigation at different locations are very close with slightly better performance of the auto-irrigation at the outlet of the watershed (Las Animas) and Rocky Ford, and better performance of the Scheduled irrigation at Timpas Creek tributary. Considering the suite of tests and illustration methods used, the results showed that the scheduled irrigation model has a significant better performance in the smaller highly agricultural tributaries while the auto-irrigation model had a slightly but not significant better performance at the outlet of the whole watershed.

These comparisons indicate that the scheduled irrigation approach is able to simulate the realistic canal irrigation and allocation processes and to provide more accurate results, especially in the tributary. However, this approach requires gathering a large amount of historical diversion data, and allocating these volumes to each CF_HRU based on water rights and a hierarchy of crop importance. Auto-irrigation algorithms based on water stress and constrained by available water supply perform well for simulating

35

irrigation practices in semi-arid, highly-managed watershed systems, and can be an adequate replacement for scheduled irrigation approached.

2.5. SUMMARY AND CONCUSIONS

In this study, the relative influence of human management features in irrigated watersheds was explored for a study region in the Arkansas River Valley in southeastern Colorado using the SWAT model. Features include canal diversions, representing each cultivated field as a hydrologic response unit with a recorded crop rotation, scheduling irrigation events based on recorded canal diversions and water rights, and canal seepage from earthen irrigation canals that run along the contours of the irrigated valley. The SWAT code was modified to add estimated canal seepage directly to the shallow aquifer along each canal. In an additional version of the model, the scheduled irrigation approach was replaced with the auto-irrigation algorithm of SWAT, which uses plant water stress to trigger irrigation events.

Results indicate that accounting for individual cultivated fields and, more importantly, canal seepage, is necessary to capture the appropriate magnitude of hydrologic processes in the study region and to accurately represent the timing and magnitude of streamflow events in the Arkansas River and its tributaries. The latter, which serve as large agricultural drains for the irrigated areas, have temporal patterns of streamflow that particularly cannot be captured without the modifications to the model. Specific conclusions include:

- Both scheduled irrigation and auto-irrigation approaches are able to capture the impact of low flow, indicating that the SWAT model can be used for water stress scenarios in irrigated regions;

- The scheduled irrigation approach performed significantly better than the auto-irrigation algorithm in the tributary to represent the realistic canal irrigation processes in the semi-arid irrigated systems;

- Auto-irrigation algorithm has slightly but not significant better performance simulating the flow amount and pattern at the outlet of the entire watershed. For those regions lack of

irrigation and allocation data, the auto-irrigation algorithm is an adequate replacement to represent hydrologic flow patterns in semi-arid irrigated systems;

- Of all the features of human management in irrigated watersheds, the inclusion of canal seepage is the most important to represent streamflow in tributaries;

- Neither irrigation approach was able to capture the correct streamflow patterns in the winter (non-irrigation) months, indicating that the groundwater flow algorithms in the SWAT model likely are not adequate to simulate groundwater flow in a heterogeneous aquifer system.

This latter limitation will be explored and improved upon in future studies, perhaps using the coupled SWAT-MODFLOW modeling code (Bailey et al., 2016) that can represent transient groundwater flow processes in heterogeneous aquifer systems.
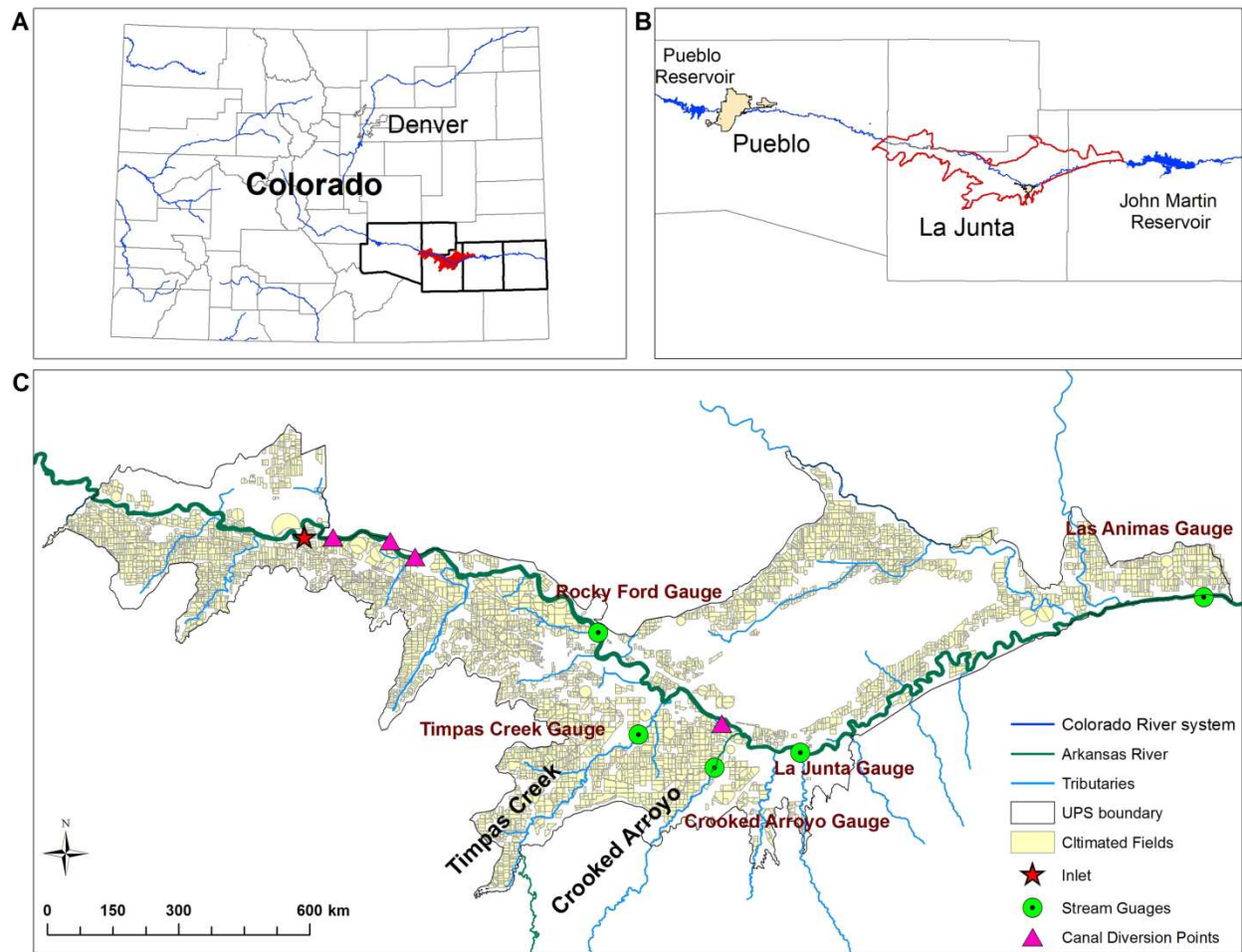
Figure 2. Location of the study region in the Lower Arkansas River Valley, showing the cultivated fields, inlet stream gauge location, outlet stream gauge locations, and canal diversion points.
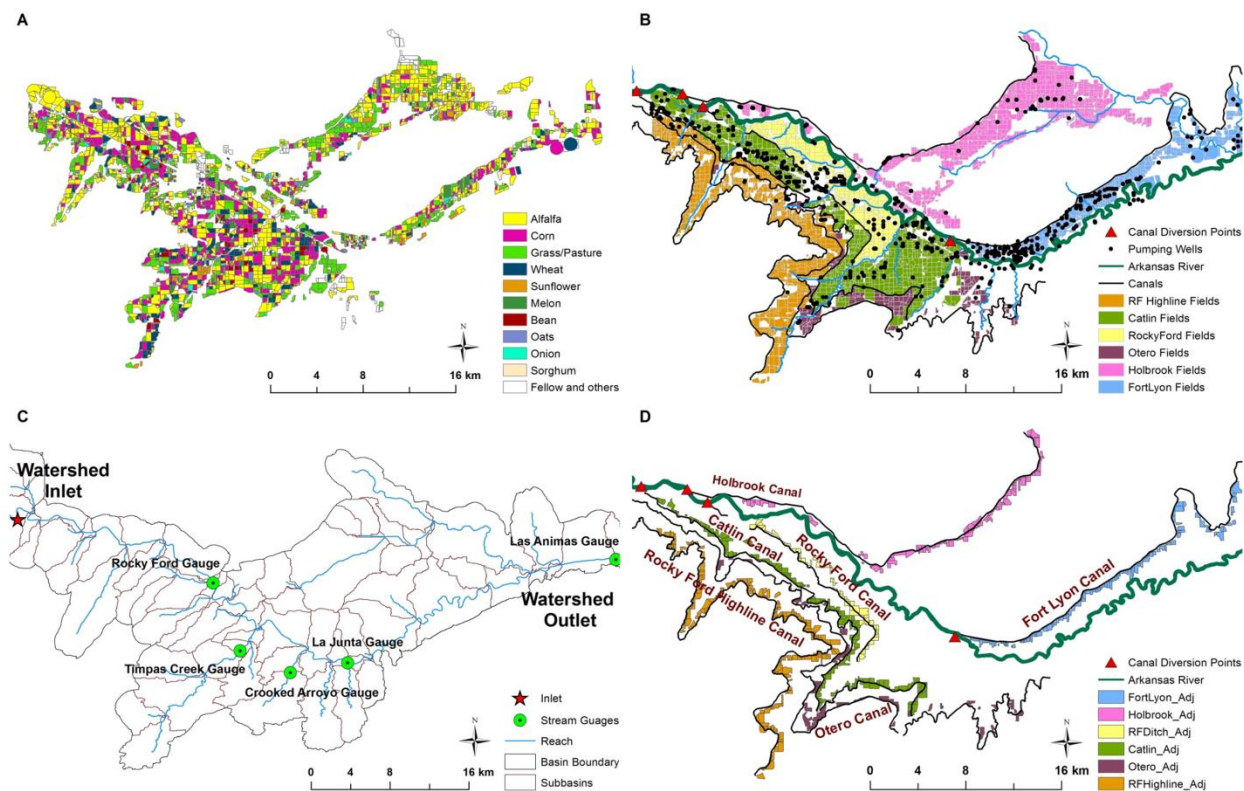
Figure 3. A. Crop type for each cultivated field for the year 2001; B. The division of the study region into irrigation canal command areas, with fields receiving irrigation water from the corresponding canal. Also shown is the location of groundwater pumping wells; C. Sub-basins generated by the SWAT model. Also shown is the inlet and outlet gauging stations. D. The canal adjacent HRUs, with each HRU receiving seepage water from the Highline, Otero, Catlin, Rocky Ford, Holbrook, and Fort Lyon canals.
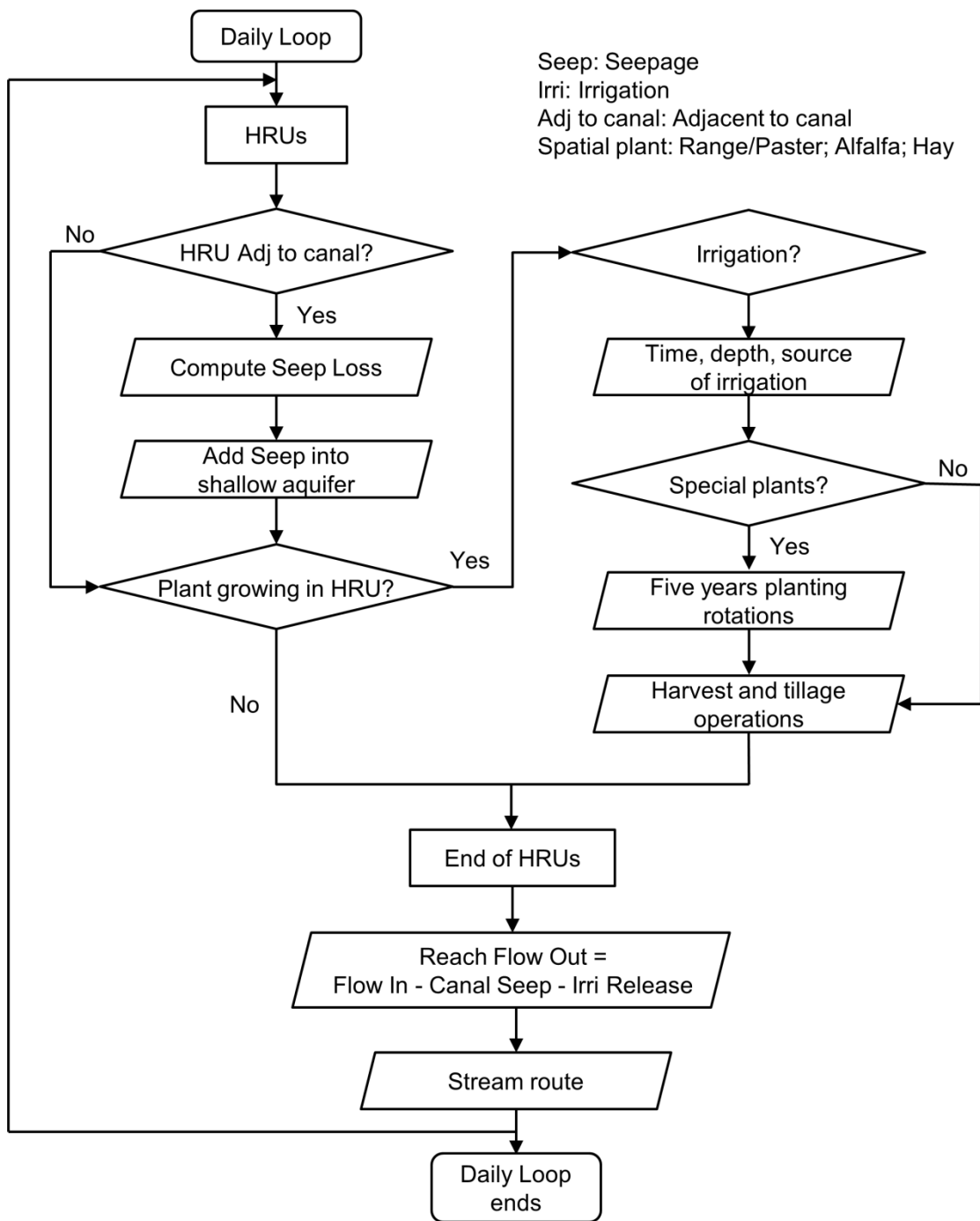
Figure 4. Diagram showing the flow of information in the SWAT modeling code. The calculated seepage loss is added into shallow aquifer through the canal adjacent HRU calculations.

A Basic SWAT HRUs

B Cultivated Field HRUs

Legend

⬜ Cultivated Field	🟥 CF_HRU #1	🟧 CF_HRU #25
🟦 HRU #1	🟦 CF_HRU #2 ...	🟪 CF_HRU #26
🟪 HRU #2	🟦 CF_HRU #3	🟫 CF_HRU #27
🟨 HRU #3	🟨 CF_HRU #4	🟩 CF_HRU #28

0   0.25   0.5   1 km
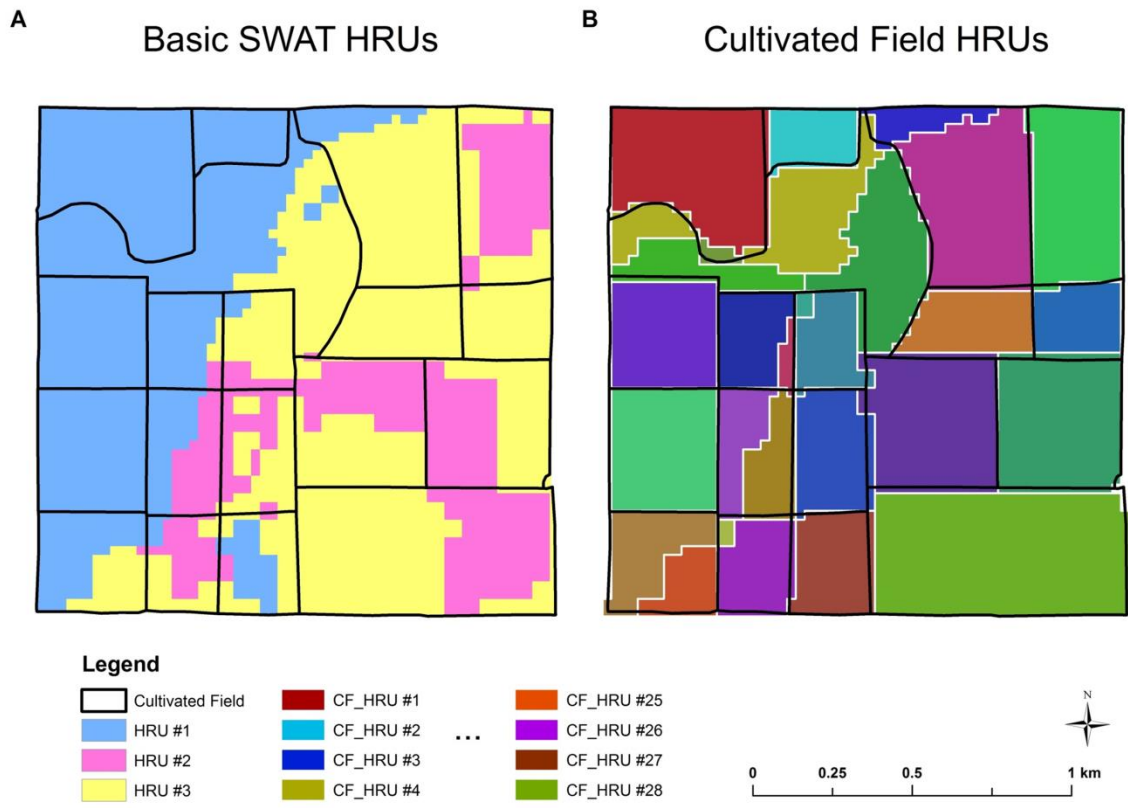
Figure 5. Schematic demonstrating the spatial interaction from the original HRUs and modified HRUs to cultivated field boundaries
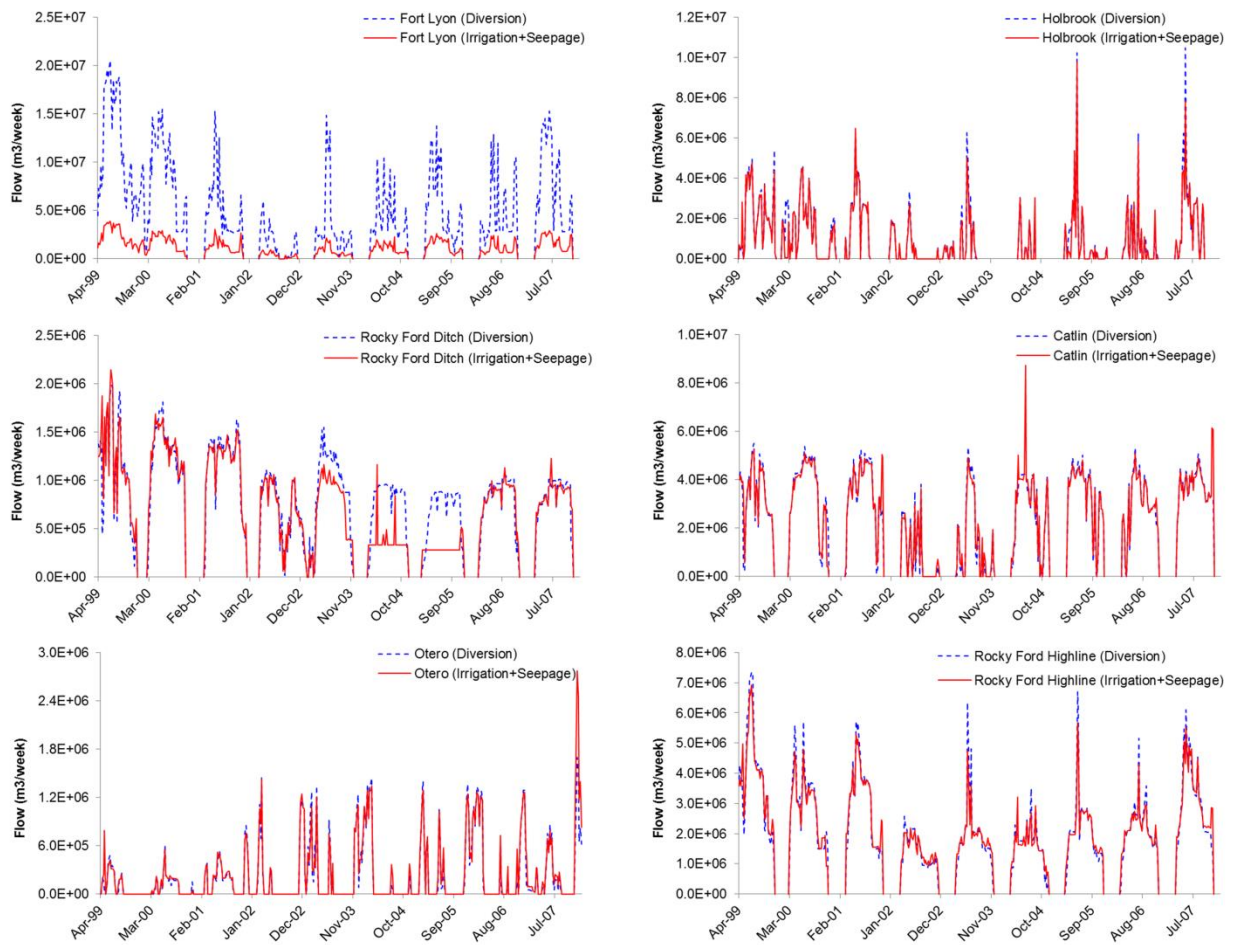
Figure 6. Comparison between the weekly recorded diversion and the calculated diversion values for each of the six canals.
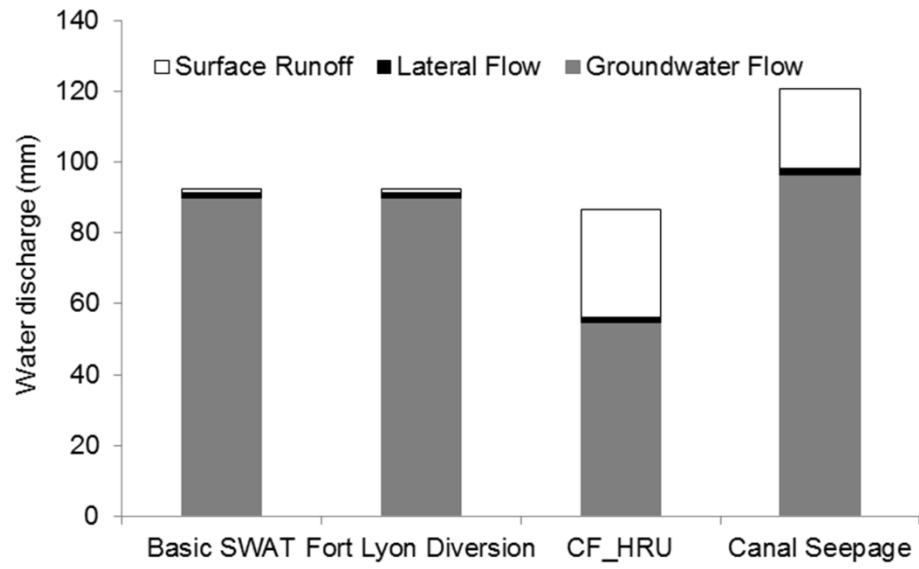
Figure 7. Annually averaged contribution from each human management feature of different pathways to the total surface water flow.
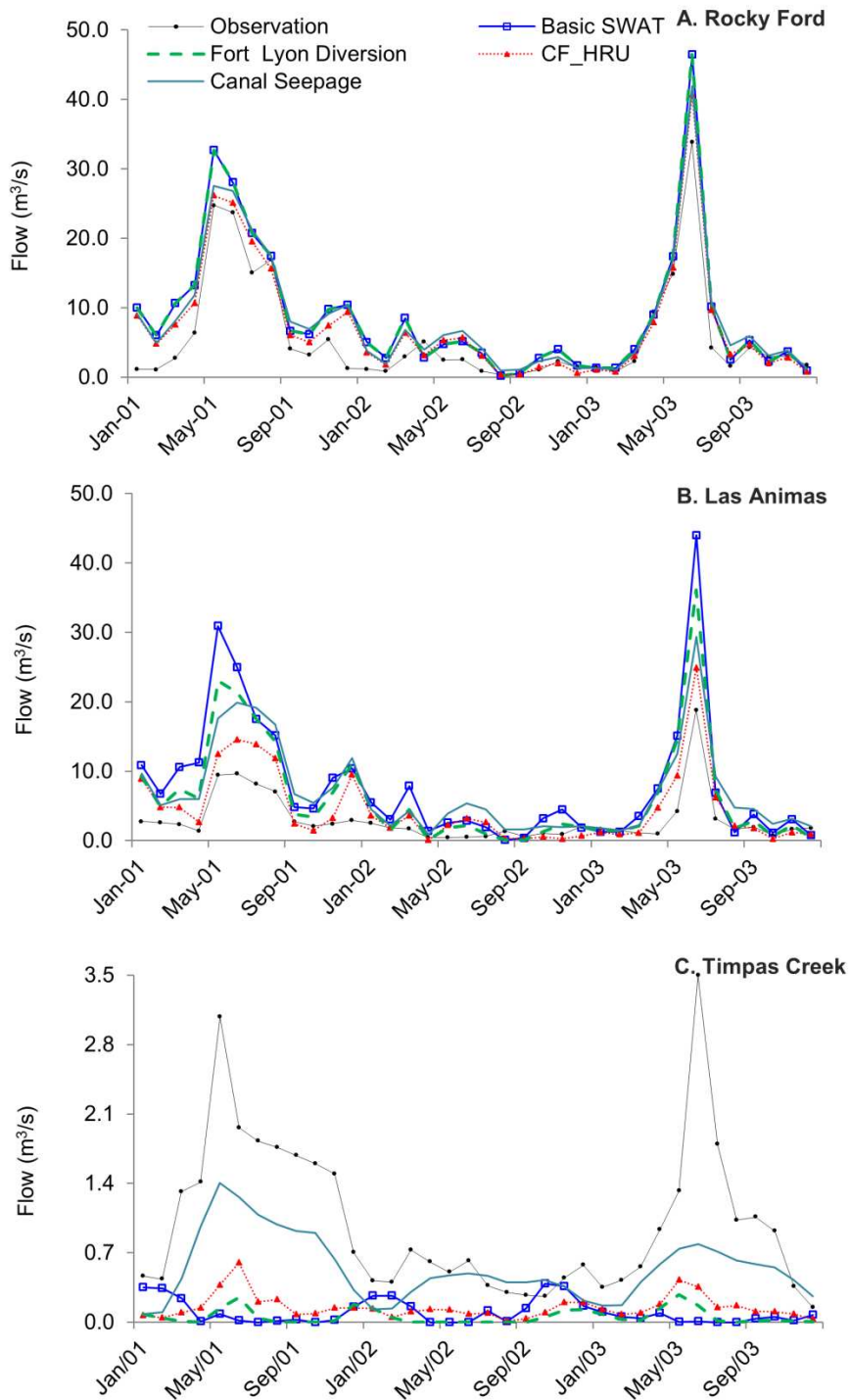
Figure 8. Comparison of simulated and observed monthly streamflow along the Arkansas River (Rocky Ford station, Las Animas station) and Timpas Creek for the basic SWAT model and subsequent model versions that include canal diversion at the Fort Lyon Canal, CF_HRUs, and canal seepage, respectively.
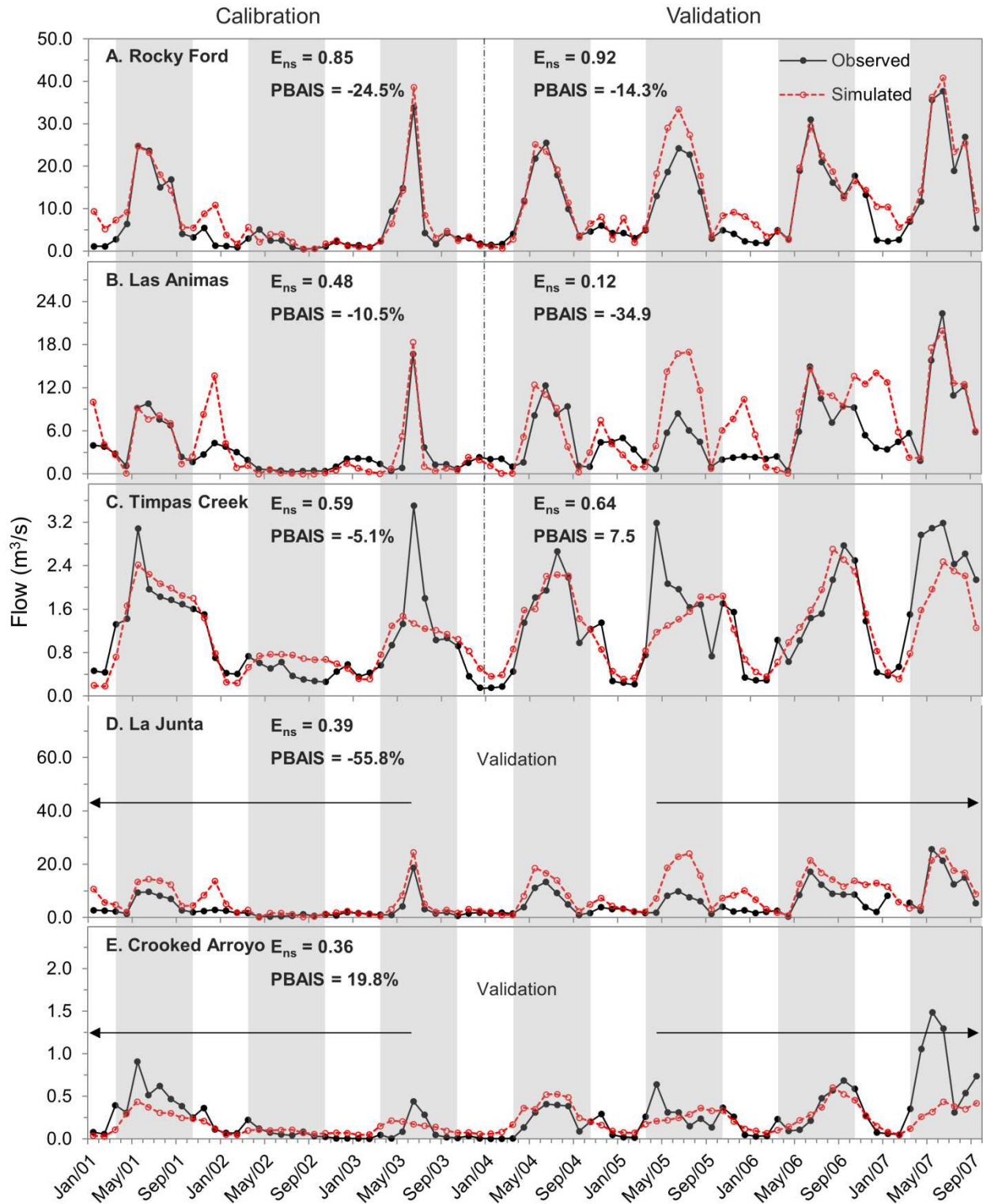
Figure 9. Monthly observed and simulated streamflow for gauging stations during the calibration and validation period for the modified SWAT model that uses CF_HRUs, canal seepage, and scheduled irrigation.
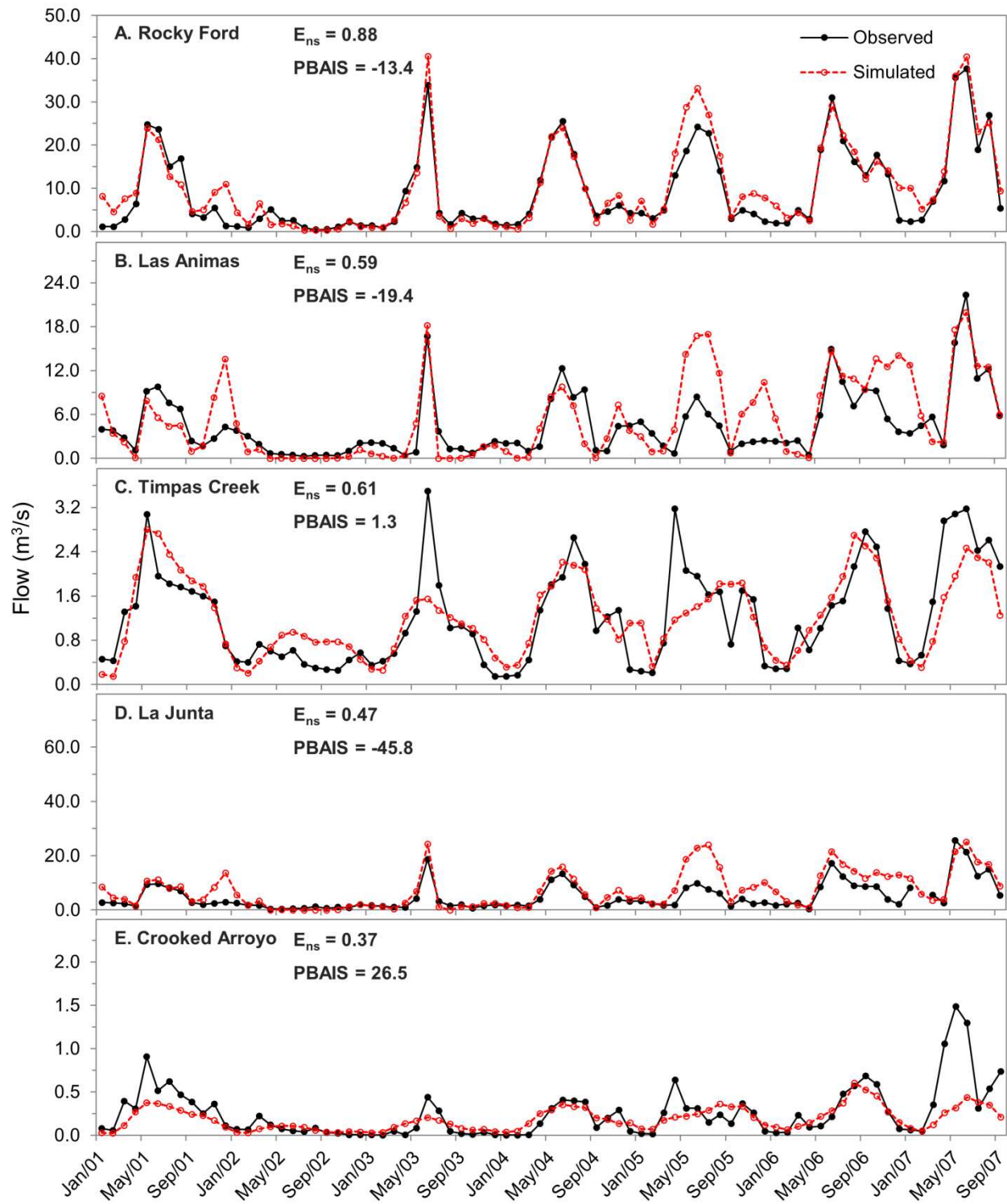
Figure 10. Monthly observed and simulated hydrographs for selected gauging stations for Auto-SWAT model.
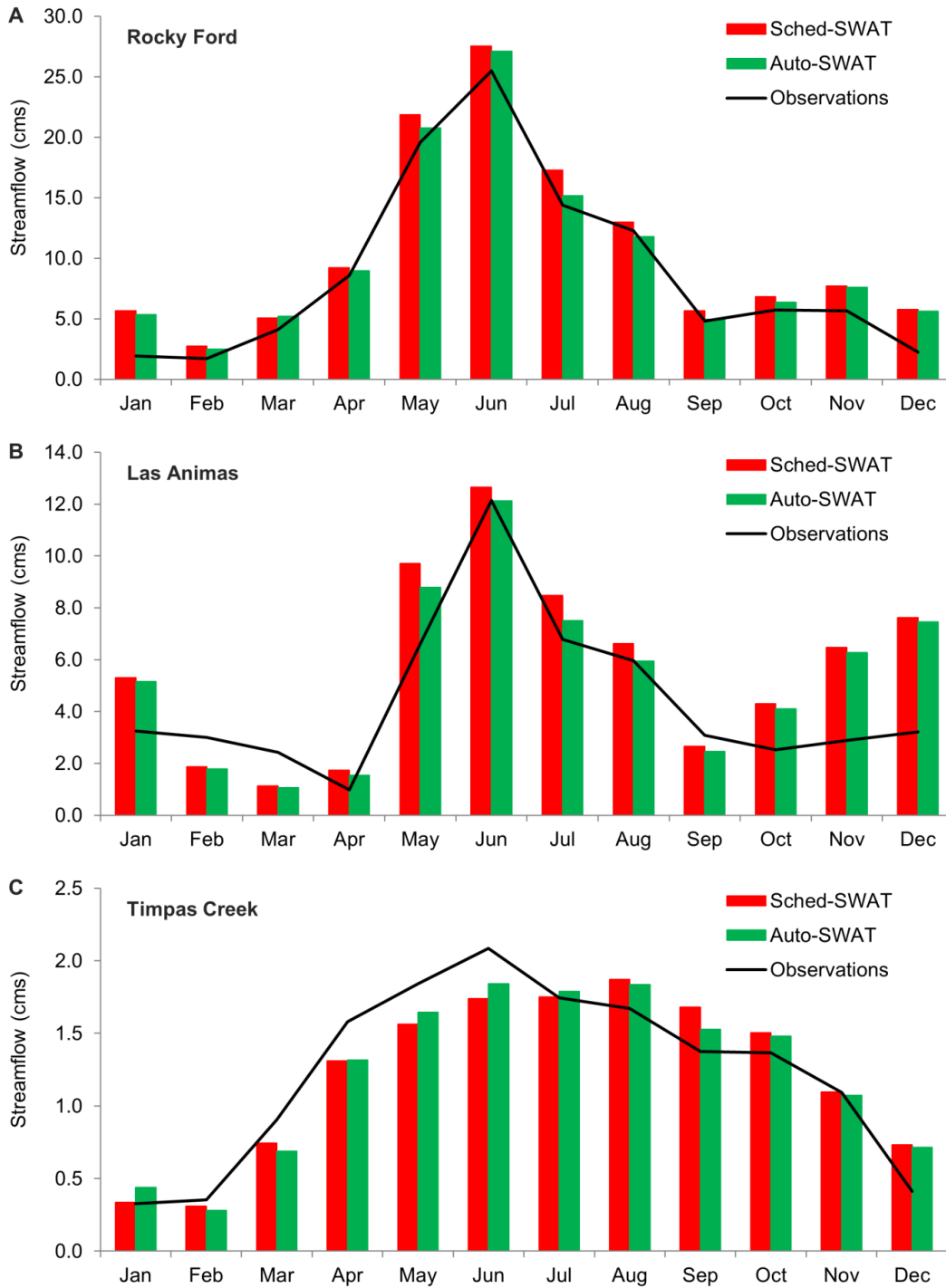
Figure 11. Comparison of monthly discharge between observed data, simulated with Sched-SWAT model, and with Auto-SWTA model.
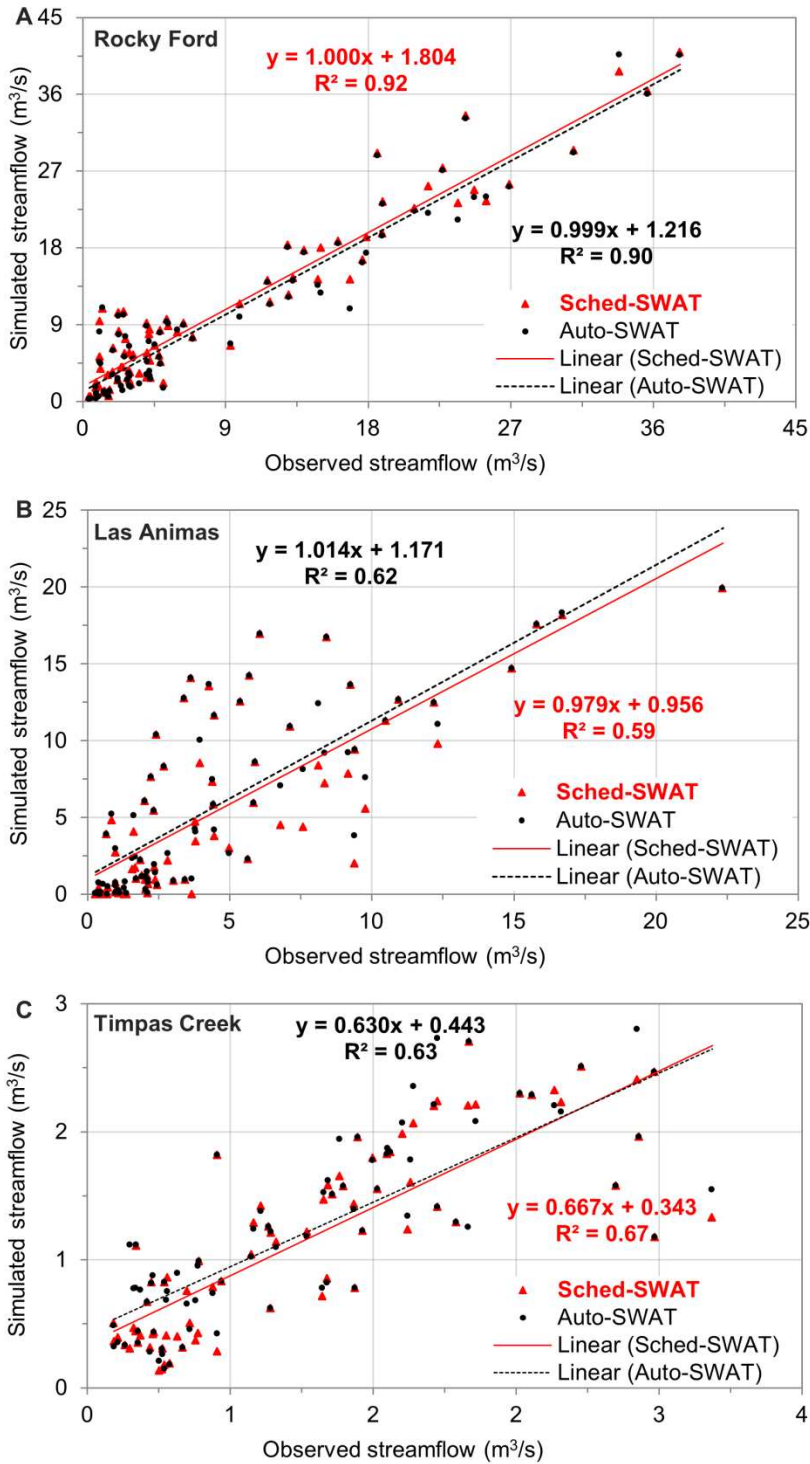
Figure 12. Scatter plots of monthly streamflow at three gauging stations for Sched-SWAT model and Auto-SWAT model.
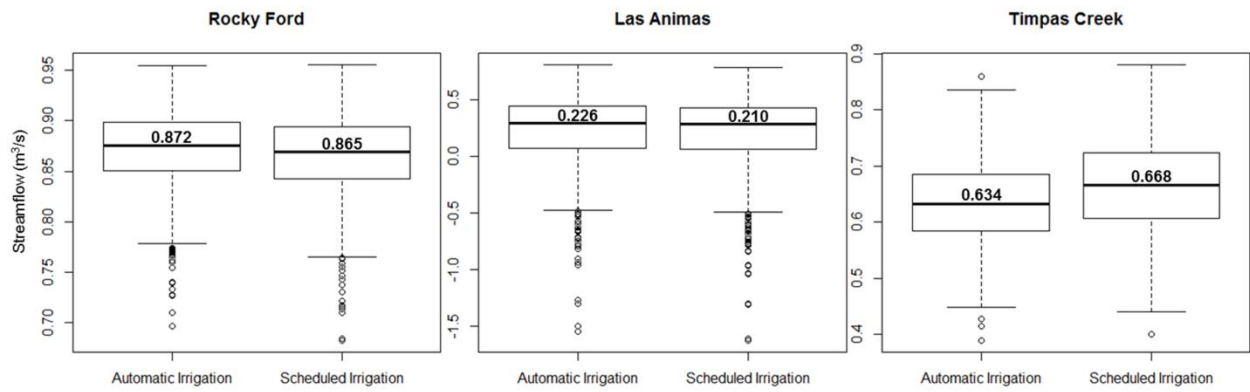
Figure 13. Boxplot of model Nash-Sutcliff coefficient (Ens) distributions of the scheduled irrigation and auto-irrigation version at Rocky Ford, Las Animas, and Timpas Creek stations, at the 0.05 significance level.

Table 1. Input datasets for the SWAT model

Date type	Data sources	Scale	Data description
DEM	The National Map System, US Geological Survey (USGS-DEM, 2010)	30 m	Elevation
Digitized Stream network	National Hydrography Dataset, US Geological Survey (NHD, 2010)	30 m	Stream network
Soil type map	US Digital General Soil Map (STATSGO) from National Resources Conservation Service (NRCS, 2012)	1/250,000	Soil physical and chemistry properties
land-use map	National Agricultural Statistics Service (NASS, 2009)	30m	Land cover map with classes of cultivated fields, water, urban, herbaceuous, shrub, and barren land
Climate	Colorado Agricultural Meteorological Network (CoAgMet, 2016)	1999-2007	Daily precipitation, max., min., temperature, wind speed, relative humidity and solor radiation
Streamflow	Colorado Diversion of Water Resources (CDWR, 2010)	1999-2007	Daily observed streamflow
Canal Diversion	Colorado's Decision Support Systems (CDSS, 2010)	1999-2007	Daily surface water diversion

Table 2. Agricultural management in the Arkansas River Valley in southeastern Colorado

Crop Type	Planting Day	Harvest Day	Plow Day
Alfalfa	30-Apr	30-Sep	20-Oct
Bean	20-May	30-Sep	20-Oct
Corn	1-May	25-Oct	14-Nov
Melon	15-May	10-Aug	30-Aug
Onion	20-Mar	15-Sep	5-Oct
Pasture	30-Aug	30-Sep	20-Oct
Pumpkin	1-Jun	30-Sep	20-Oct
Sorghum	20-May	15-Oct	4-Nov
Spring Grain	1-Apr	15-Jul	4-Aug
Squash	20-May	25-Jul	14-Aug
Sunflower	1-Jun	10-Oct	30-Oct
Vegetable	25-Apr	30-Aug	19-Sep
Winter Wheat	30-Sep	5-Jul	25-Jul

Table 3. Canal seepage estimates for the six irrigation canals in the study region. Seepage rates are provided as m^3/day-km and m^3/day.

	Fort Lyon	Holbrook	Rocky Ford	Catlin	Otero	RF Highline
Length km	37.7	38.6	20.4	50.8	94.1	102.3
Seepage rate (m^3/s-km)	0.040	0.012	0.040	0.040	0.012	0.028
Seepage (m^3/day)	1.3×10^5	4.0×10^4	7.1×10^4	1.8×10^5	9.8×10^4	2.4×10^5

Table 4. List of parameters and their ranking from the sensitivity analysis

Parameter	Definition	Range of values		
		Minimum	Maximum	Sensitivity
Parameters governing surface water response				
CN2	SCS runoff curve number for moisture condition II	-25%[a]	+25%[a]	High
ESCO	Soil evaporation sompensation factor	0.01	1	Medium
OV_N	Manning's *n* value for overland flow	0.01	30	Low
CH_N2	Manning's *n* value for the main Channel	0.01	0.07	High
CH_K2	Effective hydraulic conductivity of channel (mm/hr)	0.025	150	High
SURLAG	Surface runoff lag coefficient (days)	1	12	Low
Parameters governing subsurface water response				
SHALLST	Initial depth of water in the shallow aquifer (mm)	0	5000	High
GW_DELAY	Delay time for aquifer recharge (days)	0.001	100	High
GWQMN	Threshold depth of water level in shallow aquifered for return base flow to occur (mm)	0.01	100	Medium
ALPHA_BF	Base flow recession constant (days)	0.005	1	Low
GW_REVAP	Groundwater *revap* coefficient	0.02	0.2	Medium
REVAPMN	Threshold depth of water level in shallow aquifered for 'revap' to occor (mm)	0	1000	Low
RCHRG_DP	Deep aquifer percolation fraction	0.01	0.75	High
Parameters governing soil properties				
SOL_AWC	Available water capacity	-50%[a]	+50%[a]	Medium
SOL_K	Saturated hydraulic conductivity	0	150	Medium
Parameters governing snow response				
TIMP	Snow pack temperature lag factor	0.5	1	Low
SFTMP	Snowfall temperature (°C)	-2	20	High
SMTMP	Snow melt base temperature (°C)	-10	5	Low
SMFMX	Melt factor for snow on June 21 (mm/°C-day)	1.4	6.9	Low
SMFMN	Melt factor for snow on December 21 (mm/°C-day)	1.4	6.9	Low

Table 5. Nash Sutcliffe (E_{NS}), Percent Bias (PBIAS), and coefficient of determination (R^2) of simulated streamflow at the five gauging stations in the study region

Gauging Stations	Index	Basic SWAT model		Sched-SWAT model		Auto-SWAT model
		Calibration	Validation	Calibration	Validation	2001-2007
Rocky Ford	E_{ns}	0.66	0.53	0.85	0.92	0.88
	PBIAS	-53.1%	-45.4%	-24.5%	-14.3%	-13.4%
	R^2	0.91	0.92	0.89	0.90	0.92
Las Animas	E_{ns}	-1.69	-5.18	0.48	0.12	0.58
	PBIAS	-60.4%	-94.7%	-10.5%	-34.9%	-19.4%
	R^2	0.81	0.58	0.70	0.62	0.59
Timpas Creek	E_{ns}	-1.48	-1.49	0.59	0.64	0.64
	PBIAS	89.8%	77.2%	-5.1%	7.5%	1.3%
	R^2	0.17	0.03	0.60	0.67	0.65
La Junta	E_{ns}		-0.28		0.02	0.03
	PBIAS		-96.5%		-23.5%	13.3%
	R^2		0.10		0.07	0.07
Crooked Arroyo	E_{ns}		-0.19		0.36	0.37
	PBIAS		59.4%		19.8%	26.5%
	R^2		0.09		0.41	0.48

REFERENCES

Abbaspour, K. C., Yang, J., Reichert, P., Vejdani, M., Haghighat, S., and Srinivasan, R. (2008). *SWAT-CUP. SWAT calibration and uncertainty programs,* Swiss Federal Institute of Aquatic Science and Technology (EAWAG), Zurich, Switzerland.

Ahmadzadeh, H., Morid, S., Delavar, M., and Srinivasan, R. (2016). "Using the SWAT model to assess the impacts of changing irrigation from surface to pressurized systems on water productivity and water saving in the Zarrineh Rud catchment". *Agricultural Water Management*, *175*, 15-28.

Alarcón-Herrera, M. T., Bundschuh, J., Nath, B., Nicolli, H. B., Gutierrez, M., Reyes-Gomez, V. M., Nunez, D., Martín-Dominguez, I.R. and Sracek, O. (2013). "Co-occurrence of arsenic and fluoride in groundwater of semi-arid regions in Latin America: Genesis, mobility and remediation". *Journal of hazardous materials*, *262*, 960-969.

Arnold, J. G., Srinivasan, R., Muttiah, R. S., and Williams, J. R. (1998). "Large area hydrologic modeling and assessment part I: model development". *JAWRA Journal of the American Water Resources Association*, *34*(1), 73-89.

Arnold, J.G., Moriasi, D.N., Gassman, P.W., Abbaspour, K.C., White, M.J., Srinivasan, R., Santhi, C., Harmel, R.D., Van Griensven, A., Van Liew, M.W. and Kannan, N. (2012). "SWAT: Model use, calibration, and validation". *Transactions of the ASABE*, *55*(4), 1491-1508.

ASCE Watershed Management Committee. Irrigation, and Drainage Division (ASCE). 1993. "Criteria for evaluation of watershed models". *Journal of Irrigation and Drainage Engineering*, *119*, 429-442.

Bailey, R. T., Gates, T. K., and Ahmadi, M. (2014). "Simulating reactive transport of selenium coupled with nitrogen in a regional-scale irrigated groundwater system". *Journal of hydrology*, *515*, 29-46.

Bailey, R. T., Wible, T. C., Arabi, M., Records, R. M., and Ditty, J. (2016). "Assessing regional-scale spatio-temporal patterns of groundwater–surface water interactions using a coupled SWAT-MODFLOW model". *Hydrological Processes*, *30*(23), 4420-4433.

Behera, S., and Panda, R. K. (2006). "Evaluation of management alternatives for an agricultural watershed in a sub-humid subtropical region using a physical process based model". *Agriculture, ecosystems & environment*, *113*(1), 62-72.

Beven, K. (1997). "TOPMODEL: a critique". *Hydrological processes*, *11*(9), 1069-1085.

Bicknell, B. R., Imhoff J. C., Kittle Jr, J. L., Donigian Jr, A. S., and R. C. Johanson, R. C., 1993. *Hydrologic Simulation Program - FORTRAN (HSPF): User's Manual for Release 10* . Report No. EPA/600/R-93/174. Athens, Ga.: U.S. EPA Environmental Research Lab.

Bingner, R. L., Theurer, F. D., and Yuan, Y. (2003). *AnnAGNPS technical processes*. USDA-ARS. National Sedimentation Laboratory.

Borah, D. K., and Bera, M. (2003). "Watershed-scale hydrologic and nonpoint-source pollution models: Review of mathematical bases". *Transactions of the ASAE*, *46*(6), 1553.

Bosch, D. D., Sheridan, J. M., Batten, H. L., and Arnold, J. G. (2004). "Evaluation of the SWAT model on a coastal plain agricultural watershed". *Transactions of the ASAE*, *47*(5), 1493.

Bouraoui, F., Benabdallah, S., Jrad, A., and Bidoglio, G. (2005). "Application of the SWAT model on the Medjerda river basin (Tunisia)". *Physics and Chemistry of the Earth, Parts A/B/C*, *30*(8), 497-507.

CDSS. (2010). *Colorado's Decision Support Systems*. http://cdss.state.co.us/Pages/CDSSHome.aspx (accessed Sep. 2016).

CDWR. (2011). *Colorado Diversion of Water Resources*. http://www.dwr.state.co.us/SurfaceWater/Default.aspx (accessed Sep. 2016).

CoAgMet. (2016). *Colorado Agricultural Meteorological Network*. http://www.coagmet.com/ (accessed May. 2017).

Dechmi, F., Burguete, J., and Skhiri, A. (2012). "SWAT application in intensive irrigation systems: model modification, calibration and validation". *Journal of Hydrology*, *470*, 227-238.

Dechmi, F., and Skhiri, A. (2013). "Evaluation of best management practices under intensive irrigation using SWAT model". *Agricultural water management*, *123*, 55-64.

DHI. (1999*). MIKE SHE water movement: user manual*. Danish Hydraulic Institute, Hørsholm Denmark.

Efron, B. (1979). Computers and the theory of statistics: thinking the unthinkable. *SIAM review*, *21*(4), 460-480.

Garg, K. K., Bharati, L., Gaur, A., George, B., Acharya, S., Jella, K., and Narasimhan, B. (2012). "Spatial mapping of agricultural water productivity using the SWAT model in Upper Bhima Catchment, India". *Irrigation and Drainage*, *61*(1), 60-79.

Gassman, P. W., Reyes, M. R., Green, C. H., and Arnold, J. G. (2007). "The soil and water assessment tool: historical development, applications, and future research directions". *Transactions of the ASABE*, *50*(4), 1211-1250.

Gates, T. K., Garcia, L., and Labadie, J. W. (2006). *Toward optimal water management in Colorado's Lower Arkansas River Valley: monitoring and modeling to enhance agriculture and environment.* Completion report (Colorado Water Resources Research Institute), no. 205.

Gates, T. K., Cody, B. M., Donnelly, J. P., Herting, A. W., Bailey, R. T., and Mueller Price, J. (2009). "Assessing selenium contamination in the irrigated stream–aquifer system of the Arkansas River, Colorado". *Journal of environmental quality*, *38*(6), 2344-2356.

Gates, T. K., Garcia, L. A., Hemphill, R. A., Morway, E. D., and Elhaddad, A. (2012). *Irrigation practices, water consumption, and return flows in Colorado's lower Arkansas River Valley: field and model investigations.* Technical report (Colorado Agricultural Experiment Station), TR12-10.

Ghaffari, G., Keesstra, S., Ghodousi, J., and Ahmadi, H. (2010). "SWAT-simulated hydrological impact of land-use change in the Zanjanrood basin, Northwest Iran". *Hydrological processes*, *24*(7), 892-903.

Gosain, A. K., Rao, S., Srinivasan, R., and Reddy, N. G. (2005). "Return-flow assessment for irrigation command in the Palleru River basin using SWAT model". *Hydrological processes*, *19*(3), 673-682.

Green, C. H., and Van Griensven, A. (2008). "Autocalibration in hydrologic modeling: Using SWAT2005 in small-scale watersheds". *Environmental Modelling & Software*, *23*(4), 422-434.

Gupta, H. V., Sorooshian, S., and Yapo, P. O. (1999). "Status of automatic calibration for hydrologic models: Comparison with multilevel expert calibration". *Journal of Hydrologic Engineering*, *4*(2), 135-143.

Herczeg, A. L., Dogramaci, S. S., and Leaney, F. W. J. (2001). "Origin of dissolved salts in a large, semi-arid groundwater system: Murray Basin, Australia". *Marine and Freshwater Research*, *52*(1), 41-52.

Jang, S. S., Ahn, S. R.,and Kim, S. J. (2017). "Evaluation of executable best management practices in Haean highland agricultural catchment of South Korea using SWAT". *Agricultural Water Management*, *180*, 224-234.

Jolly, I. D., McEwan, K. L., & Holland, K. L. (2008). "A review of groundwater–surface water interactions in arid/semi-arid wetlands and the consequences of salinity for wetland ecology". *Ecohydrology*, *1*(1), 43-58.

Kannan, N., Jeong, J., and Srinivasan, R. (2010). "Hydrologic modeling of a canal-irrigated agricultural watershed with irrigation best management practices: Case study". *Journal of Hydrologic Engineering*, *16*(9), 746-757.

Kollet, S. J., and Maxwell, R. M. (2006). "Integrated surface–groundwater flow modeling: A free-surface overland flow boundary condition in a parallel groundwater flow model". *Advances in Water Resources*, *29*(7), 945-958.

Ley, T. W., Straw, D. E., and Hill, R. W. (2009). *ASCE standardized Penman-Monteith alfalfa reference ET and crop ET estimates for Arkansas River compact compliance in Colorado.* In World Environmental and Water Resources Congress 2009: Great Rivers, pp. 1-14.

Liang, X., Lettenmaier, D. P., Wood, E. F., and Burges, S. J. (1994). "A simple hydrologically based model of land surface water and energy fluxes for general circulation models". *Journal of Geophysical Research: Atmospheres*, *99*(D7), 14415-14428.

Liang, X., Wood, E. F., and Lettenmaier, D. P. (1996). "Surface soil moisture parameterization of the VIC-2L model: Evaluation and modification". *Global and Planetary Change*, *13*(1-4), 195-206.

Luo, Y., He, C., Sophocleous, M., Yin, Z., Hongrui, R., and Ouyang, Z. (2008). "Assessment of crop growth and soil water modules in SWAT2000 using extensive field experiment data in an irrigation district of the Yellow River Basin". *Journal of Hydrology*, *352*(1), 139-156.

Jang, S. S., Ahn, S. R., and Kim, S. J. (2017). "Evaluation of executable best management practices in Haean highland agricultural catchment of South Korea using SWAT". *Agricultural Water Management*, *180*, 224-234.

Martin, C. A., and Gates, T. K. (2014). "Uncertainty of canal seepage losses estimated using flowing water balance with acoustic Doppler devices". *Journal of hydrology*, *517*, 746-761.

Molina-Navarro, E., Hallack-Alegría, M., Martínez-Pérez, S., Ramírez-Hernández, J., Mungaray-Moctezuma, A., Sastre-Merlín, A. (2016). "Hydrological modeling and climate change impacts in an agricultural semiarid region. Case study: Guadalupe River basin, Mexico". *Agricultural Water Management*, *175*, 29-42.

Moore, J. E., and Wood, L. A. (1967). "Data Requirements and Preliminary Results of an Analog-Model Evaluation—Arkansas River Valley in Eastern Colorado". *Groundwater*, *5*(1), 20-23.

Moriasi, D.N., Arnold, J.G., Van Liew, M.W., Bingner, R.L., Harmel, R.D. and Veith, T.L. (2007). "Model evaluation guidelines for systematic quantification of accuracy in watershed simulations". *Transactions of the ASABE*, *50*(3), 885-900.

Moriasi, D. N., Gitau, M. W., Pai, N., and Daggupati, P. (2015). "Hydrologic and water quality models: Performance measures and evaluation criteria". *Transactions of the ASABE*, *58*(6), 1763-1785.

Morway, E.D. and Gates, T.K., 2012. "Regional assessment of soil water salinity across an intensively irrigated river valley". *Journal of Irrigation and Drainage Engineering*, *138*(5),393-405.

Morway, E. D., Gates, T. K., and Niswonger, R. G. (2013). "Appraising options to reduce shallow groundwater tables and enhance flow conditions over regional scales in an irrigated alluvial aquifer system". *Journal of hydrology*, *495*, 216-237.

Muleta, M. K., and Nicklow, J. W. (2005). "Sensitivity and uncertainty analysis coupled with automatic calibration for a distributed watershed model". *Journal of Hydrology*, *306*(1), 127-145.

Nash, J. E., and Sutcliffe, J. V. (1970). "River flow forecasting through conceptual models part I—A discussion of principles". *Journal of hydrology*, *10*(3), 282-290.

NASS. (2009). *National Agricultural Statistics Service*. https://nassgeodata.gmu.edu/CropScape/ (accessed Jan. 2017).

Neitsch, S. L., Arnold, J. G., Kiniry, J. R., Williams, J. R., and King, K. W. (2005). *Soil and water assessment tool theoretical documentation. Grassland.* Soil and Water Research Laboratory, Temple, TX.

Neitsch, S. L., Arnold, J. G., Kiniry, J. R., and Williams, J. R. (2011). *Soil and water assessment tool theoretical documentation version 2009*. Texas Water Resources Institute.

NHD. 2012. *National Hydrography Dataset, U.S. Geological Survey.* https://nhd.usgs.gov/ (accessed Jan. 2017).

Niemann, J. D., Lehman, B. M., Gates, T. K., Hallberg, N. U.,and Elhaddad, A. (2011). "Impact of shallow groundwater on evapotranspiration losses from uncultivated land in an irrigated river valley". *Journal of irrigation and drainage engineering*, *137*(8), 501-512.

NRCS. (2012). *National Resources Conservation Service, United States Department of Agriculture*. https://datagateway.nrcs.usda.gov/ (accessed Jan. 2017).

Ogden, F. L., Julien, P. Y., Singh, V. P., and Frevert, D. (2002). "CASC2D: A two-dimensional, physically-based, Hortonian hydrologic model". *Mathematical models of small watershed hydrology and applications*, 69-112.

Parajuli, P. B., Nelson, N. O., Frees, L. D., and Mankin, K. R. (2009). "Comparison of AnnAGNPS and SWAT model simulation results in USDA-CEAP agricultural watersheds in south-central Kansas". *Hydrological Processes*, *23*(5), 748-763.

Person, M., and Konikow, L. F. (1986). "Recalibration and predictive reliability of a solute-transport model of an irrigated stream-aquifer system". *Journal of Hydrology*, *87*(1-2), 145-165.

Santhi, C., Arnold, J. G., Williams, J. R., Dugas, W. A., Srinivasan, R., and Hauck, L. M. (2001). "Validation of the swat model on a large rwer basin with point and nonpoint sources". *JAWRA Journal of the American Water Resources Association*, *37*(5), 1169-1188.

Santhi, C., Muttiah, R. S., Arnold, J. G., and Srinivasan, R. (2005). "A GIS-based regional planning tool for irrigation demand assessment and savings using SWAT". *Transactions of the ASAE*, *48*(1), 137-147.

Santhi, C., Srinivasan, R., Arnold, J. G., and Williams, J. R. (2006). "A modeling approach to evaluate the impacts of water quality management plans implemented in a watershed in Texas". *Environmental Modelling & Software*, *21*(8), 1141-1157.

Servat, E., and Dezetter, A. (1991). "Selection of calibration objective fonctions in the context of rainfall-ronoff modelling in a Sudanese savannah area". *Hydrological Sciences Journal*, *36*(4), 307-330.

Susfalk, R., Sada, D., Martin, C., Young, M. H., Gates, T., Rosamond, C., Mihevc, T., Arrowood, T., Shanafield, M., Epstein, B. and Fitzgerald, B. (2008). *Evaluation of linear anionic polyacrylamide (LA-PAM) application to water delivery canals for seepage reduction*. Desert Research Institute.

Swamee, P. K., Mishra, G. C., and Chahar, B. R. (2000). "Design of minimum seepage loss canal sections". *Journal of irrigation and drainage engineering*, *126*(1), 28-32.

SWET. (2006). *Watershed Assessment Model Documentation and User's Manual*. Gainesville, Fla.: Soil and Water Engineering Technology.

Thanapakpawin, P., Richey, J., Thomas, D., Rodda, S., Campbell, B., and Logsdon, M. (2007). "Effects of landuse change on the hydrologic regime of the Mae Chaem river basin, NW Thailand". *Journal of Hydrology*, *334*(1), 215-230.

USGS-DEM. (2010). *The National Map System, US Geological Survey*. https://viewer.nationalmap.gov/advanced-viewer/ (accessed Jan. 2017).

Van Liew, M. W., Veith, T. L., Bosch, D. D., and Arnold, J. G. (2007). "Suitability of SWAT for the conservation effects assessment project: Comparison on USDA agricultural research service watersheds". *Journal of Hydrologic Engineering*, *12*(2), 173-189.

Wang, W. Y., Luo, W., and Wang, Z. R. (2005). "Surge flow irrigation with sediment-laden water in northwestern China". *Agricultural water management*, *75*(1), 1-9.

Winchell, M., Srinivasan, R., Di Luzio, M., and Arnold, J. (2013). *ArcSWAT interface for SWAT2012*. Texas Agrilife Research, United States Department of Agriculture, Agricultural Reseach Service.

Xie, X., and Cui, Y. (2011). "Development and test of SWAT for modeling hydrological processes in irrigation districts with paddy rice". *Journal of Hydrology*, *396*(1), 61-71.

Yuan, Y., Khare, Y., Wang, X., Parajuli, P.B., Kisekka, I. and Finsterle, S. (2015). "Hydrologic and water quality models: Sensitivity". *Transactions of the ASABE*, *58*(6),1721-1744.

Zheng, J., Li, G. Y., Han, Z. Z., and Meng, G. X. (2010). "Hydrological cycle simulation of an irrigation district based on a SWAT model". *Mathematical and Computer Modelling*, *51*(11), 1312-1318.

CHAPTER 3. ASSESSMENT OF SYSTEM RESPONSES IN INTENSIVELY IRRIGATED STREAM-AQUIFER SYSTEM USING SWAT-MODLFOW[1]

3.1. SUMMARY

Water management strategies need to balance water security and food production, particularly in semi-arid regions wherein irrigation is required to supplement rainfall. Irrigated stream–aquifer systems present a unique challenge in this effort, due to complex groundwater–surface water interactions and the high level of human intervention in managing irrigation practices. This paper has two objectives: first, to detail a method for constructing and applying a coupled SWAT-MODFLOW to irrigated stream–aquifer systems; and second, to use the model to quantify the effects of decreasing irrigation on hydrological responses and crop yield. The method is applied to a 734 km^2 study region in the Lower Arkansas River Valley, an alluvial valley in Colorado, USA, which has been intensively irrigated for over 100 years and is threatened by shallow water tables. Therefore, a reduction in applied irrigation amounts has the double benefit of conserving water and decreasing waterlogging, given that crop yield can be maintained for food production. The results indicate that an approximate 10% decrease in total applied irrigation water results in decreases of 6% in surface runoff, 8% in evapotranspiration, and 4% in recharge water. It also results in an increase of 4% in groundwater return flow to the Arkansas River, and an actual increase in groundwater levels due to the decrease in groundwater pumping, pointing to the need for targeted irrigation reduction strategies to decrease waterlogging occurrence. The irrigation reduction yields an average 9% decrease in corn and alfalfa yield. This modeling approach is in general transferable to other similar irrigated river valleys.

3.1. INTRODUCTION

The increasing scarcity of water is an immediate threat to the sustainable development of areas around the world. Water resource managers faces the growing challenges of providing sustainable water supplies while maintaining and even increasing crop productivity, all in the face of increasing demand, limited resources, and the variation of streamflow and groundwater volumes due to short-term human management and long-term climatic patterns (Lobell et al., 2010; Martin-Carrasco et al., 2013; Robertson et al., 2018; Törnqvist and Jarsjö, 2012). The optimum management of available groundwater and surface water resources is particularly difficult in irrigated stream–aquifer systems due to the interaction between groundwater and surface water and the high degree of human intervention in providing irrigation water to cultivated fields. Both groundwater and surface water are used for irrigation, with recharge to the alluvial aquifer providing return flow to streams (Aliyari et al., 2019; Cai et al., 2003; Droogers and Bastiaanssen, 2002; Niemann et al., 2011; Pokhrel et al., 2015). However, in many regions, high water tables result in waterlogging, soil salinization, and nutrient accumulation in the aquifer and downstream areas (Burkhalter and Gates, 2005; Gates et al., 2012; Pimentel et al., 1997; Qureshi et al., 2010; Scanlon et al., 2007; Tanji and Kielen, 2002). Therefore, water management strategies in these regions must balance water conservation with crop yield while also seeking to lower groundwater levels.

Due to the complexity in these systems, watershed-scale hydrological models have been essential tools to capture the major hydrological processes and investigate solutions through alternative management strategies (Borah and Bera, 2003; Devia et al., 2015; Francesconi et al., 2016; F. Schoumans et al., 2009). Some of the commonly used models focus on land surface processes, and include the Agricultural NonPoint Source pollution model (AGNPS (Young et al., 1989)), the Hydrological Simulation Program—Fortran (HSPF (Bicknell et al., 1993)), the Hydrologic Modeling System (HEC-HMS; (Charley et al., 1995)), the KINematic runoff and EROSion model (KINEROS (Woolhiser et al., 1990)), the Soil and Water Assessment Tool (SWAT (Arnold et al., 1998)), the Soil and Water Integrated Model (SWIM (Krysanova et al., 2000)), and the CASCade of planes in 2-Dimentions (CASC2D (Ogden et al., 2002)).

SWAT, the most popular of these, is considered a promising tool for continuous simulations in predominantly agricultural watersheds, and often is used to assess changes in water due to land use and agricultural management practices (Gassman et al., 2007; Jang et al., 2017; L. Chiang et al., 2010; L. T. Ghebremichael et al., 2010; Strehmel et al., 2016). For example, SWAT was used to evaluate impacts of various dairy farming facts on land-use changes in the 3050 km^2 Sondu River basin in Kenya (Jayakrishnan et al., 2005), and to analyze the implementation of land management practices to improve water quantity and maintain crop production in Central German (Ullrich and Volk, 2009). In the Midwest United States, a study used the SWAT model to explore the response of crop yield to climate variability and estimate crop yield under different drought and aeration stresses conditions (Wang et al., 2016). SWAT also has been applied in the Aral Sea drainage basin in northwest Iran to access water savings as a result of improved irrigation techniques (Ahmadzadeh et al., 2016). This study showed that changing the traditional irrigation system to a pressurized irrigation system can lead to basin level water conservation and increase crop production. However, they did not capture the individual hydrological responses, especially the interactions of groundwater and surface water (Fleckenstein et al., 2010). The current SWAT model often performs poorly in watershed systems wherein groundwater discharge is a significant component of streamflow (Chu and Shirmohammadi, 2004; Gassman et al., 2007; Spruill et al., 2000), due to lack of consideration of geographic location of groundwater and spatially-varying aquifer characteristics. In addition, the influence of pumping wells on groundwater head gradients cannot be simulated.

Spatio-temporal hydrological processes and water management assessment can also be addressed through integrated models such as CATchment HYdrology (CATHY (Paniconi et al., 2003)), the Ground-water and Surface-water Flow Model (GSFLOW (Markstrom et al., 2008)); Parallel groundwater Flow (ParFLOW (Kollet and Maxwell, 2008)), HydroGeoSphere (Therrien et al., 2010), OpenGeoSys (OGS (Kolditz et al., 2012)), and MIKE SHE (Refsgaard, 1997). Examples of applying these integrated models for investigating management strategies include the application of GSFLOW to the second largest inland river basin in China (Wu et al., 2016) to perform temporal optimization for the conjunctive use of surface water and groundwater for irrigation, and applying MIKE SHE to analyze the influence of groundwater

dynamics in the estimation of hydrology–land surface feedback in a 225 km^2 region in Kansas (Larsen et al., 2016). While many studies focus on assessing groundwater surface–water interactions under climate change (Scibek et al., 2007; Ward et al., 2006), agronomic and environmental feedbacks (Ahrends et al., 2008; Cai et al., 2003; Shultz et al., 2018; Wei et al., 2018a), and wetland interactions (Anibas et al., 2012; Bauer et al., 2006), there is a need for an assessment of land management practices on hydrological processes and agronomic responses in a fully integrated stream–aquifer systems wherein major human interventions in managing irrigation practices occur.

The objective of this study is twofold: first, to detail a method for constructing and applying a coupled SWAT-MODFLOW (modular three-dimensional finite-difference groundwater model - MODFLOW) to irrigated stream–aquifer systems; and second, to use the model to quantify the effects of decreasing irrigation on hydrologic responses and food production (i.e., crop yield). System responses include stream flow, groundwater elevation, groundwater discharge to streams, and crop yield. The objective will be accomplished through the use of a coupled groundwater surface SWAT-MODFLOW model that links SWAT with MODFLOW (Harbaugh, 2005), which is a widely used groundwater flow model. Whereas previous model applications to this study region focused on unsaturated zone flow and groundwater flow (Morway et al., 2013) (MODFLOW using the River package) and unsaturated zone flow, groundwater flow, and streamflow (Shultz et al., 2018) (MODFLOW using the Streamflow Routing package), the use of SWAT-MODFLOW provides a representation of all major hydrologic processes, including surface runoff and soil lateral flow. In addition, the inclusion of SWAT allows for the simulation of crop yield. Although the model is based on the published SWAT-MODFLOW modeling code (Bailey et al., 2016), it has been modified to include detailed representations of canal diversion, canal seepage, applied irrigation amounts of surface water (canals), and groundwater (pumping wells) for each field, and the evapotranspiration of shallow groundwater. The model is applied to a 732 km^2 region of the Lower Arkansas River Valley (LARV) in southeastern Colorado, an intensively irrigated system in which shallow water tables have caused waterlogging and associated soil salinization in recent decades. The model is calibrated and tested against land surface and subsurface system-response variables as well as crop yield.

Section 2 provides a brief theoretical overview of SWAT, MODFLOW, and the coupled SWAT-MODFLOW model, followed by modifications of the SWAT-MODFLOW code to enhance model capability in irrigated stream–aquifer systems. Section 3 demonstrates the method of applying the modified SWAT-MODFLOW code to the LARV, and Section 4 provides results and a discussion.

3.2. MODEL CONSTRUCTION AND COMPOSITION

3.2.1 Overview of SWAT and MODFLOW

The Soil and Water Assessment Tool (SWAT) is a continuous time, physically-based, and spatially semi-distributed model (Arnold et al., 1998). It has been successfully used to test and evaluate eco-hydrological processes containing surface and soil water flow, nutrient mass transport, food production, and land-use management practices at the watershed scale (Baker and Miller, 2013; Garg et al., 2012; Geza and McCray, 2008; Kundu et al., 2017; Srinivasan et al., 2010; Zhang et al., 2011). The watershed is typically divided into multiple sub-basins based on topography. Hydrologic response units (HRUs) in each sub-basin are created by lumping similar land-use and soil layers in which the vertical flows and nutrient transport are calculated. The output from each HRU is routed according to the channel routing algorithm to the watershed outlet. A main disadvantage of SWAT is its lumped, linear reservoir approach, which oversimplifies the groundwater processes. It results in significant conceptual limitations regarding the physical representation of the aquifer heterogeneity, groundwater flow, and the surface and subsurface interactions in the hydrological system.

The modular three-dimensional finite-difference groundwater model (MODFLOW) is a physically based, fully distributed model (Harbaugh, 2005). It uses the finite different approach to solve the groundwater flow equations for the hydraulic head in each grid cell based on sources and sinks (e.g., recharge, pumping), initial and boundary conditions, and aquifer parameters (e.g., river conductance, specific storage, specific yield, and hydraulic conductivity). MODFLOW has various packages that simulate different hydrological processes, such as soil deep percolation (i.e., water that leaves the bottom of the soil profile) is considered by recharge package (RCH), groundwater pumping/injection is represented

by well package (WEL), groundwater discharge/recharge is simulated by the river package (RIV) along the river grid cells, and the evapotranspiration package (EVT) evaluates groundwater upflux to evapotranspiration when the groundwater table raises into the root zone. A recent version is MODFLOW-NWT, which performs well in unconfined groundwater systems with the complex non-linear drying and rewetting processes (Niswonger et al., 2011). MODFLOW lacks a meaning of specifying the conditions in terms of hydrological processes at the watershed surface. Therefore, it is often linked with land surface models such as SWAT (Bailey et al., 2016; Guzman et al., 2015; Kim et al., 2008; Sophocleous and Perkins, 2000), as is done in the study we addressed in this paper.

3.2.2 SWAT-MODFLOW Linkage

The SWAT-MODFLOW modeling code (Bailey et al., 2016) combines the SWAT 2012 and MODFLOW-NWT, a Newton-Raphson formulation for MODFLOW-2005, into a single FORTRAN code, which replaces the SWAT groundwater module with the MODFLOW code. The fundamental linkage between the two models is based on mapping schemes that occur on a daily time step that passes SWAT-calculated deep percolation as a recharge to the MODFLOW grid cell. Then, the MODFLOW-calculated hydraulic head is compared with the SWAT stream channels to determine stream–aquifer interactions on a daily time step. The SWAT HRUs are first split into disaggregated HRUs (DHRUs), in which each DHRU contains a geographical location to store SWAT daily calculations (e.g., soil deep percolation). All the mapping information is stored in four text inputs files that are read at the beginning of the simulation. Within the framework, SWAT simulates surface and soil zone processes (e.g., stream stage, surface runoff, overland flow, lateral flow, surface evapotranspiration, and plant growth), while MODFLOW simulates groundwater hydrology in each grid cell (e.g., groundwater elevation, three-dimensional groundwater flow, and surface–groundwater interactions). The main steps in the daily loop of the SWAT-MODFLOW code are shown in Figure 14.

3.2.3 SWAT-MODFLOW Modifications

Modifications to the SWAT-MODFLOW code are made for simulating irrigation-related processes in the irrigated stream–aquifer system. These include new subroutines for groundwater irrigation and groundwater evapotranspiration, as detailed in the following sections.

3.2.3.1 Irrigation Events

The SWAT automatic irrigation algorithm is applied to represent irrigation events that can be triggered based on plant water demand (Wei et al., 2018b). Irrigation water can be provided either by surface water through earthen canals or by groundwater through pumping wells. For surface water irrigation, the standard SWAT procedure is used by specifying the sub-basin reach from which the surface water is derived, representing canal diversions from the main stem of the river. For groundwater irrigation, as can be seen in Figure 14, daily pumping rates are specified in the MODFLOW's WEL package input file, with these volumes converted to irrigation depths for application to SWAT HRUs on the following day. The conversion of volumes to depths and the application to SWAT HRUs are performed using new subroutines within the SWAT-MODFLOW code. To employ this new model linkage, the model user must prepare a file (swatmf_irrigate.txt) that contains the following information:

- HRUs and associated sub-basin assigned to each pumping well, with the pumping well designated by a row and column within the MODFLOW grid;

- Conveyance efficiency for each subbasin (percentage of pumped groundwater that is lost between the well and the field of application, representing loss from an earthen canal); and

- Runoff ratio (percentage of applied irrigation water that runs off the field).

The depth of irrigation water to the groundwater-supplied HRU via a pumping well is calculated as:

$$V_{sub-irr,i} = \sum Q_{pump,n,i} \times R_{convey,i} \tag{1}$$

$$D_{sub-irr,i} = \frac{V_{sub-irr,i}}{A_i} \times 1000 \tag{2}$$

$$aird_j = D_{sub-irr,i} \times (1 - R_{runoff,i}) \tag{3}$$

where $V_{sub-irr,i}$ is the total volume of irrigation water provided to SWAT sub-basin i (m³/day); $Q_{pump,n,i}$ is the amount of water pumped for a specified grid cell n for a given sub-basin i (m³/day); $R_{convey,i}$ is conveyance efficiency for a given sub-basin i; $D_{sub-irr,i}$ is the depth of irrigation provided to SWAT sub-basin i (mm), with the 1000 included to convert from meters to mm; A_i is the total HRU area that receives irrigation water in a given sub-basin i; $aird_j$ is the amount of irrigation water applied to a given HRU j; and $R_{runoff,i}$ is the runoff efficiency for a given sub-basin i. The irrigation depths for the groundwater-supplied HRUs are applied on the following day.

3.2.3.2 Groundwater Evapotranspiration

Due to the presence of shallow water tables in many semi-arid irrigated regions, the volume of groundwater removed via evapotranspiration (ET) is calculated as a linearly varying function of depth below the water table using MODFLOW's EVT package. The EVT package simulates the influence of direct evaporation and plant transpiration in removing water from the saturated groundwater regime based on the following assumptions: (1) when the groundwater elevation is at or above the root zone, which is the bottom layer of SWAT soil profile, ET from the water table occurs with a user specified maximum rate; (2) when the groundwater elevation is below a specified extinction depth, ET from the saturated zone ceases; (3) between these two limits, ET from the water table varies linearly with groundwater elevation (Harbaugh et al., 2000). The maximum evapotranspiration rate $EVTR$ provided to the EVT package is calculated as the difference between the potential ET rate (PET) (mm) calculated by SWAT and the actual ET rate (AET) (mm) simulated by SWAT:

$$EVTR = PET - AET \tag{4}$$

with the assumption that a portion of the PET rate can be satisfied by the shallow water table.

Therefore, this coupling process is effective in the new coupling code when the groundwater table is within the root zone. With other SWAT-MODFLOW interactions, groundwater ET is simulated on a daily time step.

3.3. SWAT-MODFLOW APPLICATION TO IRRIGATED STREAM-AQUIFER SYSTEM

3.3.1 Study Region: Lower Arkansas River Valley, Colorado

The modified SWAT-MODFLOW code is illustrated in application to a 732 km^2 irrigated stream–aquifer system along the Lower Arkansas River Valley (LARV) in southeastern Colorado (Figure 15A). In this study region, the snowmelt-derived Arkansas River runs through a shallow sandy alluvial aquifer (10–20 m in thickness) that contains two main tributaries, Timpas Creek and Crooked Arroyo. The average temperature is 13.6 °C, with the monthly temperature varies between −7/9 °C (low/high) and 16/33 °C in December and July, respectively. The mean annual crop reference evapotranspiration (ETr; Alfalfa reference equation) is about 1650 mm, which is much larger than the mean annual precipitation of 273 mm (Figure 16). Two-thirds of the annual rainfall occurs between April and August, primarily during brief but intense thunderstorms.

The climate is semi-arid, which requires irrigation to supplement rainfall for crop growth. Over the past century, irrigation has been practiced either through diverting water from the Arkansas River into an extensive network of earthen canals (Figure 15A green lines), or more recently from the aquifer through a network of 575 pumping wells (Figure 15A black dots). From 89 groundwater observation wells (Figure 15E red dots), the groundwater table is 2–20 m below the surface. Groundwater recharge is provided by the infiltration of precipitation, percolation of applied irrigation, and seepage from river, canals, and ditches (Dennehy et al., 1995), with the increased groundwater head creating a gradient that produces discharge to the stream network, creating baseflow for the river. Cultivation and associated irrigation occurred between March–November. Figure 15B shows the crop type information for each cultivated field in 1999, provided by information from the Farm Service Agency located in Rocky Ford, Colorado. Alfalfa, corn, and wheat are the dominant crop types in the LARV.

3.3.2 Model Application

The SWAT-MODFLOW model for the study region uses the calibrated SWAT model (Wei et al., 2018b) and the calibrated MODFLOW model (Morway et al., 2013), with the latter developed to study the impacts of human management features on hydrological processes in an irrigated watershed.

71

The SWAT model used for the study area was developed by a former study (Wei et al., 2018b). The region includes 72 sub-basins (Figure 15D). As described in the previous paper (Wei et al., 2018b), a method was developed to apply SWAT to intensively managed irrigated watershed, which included: (1) designating each cultivated field as an HRU; (2) manipulating realistic crop rotations by changing the management files (*.mgt) for each HRU; and (3) applying SWAT's automatic irrigation function to trigger irrigation events based on plant water demand for both surface water and groundwater irrigation. This method required modifications to the input files and resulted in 5270 HRUs. The source of surface irrigation water for all HRUs in a given canal command area was specified to the section of the Arkansas River coinciding with the point of diversion based on the Colorado Division of Water Resources. Groundwater irrigation was specified to HRUs surrounded by the groundwater pumps. Additional details on model construction have been provided by the original SWAT study (Wei et al., 2018b). The model was run from April 1999 to Feburary 2016, with simulated streamflow tested against observed hydrographs at five stream gauges (See Figure 15D for location) (Wei et al., 2018b).

The original MODFLOW model encompasses the central cultivated region with an area of 506 km^2. The region was discretized into finite difference grid cells with uniform dimensions of 250 m × 250 m, consisting of 213 east–west oriented rows and 127 north–south oriented columns (see Figure 15D in light grey) with 7777 activated cells (see Figure 15D in dark grey) in the model domain. The model consists of 1943 river cells, of which 1089 represent the Arkansas River and tributaries (Figure 15E in blue), and 1065 represent irrigation canals (Figure 15E in green). Canal seepage was estimated by MODLOW RIV package, with hydraulic heads specified along the canals based on estimated data from the fields. The aquifer was discretized vertically into two layers of varying thickness based on the local hydrogeological units, with a third layer representing the shale bedrock. The MODFLOW WEL package simulated groundwater pumping processes, while the unsaturated-zone processes were represented using the UZF1 package, including weekly infiltrated irrigation and precipitation depths, potential evapotranspiration, and unsaturated zone flow for each grid cell. Surface water and groundwater interactions were estimated using the RIV package. The model was tested against water table elevation, groundwater return flow to the river network, and ET.

The spatial extent of the coupled SWAT-MODFLOW model is shown in Figure 15D. The SWAT-MODFLOW linkage has the ability to use SWAT and MODFLOW models of different spatial extent. The original functionality of each model is retained beyond the overlap area. The modification to the original MODFLOW was the replacement of the UZF1 package by the EVT and RCH packages. As described in Section 2.3.2, groundwater ET processes are simulated using the EVT package. Daily diverted volumes from the Arkansas River to irrigation canals are simulated as point sources along SWAT stream channels.

The basic procedure of linking two models is processed using ArcGIS. Both DHRUs and SWAT stream networks are intersected with the MODFLOW grid to provide necessary data for the linking files. In this study, a total of 57,168 DHRUs were created. Figure 17 demonstrates the shape file interactions and specific input parameters required to perform the linkage between SWAT and MODFLOW, with sub-basin 67 used as an example. The spatial relationship between HRUs and DHRUs, DHRUs and MODFLOW grid cells, SWAT stream channels and MODFLOW river cells, and SWAT subbasins/HRUs and MODFLOW pumping wells are saved into text files, read by code, and stored in memory for use throughout the simulation. The model is run for the 1999–2016 time period, with the original MODFLOW model (Morway et al., 2013) extended from 2009 to 2016 using pumping data and land-use data.

3.3.3 Model Calibration

The SWAT-MODFLOW model is calibrated using a combination of automated and manual procedures. The automatic parameter estimation is carried out with SWAT-CUP 2012 using the Sequential Uncertainty Fitting Algorithm (SUFI2 (Abbaspour et al., 2015)), and following the procedure in the original SWAT study (Wei et al., 2018b) for the stream discharge. In addition to the original parameters(Wei et al., 2018b), two extra model parameters—plant uptake compensation factor (EPCO) and depth from soil surface to bottom of layer (SOL_Z), which influence the processes of evapotranspiration and recharge—are included in the calibration. After model coupling, the SWAT groundwater module is turned off and replaced by the MODFLOW. Therefore, SWAT groundwater parameters were excluded from the automatic SWAT-CUP calibration. The new calibrated value ranges are shown in Table 6. The influence of MODFLOW parameters in the RIV package (Cond—riverbed hydraulic conductance) and the UPW package (i.e., S_y—

73

specific yield, S_s—specific storage) was determined using a one-at-a-time sensitivity analysis. Ten values were assigned to each parameter while keeping all the others constant, thereby testing the sensitivity of streamflow to the change in each parameter (Abbaspour et al., 2015; Molina-Navarro et al., 2019). MODFLOW hydraulic conductivity was not included in the calibration process, since it was calibrated in the original MODFLOW study (Morway et al., 2013). Figure 15C shows the hydraulic conductivity for the first layer of the MODFLOW model.

The model was tested against monthly streamflow, groundwater head, and crop yield. Simulated monthly streamflow was compared to the measured streamflow from the Colorado Division of Water Resources (CDWR) at three gauges along the Arkansas River (Rocky Ford, La Junta, and Las Animas) and two tributaries (Timpas Creek and Crooked Arroyo) (see Figure 15D). Model performance is estimated using statistical metrics, including the Nash–Sutcliffe efficiency (NSE (Nash and Sutcliffe, 1970)) and the coefficient of determination (R^2). These performance of NSE ranges from negative infinity to one, with values approaching one indicating a better match between simulated and observed values. The groundwater head is compared with the observed head for the 89 wells shown in Figure 15E, with several wells selected for a time-series comparison.

Simulated and observed crop yields are compared for alfalfa and corn, which are the two major crops in the study region. No further calibration was provided for crop yield. Crop yields simulated by SWAT are compared with county-level USDA National Agricultural Statistical Survey (NASS) data (https://quickstats.nass.usda.gov/). Due to the data availability from NASS, the period of 2001–2006 is selected. The simulated corn yield and alfalfa yield are aggregated to county level and compared with the NASS values that are reported yearly value for the same region. NASS reports corn and alfalfa yields in bushel per acre and tons per acre, with moisture of 15.5% and 20%, respectively. Since SWAT reports crop yield in tons per hectare, the following equation is used to convert bushels per acre to tons per hectare:

$$1\frac{bushel}{acre} = \frac{62.77}{1000} \times \frac{tons_{dry-corn}}{hectare} / (1-moisture) \tag{5}$$

During harvest time, the SWAT model simulates crop yield at 20% moisture content (Neitsch et al., 2011; Srinivasan et al., 2010); therefore, the simulated crop yield is multiplied by 0.8 to compare with the dry mass in the equation above.

3.3.4 Simulation of Irrigation Reduction Scenario

In intensively irrigated regions, irrigation water can have a significant impact on the entire hydrological system. In this study, the automatic irrigation method is used to trigger irrigation events based on plant water demand (Wei et al., 2018b), with irrigation water provided by either the Arkansas River via irrigation canals or by groundwater pumping as specified in MODFLOW's WELL package. When plant stress occurs, irrigation will be triggered, and water will be applied based on the water avalibility in the source. The baseline SWAT-MODFLOW model applies a threshold value of 0.9 to trigger crop irrigation. To explore the impacts of reducing irrigation water on streamflow, groundwater levels, groundwater ET rate, and crop yield, the water stress threshold is set to 0.5 (i.e., the model will automatically apply water to the HRU when the daily actual plant growth is reduced by 50% due to water stress) to decrease the surface water irrigation, and the groundwater pumping rates are decreased in the MODFLOW WELL to decrease groundwater irrigation.

3.4. RESULTS AND DISCUSSION

3.4.1 Water Balance

Results are first shown to demonstrate the relative flow components in the irrigated watershed. Figure 18 shows the partitioning of monthly average water yield (mm) to the river network calculated by SWAT-MODFLOW. For this study region, the amount of water entering the Arkansas River and its tributaries is dominated by groundwater discharge (74–97%), followed by surface runoff (2–25%) and lateral flow (less than 1%), which matches with the SWAT modeling results from (Wei et al., 2018b). Figure 19A gives the main components of average annual water budget, with depths of changing calculated by dividing by the area of the watershed. Surface water (198.6 mm) makes a higher contribution to irrigation than well pumping (59 mm) as the input source of irrigation water in the district (Gates et al., 2012).

Evapotranspiration is the most important output, with an average depth of 414.8 mm. It could be found out that the surface water and groundwater interactions are very strong. Water yield to the stream is dominated by return flow (202.5 mm), which accounts for 86% of the water yield.

3.4.2 Streamflow

The monthly streamflow comparison between observed and simulated results along the Arkansas River at the stream gauges of Rocky Ford, La Junta, and Las Animas are shown in Figure 20. Overall, the model is able to capture the seasonal flow patterns very well. A statistical comparison of simulated streamflow at five gauging stations are given in Table 7. The values for monthly streamflow are considered to be 'very good' for NSE >0.8 and R^2 >0.85, respectively (Moriasi et al., 2015), but poor for the two main tributaries (Timpas Creek and Crooked Arroyo). Simulated discharge for the tributaries, which act as drains for irrigation tail-water runoff and groundwater return flows, are lower than observed streamflow, which is likely because of the difficulty of physically matching the pattern of irrigation return flow from hundreds of irrigated fields. The same issue was reported by another study (Shultz et al., 2018) in their groundwater model of flow and selenium transport in the study region. Another reason for the mismatch is that the model ignores any streamflow generated from upland catchments beyond the irrigated areas, which can happen during occasional intense precipitation events.

3.4.3 Groundwater Elevation

The general results of the simulated groundwater levels are shown in Figure 21. The annual average groundwater level (m) is shown in Figure 21A, with the hydraulic head ranging from 1195 m to 1320 m, decreasing from southwest to east. The spatial pattern of groundwater elevation is similar to the surface elevation, with the highest and lowest head occurring in the southwest and east regions, respectively. Figure 21B shows the cell-wise depth to the water table, which was calculated by the difference between ground surface elevation and the simulated groundwater level. It shows that the water table depths range from 0 m to 23 m, with the shallowest depths along the Arkansas River corridor and tributaries.

The difference between simulated and measured groundwater levels at the 89 observation wells (see Figure 15E) (a total of 9444 measurements) is summarized by a relative frequency plot of groundwater

level in Figure 22. The results from the original MODFLOW model (Morway et al., 2013) also are shown (grey boxes). The average of the residuals for the SWAT-MODFLOW (−0.21 m) is similar to the original MODFLOW results (−0.22 m). The root mean square error (RMSE) of the simulated values compared to the observation values is 2.32 m. The differences in the distribution of groundwater levels between two models are similar to each other. These residuals demonstrate that the model can provide an acceptable representation for the groundwater levels in the region.

Further analysis can be performed by comparing the simulated and observed hydraulic head at 10 observation wells spread throughout the study region. Hydrographs for the time period 1999 to 2015 are shown in Figure 23. In general, simulated results are within the estimated error range of the measured head values of ±0.5 m (grey bars in Figure 23), with the errors accounting for the possible range of head values that can occur within a 250 m × 250 m area of the aquifer (i.e., the size of the grid cell). The model accurately captures the within-season and long-term trends of groundwater elevation magnitude. As can be seen in Figure 23, there are still several locations that have a significant mismatch between simulated and observed values (Well 12, Well 73, and Well 93). These discrepancies are likely due to the inaccurate recharge provided by SWAT (Arnold et al., 2000; Sun and Cornish, 2005), especially along the ungauged tributaries at the north region of the model. Moreover, it is realistic that the aquifer properties are not unique within a 250-m grid cell to induce a significant head change during certain periods. The hydraulic head estimated at the center of each cell could possibly be different from the observation value if the monitoring well is located at the edge of the grid cell.

3.4.4 Surface Water–Groundwater Interactions

The average simulated groundwater return flows to the Arkansas River is 1.8×10^6 m^3/week over the period November 2007 to December 2010, which is similar to the average value of 1.2×10^6 m^3/week calculated from a river water balance of the study region (Gates et al., 2018).

Simulated annual average surface and groundwater interactions (m^3/day) for each of the 731 river cells during the 1999–2016 period are shown in Figure 24, which is important to quantify spatio-temporal patterns of surface water seepage and groundwater discharge in the watershed. Blue bars represent seepage

from stream to aquifer, whereas green–yellow–red bars indicate groundwater discharge from the aquifer into the river network. It can be seen that the vast majority of surface and groundwater interactions is discharged from the aquifer to the river. The average interaction rates vary from -1611 m^3/day to 7126 m^3/day, with a standard deviation of 556 m^3/day, which demonstrates a highly spatio-variable groundwater discharge based on different hydrological conditions.

3.4.5 Groundwater ET

The annual average groundwater ET rate simulated by the model is 31.8 mm. The spatial pattern of the groundwater ET rate during the simulation period is shown in Figure 25, which is displayed as an average daily rate leaving the saturated zone during the irrigation season (March to November) (Figure 25A) and the non-irrigation season (Figure 25B). Groundwater ET occurs mainly along the Arkansas River corridor and tributaries. Overall, the average amount of groundwater ET is approximately constant over the simulation period, with the rates decreasing from the irrigation season to the non-irrigation season. Magnitudes and spatial patterns of groundwater ET are very similar to the results of the original MODFLOW model (Morway et al., 2013).

3.4.6 Crop Yield

Crop yield is one of the most important factors to estimate water productivity, especially in the Colorado area (Ahmadzadeh et al., 2016; Dozier et al., 2017). In this study, we compared the simulated crop yields in Otero County with the NASS reported mean yields of corn and alfalfa on an annual basis, as the majority of irrigated fields are located in this county (Figure 15A). Figure 26 A,B present the annual comparison of predicted and observed corn yield and alfalfa yield, respectively in Otero County for the years 2001–2006. The error bars on the plots represent the standard deviation of all the simulated values. It is shown that the model can capture the annual variation in crop yields quite well, with the annual average yield of 9.7 tons/ha and 7.4 tons/ha for corn and alfalfa, respectively. The percent bais (PBIAS) is 3.1% and 1.5% for corn yield and alfalfa yield, respectively. In this model, we assigned the management practices (e.g., crop rotation, fertilizer, harvest, and tillage) at the HRU scale according to the actual farm-scale conditions (Wei et al., 2018b), which helps to improve model performance. Although the model tends to underestimate both corn

and alfalfa yields in 2006 and overestimate alfalfa in 2003 and 2004, the objective is to capture the regional trends in total crop yield.

3.4.7 Quantifying the Impacts of the Irrigation on System Responses

Figure 19B gives the main components of the water budget for the reduced irrigation scenario. As expected, surface water and groundwater irrigation decreases (6.4 mm and 26.2 mm), respectively, in the control of water stress threshold and pumping rate and less consumptive use by crops. As a result of the lower irrigation application rates, the ET flux is decreased by 32.8 and the surface runoff is decreased by 2 mm, which also decreases recharge by 5.7 mm. However, the water table is influenced more by the decrease in pumping than the decrease in recharge, resulting in higher water table elevation, which drives more groundwater into the river network (i.e., increase in return flow from 202.5 mm to 211.2 mm, 4.3%). This is also demonstrated by the annual average increase in groundwater elevation (Figure 27), which is calculated by taking the difference between the reduced irrigation scenario and the baseline scenario. As expected, the water table increases in areas of pumping wells (see Figure 15E) due to the strong causal relationship between pumping and sustained shallow water tables, but decreases in areas of surface water irrigation due to the decrease in recharge. The overall average increase in water table elevation is 65 mm (Figure 19), thus leading to the increase in groundwater return flow (202.5 mm to 211.2 mm). The percentage increase in streamflow in the Arkansas River is shown in Figure 28, with the increase occurring due to less water diverted for surface water irrigation and more groundwater return flow.

The percentage increase in return flow for each of the river cells during the simulation period is shown in Figure 29, with green–yellow–red bars representing groundwater return flow. It can be seen from this figure that the majority of river cells are gaining return flows for the reduced irrigation scenario, with the highest percentage increase of 31%. This is an important result—implementing a basin-wide decrease in irrigation water for both surface water irrigation and groundwater irrigation does not necessarily improve waterlogging occurrence, and can actually increase the groundwater loading of salts, nitrate, phosphorus, and trace elements (selenium, uranium) due to an increase in groundwater return flow. This may be due to the close proximity of the pumping wells to the Arkansas River; therefore, the areas that control

79

groundwater discharge to the Arkansas River have higher water tables than those in the baseline scenarios. However, in general, a targeted approach must be taken that focuses on decreasing surface water irrigation and allowing the groundwater pumps to continue operation (e.g. the BMPs tested by Morway et al. (2013)). This will maintain deep water tables and decrease the recharge, therefore preventing waterlogging.

To complete the analysis of trade-offs, the change in crop yield between the baseline scenario and the reduced irrigation scenarios must be quantified. For the multi-year average assessment, the average yield under the reduced irrigation scenario for the entire irrigated fields is 8.9 tons/ha and 6.7 tons/ha for corn and alfalfa, respectively. The average production for these corn and alfalfa crops is shown by an HRU in Figure 29. Two types of assessments are conducted over the 18-year simulation period to compare the average crop production under the reduced irrigation condition: (1) annual spatial yield (Figure 29 A,B) and (2) yield reduction between the reduced irrigation scenario and the baseline scenario (Figure 29 C,D). We observed that corn has a higher yield in the central part of the study region, while the alfalfa yield has a wider spread and shows high yield in the north region. In general, the reduced irrigation scenario leads to a widespread reduction in crop yield, with a few locations of increased crop yield. The average reductions in crop yield are 8.8% and 9.2% for corn and alfalfa, respectively. Figure 29C,D shows that 5.9% and 6.3% of the corn field and alfalfa field experienced more than 20% reductions in crop production, respectively. Results also show that some fields do not have significant crop yield change under the irrigation scenario. Those fields could likely receive the extra irrigation water that is saved by the reduced surface water triggered by auto-irrigation water stress, so that the crop yield could decrease more slowly when the irrigation amount approaches the crop water demand (English, 1990; Zhang et al., 2018).

3.5. SUMMARY AND CONCLUSIONS

This paper presents the application of a new version of the SWAT-MODFLOW code (Bailey et al., 2016) to a 732 km^2 irrigated stream–aquifer system in the Lower Arkansas River Valley, Colorado. The model accounts for the influence of irrigation applications, canal diversions, earthen canal seepage, and groundwater pumping. The model provides a detailed description of surface and groundwater flow

processes, thereby enabling a detailed description of watershed processes such as surface runoff, ET, infiltration, soil lateral flow, recharge, groundwater ET, three-dimensional groundwater flow in a heterogeneous aquifer system with sources and sinks, spatio-temporal groundwater and surface water interactions (e.g., groundwater discharge to the river network), and streamflow. Model performance was tested against stream discharge, groundwater levels, groundwater return flow, and crop yield. Therefore, this paper serves as a guideline for implementing SWAT-MODFLOW models in irrigated watersheds wherein streamflow is influenced by groundwater-surface water interactions.

The model was used to explore the effects of reducing irrigation rates on hydrologic responses (surface runoff, recharge, water table elevation, return flows, streamflow) and crop yield. The results reveal that jointly decreasing surface water irrigation and groundwater irrigation yields an overall increase in water table elevation, with the decrease in pumping having a stronger influence than the decrease in recharge on groundwater levels. The higher groundwater levels enhance the prospect of waterlogging and salinization, and increase the groundwater gradient to the river, increasing the groundwater discharge rates to the Arkansas River, and resulting in an increase in the loading of salts and pollutants to the stream. This will be addressed in future studies using a coupled surface/subsurface nutrient transport model. In addition, 8.8% (corn) and 9.2% (alfalfa) crop reduction are observed in the reduced irrigation scenario.

This study points to the need for targeted irrigation reduction scenarios that will decrease shallow water tables while also maintaining crop yields. It is likely that this will be targeting surface water irrigation for irrigation reduction, with groundwater pumping for irrigation allowed to continue to (1) maintain the basin-wide crop yield and (2) maintain adequately deep water tables to prevent waterlogging. The results discussed here only concern system hydrological responses. The nutrient fate and transport, as well as plausible best management practices for controlling contaminant pollution need to be addressed in intensively irrigated stream–aquifer systems in order to provide water resources managers with a detailed description of the alternative management options.
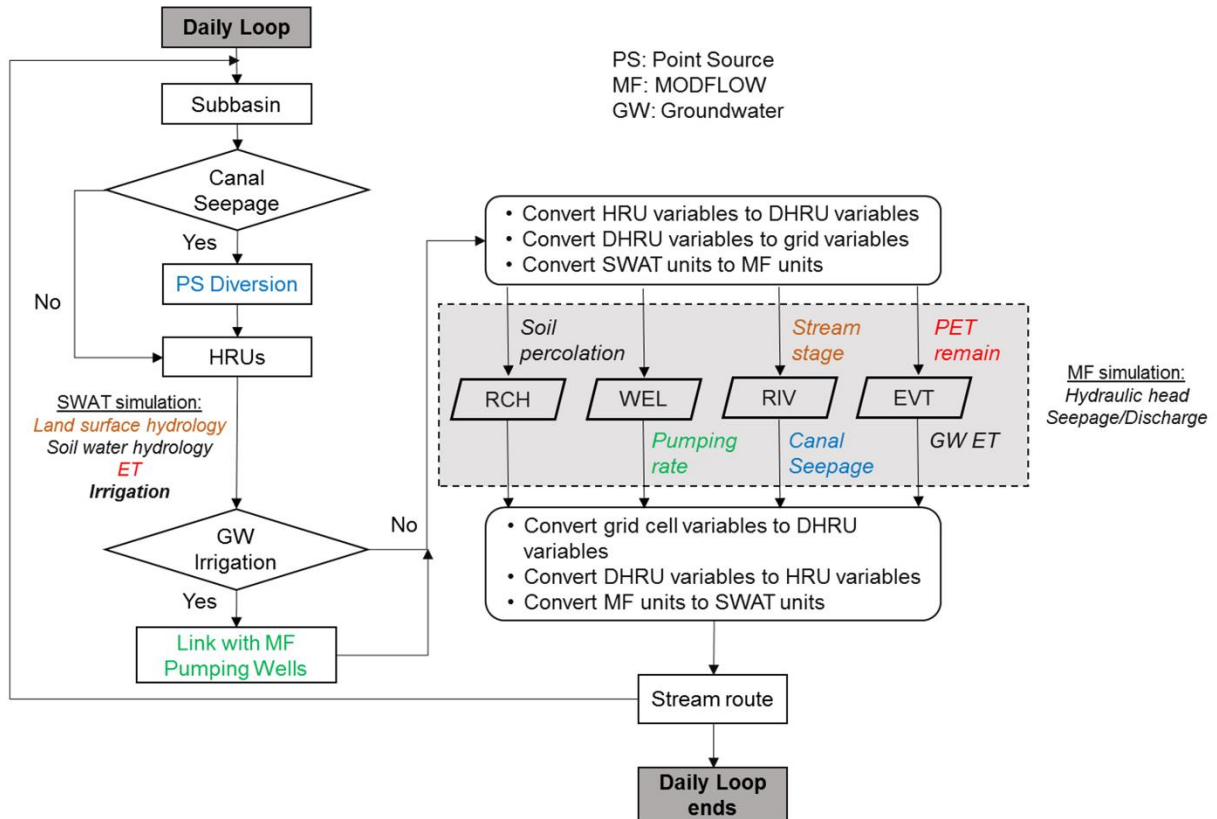
Figure 14. Flow of information in modified SWAT-MODFLOW modeling code, showing the calling of MODFLOW as a subroutine within the main SWAT structure.
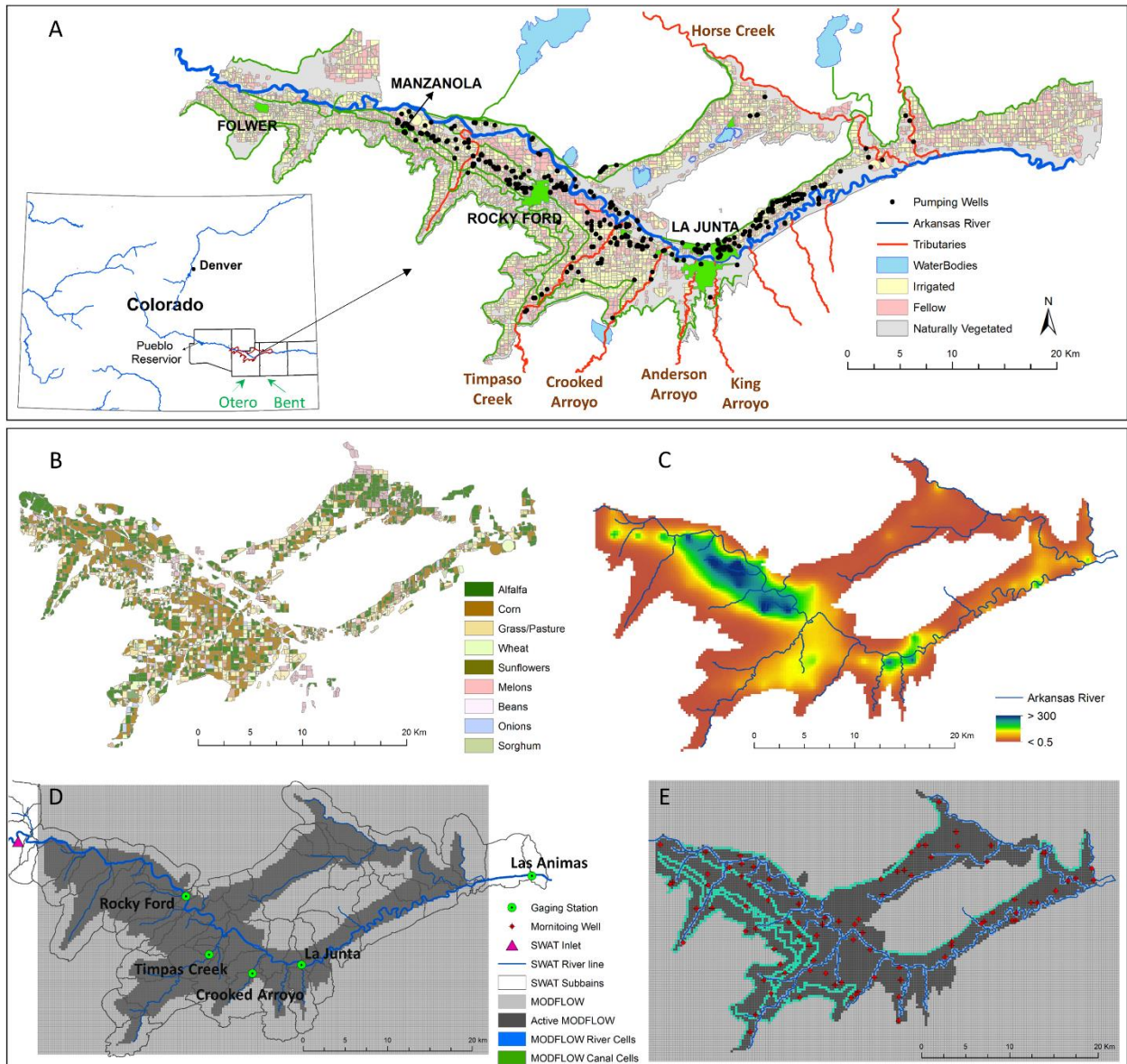
Figure 15. (A) Location of the study region in Colorado; (B) crop type for each cultivated field for the year 1999; (C) Horizontal hydraulic conductivity (m/day) for layer 1; (D) subbasins generated by the SWAT model; also shown is the inlet and outlet gauging stations; (E) MODFLOW grid cells; also shown the 89 monitoring well locations and MODFLOW river cells.
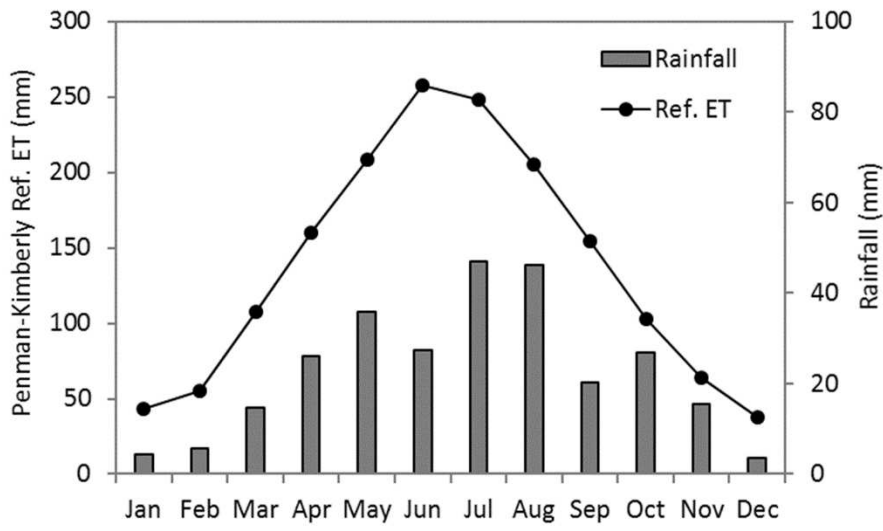
Figure 16. Monthly average rainfall and reference evaporation in the study region.
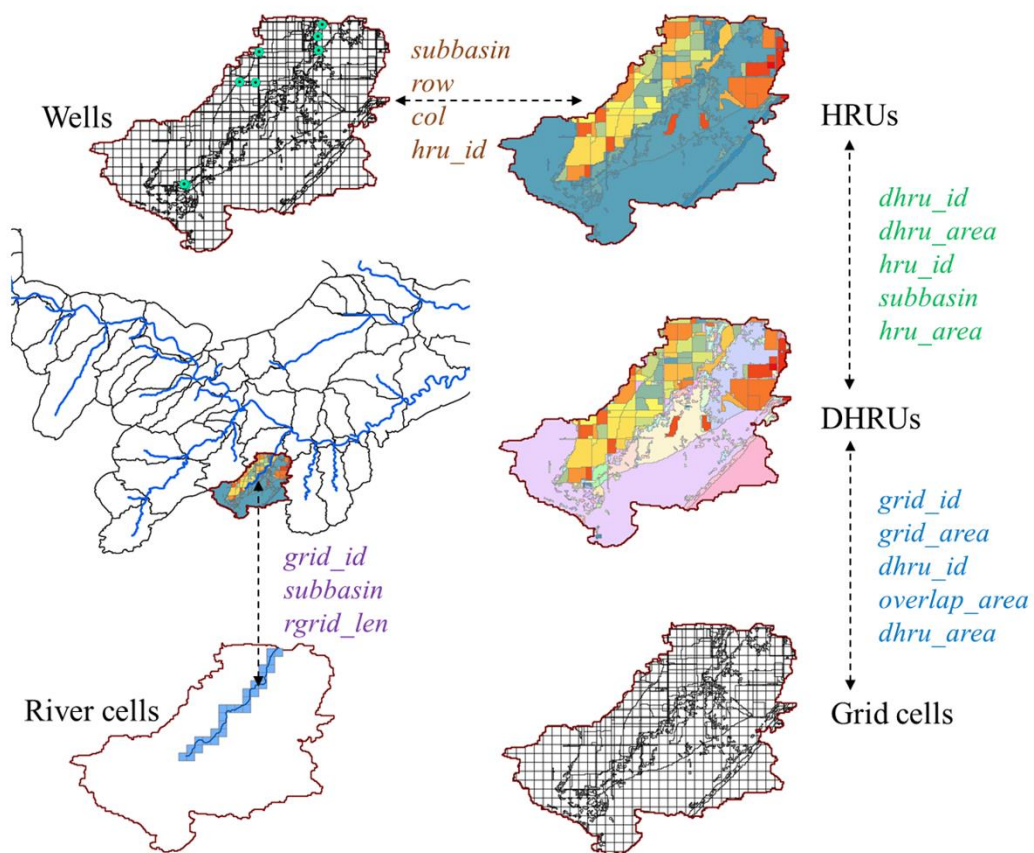
Figure 17. Information necessary to convert model output from HRUs to geographically-located disaggregated HRUs (DHRUs), from DHRUs to MODFLOW grid cells, from SWAT subbasin rivers to MODFLOW river cells, and from MODFLOW pumping wells to SWAT DHRUs.
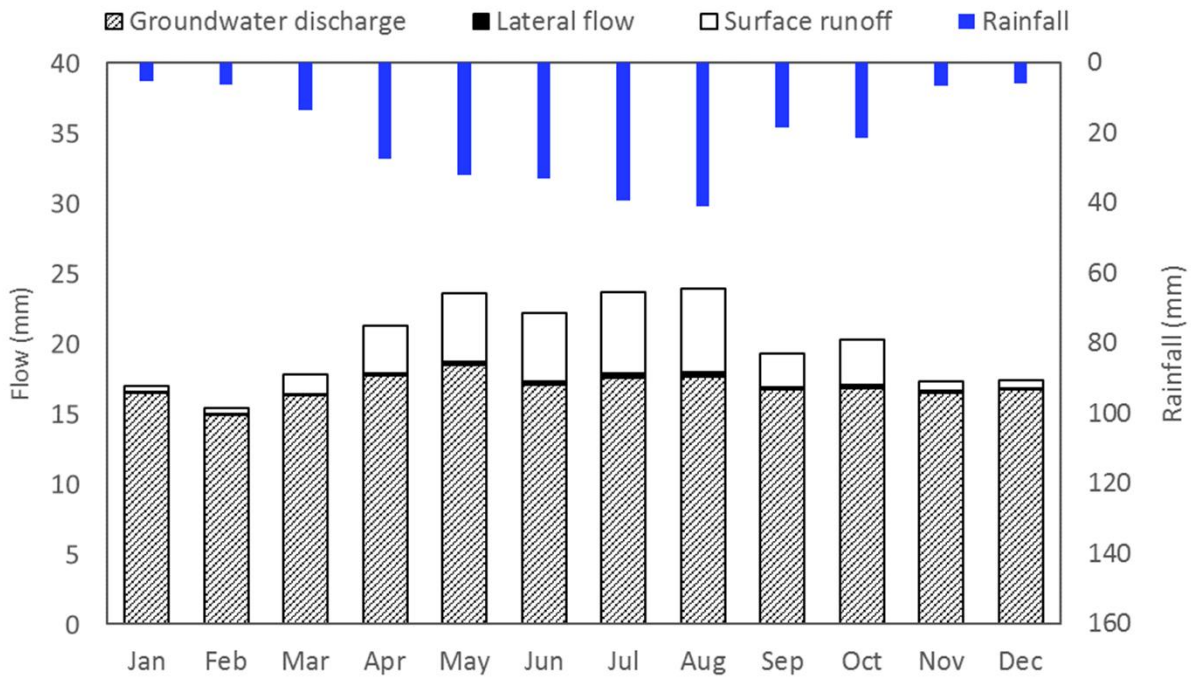
Figure 18. Monthly average water budget and rainfall in the study region.
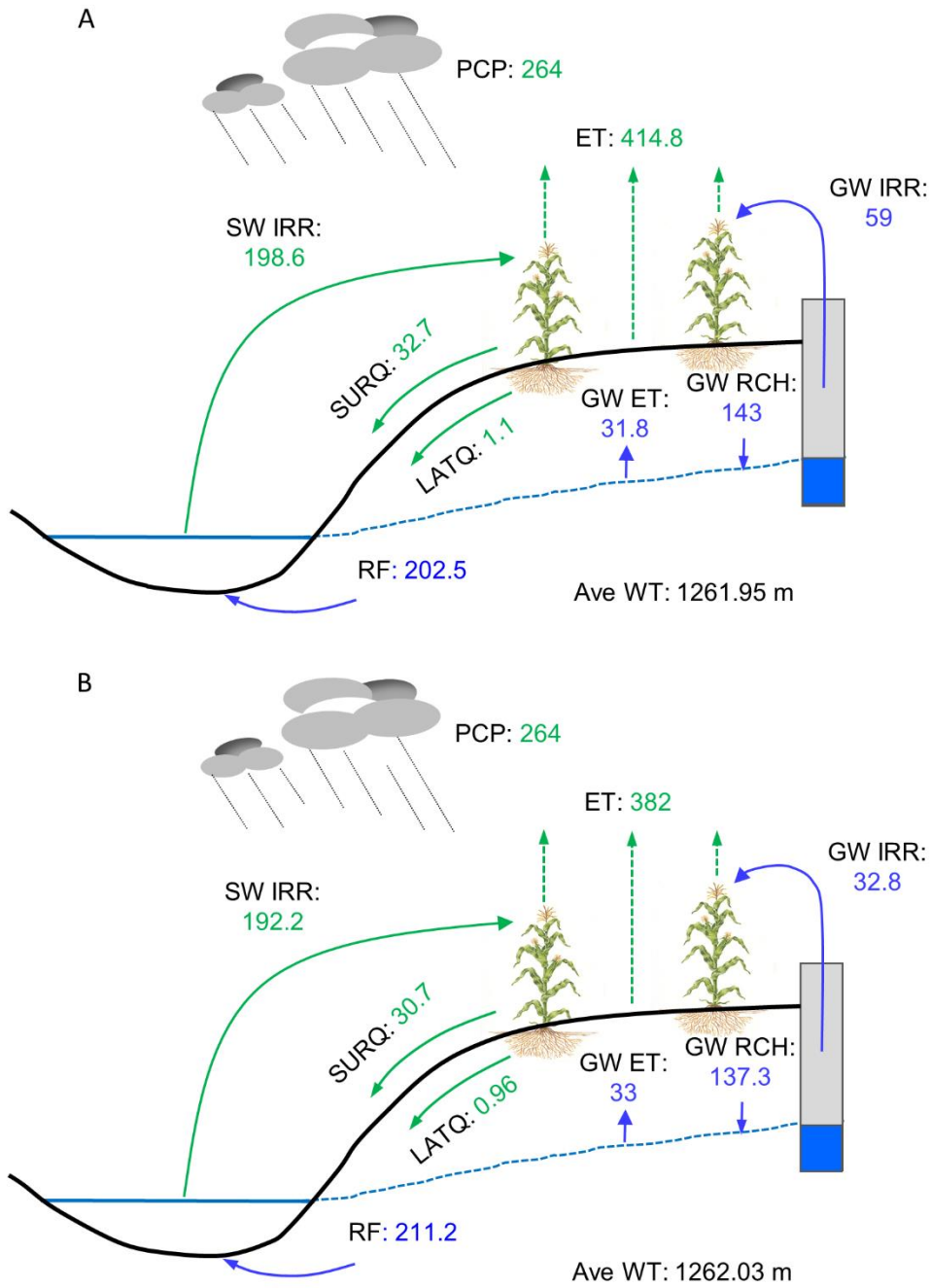
Figure 19. Water budget scheme for the entire study region for (A) baseline scenario and (B) reduced irrigation scenario, with domain-wide values reported in mm and water table elevation reported in m.
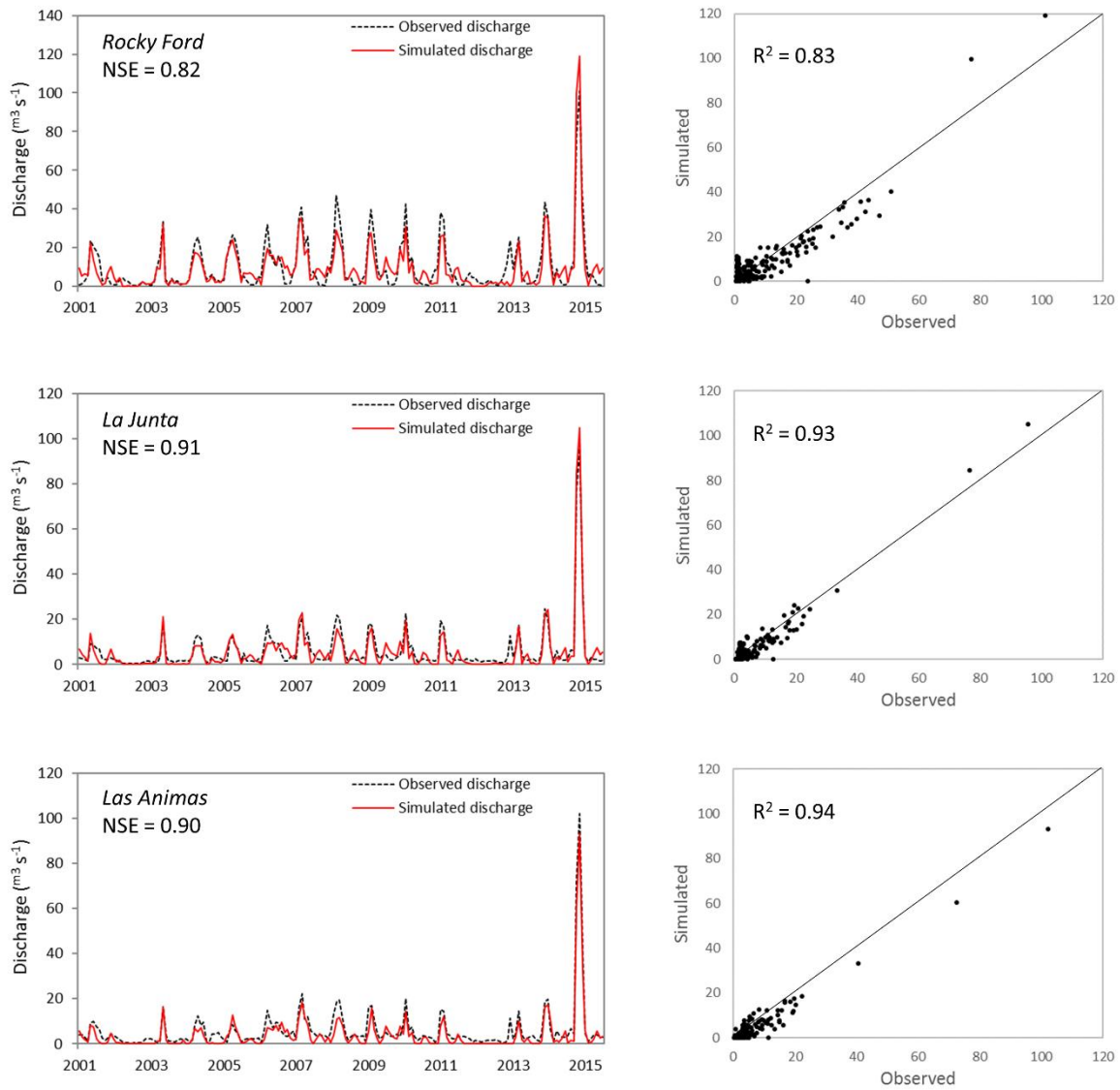
Figure 20. Comparison of SWAT-MODFLOW simulated and observed stream flow at Rocky Ford, La Junta, and Las Animas (outlet) (see Figure 15B), with corresponding coefficient of determination.
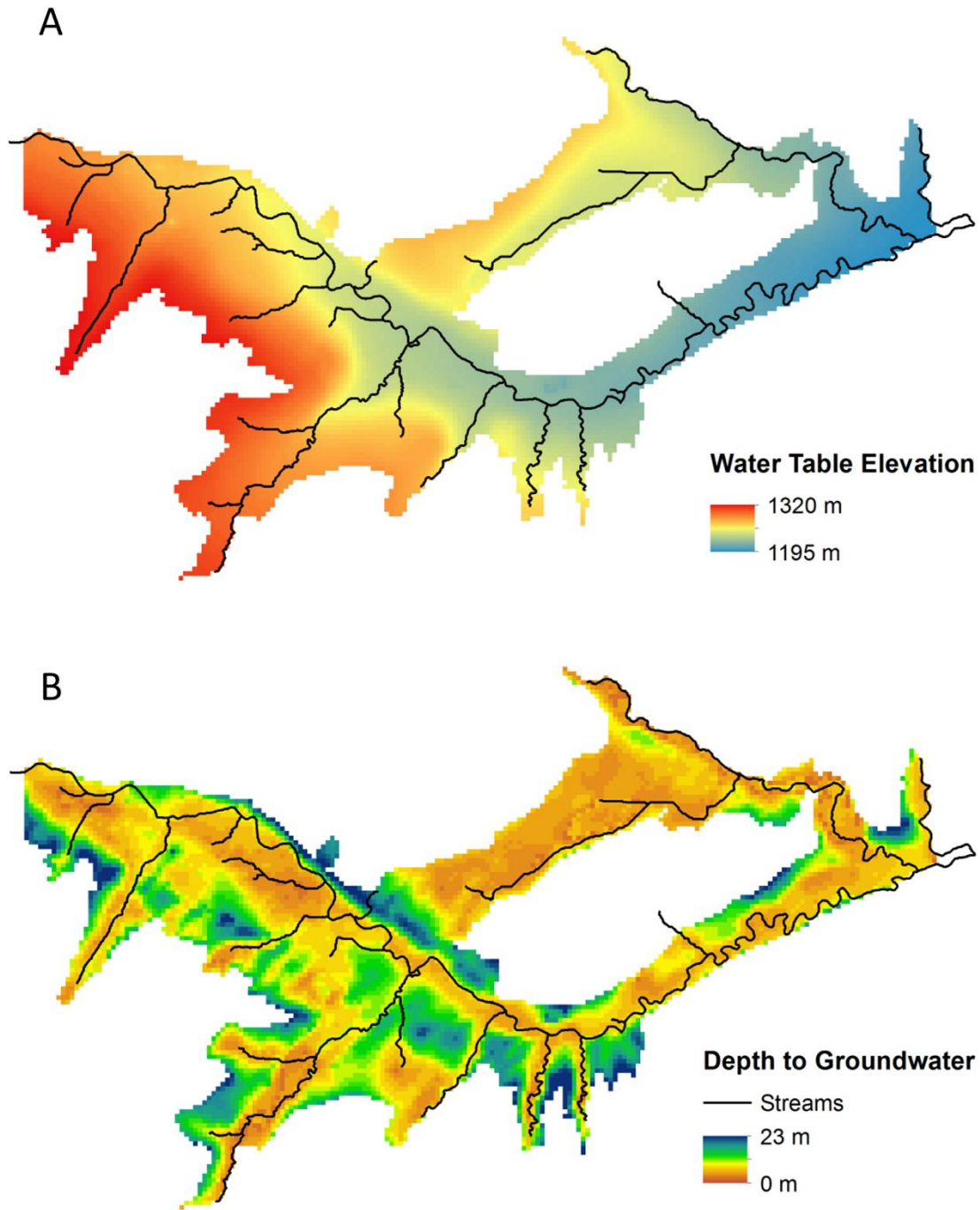
Figure 21. Annual average cell-wise plots for active MODFLOW grid cells in the study region over the 1999-2016 time period: (A) water table elevation and (B) depth to groundwater table.
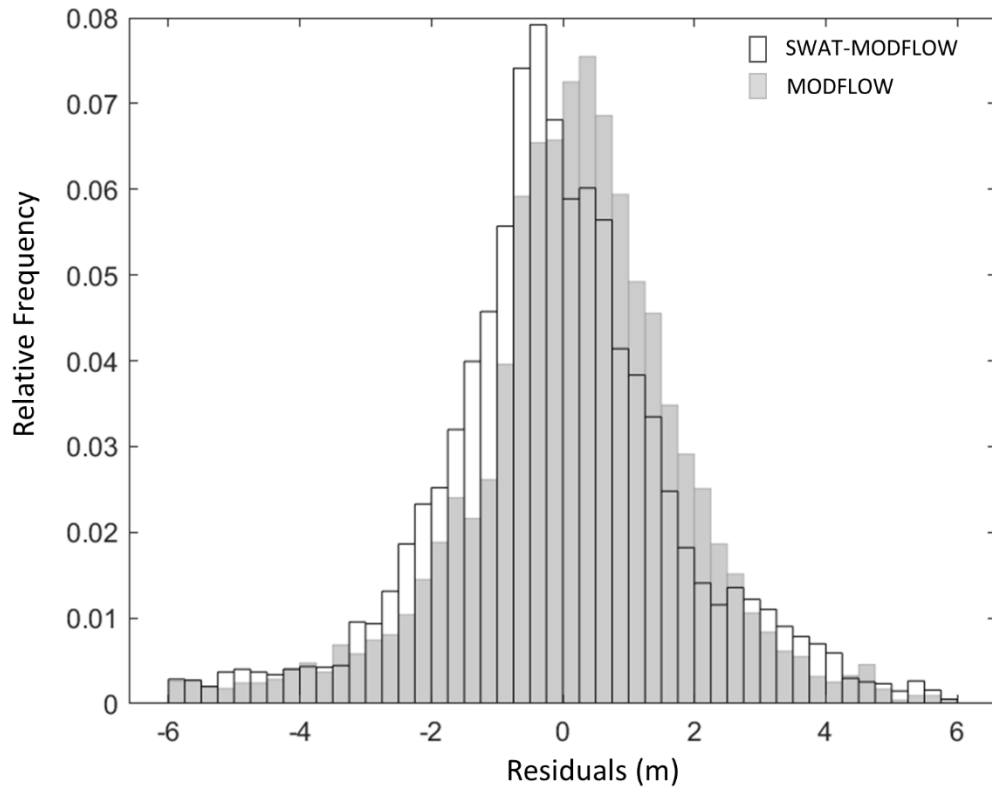
Figure 22. Residuals of simulated groundwater elevation head for (A) SWAT-MODFLOW model and (B) MODFLOW model
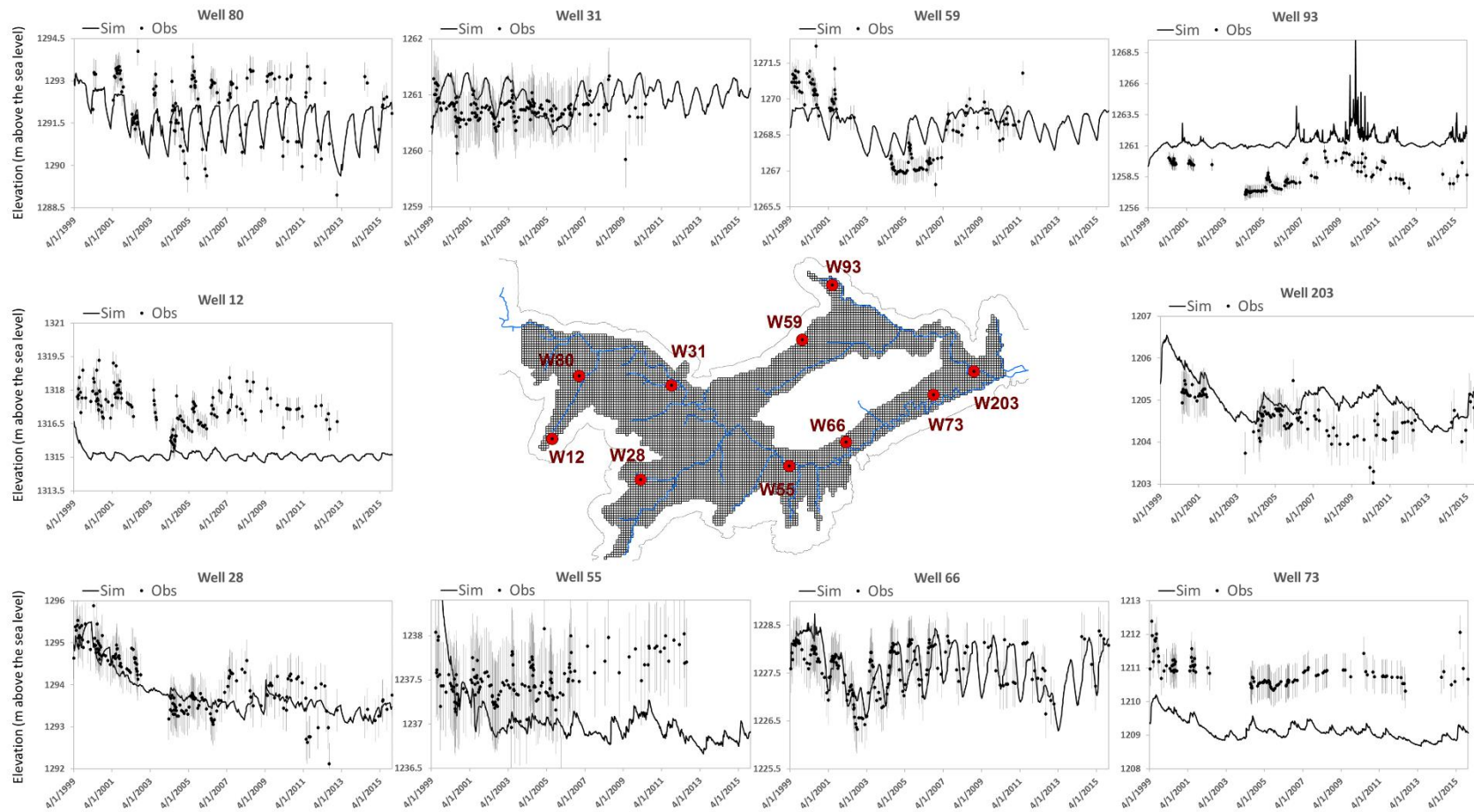
Figure 23. Spatial and temporal groundwater elevation distribution in cells containing monitoring wells at ten locations over 1999-2016 time period. Grey bars shown on observations indicate 0.5 m range.
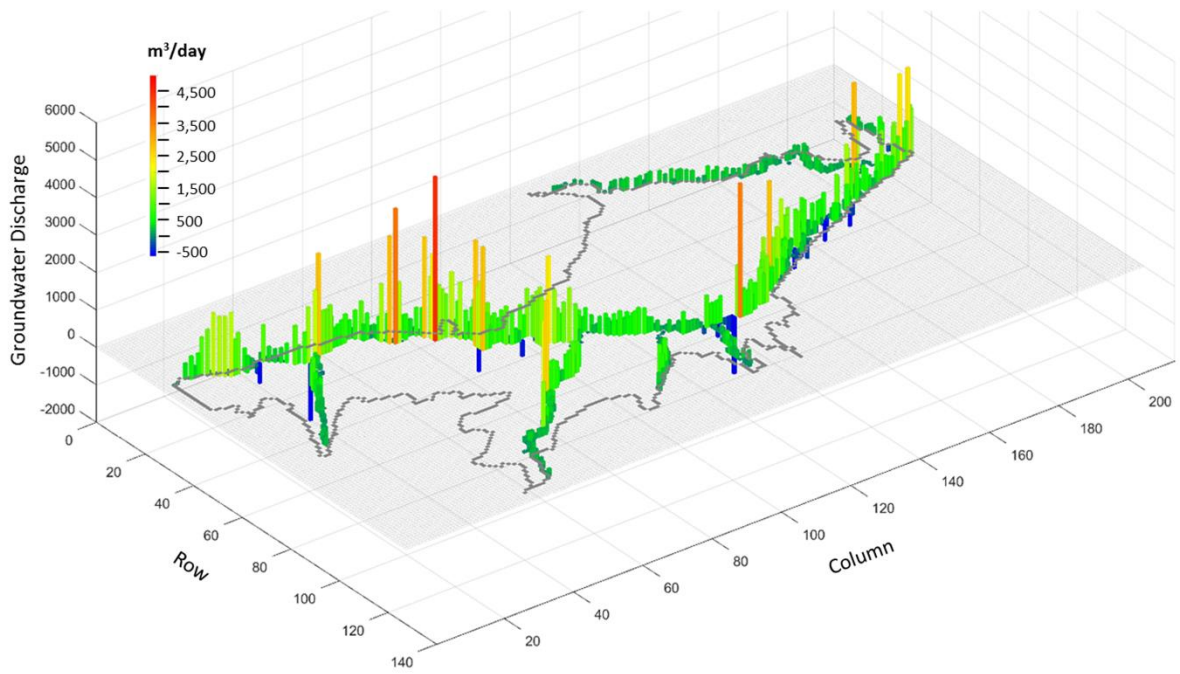
Figure 24. 3-D simulated average annual groundwater discharge (m3/day) from the aquifer to the stream over the 1999-2016 time period.
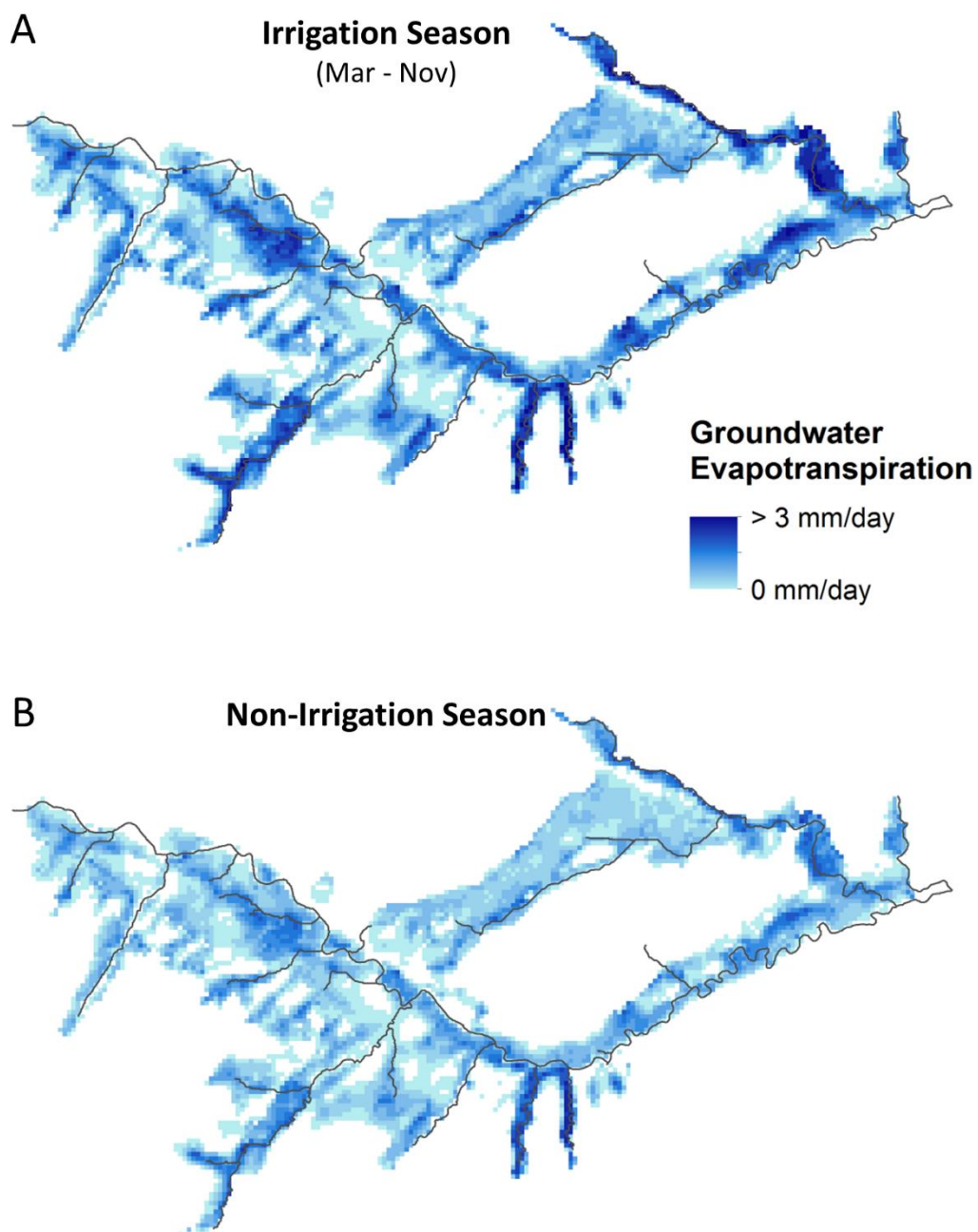
Figure 25. Departure from annual groundwater upflux to ET for the irrigation season and non-irrigation season over the 1999-2016 time period.
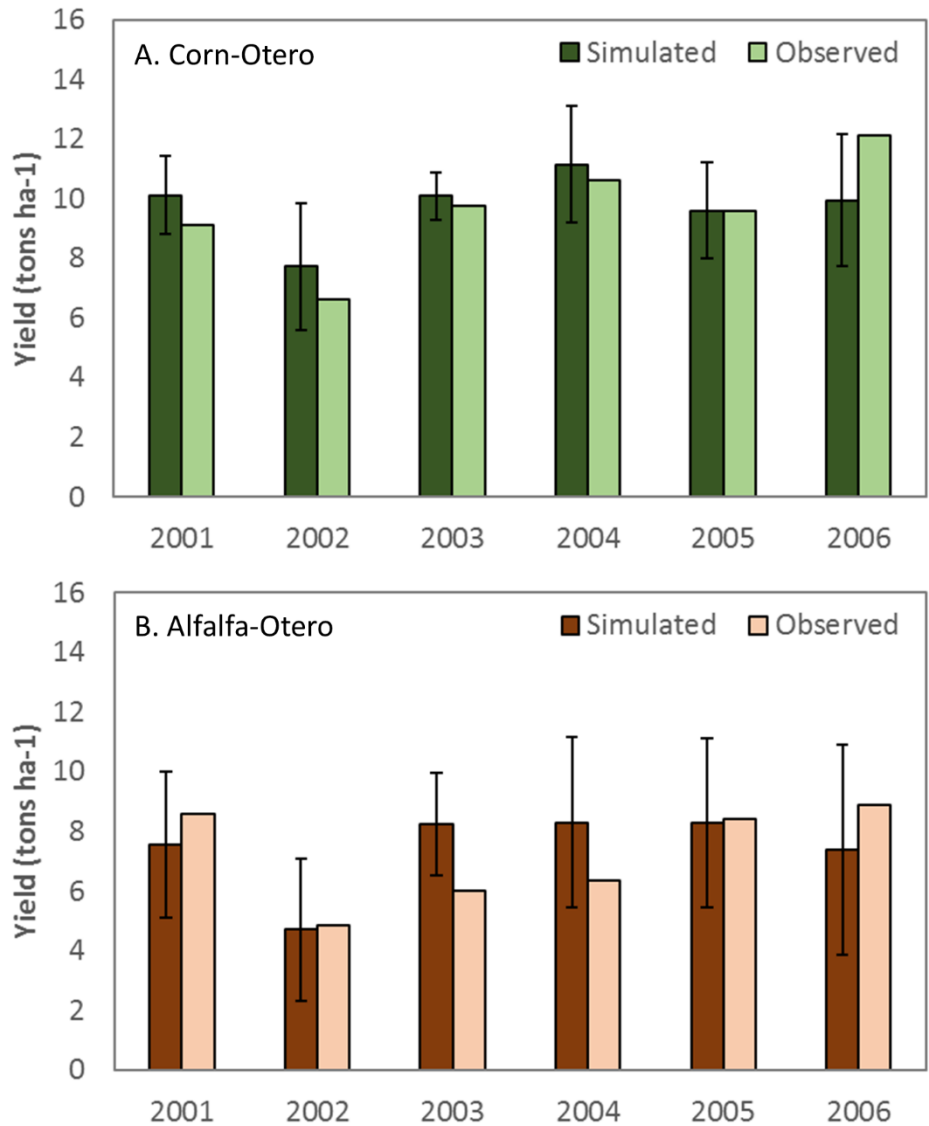
Figure 26. Average corn and alfalfa comparison between NASS reported and simulated values in Otero County over the 2001-2006 time period. Upper and lower bars indicate one standard deviation derived from simulated values.

94
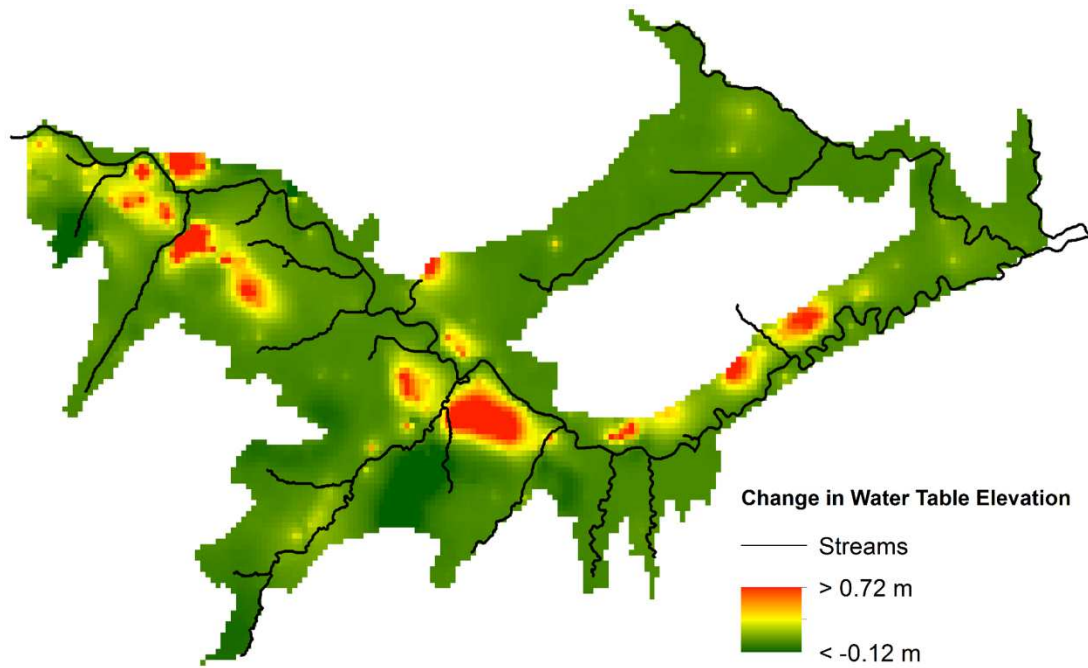
Figure 27. Average increase in groundwater level between the reduced irrigation scenario and the baseline scenario over the 1999-2016 time period.
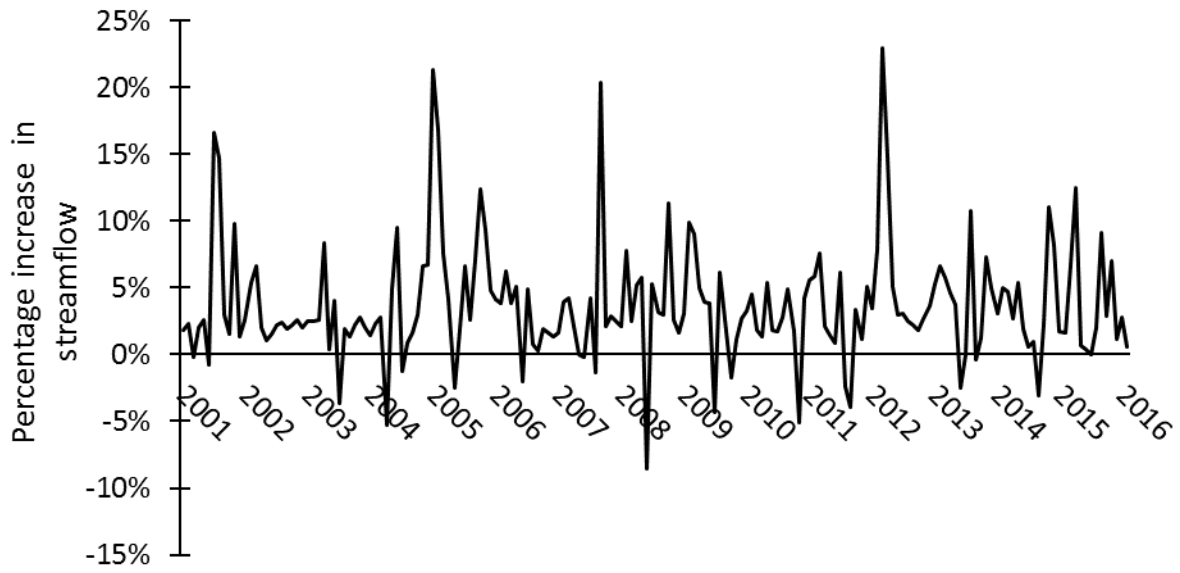
Figure 28. Percentage increase of streamflow between reduced irrigation scenario and baseline scenario indicates the impact of irrigation results to streamflow at the outlet of the watershed.
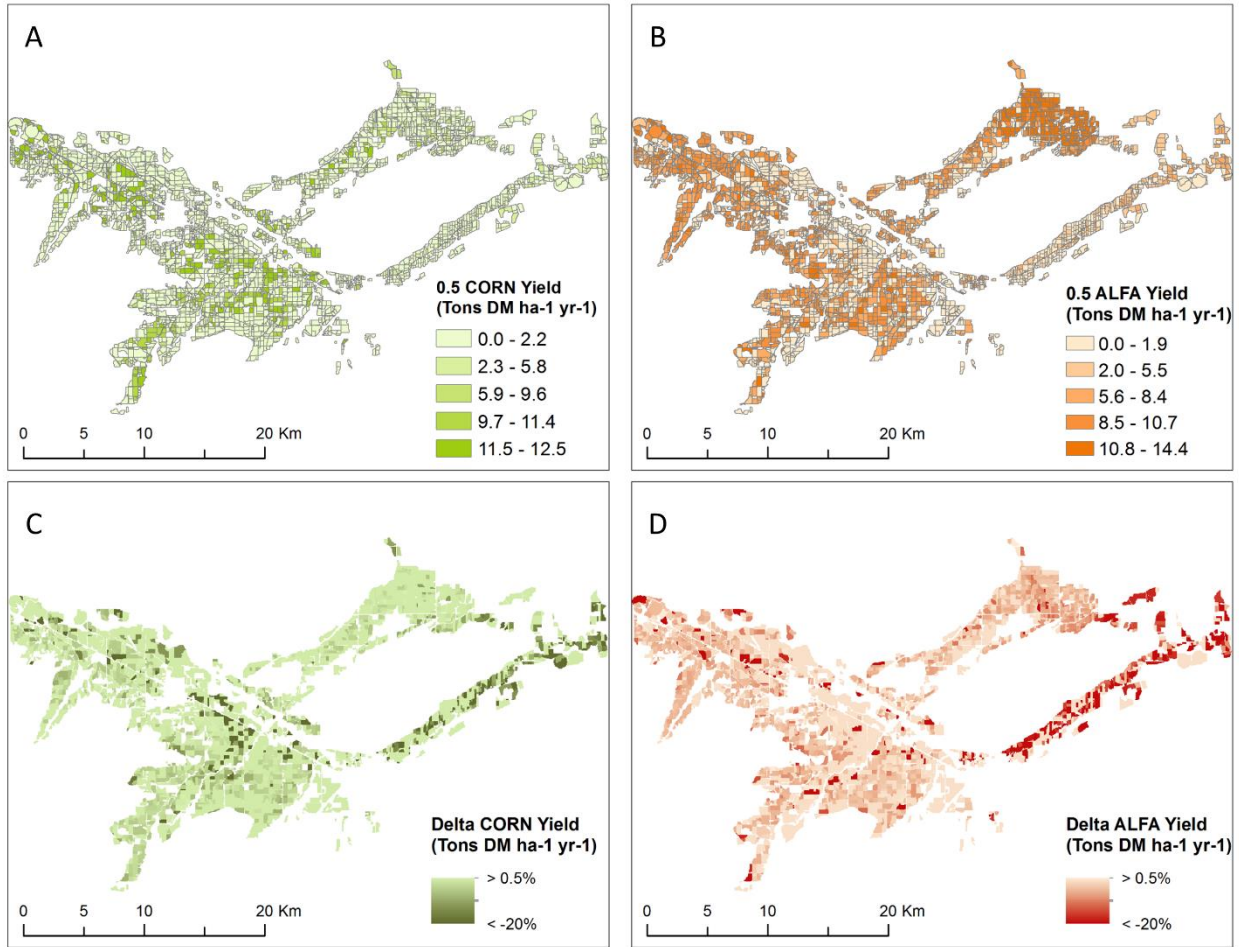
Figure 29. Spatial distribution of species-specific crop yield averaged over 1999-2016 time period for (A) corn, (B) alfalfa under 0.5 scenario. (C) and (D) shows the percentage decreases in crop yield after reducing irrigation water for corn and alfalfa, respectively.

Table 6. List of parameters that produced for SWAT-MODFLOW calibration

Parameter	Definition	Calibrated values
Parameters governing surface water response		
CN2	SCS runoff curve number for moisture condition II	+25%
EPCO	Plant uptake compensation factor	0.85
CH_N2	Manning's *n* value for the main Channel	0.22
CH_K2	Effective hydraulic conductivity of channel (mm/hr)	22.91
OV_N	Manning's *n* value for overland flow	7.86
SURLAG	Surface runoff lag coefficient	3.28
Parameters governing soil properties		
SOL_Z	Depth from soil surface to bottom of layer (mm)	2076
SOL_K	Saturated hydraulic conductivity	-19%
SOL_AWC	Available water capacity	-10%
SOL_ZMX	Maximum rooting depth of soil profile	-5%
Parameters governing snow response		
TIMP	Snow pack temperature lag factor	0.61
SFTMP	Snowfall temperature (°C)	-1.22
SMTMP	Snow melt base temperature (°C)	-0.34
SMFMX	Melt factor for snow on June 21 (mm/°C-day)	2.12
SMFMN	Melt factor for snow on December 21 (mm/°C-day)	1.58
Parameters governing groundwater response		
COND	Riverbed hydraulic conductance (m^2/s)	0.00134 - 39.55
S_y	Specific yield	0.01 – 0.36
S_s	Specific storage (1/m)	1.69×10^{-5}

Table 7. Values of performance calculated for comparing simulated and observed streamflow at the five gauging stations within the study region

Gauging Stations	Statistical Comparison	Model performance
Rocky Ford	NSE	0.823
	R^2	0.831
La Junta	NSE	0.909
	R^2	0.923
Las Animas	NSE	0.902
	R^2	0.942
Timpas Creek	NSE	0.132
	R^2	0.665
Crooked Arroyo	NSE	0.117
	R^2	0.443

REFERENCES

Abbaspour, K.C., Rouholahnejad, E., Vaghefi, S., Srinivasan, R., Yang, H., Kløve, B., 2015. A
continental-scale hydrology and water quality model for Europe: Calibration and uncertainty of a
high-resolution large-scale SWAT model. Journal of Hydrology 524, 733–752.
https://doi.org/10.1016/j.jhydrol.2015.03.027

Ahmadzadeh, H., Morid, S., Delavar, M., Srinivasan, R., 2016. Using the SWAT model to assess the
impacts of changing irrigation from surface to pressurized systems on water productivity and water
saving in the Zarrineh Rud catchment. Agricultural Water Management, Agricultural water and
nonpoint source pollution management at a watershed scale: PART I Overseen by: Brent Clothier
175, 15–28. https://doi.org/10.1016/j.agwat.2015.10.026

Ahrends, H., Mast, M., Rodgers, Ch., Kunstmann, H., 2008. Coupled hydrological–economic modelling
for optimised irrigated cultivation in a semi-arid catchment of West Africa. Environmental Modelling
& Software 23, 385–395. https://doi.org/10.1016/j.envsoft.2007.08.002

Aliyari, F., Bailey, R.T., Tasdighi, A., Dozier, A., Arabi, M., Zeiler, K., 2019. Coupled SWAT-
MODFLOW model for large-scale mixed agro-urban river basins. Environmental Modelling &
Software 115, 200–210. https://doi.org/10.1016/j.envsoft.2019.02.014

Anibas, C., Verbeiren, B., Buis, K., Chormański, J., De Doncker, L., Okruszko, T., Meire, P., Batelaan,
O., 2012. A hierarchical approach on groundwater-surface water interaction in wetlands along the
upper Biebrza River, Poland. Hydrol. Earth Syst. Sci. 16, 2329–2346. https://doi.org/10.5194/hess-
16-2329-2012

Arnold, J.G., Muttiah, R.S., Srinivasan, R., Allen, P.M., 2000. Regional estimation of base flow and
groundwater recharge in the Upper Mississippi river basin. Journal of Hydrology 227, 21–40.
https://doi.org/10.1016/S0022-1694(99)00139-0

Arnold, J.G., Srinivasan, R., Muttiah, R.S., Williams, J.R., 1998. Large Area Hydrologic Modeling and Assessment Part I: Model Development1. JAWRA Journal of the American Water Resources Association 34, 73–89. https://doi.org/10.1111/j.1752-1688.1998.tb05961.x

Bailey, R.T., Wible, T.C., Arabi, M., Records, R.M., Ditty, J., 2016. Assessing regional-scale spatio-temporal patterns of groundwater–surface water interactions using a coupled SWAT-MODFLOW model. Hydrological Processes 30, 4420–4433. https://doi.org/10.1002/hyp.10933

Baker, T.J., Miller, S.N., 2013. Using the Soil and Water Assessment Tool (SWAT) to assess land use impact on water resources in an East African watershed. Journal of Hydrology 486, 100–111. https://doi.org/10.1016/j.jhydrol.2013.01.041

Bauer, P., Gumbricht, T., Kinzelbach, W., 2006. A regional coupled surface water/groundwater model of the Okavango Delta, Botswana. Water Resources Research 42. https://doi.org/10.1029/2005WR004234

Bicknell, B.R., Imhoff, J.C., Kittle Jr, J.L., Donigian Jr, A.S., Johanson, R.C., 1993. Hydrologic simulation program-FORTRAN (HSPF): User's Manual for Release 10.

Borah, K.K., Bera, M., 2003. WATERSHED-SCALE HYDROLOGIC AND NONPOINT-SOURCE POLLUTION MODELS: REVIEW OF MATHEMATICAL BASES. Transactions of the ASAE 46, 1553–1566. https://doi.org/10.13031/2013.15644

Burkhalter, J.P., Gates, T.K., 2005. Agroecological Impacts from Salinization and Waterlogging in an Irrigated River Valley. Journal of Irrigation and Drainage Engineering 131, 197–209. https://doi.org/10.1061/(ASCE)0733-9437(2005)131:2(197)

Cai, X., McKinney, D.C., Rosegrant, M.W., 2003. Sustainability analysis for irrigation water management in the Aral Sea region. Agricultural Systems 76, 1043–1066. https://doi.org/10.1016/S0308-521X(02)00028-8

Charley, W., Pabst, A., Peters, J., 1995. The Hydrologic Modeling System (HEC-HMS): Design and Development Issues. (No. HEC-TP-149). HYDROLOGIC ENGINEERING CENTER DAVIS CA.

Chu, T.W., Shirmohammadi, A., 2004. Evaluation of the SWAT model's hydrology component in the piedmont physiographic region of Maryland. Transactions of the ASAE 47, 1057.

Dennehy, K.F., Litke, D.W., McMahon, P.B., Heiny, J.S., Toetz, T.M., 1995. Water quality assessment of the South Platte River basin, Colorado, Nebraska, and Wyoming–Analysis of available nutrients, suspended sediment and pesticide data, water years 1980–92 (No. 94–4095).

Devia, G.K., Ganasri, B.P., Dwarakish, G.S., 2015. A Review on Hydrological Models. Aquatic Procedia, INTERNATIONAL CONFERENCE ON WATER RESOURCES, COASTAL AND OCEAN ENGINEERING (ICWRCOE'15) 4, 1001–1007. https://doi.org/10.1016/j.aqpro.2015.02.126

Dozier, A.Q., Arabi, M., Wostoupal, B.C., Goemans, C.G., Zhang, Y., Paustian, K., 2017. Declining agricultural production in rapidly urbanizing semi-arid regions: policy tradeoffs and sustainability indicators. Environ. Res. Lett. 12, 085005. https://doi.org/10.1088/1748-9326/aa7287

Droogers, P., Bastiaanssen, W., 2002. Irrigation performance using hydrological and remote sensing modeling. Journal of Irrigation and Drainage Engineering 128, 11–18.

English, M., 1990. Deficit irrigation. I: Analytical framework. Journal of irrigation and drainage engineering 116, 399–412.

Fleckenstein, J.H., Krause, S., Hannah, D.M., Boano, F., 2010. Groundwater-surface water interactions: New methods and models to improve understanding of processes and dynamics. Advances in Water Resources, Special Issue on ground water-surface water interactions 33, 1291–1295. https://doi.org/10.1016/j.advwatres.2010.09.011

Francesconi, W., Srinivasan, R., Pérez-Miñana, E., Willcock, S.P., Quintero, M., 2016. Using the Soil and Water Assessment Tool (SWAT) to model ecosystem services: A systematic review. Journal of Hydrology 535, 625–636. https://doi.org/10.1016/j.jhydrol.2016.01.034

F. Schoumans, O., Silgram, M., J. Walvoort, D.J., Groenendijk, P., Bouraoui, F., E. Andersen, H., Porto, A.L., Reisser, H., Gall, G.L., Anthony, S., Arheimer, B., Johnsson, H., Panagopoulos, Y., Mimikou, M., Zweynert, U., Behrendt, H., Barr, A., 2009. Evaluation of the difference of eight model

applications to assess diffuse annual nutrient losses from agricultural land. Journal of Environmental Monitoring 11, 540–553. https://doi.org/10.1039/B823240G

Garg, K.K., Bharati, L., Gaur, A., George, B., Acharya, S., Jella, K., Narasimhan, B., 2012. Spatial mapping of agricultural water productivity using the SWAT model in Upper Bhima Catchment, India. Irrigation and Drainage 61, 60–79.

Gassman, P.W., Reyes, M.R., Green, C.H., Arnold, J.G., 2007. The soil and water assessment tool: historical development, applications, and future research directions. Transactions of the ASABE 50, 1211–1250.

Gates, T.K., Cox, J.T., Morse, K.H., 2018. Uncertainty in mass-balance estimates of regional irrigation-induced return flows and pollutant loads to a river. Journal of Hydrology: Regional Studies 19, 193–210. https://doi.org/10.1016/j.ejrh.2018.09.004

Gates, T.K., Garcia, L.A., Hemphill, R.A., Morway, E.D., Elhaddad, A., 2012. Irrigation practices, water consumption, & return flows in Colorado's lower Arkansas River Valley: field and model investigations (Technical Report No. No. TR12-10). Colorado Agricultural Experiment Station.

Geza, M., McCray, J.E., 2008. Effects of soil data resolution on SWAT model stream flow and water quality predictions. Journal of Environmental Management 88, 393–406. https://doi.org/10.1016/j.jenvman.2007.03.016

Guzman, J.A., Moriasi, D.N., Gowda, P.H., Steiner, J.L., Starks, P.J., Arnold, J.G., Srinivasan, R., 2015. A model integration framework for linking SWAT and MODFLOW. Environmental Modelling & Software 73, 103–116. https://doi.org/10.1016/j.envsoft.2015.08.011

Harbaugh, A.W., 2005. MODFLOW-2005, the US Geological Survey modular ground-water model: the ground-water flow process. US Department of the Interior, US Geological Survey Reston, VA.

Harbaugh, A.W., Banta, E.R., Hill, M.C., McDonald, M.G., 2000. MODFLOW-2000, The U. S. Geological Survey Modular Ground-Water Model-User Guide to Modularization Concepts and the Ground-Water Flow Process (No. 00–92).

Jang, S.S., Ahn, S.R., Kim, S.J., 2017. Evaluation of executable best management practices in Haean highland agricultural catchment of South Korea using SWAT. Agricultural Water Management, Agricultural water and nonpoint source pollution management at a watershed scale Part II Overseen by: Dr. Brent Clothier 180, 224–234. https://doi.org/10.1016/j.agwat.2016.06.008

Jayakrishnan, R., Srinivasan, R., Santhi, C., Arnold, J.G., 2005. Advances in the application of the SWAT model for water resources management. Hydrological Processes 19, 749–762. https://doi.org/10.1002/hyp.5624

Kim, N.W., Chung, I.M., Won, Y.S., Arnold, J.G., 2008. Development and application of the integrated SWAT–MODFLOW model. Journal of Hydrology 356, 1–16. https://doi.org/10.1016/j.jhydrol.2008.02.024

Kolditz, O., Bauer, S., Bilke, L., Böttcher, N., Delfs, J.O., Fischer, T., Görke, U.J., Kalbacher, T., Kosakowski, G., McDermott, C.I., Park, C.H., Radu, F., Rink, K., Shao, H., Shao, H.B., Sun, F., Sun, Y.Y., Singh, A.K., Taron, J., Walther, M., Wang, W., Watanabe, N., Wu, Y., Xie, M., Xu, W., Zehner, B., 2012. OpenGeoSys: an open-source initiative for numerical simulation of thermo-hydro-mechanical/chemical (THM/C) processes in porous media. Environ Earth Sci 67, 589–599. https://doi.org/10.1007/s12665-012-1546-x

Kollet, S.J., Maxwell, R.M., 2008. Capturing the influence of groundwater dynamics on land surface processes using an integrated, distributed watershed model. Water Resources Research 44. https://doi.org/10.1029/2007WR006004

Krysanova, V., Wechsung, F., Arnold, J., Srinivasan, R., Williams, J., 2000. SWIM (soil and water integrated model) (PIK-69 No. PIK-69). Potsdam-Institut fuer Klimafolgenforschung (PIK), Potsdam (Germany).

Kundu, D., Vervoort, R.W., Ogtrop, F.F., 2017. The value of remotely sensed surface soil moisture for model calibration using SWAT. Hydrological Processes 31, 2764–2780. https://doi.org/10.1002/hyp.11219

L. Chiang, I. Chaubey, M. W. Gitau, J. G. Arnold, 2010. Differentiating Impacts of Land Use Changes from Pasture Management in a CEAP Watershed Using the SWAT Model. Transactions of the ASABE 53, 1569–1584. https://doi.org/10.13031/2013.34901

L. T. Ghebremichael, T. L. Veith, M. C. Watzin, 2010. Determination of Critical Source Areas for Phosphorus Loss: Lake Champlain Basin, Vermont. Transactions of the ASABE 53, 1595–1604. https://doi.org/10.13031/2013.34898

CHAPTER 4. EVALUATING BEST MANAGEMENT PRACTICES FOR NITRATE AND PHOSPHORUS REDUCTION IN INTENSIVELY IRRIGATED STREAM-AQUIFER SYSTEMS USING SWAT-MODFLOW-RT3D

4.1. SUMMARY

In irrigated semi-arid watersheds, over-fertilization often leads to nitrogen (N) and phosphorus (P) contamination in aquifers and river systems. Watershed modelling tools often are used to evaluate the effect of management practices on nutrient contamination levels. In this study, we present a numerical model that simulates the fate and transport of nitrate (NO_3) and soluble P in an irrigated stream-aquifer system at the regional scale. The model is based on the coupled flow model SWAT-MODFLOW, with the groundwater reactive transport model RT3D included to simulate the reactive groundwater transport of NO_3 and P and their interactions with the soil zone and stream network. The SWAT-MODFLOW-RT3D is a single model executable that can be applied to watersheds wherein groundwater flow is a major component of overall watershed water yield. The model is tested in a highly-managed 732 km^2 region in the Lower Arkansas River Valley, southeast of Colorado, with model results compared to observed groundwater nutrient concentration, in-stream nutrient concentration and loading, and crop yield. A total of 28 best management practices (BMPs) scenarios are evaluated regarding their impact on NO_3 and P contamination in groundwater and river water. The most effective individual BMP in most areas is to decrease fertilizer by 30%, resulting in average NO_3-N and soluble P concentrations within the region could be reduced by 14% and 9%, respectively. This individual BMP could lower the average NO_3-N concentrations by 19% and soluble P concentrations by 2%. Combinations of using 30% irrigation reduction, 30% fertilization reduction, 60% canal seepage reduction, and conservation tillage are predicted to have the greatest overall impact to lower groundwater concentrations in NO_3-N up to 41% and soluble P concentrations up to 8%. Focusing BMPs on localized problem areas shows great promise in reducing contamination while maintaining region-wide crop yield. SWAT-MODFLOW-RT3D can be a

useful tool to examine NO_3 and P transport and quantify BMP effects in groundwater-driven watersheds worldwide.

4.2. INTRODUCTION

Nitrogen (N) and phosphorus (P) are essential elements for plant growth, but their application in agricultural areas has resulted in a serious environmental issues for both surface water and groundwater (Monaghan et al., 2005; Dechmi and Skhiri, 2013; Cerro et al., 2014). Between 1964 and 1999, irrigation activities and food production doubled, resulting in a 7-fold increase in the use of N based fertilizer and a 3-fold increase in P based fertilizer (Huizenga et al., 2017). The enrichment of N and P in the agricultural system has resulted in the eutrophication of lakes and rivers that is now acknowledged as one of the major environmental concerns throughout the world (Omernik et al., 1981; Smith, 2003; Volk et al., 2009). In Europe, more than half of all surface water bodies are impaired by nutrient pollution (Poikane et al., 2019). However, established nutrient standards of N and P vary by water type and by environmental agency. In Europe, established threshold concentrations of N range between 0.25-35 mg/L for lakes and reservoirs and 0.25-4.0 mg/L for streams and rivers, whereas in the USA the state-prepared thresholds range from 0.1-4.0 mg/L for lakes/reservoirs and 0.1-10 mg/L for streams/rivers (Poikane et al., 2019; USEPA, 2019). For P, threshold concentrations range from 5 to 500 for lakes/reservoirs and from 5 to 2500 for streams/rivers (Poikane et al., 2019; USEPA, 2019).

NO_3 and soluble P can be transported to streams via surface runoff, soil lateral flow, and groundwater return flow. NO_3 is highly mobile in soil water and groundwater with minimal sorption. When fertilizer application exceeds the crop demand and denitrification capacity of the soil, NO_3 can dissolve and leach into the underlying alluvial aquifer, and then load to streams via groundwater discharge. P is usually considered to be highly immobile, with significant sorption to soil colloids or organic matter in top soil or the shallow subsurface. High soluble P concentrations occur in surface runoff after irrigation events or rainfall events and can leach to the water table and be transported back to streams during surface and groundwater interactions. For many irrigated agricultural systems, reactive

transport of NO_3 and soluble P in the aquifer system has a strong influence on the storage of N and P, and greatly affects the timing and amount of N and P mass loading to surface water. Understanding and accounting for nutrient storage and transport is essential for assessing baseline conditions in a given watershed and identifying effective nutrient management strategies. This is especially true for highly-managed agricultural watersheds, where complex hydrologic pathways can occur between surface water and groundwater.

Numerous methods have been proposed to identify best management practices (BMPs) for nutrient management. BMPs include efficient use of irrigation water (Abdelraouf and Ragab, 2018; Li et al., 2018; Zhang et al., 2018), decreasing fertilizer loading (Almasri and Kaluarachchi, 2007; Schilling and Wolter, 2009), enhancing soil covers (Gaynor and Findlay, 1995; Bosch et al., 2013; Almendinger and Ulrich, 2017), and associated combinations (Novotny, 2002; Rong and Xuefeng, 2011; Chukalla et al., 2018; Liu et al., 2019). Often, the effect of proposed BMPs on N and P concentrations and loadings is evaluated using computational modeling tools. The Soil and Water Assessment Tool (SWAT), a watershed model that simulates water and nutrient transport via surface runoff, lateral flow, groundwater flow, and streamflow using water and nutrient balances on a daily time step, is the most commonly used model to assess nutrient BMPs, with hundreds of studies published since the year 2000 (e.g. Secchi et al. , 2007; Tuppad et al., 2010a; Waidler et al., 2011; Özcan et al., 2017), with many studies focusing solely on P (Santhi et al., 2001; Dechmi and Skhir, 2013; Rousseau et al., 2013; Lamba et al., 2016; Taylor et al., 2016; Malago et al., 2017). Other modeling tools include simplifications of SWAT for field-scale nutrient export (White et al., 2010) or simple models that link source areas to water bodies using digital elevation models and travel time indices (Kovacs et al., 2008; Buchanan et al., 2013). A final group of models use physical-based, spatially-distributed groundwater flow and solute transport models such as MODFLOW, UZF-RT3D, and RT3D-OTIS. UZF-RT3D (Bailey et al., 2014) simulates the fate and transport of nitrogen species in variably saturated groundwater systems, whereas RT3D-OTIS links UZF-RT3D with a 1D surface water transport model. These models have been used to quantify the impact of nitrogen-focused BMPs in an irrigated stream-aquifer system (Bailey et al., 2015; Shultz et al., 2018).

While each model type works well for selected watersheds, major components of N and P transport in watershed systems are either treated simplistically or are not included. SWAT simulates both N and P transport, but its simplified representation of groundwater flow processes and groundwater-surface water interaction often results in poorly performance in watershed systems wherein groundwater discharge is a significant component of stream flow (Chu and Shirmohammadi, 2004; Gassman et al., 2007). As a result, accurate timing and amount of water and nutrient loading from the aquifer to the stream cannot be produced. Conversely, aquifer-focused models such as UZF-RT3D and RT3D-OTIS simulate physically-based, spatially-distributed (PBSD) groundwater flow and groundwater-surface water interactions in heterogeneous aquifer system, but neglect key hydrologic pathways (surface runoff, lateral flow) and do not include the transport of P species. Wei et al. (2018) included NO_3 transport to SWAT-MODFLOW (Bailey et al., 2016), which includes PBSD groundwater flow, but was not applied to BMPs and did not include P transport. To our best knowledge, no study has developed a comprehensive tool for assessing the effectiveness of BMPs to reduce both N and P in a highly-managed stream-aquifer system.

The objective of this paper is two-fold: 1) present a version of SWAT-MODFLOW-RT3D that simulates fate and transport of both NO_3 and soluble P in agricultural watersheds, thereby building off the work of Wei et al. (2018a); and 2) use the model to evaluate the effect of best management practices (BMPs) on NO_3 and soluble P storage and contamination in an intensively irrigated stream-aquifer system. For the latter, nutrient concentration and loading will be assessed for both the aquifer and the river system. The model is applied to a 732 km^2 region of the Lower Arkansas River Valley (LARV) in southeastern Colorado, and builds on the work of Bailey et al. (2015a) who assessed BMP impact on groundwater NO_3 concentrations and loading, and Shultz et al. (2018), who assessed BMP impact on NO_3 concentrations in the the coupled groundwater-surface water system.

The remainder of the paper is structured as follows: a description of SWAT, MODFLOW, RT3D, and the coupled SWAT-MODFLOW-RT3D model, including N and P cycling and transport modification, is presented in section 2; Section 3 presents the application of the model to baseline

conditions in the LARV study region; Section 4 outlines proposed BMPs and a presentation of modeling

results and an overall ranking of BMPs; Section 5 provides a summary and conclusions.

4.3. SWAT-MODFLOW-RT3D FOR N AND P TRANSPORT

This section first introduces the SWAT and MODFLOW models, followed by the previous version of

SWAT-MODFLOW-RT3D for NO_3 transport (Wei et al., 2018a) and then modifications to SWAT-

MODFLOW-RT3D to simulate both NO_3 and P transport and include nutrient mass in irrigation water.

Figure 30 shows the N and P processes simulated in the new version of SWAT-MODFLOW-RT3D,

which will be explained in detail in Section 4.3.5.

4.3.1 SWAT Model for N and P Transport

The SWAT model is a physically based, spatially semi-distributed watershed model (Arnold et al.,

1998) that computes water and nutrient mass balances operating on a daily time step. The model has been

widely used to evaluate the impact of different agricultural conservation practices in large, complex

watersheds under varying management conditions (Arabi et al., 2007; Dechmi and Skhiri, 2013)(MORE).

In SWAT, the watershed is divided into subbasins based on the river network and user defined threshold

drainage area. Each subbasin is further divided into hydrologic response units (HRUs) with homogeneous

land use, slope, and soil characteristics. The HRU is the smallest landscape component of SWAT, with

output (water fluxes and nutrient fluxes) from each HRU within a subbasin summed and loaded to the

subbasin channel, and the resulting flow and loads are routed through channels to the watershed outlet.

The model integrates all relevant eco-hydrologic processes including weather, surface flow, soil erosion,

subsurface flow, infiltration, percolation, evapotranspiration (ET), crop growth and irrigation, land use

management, and nutrient transport through watersheds.

The SWAT model simulates N and P transformation through several forms between organic and

inorganic pools in the nutrient cycle within the root zone (Tuppad et al., 2010b). In SWAT, nutrients are

introduced into the system through atmospheric fixation, plant residue, and fertilization, while nutrient

loss from soil includes surface runoff, plant uptake, leaching, lateral subsurface flow, and groundwater

flow. SWAT in-stream nutrient dynamics are simulated using QUAL2E kinetic routines (Brown and Barnwell, 1987; Arnold et al., 2013) and in-stream transport algorithms.

4.3.2 MODFLOW Model

The groundwater flow model MODFLOW (Harbaugh, 2005) is a physically based, fully distributed model that solves the three-dimensional groundwater flow equation using the finite difference method. The aquifer domain is discretized laterally and vertically into finite-difference grid cells, with a water balance equation written for each grid cell. Sources and sinks can include recharge, groundwater ET, pumping, and groundwater-surface water exchange. Aquifer properties (specific yield, specific storage, hydraulic conductivity) also are specified for each grid cell. The system of equations, with one equation for each grid cell, is solved for groundwater head at each model time step. A new version of MODFLOW, MODFLOW-NWT (Niswonger et al., 2011) is well-suited for highly nonlinear problems. Results simulated by MODFLOW (i.e. groundwater head, groundwater flow rates, sources/sinks rates) can be used by groundwater solute transport models such as PHT3D (Prommer et al., 2003; Laattoe et al., 2017), MT3DMS (Pulido-Velazquez et al., 2015; Ehtiat et al., 2018), and RT3D (Clement, 1997; Bailey et al., 2014b). Among these, RT3D solves multi-species chemical reactions simultaneously using an ordinary differential equation (ODE) solver, thus allowing for the concentration of multiple chemical species to be updated simultaneously. Therefore, it allows the concentration of a solute to influence the reaction rates of other chemical species.

4.3.3 SWAT-MODFLOW Model

Several studies have presented a linked modeling system between SWAT and MODFLOW (Sophocleous and Perkins, 2000; Kim et al., 2008; Bailey et al., 2016). The most recent version (Bailey et al., 2016) imbeds the MODFLOW subroutines within the SWAT modeling code, with SWAT calling MODFLOW during each daily time step. Recharge and potential ET from each HRU are passed to MODFLOW grid cells via mapping routines, and groundwater head and groundwater-surface water exchange rates are passed from MODFLOW grid cells to SWAT HRUs and SWAT subbasin channels, respectively. SWAT routines then route water through the subbasin channels, to the watershed outlet.

Therefore, SWAT simulates surface runoff and soil lateral flow to subbasin channels, whereas MODFLOW simulates groundwater discharge to subbasin channels. Within this framework, MODFLOW also simulates river seepage to the aquifer, if the water table adjacent to a stream is below the stream stage. This version of SWAT-MODFLOW has been used worldwide in recent years (Semiromi and Koch, 2019; Gao et al., 2019; Chunn et al., 2019; Aliyari et al., 2019; Molina-Navarro et al., 2019) to assess watershed water resources and quantify the impact of pumping and climate change on streamflow and groundwater levels.

4.3.4 RT3D Model

The numerical code Reactive Transport in 3 Dimensions (RT3D) simulates the groundwater reactive transport of one or more solutes by solving the advection-dispersion-reactive (ADR) mass balance equation (Clement, 1997; Clement et al., 1998). RT3D uses the same finite-difference grid as the MODFLOW mode, which provides cell-by-cell groundwater hydraulic head, 3D flux rates, and groundwater sources and sinks (e.g. recharge, pumping). The ADR equations for a set of solutes in saturated porous media are written as:

$$\frac{\partial C_k}{\partial t} R_k = -\frac{\partial}{\partial x_i}\left(v_i C_k\right) + \frac{\partial}{\partial x_i}\left(D_{ij}\frac{\partial C_k}{\partial x_j}\right) + \frac{q_s}{\phi}C_{s_k} + r_k \qquad k = 1,2,\ldots,m \tag{1}$$

where m is the total number of aqueous-phase species, C_k $[M_f L_f^{-3}]$ is the solute concentration of the kth species in aqueous phase; D_{ij} $[L^2 T^{-1}]$ is the hydrodynamic dispersion coefficient, which can be assumed to be independent of solute concentration; v $[L_b T^{-1}]$ is the average groundwater velocity where b denotes the bulk phase; ϕ $[L_f^3 L_b^{-3}]$ is soil porosity; q_s $[L_f^3 T^{-1} L_b^{-3}]$ is the volumetric flux of water representing sources and sinks of the species; C_{s_k} $[M_f L_f^{-3}]$ is the concentration of the source or sink; r_k $[M_f L_f^{-3} T^{-1}]$ represents the rate of all reactions that occur in the aqueous phase for the kth species; and R_k is the retardation coefficient for the kth species, representing linear sorption with aquifer sediment surface sites. Therefore, the change of solute concentration through time is represented by the four terms on the right-hand-side of Equation (1): advection, dispersion, sources and sinks mixing, and kinetic chemical reactions.

4.3.5 SWAT-MODFLOW-RT3D

4.3.5.1 Previous Version: Nitrogen Transport

The study of Wei et al. (2018) included RT3D into the SWAT-MODFLOW (Bailey et al., 2016) modeling framework for comprehensive transport of NO_3 in a watershed setting (i.e. surface runoff, soil lateral flow, spatially-distributed groundwater flow). The RT3D model subroutines are imbedded into the MODFLOW routines, with RT3D called each daily time step. MODFLOW passes groundwater head, groundwater flux rates, and groundwater sources/sink rates to the RT3D grid cells, which then solves for NO_3 groundwater concentration at each grid cell and groundwater NO_3 loadings to streams, with the latter passed to SWAT subbasin channels for in-stream NO_3 loading through the watershed stream network. The model was applied to the Upper Klamath Basin in southern Oregon, with model output tested against in-stream NO_3 loadings and groundwater NO_3 concentration (Wei et al., 2018). The following ADR equation was used for NO_3 groundwater transport:

$$\frac{\partial C_{NO_3}}{\partial t} R_{NO_3} = -\frac{\partial}{\partial x_i}\left(v_i C_{NO_3}\right) + \frac{\partial}{\partial x_i}\left(D_{ij} \frac{\partial C_{NO_3}}{\partial x_j}\right) + \frac{q_s}{\phi} C_{s_{NO_3}} + r_{NO_3} \tag{2}$$

with the rate law for denitrification defined using a single-Monod expression:

$$r_{NO_3} = -\mu_{NO_3} C_{NO_3}\left(\frac{C_{NO_3}}{K_{NO_3} + C_{NO_3}}\right) \tag{3}$$

where μ_{NO_3} is the first-order rate constant (d^{-1}) for denitrification and K_{NO_3} is the Monod half-saturation constant [$M_f L_f^{-3}$] for NO_3. Since NO3 does not sorb, R_{NO_3} in equation (2) is set to 0 for all grid cells.

4.3.5.2 Model Modifications

P Transport

For this study, the SWAT-MODFLOW-RT3D modeling code of Wei et al. (2018) was amended to include transport of soluble P in the aquifer and P mass loading exchange between the aquifer and the stream network. The cycling and transport of N and P species in the land surface / soil / aquifer system as

simulated by SWAT-MODFLOW-RT3D is shown in Figure 30. Within this system, nutrient mass enters the subsurface via atmospheric fixation and fertilizer loading. Within the soil zone, organic P can be mineralized to soluble P, which then can attach to mineral surfaces via sorption. Organic N can undergo ammonification to ammonium (NH_4), which can be changed to nitrate (NO_3) through nitrification and then denitrified to nitrogen gas (N_2). NO_3, NH_4, and soluble P can be either taken up by crop roots and be removed from the system through harvest processes or loaded back to the stream network through lateral flow in the soil zone. Meanwhile, those species can leach downward to the water table through deep percolation and return via upflux, where they undergo 3D transport in the saturated zone and can be loaded back to the stream via groundwater discharge. NO_3 and P mass can also be transferred from the aquifer to the land surface via groundwater pumping for irrigation.

In addition to the ADR equation for NO_3 (equation 2), the following ADR is included for soluble P transport in the groundwater system:

$$\frac{\partial C_{PO_4}}{\partial t} R_{PO_4} = -\frac{\partial}{\partial x_i}\left(v_i C_{PO_4}\right) + \frac{\partial}{\partial x_i}\left(D_{ij}\frac{\partial C_{PO_4}}{\partial x_j}\right) + \frac{q_s}{\phi}C_{s_{PO_4}} + r_{PO_4} \tag{4}$$

Unlike NO_3, soluble P sorbs strongly to soil and aquifer sediments, and hence R_{PO_4} is > 1. As solute P has no appreciable reduction rate in groundwater system, r_{PO_4} is set to 0. Although this study simulates only NO_3 and P transport in the aquifer, other reactive solutes could be implemented into the RT3D reaction module.

N and P Mass in Irrigation Water

Another modification to the SWAT-MODFLOW-RT3D code for this study is the inclusion of NO_3 and P mass in irrigation water. For many watersheds, the high concentration of NO_3 and P in river water and groundwater can add appreciable amounts of solute mass to the land surface during irrigation events. In particular, if pumped groundwater is used for irrigation, irrigation water chemistry can be changed significantly due to the typically much higher concentration of nutrients in groundwater than in surface

water (McMahon and Böhlke, 1996). However, the original SWAT modeling code does not account for nutrient mass in irrigation water.

In this study, the SWAT modeling code was modified to account for the loading of NO_3 and soluble P mass to the soil profile via irrigation water from both surface water (canal diversions) and groundwater (aquifer). If the irrigation water source is a subbasin reach (surface water irrigation), the concentration (mg/L) of NO_3 and soluble P is used to calculate nutrient mass (kg ha^{-1}) that can be added to the first soil layer of the corresponding HRU, with the applied nutrient mass removed from the source of the corresponding reach. If the irrigation water is provided by the shallow aquifer (groundwater irrigation), the nutrient mass (kg ha^{-1}) of NO_3 and P each species is added to the first soil layer of the corresponding HRU and then subtracted from the corresponding shallow aquifer. For both sources, the nutrient mass in the irrigation water (kg ha^{-1}) is calculated as the product of concentration in the reach water and the volume of applied irrigation water, divided by the HRU area.

4.4. SWAT-MODFLOW-RT3D APPLICATION TO IRRIGATED STREAM-AQUIFER SYSTEM

4.4.1 Description of study region

The Lower Arkansas River Valley (LARV) in southeastern Colorado has a long history of rich agricultural production, and currently faces challenging issues due to extremely shallow water tables resulting from more than 100 years intensive irrigation, seepage from earthen canals, and inefficient drainage systems (McMahon and Böhlke, 1996; Gates et al., 2012; Bailey et al., 2012).

The study area is a semi-arid region located within the LARV in southeastern Colorado (Figure 31A), with average annual precipitation of 273 mm. The average temperature is 13.6 °C, with the monthly temperatures ranging from -12.6 °C in January to 35.9 °C in July. It encompasses a total of 732 km^2, of which about 330 km^2 is agricultural fields with intensive cultivation. Major crops in order of planted area are alfalfa, followed by sorghum, corn, grass/pasture, sunflower, melons, oats, onion, and soybeans (USDA NASS COLORADO FIELD Office 2007, see Figure 31B). The growing season commences mid to late-March and ends in early November, with earthen irrigation canals receiving water

115

from the Arkansas River during the period of March 15th to November 15th. The vast majority of irrigation water is derived from one of six principal irrigation canals (Rocky Ford Highline, Catlin, Otero, Rocky Ford Ditch, Fort Lyon, and Holbrook), with supplemental irrigation water provided by > 500 groundwater pumping wells (Figure 31A).

Over-fertilization on cultivated fields has resulted in high surface and groundwater NO_3 concentrations, assessed by numerous monitoring data (stream sample sites, groundwater observation wells). In the study region, the first set of field data was collected and analyzed for NO_3-N between June 2006 and July 2011, with a total of 270 surface water samples (NO_3-N and soluble P) and 598 groundwater samples (NO_3-N and soluble P) were taken. Samples were taken from 20 surface sites and 25 monitoring wells (Figure 31C) during 18 sampling events. Samples from an addition 64 observation wells were taken during several sampling events during this same period (Figure 31C). The second set of field data was gathered between June 2014 and February 2016, with both concentrations of NO_3-N and soluble P sampled at the same surface sites (a total of 71 samples) and at the same monitoring wells (a total of 193 samples). From both data sets, the average NO_3-N and soluble P concentration in surface water is 1.83 mg L^{-1} and 0.16 mg L^{-1}, respectively. Compared to the Colorado interim nutrient standard of 2.01 mg L^{-1} and 0.17 mg L^{-1} for total N and total P, 34% and 30% of samples exceeded the standard for NO_3 and soluble P, respectively. For groundwater, average monitored concentrations for NO_3-N and soluble P are 4.83 mg L^{-1} and 0.13 mg L^{-1}, with maximum values of 66 mg L^{-1} and 1.1, respectively. More details of observed data will be presented with model results in Section 4.4.4.

4.4.2 SWAT-MODFLOW-RT3D model set up for the LARV

A previously calibrated and tested SWAT-MODFLOW model for the LARV study region is used to link with RT3D to simulate nutrient fate and transport in the study region. The SWAT-MODFLOW is detailed in Wei and Bailey (2019), constructed by linking a calibrated SWAT model (Wei et al., 2018b) that accounts for canal seepage and crop rotations, with a calibrated MODFLOW model (Morway et al., 2013) for the study area. The model includes new subroutines for groundwater irrigation and groundwater evapotranspiration and provides a detailed description of surface and groundwater flow processes, thereby

116

enabling a specific description of watershed processes including streamflow, ET, surface runoff, soil later flow, infiltration, recharge, 3D groundwater flow in a heterogeneous aquifer system with various sources and sinks, groundwater ET, and spatio-temporal groundwater and surface water interactions.

The spatial extent of the SWAT-MODFLOW model, which is used in this study for SWAT-MODFLOW-RT3D, is shown in Figure 31C. The model domain contains 5270 HRUs and 72 subbasins, with each cultivated field designated as an individual HRU. Thus, management operations such as irrigation application, plant growth, fertilizer application, harvest and kill, and tillage operation can be applied to each HRU to mimic real-world conditions. Specific management operations for each crop type is listed in Table 8, with the values provided via expert opinion from research scientists at the Arkansas Valley Research Center (AVRC) located within the study region. The management input file (.mgt) for HRUs accommodates crop rotation in continuous years. An example of the management file with corn and onion rotation is provided in Table 9. The auto-irrigation algorithms in SWAT were used to trigger irrigation events based on plant water demand for both surface water and groundwater irrigation.

The MODFLOW finite difference grid contains 7777 active cells horizontally (see Figure 31C), with a uniform cell size of 250 m x 250 m. The aquifer is discretized vertically into 3 layers: 2 for the alluvial aquifer and one for the shale bedrock, which is approximately 15 m below ground surface. Canal seepage from each of the six earthen canals is simulated using MODFLOW's River package, with the corresponding canal diverted flows specified as point sources in SWAT. SWAT simulated stream stages are treated as an input of MODFLOW River package to represent canal water elevations. For groundwater irrigation, daily pumping rates are specified in MODFLOW's Well package, with the volume converted to depths and applied to SWAT HRUs (Wei et al., 2018b). Example output of stream discharge (at the watershed outlet near Las Animas, Colorado), water table depth, and recharge rates from the calibrated SWAT-MODFLOW model are shown in Figure 32. For the stream hydrograph, NSE and R^2 are 0.9 and 0.94 respectively, which is considered to be 'very good' (Moriasi et al., 2015). The shallowest water table occurs along the river corridors of the Arkansas River and the tributaries, with the deepest water table occurring away from the river network.

117

The simulation period for SWAT-MODFLOW-RT3D is from April 1999 to February 2016, with the first two years specified as a warm-up period. Initial groundwater NO_3 and P concentrations for each RT3D grid cell are provided by an 18-year spin up simulation. This spin up period was prepared by repeating the weather, crop management operation, and pumping stresses for the year 2005 for 18 years until the groundwater solute concentrations achieved a steady seasonal fluctuation. Then, the output solute concentrations were used to provide initial concentration for the calibration period of simulation. Initial values for μ_{NO_3}, K_{NO_3}, and the sorption partition coefficient for soluble P k_{d,PO_4} were set to 0.0005, 10, and 1.5, respectively.

Model calibration was carried out using a combination of manual and automated methods. One-at-a-time sensitivity analysis was performed manually for the parameters governing nutrient fate and transport in SWAT and RT3D, respectively. Up to 20 values within a realistic range were assigned to each parameter, while keeping the other parameters constant, to test the sensitivity of the in-stream mass loading to each parameter (Tuppad et al., 2010b; Douglas-Mankin et al., 2010; Dechmi et al., 2012; Özcan et al., 2017). Parameters shown in Table 10 were found to be the most influential on nutrient in-stream loading at the outlet of the study region. Then, automated parameter estimation was performed with the SWAT Calibration and Uncertainty Procedures (SWAT-CUP) software tool, using the Sequential Uncertainty Fitting Algorithm (SUFI2) (Abbaspour et al., 2015). This allows modifications for SWAT parameters only. The in-stream mass loading at the outlet was first calibrated by SWAT-CUP with the parameters listed in Table 10 (five iterations with a total of 2500 simulations), following the procedure used in the original SWAT model for the study region (Wei et al., 2018b). Monthly NO_3-N mass loading was provided by Gates et al. (2018), who performed a stochastic mass balance on the Arkansas River network system using measured stream discharge rates, river stages, NO_3-N concentrations, and electrical conductivity in the streams. Monthly soluble P loading was estimated using the program LOAD ESTimator (LOADEST) (Runkel et al., 2004) by combining the observed in-stream concentrations with daily flow rates, with soluble P concentration available from June 2014 to February

2016. Then, manual calibration was performed using the groundwater transport parameters μ_{NO_3}, K_{NO_3}, and k_{d,PO_4}, based on published values (McMahon and Böhlke, 1996; McMahon et al., 1999; Bailey et al., 2014a). Finally, SWAT-CUP was re-run with 500 simulations to fine-tine SWAT nutrient parameters. To evaluate the improvement of SWAT-MODFLOW-RT3D model over the original SWAT model, the calibrated parameter set was applied directly to the SWAT model with the modified irrigation method (described in section 2.1). Model performance is estimated using statistical measures Nash-Sutcliffe efficiency NSE (Nash and Sutcliffe, 1970) and coefficient of determination R^2.

The model is tested against observed groundwater nutrient concentrations, in-stream nutrient concentrations, in-stream nutrient loadings, and crop yield. Simulated crop yields are compared with county-level observed data provided by the National Agricultural Statistical Survey (NASS) (https://quickstats.nass.usda.gov/). Alfalfa and corn are selected since they are the two major crops in the Otero County, wherein resides the majority of irrigated fields in the model domain. Since SWAT reports crop yield in tons per hectare, the following equation is used to convert bushels per acre to tons per hectare:

$$1\frac{bushel}{acre} = \frac{62.77}{1000} \times \frac{tons_{dry-corn}}{hectare} / (1 - moisture) \qquad (5)$$

During harvest time, the SWAT model simulates crop yield at 20% moisture content (Neitsch et al., 2011; Srinivasan et al., 2010); therefore, the simulated crop yield is multiplied by 0.8 to compare with the dry mass in the equation above. No targeted calibration was performed for crop yield.

4.5. BASELINE MODEL RESULTS

4.5.1 Groundwater nutrient concentrations

A cell-by-cell modelled results for average nutrient concentration is shown in Figure 33(A) and Figure 34(A). It indicates the spatial distribution of simulated groundwater NO_3-N and soluble P averaged over the 1999-2016 simulation period, with the NO_3-N concentrations ranges from 0.01 to 59.3 mg L^{-1} and soluble P values ranging from 0 to 2.12 mg L^{-1}. As can be seen from the figures that high

concentration values of both species typically located along the river corridor. Further comparison between simulated nutrient concentration at four groundwater monitoring wells spread throughout the study region are exhibited in Figure 33(B-E) for NO_3-N and in Figure 34(B-E) for soluble P, with the location of wells shown in Figure 33(A) and Figure 34(A). These comparisons indicate an acceptable match between the simulated and observed values for the magnitude of each species. For NO_3-N simulation, increases and decreases in concentration are generally captured by the coupled model, while simulated soluble P does not have seasonal fluctuation during the simulation period. There are still several locations and periods that have a significant mismatch between observed and simulated values (Well 74 for soluble P), which is common in regional scale modelling studies that the aquifer properties within a 250-m grid cell between observation and simulation are dissimilar. The observed nutrient concentrations from observation wells have uncertainty and the averaged observation solute value over a spatial grid cell area is hard to know.

When comparing the average of the measured values in the observation wells (4.83 mg L^{-1} for NO_3-N and 0.13 mg L^{-1} for soluble P) with the average simulated values from all grid cells (4.91 mg L^{-1} for NO_3-N and 0.12 mg L^{-1} for soluble P), it seems match with each other really well. Figure 35 shows the global comparison of frequency distribution of NO_3-N and soluble P concentration in the groundwater respectively, with distributions plotted using the observed values from all of the monitoring wells (see Figure 31C) (a total of 746 measurements for NO_3-N and 124 for soluble P) and the simulated values from the second layer of the coupled model (pumping well is located in layer 2). Previous comparisons are performed based on the annual average concentrations, whereas this frequency plots analyzes the relative frequency of concentrations within a given interval in order to demonstrate the model performance of the spatiotemporal statistics of each species. According to the figure, the general shape and magnitude of frequency for each concentration interval is similar to the frequency from the observed data, especially for NO_3-N. However, soluble P concentration is overestimated for the low range (< 0.1 mg L^{-1}) and underestimates for the mid-range (0.1 – 0.25 mg L^{-1}), indicating the SWAT-MODFLOW-RT3D model predicts a large amount of simulated low soluble P concentration grid cells in the beyond

the stream corridors (Figure 35A). The bias is likely due to the majority of monitoring well are located along the stream corridors and the relative frequency of the low values is not as much as the observed values.

4.5.2 Groundwater nutrient mass loading to surface water

Averaged spatial distribution of simulated mass loading of NO_3-N and soluble P to the river system occur along the Arkansas River and the tributaries during the 1999-2016 period are shown in Figure 36. Values are plotted for 731 river cells within the study region. Blue bars indicate mass loading from stream into aquifer, whereas green-yellow-red bars represent mass loading from the aquifer into the river network. It shows that the vast majority of nutrient loading happens from the aquifer into the river (i.e. positive values), the averaged NO_3-N mass ranging from -97 kg to -907 kg and solute P mass ranging from -5.4 kg to 36.8 kg. In this study region, the nutrient mass loading is highly spatial variable due to different local hydrological conditions and groundwater nutrient concentrations.

For the entire study area, the 18 years average daily loading is 17.4 kg for NO_3-N and 0.34 kg for soluble P. The individual subbasin loading has tremendous variability ranging from -8.3 kg to 196.3 kg and -0.2 kg to 4.8 kg for NO_3-N (Figure 36C) and soluble P (Figure 36D), respectively. Thus, the figures provides a very good spatial pattern for high-loading subbasins. The highlighted subbasins in Figure 36C and Figure 36D are the top 6 regions that respectively contains 50% and 60% of total mass loading of NO_3-N and soluble P from the aquifer into the watershed, and these severe areas could be potentially targeted for further BMP reduction.

4.5.3 Nutrient in-stream loading and concentration

Monthly time series plots of simulated and measured nitrate and solute phosphorus in-stream loading at the outlet of the watershed is shown in Figure 37(A) and Figure 38(A), respectively. Black line with round dots represent the observation values and red lines with triangle dots represent simulations from the SWAT-MODFLOW-RT3D model. As can be seen from the figures, the coupled model is able to track the spatiotemporal variability and magnitude of in-stream loading for both species quite well. The statistical NSE for nitrate in-stream loading during calibration and validation period is 0.51 and 0.72, represent

'good' and 'very good' performance based on Moriasi (2015). Solute phosphorus in-stream loading is considered to be 'very good' for NSE of 0.82. There is a marked improvement for SWAT-MODFLOW-RT3D model as compared to the nutrient in-stream results with SWAT model (Wei et al., 2018b) (green lines with rectangular dots in Figure 37(A) and Figure 38(A)). The SWAT model consistently underestimates the nitrate and solute phosphorous in-stream loading, especially during the irrigation season. A statistical comparison of simulated in-stream loading at the outlet is given in Table 11.

The coupled model is further tested by comparing the daily simulated and observed nutrient in-stream concentration at another two stream gauges SW-12 and SW-63 (location is shown in Figure 31C). The horizontal black line and dot line respectively represent the Colorado interim standard in warm water and in code water. Time series comparisons for NO_3-N concentration are plotted from January 2006 to February 2016 (Figure 37B,C) whereas soluble P concentrations are only compared from January 2014 to February 2016 (Figure 38B,C) due to the availability of the observation data. In general, simulated results are within the estimated standard error of the measured head values of ±1.6 mg L^{-1} and ±0.2 mg L^{-1} for nitrate and solute phosphorus, respectively, demonstrating the ability of the SWAT-MODFLOW-RT3D model to accurately simulate in-stream loading. Moreover, the coupled model has a better performance for NO_3-N simulation compared with soluble P, which could like because of the lower number of soluble P samples and lack of observed sediment data, which can be used for more accurate calibration.

4.5.4 Crop yield

Annual comparison between observed and simulated corn yield and alfalfa yield is presented in Figure 39. Due to the data availability from NASS, results during 2001 to 2006 are compared in this study. Black boxes and grey boxes are representing simulated corn and alfalfa yields under the baseline scenario, respectively, while purple dash line and orange dash lines represent observed corn and alfalfa values. Based on the figures, the coupled model was able to predict variations in crop yield, with annual average yield of 9.7 tons ha^{-1} for corn and 7.3 tons ha^{-1} for alfalfa. As explained before, we specified different management scenarios including the irrigation water and fertilizer input, planting and harvest time, etc., which helps to improve the crop yield results.

4.6. QUANTIFYING THE EFFECT OF BMPS ON NO_3 AND P

This section describes the method of implementing and analyzing the BMPs, with results presented and discussed. Analysis is performed in terms of the ability of a given BMP to decrease NO_3-N and soluble P in-stream concentrations, groundwater concentrations, solute mass loadings from groundwater to the surface river systems, and solute mass loading into each subbasin. Results are compared with baseline model results described in Section 4.5. Following an analysis of domain-wide BMP implementation, results of spatial BMP targeting also will be presented.

4.6.1 Description of BMP simulations

The tested Best Management Practices (BMPs) in this study are related to irrigation management, nutrient management, water conveyance efficiency, and tillage operations. A total of 28 BMP scenarios were evaluated (Table 12), with 20 combination BMPs.

Irrigation management consists of using the optimum irrigation practices, for example by replacing the traditional flood irrigation to more efficient drip/sprinkler irrigation. This improved efficiency can be achieved by adjusting the irrigation efficiency (IRR_EFF) and the surface runoff ratio (IRR_ASQ) through auto-irrigation operations in the SWAT management files. For irrigation reduction (IR) scenarios, IRR_ASQ were decreased by 10% and 30% (IR10 and IR30) and IRR_EFF were increased by 10% and 30%, respectively, so that the decreased irrigation water would lower surface runoff and soil percolation, which result in net reductions of solute transportation and mass loading into stream systems.

In Colorado, farmers commonly apply fertilizers in excess of what is required for optimal crop yield (Halvorson et al., 2002). Nutrient management to reduce the availability of excess nutrients is simulated by by controlling the applied fertilizer amount (FRT_KG) in the SWAT management files. Two different fertilization reduction (FR) scenarios were developed by reducing the fertilizer amount by 10% (FR10) and 30% (FR30). These levels of reduction are judged reasonable to avoid appreciable crop yield decrease. Analysis of the impact on crop yield will be discussed with results.

Seepage loss from earthen irrigation canals in the LARV varies from 0.012 $m^3s^{-1}km^{-1}$ to 0.04 $m^3s^{-1}km^{-1}$ (Susfalk et al., 2008) and provides a considerable source of recharge to shallow groundwater. In this

study, seepage reductions (SR) were specified to 40% (SR40) and 60% (SR60), which can be achieved by lowering the canal bed conductance in the MODFLOW RIVER package (Morway et al., 2013). In the LARV, seepage reduction is possible through canal lining and sealing, which has been tested by Martin and Gates (2014) by using linear anionic polyacrylamide to decease seepage losses (Martin 2014). The higher percent of seepage reduction indicates a higher level of labor and material investment.

Land use management scenarios involving conservation tillage (CT) and no tillage (NT) operations were developed. In the current situation, the tillage operations are being carried out with conventional tillage including disk plow and moldboard plow. These two practices increase the amount of residue on the surface between the period of harvest and planting the next crop (Tuppad et al., 2010b). Conservation tillage leaves at least 30% of the soil surface covered with crop residue while no tillage is carried out by planting crop in the soil without any tillage operation. In SWAT, these tillage operations differ in terms of the mixing efficiency (EFFMIX) and depth of mixing (DEPTIL), which specify the fraction of residue on surface that are mixed uniformly through the soil depth. Specific values for each parameter are listed in Table 11.

Scenarios 1-8 include individual BMPs application, with each BMP analyzed over a conservative and an aggressive level. Scenarios 9-12, 13-24, and 25-28 represent the adoption of 2, 3, and 4 concurrent BMPs, respectively. Due to the uncertainty associated with the land use management, tillage operations were considered as a single BMP with no respective level assigned to it. In order to limit the total number of BMP combinations associated with the computational time, only BMPs with the same respective levels of implementation (i.e. irrigation management, nutrient management, and water conveyance efficiency) were combined together for 3 BMPs and 4 BMPs in this study.

The impact of BMP implementation on water quality is presented as percent reductions from the calibrated baseline SWAT-MODFLOW-RT3D model for the same period (1999-2016). Each BMP was simulated individually with all inputs except the parameters used to represent a BMP kept constant of the calibrated value. The percent reduction was calculated as follows:

$$Reduction(\%) = \frac{\sum_{i=1}^{n} \frac{preBMP_i - postBMP_i}{preBMP_i} \times 100}{n} \qquad (6)$$

Where *preBMP* and *postBMP* are model outputs for month *i* before and after implementation of

BMP, respectively. *n* is the total months during the simulated period. A positive value indicates that the

BMP reduced the outputs compared to the baseline condition where as a positive value indicates that the

BMP results in increased outcomes.

4.6.2 BMP Results

4.6.2.1 Changes in nutrient groundwater concentrations

Average percent reduction in NO_3-N and soluble P in the aquifer for each of the BMP scenarios

throughout the 18-yr simulation period is summarized in Figure 40. The average nutrient reduction rates

were computed using the simulation values in the second layer of the model, which is the depth that

monitoring wells located at. For each BMP set, the impact on reducing groundwater concentrations

increases with the increasing level of implementation, which is similar to (Bailey et al., 2015a, 2015b). Of

the individual BMPs, FR10, and SR40 were found to be effective at decreasing NO_3-N groundwater

concentration by 4% and 3%, respectively, and decreasing soluble P by 1% and 1%, respectively, under

scenarios with the conservative level of implementation. FR30 and IR30 under the aggressive level of

implementation could decrease the amount of nutrient leaching into the aquifer system, as a result, NO_3-N

concentration reduced by 19%, 12%, respectively, and soluble P reduced by 2% and 1% respectively. The

conservation IR10 scenarios (Scenario 1) yield a negligible decrease, with 0.4% rate for NO_3-N and

0.05% for soluble P. As a reminder, irrigation reduction scenario is essentially increase the irrigation

efficiency rate. 10% of increase in irrigation efficiency could likely result in several issues

including lower the water content and increase the leaching time (Bailey et al., 2015a). It is

interesting to note that compared with the NT scenario (Scenario 8), the CT scenario (Scenario 7)

resulted in a better reduction in groundwater nutrient concentration, which is because of the

increased infiltration simulated by NT scenario causing more nutrient leaching into the aquifer

system. When comparing Figure 40A and Figure 40B, it can be seen that all the BMP scenarios are more efficient to reduce the NO_3-N concentrations that the average percent reduction for NO_3-N was 15% with the highest rate of 41%, whereas for soluble P the average percent was only 3% with the highest rate of 8%. This is because the majority of soluble P was attached to soil surface when leaching through the soil profile.

The cell-wise spatial distribution in nutrient concentration decreases are illustrated in Figure 41 A,C for the selected combined BMP of IR30-FR30-SR60-CF scenario (Scenario 27), the highest reduction scenario. It shows the difference in the computed time-averaged groundwater concentration for the baseline scenario shown in Figure 35A and Figure 36A for NO_3-N and soluble P, respectively. Decreases in concentrations are represented by blue-green-yellow colors while increases in concentrations are showed in orange-red colors. The contour plots exhibit a large spatial variability of lowing the nutrients concentrations by this BMP, with an average concentration decrease in NO_3-N and soluble P of 1.81 mg L^{-1} and 0.005 mg L^{-1}, respectively. Although increases in concentration occur in a few of grid cells, some locations also show a substantial decrease (up to 18 mg L^{-1} for NO_3-N and 0.29 for soluble P). Furthermore, the majority regions were experiencing a decrease of above 90% for NO_3-N and above 40% for soluble P, respectively. These results also shown in the histogram of cell-by-cell percent reduction (Figure 41 B,D). For NO_3-N, 81% of the cells have a decrease greater than 20% and 54% of the cells have a decrease greater than 50%. Soluble P reduction is impressive as well that 31% of cells have a decrease greater than 10% and 82% of the cells have a decrease greater than 3%.

4.6.2.2 Changes in nutrient mass loading to surface water

Simulated reductions in NO_3-N and soluble P mass loading to the river system occurred along the Arkansas River and its tributaries from aquifer system over the 18 years simulation period

are summarized in Figure 42A. Of the individual BMP scenarios, the seepage reduction

scenarios were quite efficiency in decreasing both nutrient loading from groundwater to the

streams, with reduction rate of 39% for NO_3-N and 34% for soluble P, respectively, for

aggressive SR scenario (Scenario 6), and 14% for NO_3-N and 16% for soluble P, respectively,

for conservative SR scenario (Scenario 5). Seepage reductions could result in a decrease in deep

percolation to the groundwater system. Therefore, lower water tables resulting from the

decreased seepage rate could cause a decrease in return flow and thus lead to a corresponding

decrease in nutrient mass loading to rivers. The most effective type of combined BMP occurred

to be the aggressive IR30-FR30-CT-SR60 (Scenario 27), with the reduction of 63% for NO_3-N

and 49% for soluble P, respectively. Reduction in mass loading can be achieved by changing the

return flow rate entering into the stream system and by changing the nutrient concentration in the

return flow. Since IR10 and NT scenarios did not sufficiently affect groundwater concentration,

their impact on mass loading were negligible as well.

Selected temporal variability of simulated reductions in nutrient mass loadings from aquifer to

the rivers are shown for scenarios IR30, SR60, FR10-SR40-NT, and IR30-FR30-CT-SR60 in

Figure 42 B,C. As can be seen from the figure, the combined 4 BMP had the strongest impact on

decreasing NO_3-N and soluble P concentrations, followed by the 3 BMP scenario. For

implementations of IR30 and SR60, water losses from the baseline condition were diverted as

part of gross irrigation application and returned to the river could be left in the river to reduce

return flow. IR30 had higher impact for NO_3-N mass loading while SR60 was more efficient for

soluble P, since soluble P had significant lower reduction rate in groundwater leads to a lower

soluble P concentration within the return flows.

Figure 43 summarized the removal efficiency of nutrient mass loading from aquifer into each subbasin for the selected BMPs. As shown in the figure, the 4 BMP scenarios is the most efficient one, with the average reduction rate of 34% for NO3-N and 17% soluble P, respectively. The subbasin loading plots displays substantial spatial variability in the effectiveness of lowing mass loading, representing the BMPs have larger influence in some part of the watershed than others.

4.6.2.3 Changes in nutrient in-stream concentrations to the river system

The overall average percent reductions in NO_3-N and soluble P in-stream concentration at the outlet of the study region (See Figure 31B) are summarized for each of the 28 BMPs in Figure 44A. Figure 44A shows that IR10 has negative effect on reduce NO_3-N and soluble P in-stream concentration and actually result in a slightly increase of the concentration at the outlet. This increase is likely due to the increase of irrigation efficiency is not improved enough to match with the decrease of runoff ratio so that the same amount of fertilizer being applied to field cannot be diluted by the surface runoff, resulting in a higher nutrient concentration in the surface water. It has been demonstrated by IR10-FR10 (Scenario 9) that in-stream concentration has been reduced by 14% and 9% for NO_3-N and soluble P, respectively, with an extra 10% fertilizer reduction combined with 10% irrigation reduction. The FR30 is found to be the most effective individual BMP for lowing NO_3-N (25%) and soluble P (20%) at the aggressive level, followed by SR60 (17% for NO_3-N and 8% for soluble P) and CT (14% NO_3-N, 5% for soluble P). Scenario 27 again is the most effective type of combined BMP, resulting in an average reduction of 52% and 40%, respectively, at the aggressive level.

The influence of NT (Scenario 8) is negligible for in-stream NO_3-N (0.14%) and soluble P concentration (2%) as well. CT (Scenario 7) seems to be better than NT since the simulated percent reductions were 14% for NO_3-N and 5% for soluble P, respectively. This result was first

due to the fact that CT practice did mix the residues properly with the soil compared with NT operations. The build-up of residues for NT practice were easily getting into the stream with surface runoff, resulting in increased the nutrient concentrations in the surface water (Powlson and Jenkinson, 1981). The relatively low impact of NT on nutrient mass loading into river also affect the nutrient concentration in surface water since this study area is a groundwater dominant region. In general, CT has a higher impact on nutrient concentrations for this study area. However, if combined with the other BMPs, the reduction rates increases from 5% and 5% for NO_3-N and soluble P, respectively of the conservative scenario 12, to 48% and 35% for NO_3-N and soluble P of the aggressive scenario 24.

Time series NO_3-N and soluble P median concentrations simulated over both Arkansas River and the tributaries under baseline scenario and selected conservative and aggressive BMPs are shown in Figure 44 B and C, respectively. In order to show the reduction more clearly, these figures are plotted through the 2006 to 2016 period. The conservative BMPs include scenario 9 (IR10-FR10) and Scenario 21 (IR10-SR40-CT) and the aggressive BMPs include Scenario 4 (FR30) and Scenario 27 (IR30-FR30-SR60-CT). As can be seen from the figure, all the scenarios showed a continuous reduction over the simulation period, with the most impressive reduction generated by Scenario 27 that the entire simulated NO_3-N and soluble P median concentrations were predicted under the Colorado standard (grey dash line in Figure 44B and C). The plot also reveal a slightly trend that the impact of BMPs was increasing gradually over the simulation period, due to the very slow movement of flow and nutrients in groundwater. Therefore, conservative BMPs could also work to achieve the Colorado standard for a longer time period.

4.6.2.4 Changes for spatially targeted BMPs

In general, combinations of the aggressive IR30-FR30-CT-SR60 (Scenario 27) is predicted to have the greatest overall impact to the nutrient reduction, while FR30 (Scenario 4) is the most

effective singular BMP. The impact of Scenario 27 on the crop productions is presented in

Figure 39. The average reduction in crop yield are 24% and 4% for corn (red boxes) and alfalfa

(green boxes), respectively. In the case of alfalfa, the lower impact is due to it is a perennial

legume fixing nitrogen from the air, N fertilizers are generally only needed for early stage of its

establishment (Davis et al., 2005). In addition, Scenario 4 resulted in a 36% corn reduction for

the entire region. For the economic sustainability of irrigated agriculture, it is important to

consider the impact of the BMP scenarios on farmer's profits.

Since uniformly applying BMPs throughout the entire watershed have significant influence on

corn production, 6 subbasins, as discussed in section 3.4.3 were selected to apply the most

efficient combined BMP (4 BMPs) and individual BMP (FR30), and left the rest subbasins to be

the baseline condition in order to remediate water quality while maintain the majority of crop

yield. Figure 45 shows the predicted NO_3-N and soluble P median concentration for the

Arkansas River and its tributaries after specified targeted FR40 and targeted 4 BMPs. For

example, purpose line and black line respectively represent the NO_3-N median temporal

distribution after uniformly and targeted applied FR40 BMPs, while black dash line is the

baseline condition and grey line is the Colorado interim standard for total N. Figure 45 reveals

the targeted BMPs also have impact on reducing in-stream concentrations, but not as substantial

as the reduction of uniformly applied BMPs. Since the plots also reveals a trend of increasing

impact over time, it will take longer time for uniformly applied BMPs for their full effects to be

reached. Groundwater cell-wise reduction based on the targeted 4 BMP scenario is presented in

Figure 41B,D with red boxes represent NO_3-N and green boxes represent soluble P, respectively.

It indicates similar results with in-stream concentration reduction that the targeted applied BMPs

is decreasing the nutrients' concentrations, however, their effectiveness is less than the uniformly

applied BMPs. With regarding to corn production, the impact of the targeted 4-BMP scenario and targeted FR30 scenario lead to a 13% and 20% reduction rate, better than the uniformly 4-BMP scenario. Overall, crop production and nutrient remediation is strongly impacted by the region of investigated implementation. When applying BMPs only in 6 targeted subbasins, many areas of the study region can have a significant decrease in NO_3-N and soluble P. Therefore, regional impact can potentially be achieved by focusing BMPs on localized problem areas.

4.7. SUMMARY AND CONCLUSIONS

This paper presents a physically-based, spatially-distributed model that simulates NO_3 and soluble P fate and transport in a coupled stream-aquifer system and applies the model to investigate the impact of water and land management BMPs on NO_3 and P in this system. The SWAT-MODFLOW-RT3D model (Wei et al., 2018) was modified to include soluble P groundwater transport, and accounts for the major processes that govern NO_3-N and soluble P movement, transformation, and storage in intensively managed irrigated stream-aquifer systems, including application of irrigation water from surface canals and pumping wells, crop growth and rotation, seepage of canal water, infiltration and percolation of irrigation water, loading of N and P fertilizer, sorption, denitrification, and groundwater-surface water interactions. Due to the elevated nutrient concentrations in the irrigation system, the cycling of N and P mass in irrigation water was also included in the modeling code.

The model was tested in a 732 km^2 irrigated stream-aquifer system in the Lower Arkansas River Valley, Colorado during the 1999 – 2016 time period, with model output compared to observed groundwater concentration, in-stream loading, in-stream concentration, and crop yield for both NO_3 and P. The tested model was used to evaluate the potential impact of water and land best management practices (BMPs) to decrease NO_3-N and soluble P concentrations in the

groundwater, mass loading to river, and stream concentrations relative to baseline conditions. BMPs include nutrient management and aggressive irrigation management (IR30), and conservation tillage are showed to be efficient at lowing NO_3-N concentration in groundwater while water conveyance efficiency are simulated to effectively decrease soluble mass loading into river. Conservative irrigation management (IR10) and no tillage are not impactful as other BMPs. Results also demonstrate that FR30 and SR60 implementation can have a significant reduction on in-stream concentration. Benefit of BMPs in combination with one another is also revealed by this study. The IR30-FR30-CT-SR60 combination seems to be have the most significant reduction for both NO_3-N and soluble P contamination. However, efficient corn productivity cannot be achieved by the combination implementation. Modelling results can help policy makers to effectively design programs to maximize nutrient reductions and minimize the cost in compensating the farmers for their yield loss.
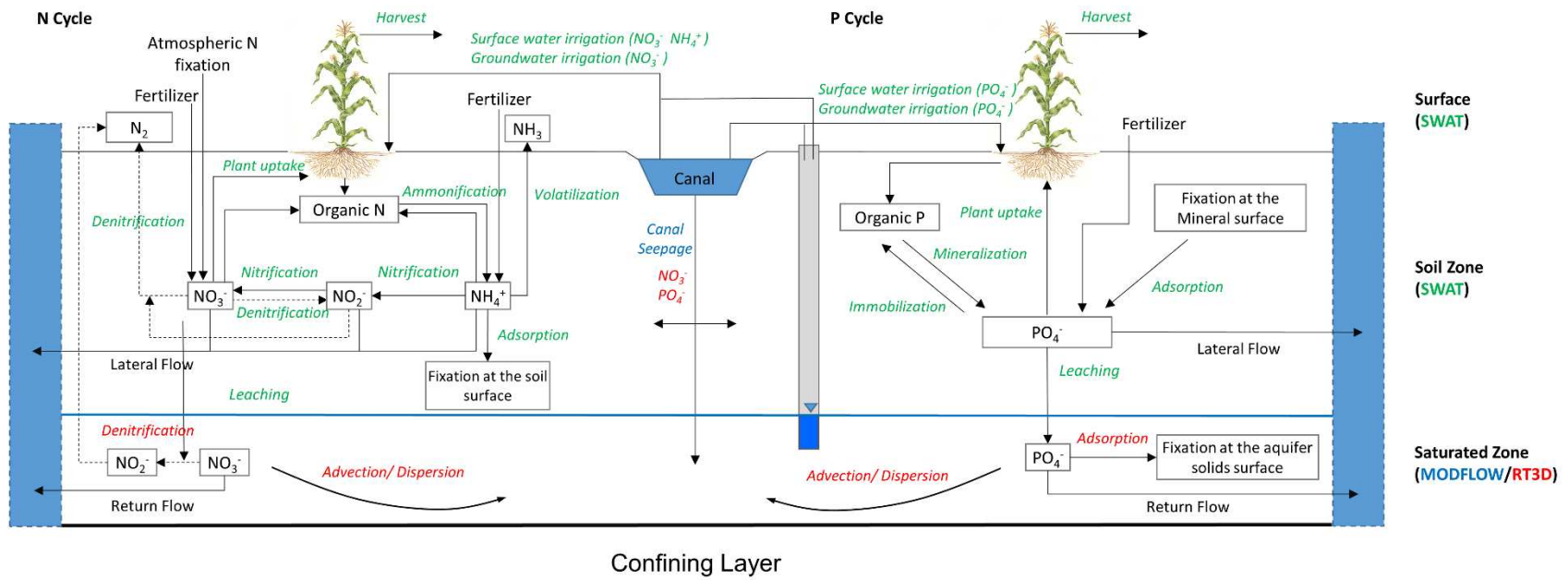
Figure 30. Nitrogen and phosphorus transformation simulated in SWAT-MODFLOW-RT3D model.
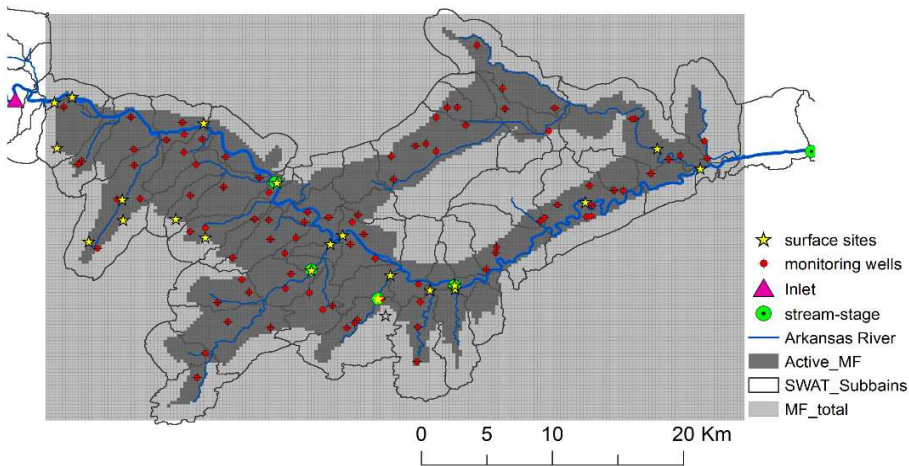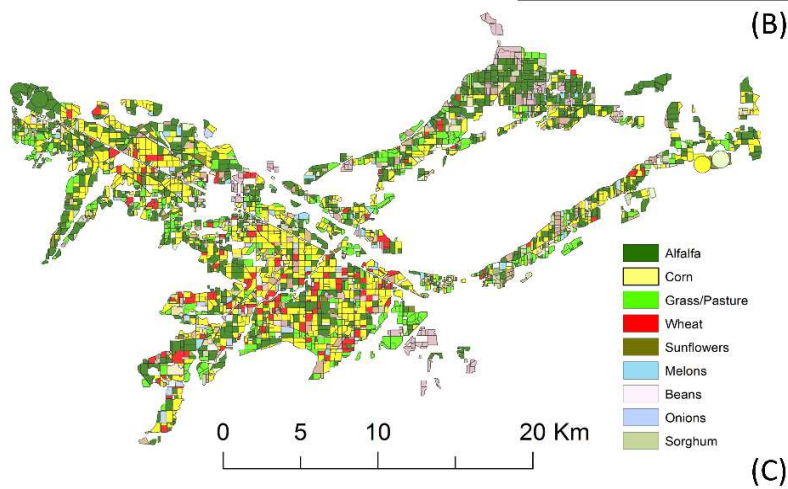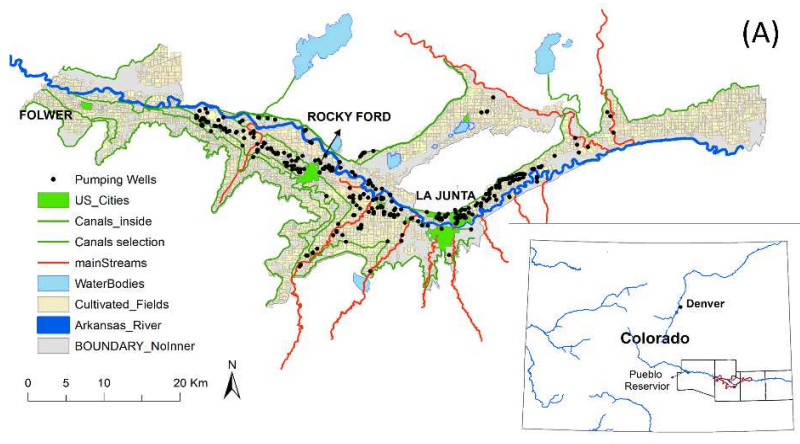
Figure 31. (A) Location of the study region in Colorado; (B) crop type for each cultivated field for the year 2001; (C) subbasins created by SWAT and MODFLOW grid cells; surface water sites and monitoring wells are also shown
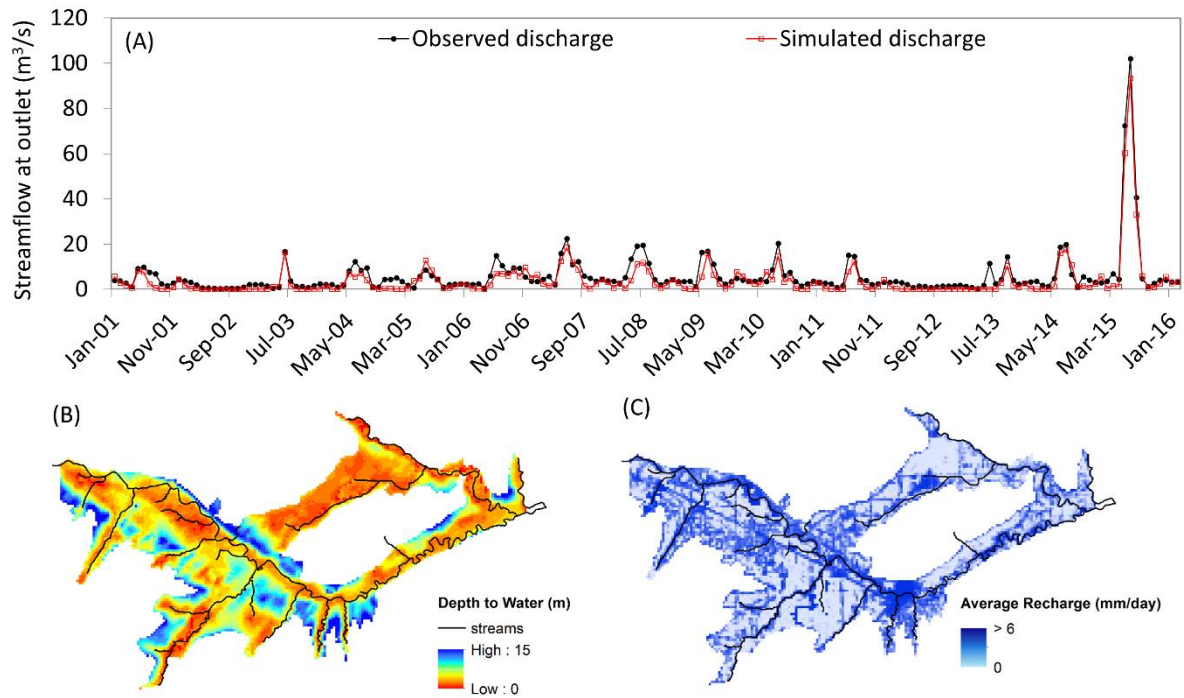
Figure 32. (A) Observed and SWAT-MODFLOW simulated time series of stream discharge (m3/s) at the outlet of the study area, from Wei et al. (2018); Annual average cell-wise plots for active MODFLOW grid cells in the study region over the 1999–2016 time period: cell-by-cell maps of (B) depth to groundwater table and (C) recharge rates.
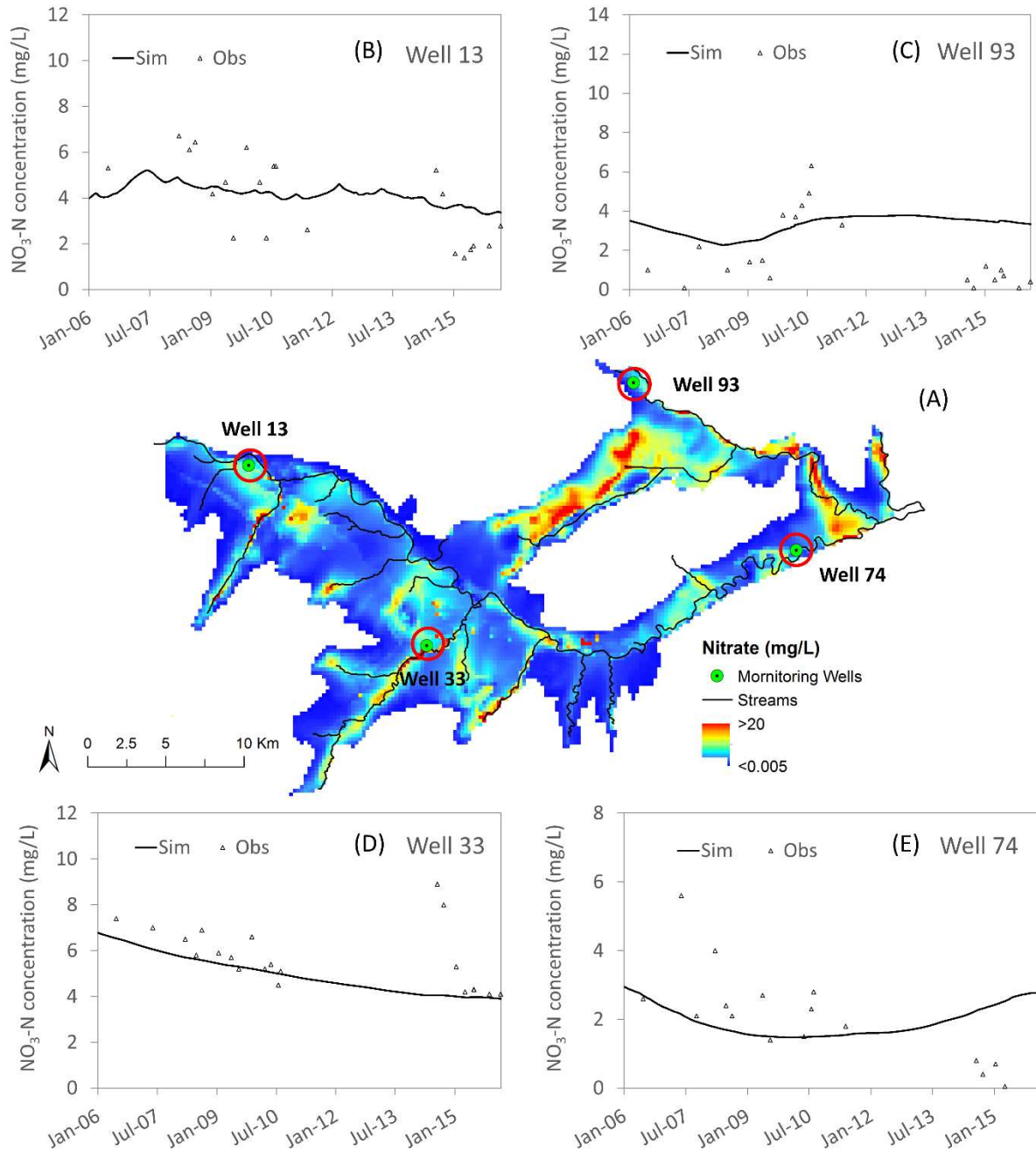
Figure 33. (A) Average cell-wise groundwater NO_3-N concentrations with the observation wells' locations; (B), (C), (D), and (E) are the model performances in predicted NO_3-N concentrations at different monitoring wells
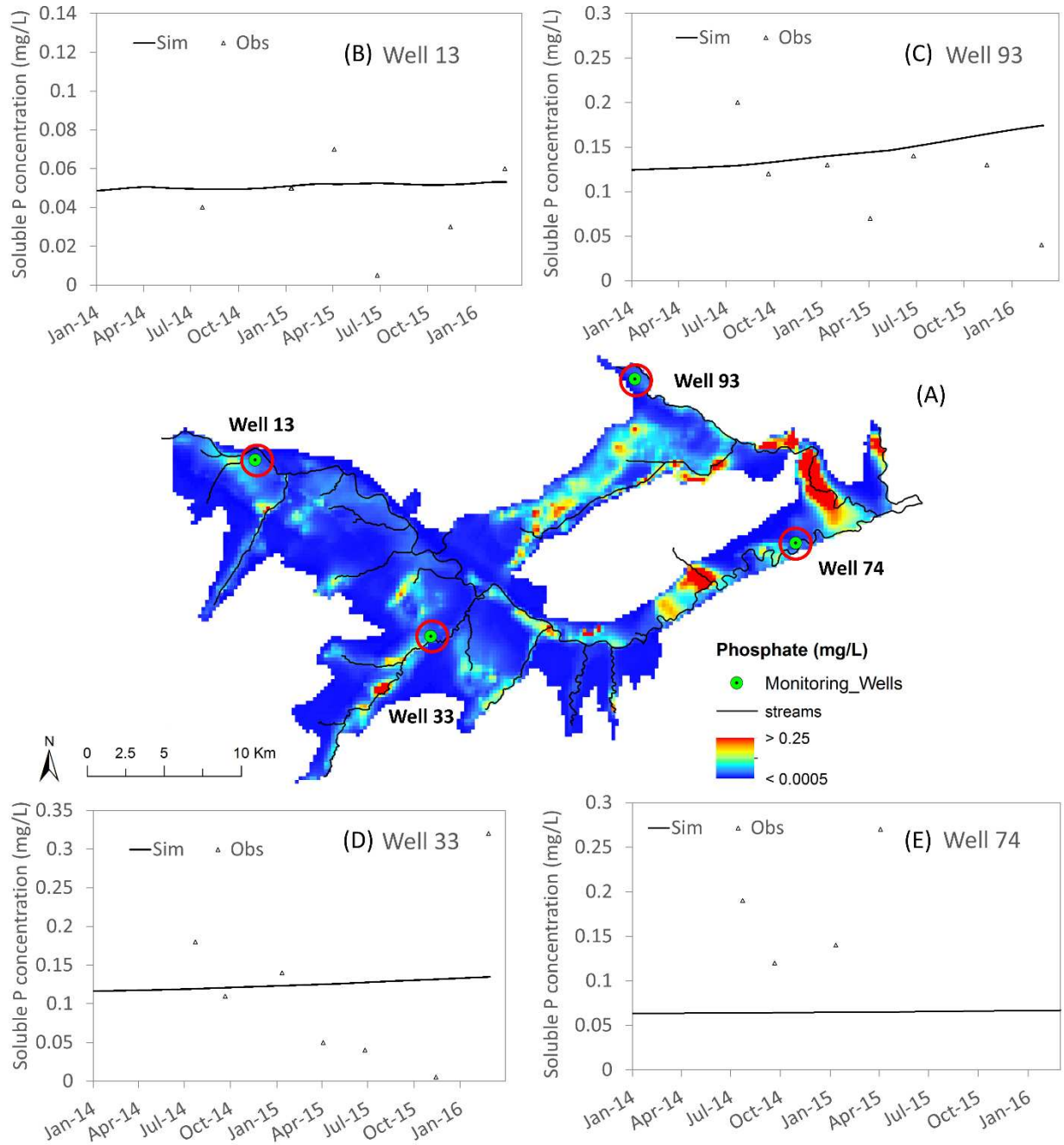
Figure 34. (A) Average cell-wise groundwater soluble P concentrations with the observation wells' locations; (B), (C), (D), and (E) are the model performances in predicted Soluble P concentrations at different monitoring wells
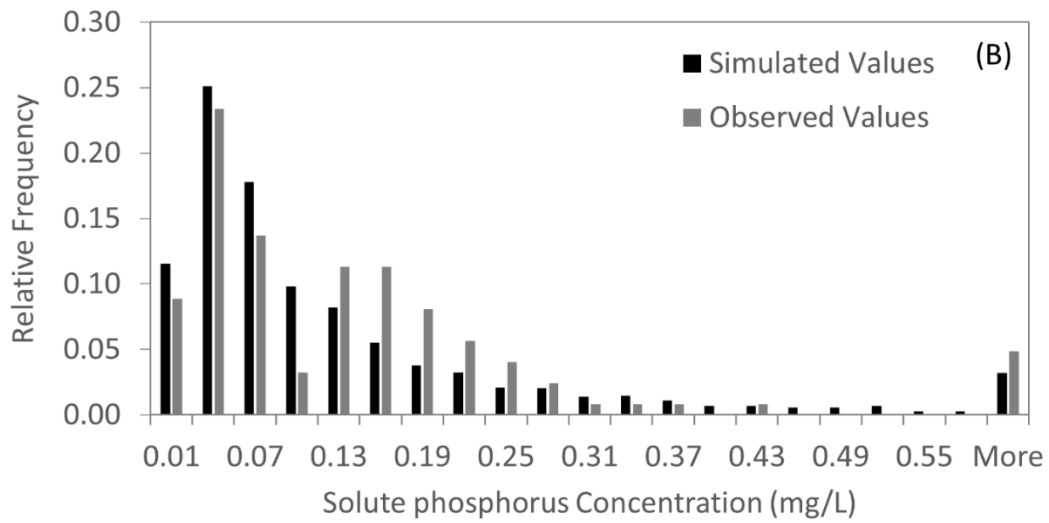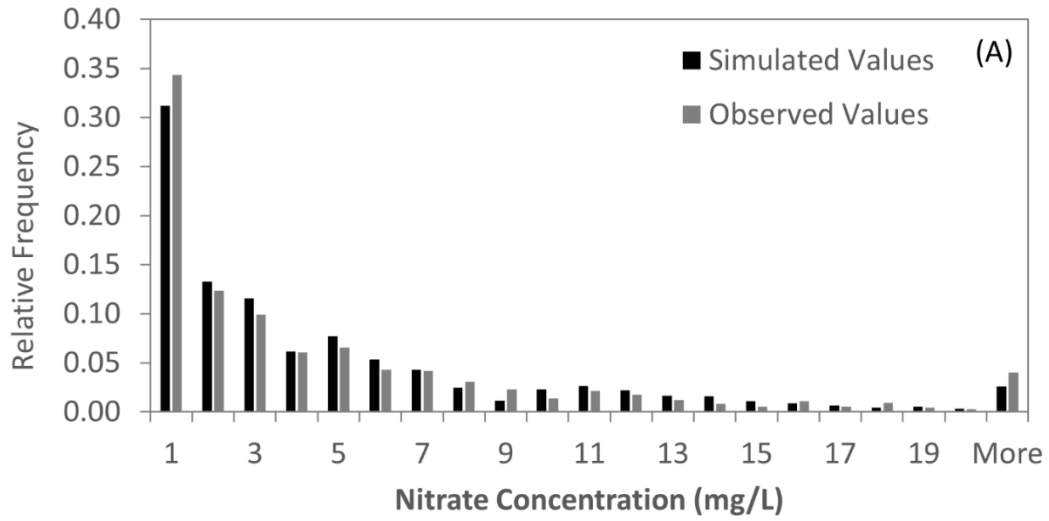
Figure 35. Frequency distribution of observed and simulated values of (A) NO_3-N concentrations and (B) soluble P concentrations.
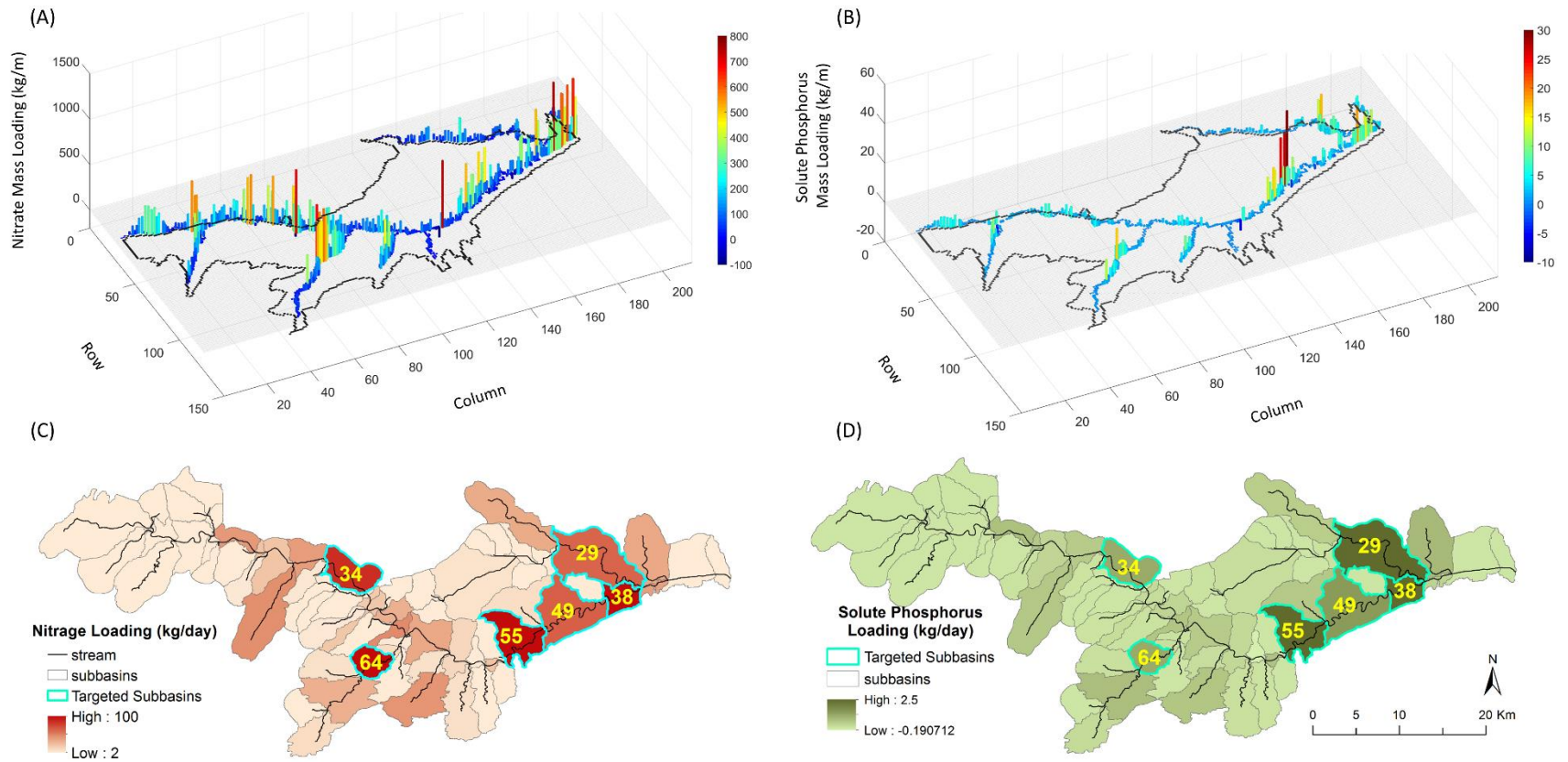
Figure 36. Three-dimensional (3D) simulated annual average (A) NO$_3$-N and (B) from the aquifer to the Arkansas River network over the 1999–2016 time period; Annual average (C) NO$_3$-N and (D) mass loading from the aquifer to the subbasins over the 1999-2016 time period, with the top 6 loading subbaisns highlighted.
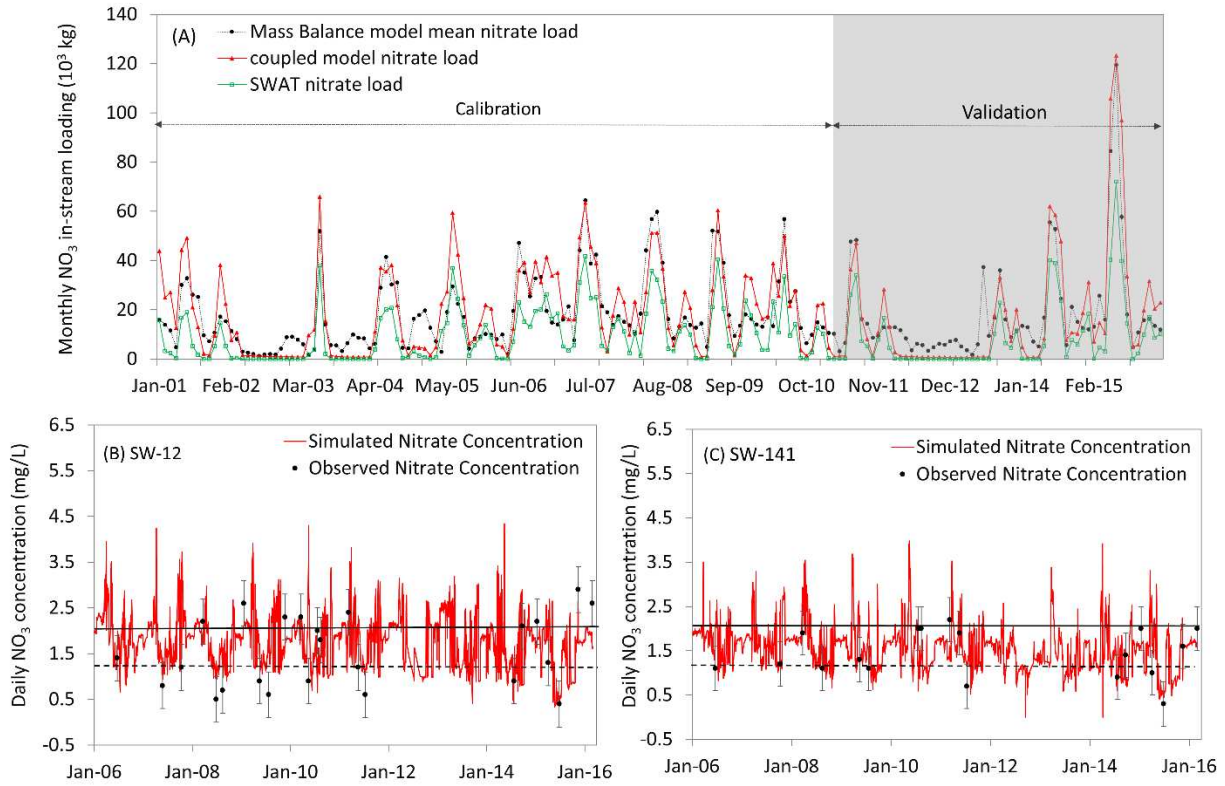
Figure 37. (A) Monthly time series NO3-N in-stream loading at the outlet of the study region. Results of both SWAT-MODFLOW-RT3D simulation and the SWAT model are shown; Daily time series NO3-N in-stream concentration comparison between simulated results from SWAT
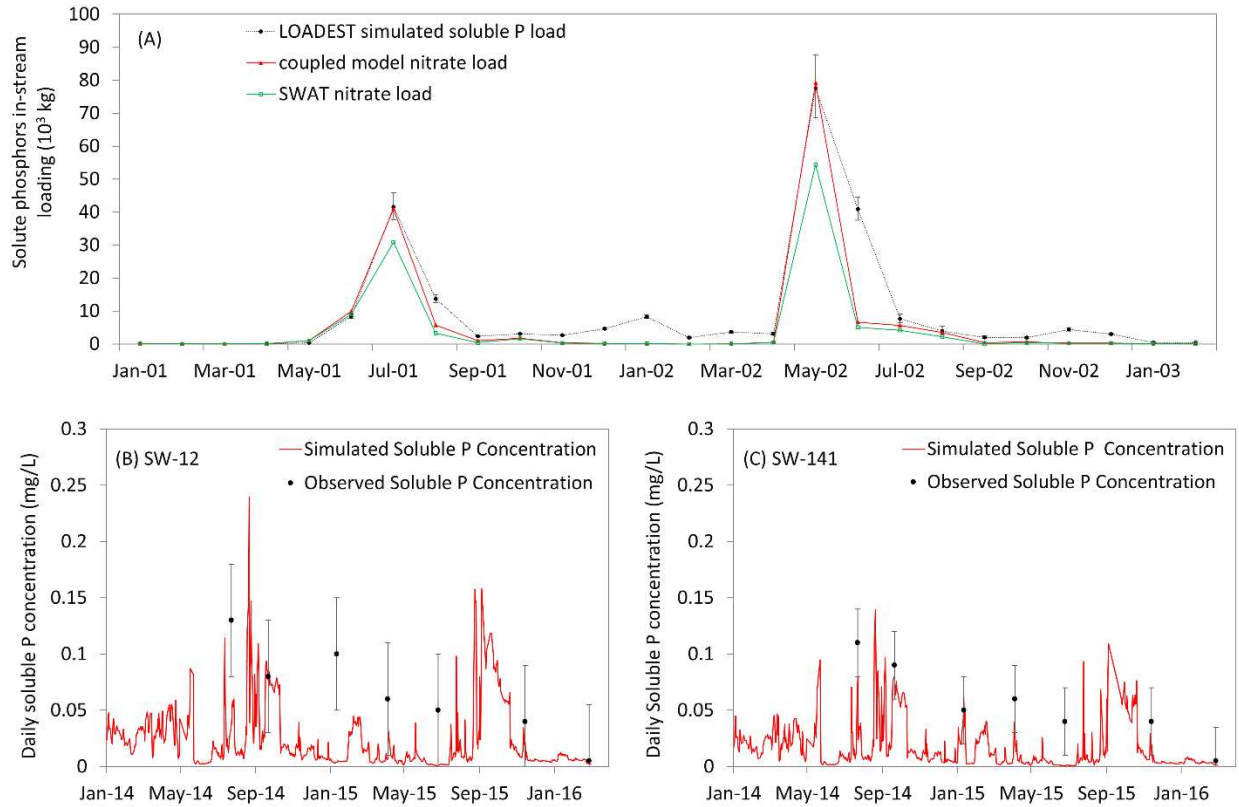
Figure 38. (A) Monthly time series soluble P in-stream loading at the outlet of the study region. Error bars represent standard errors of the LOADEST model. Results of both SWAT-MODFLOW-RT3D simulation and the SWAT model are shown; Daily time series soluble P in-stream concentration comparison between simulated results from SWAT-MODFLOW-RT3D model and observed values for (B) SW-12 and (C) SW-14
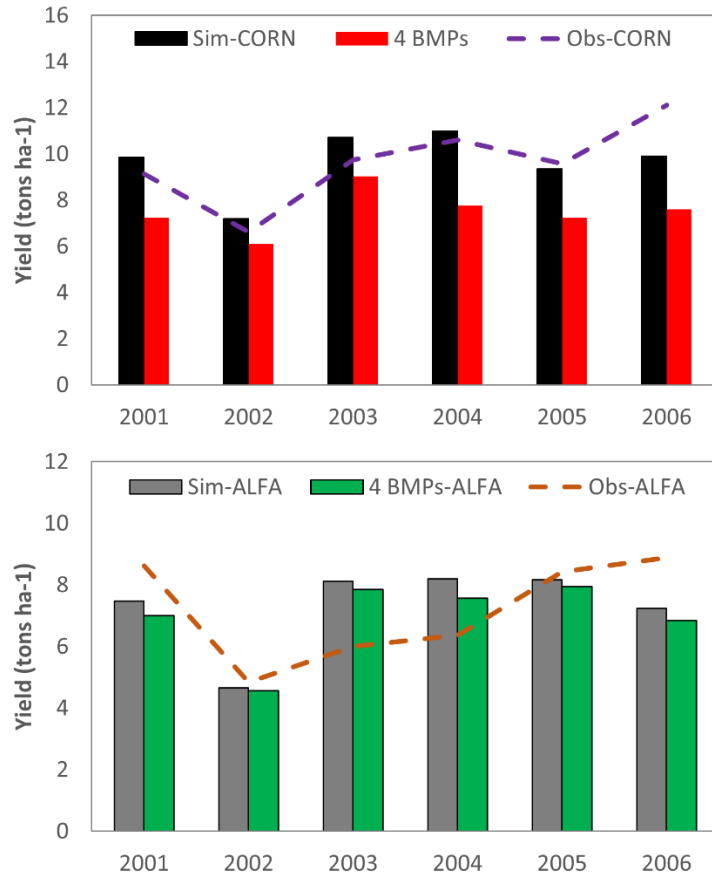
Figure 39. Average crop yields for corn and alfalfa comparison between NASS reported and simulated values in Otero County over the 2001–2006 time period for baseline scenario and 4 BMPs scenarios.
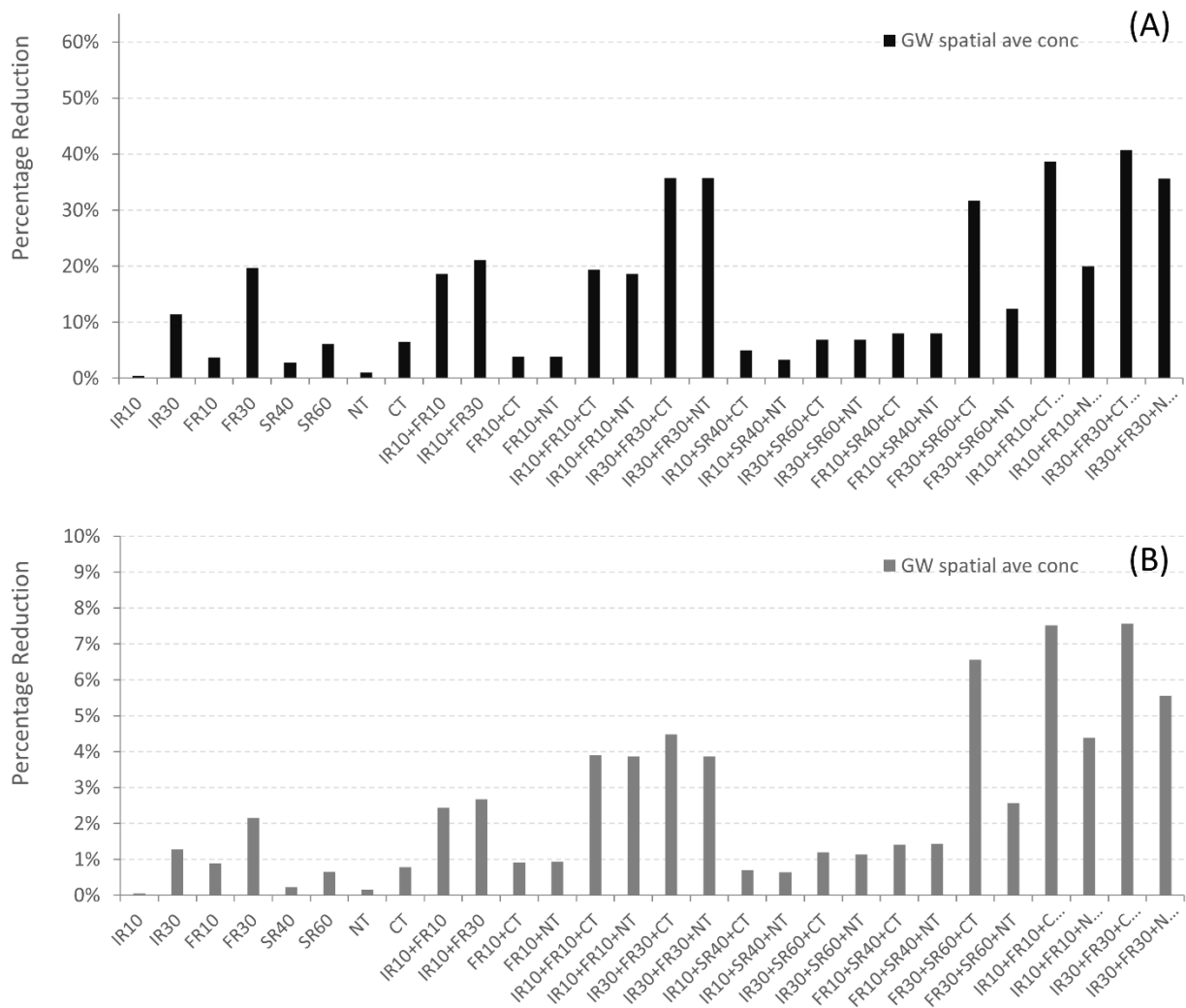
Figure 40. Percent average reduction rate in (A) NO$_3$-N and (B) soluble P groundwater concentration for the BMPs compared to the baseline condition.
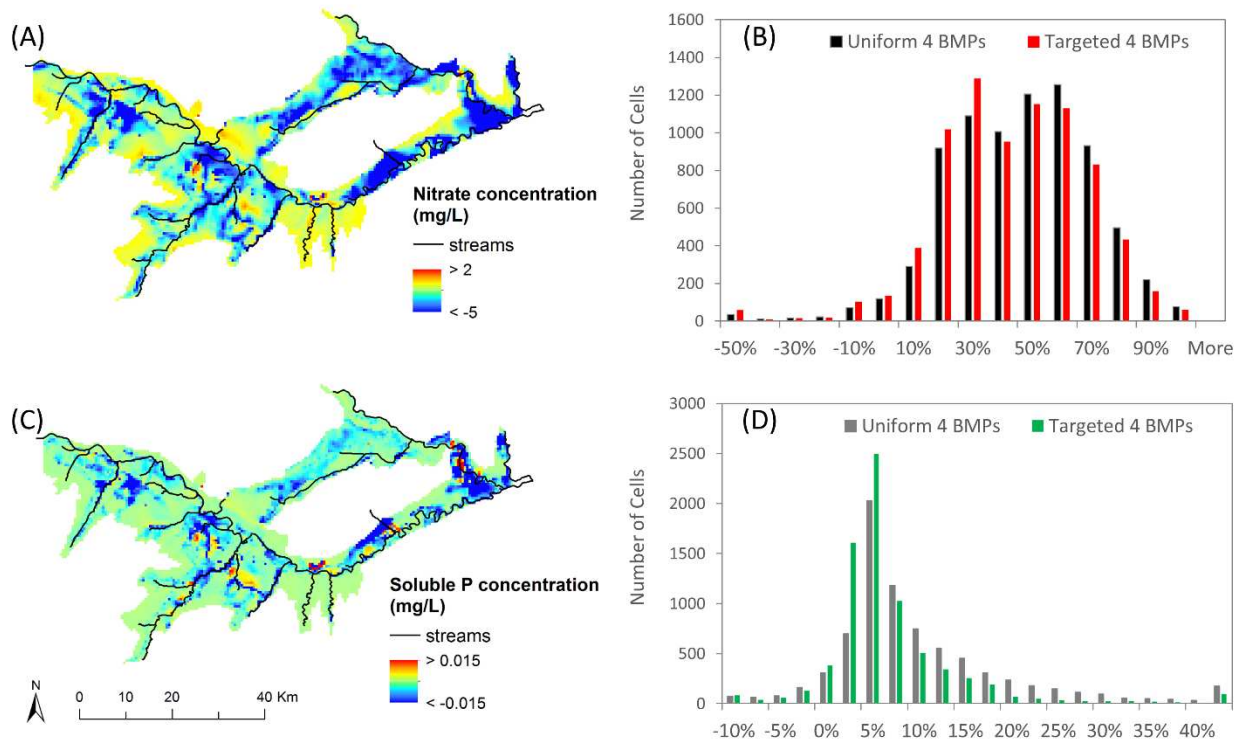
Figure 41. Difference between the simulated baseline and IR30-FR30-SR60-CT BMP values of groundwater (A) NO_3-N concentration and (C) soluble P concentration averaged temporally over the 18 years period; Histogram of cell-by-cell percent difference in (B) NO_3-N concentration and (D) soluble P concentration for uniform 4 BMPs scenario (IR30-FR30-SR60-CT BMP) and targeted 4 BMPs scenarios.
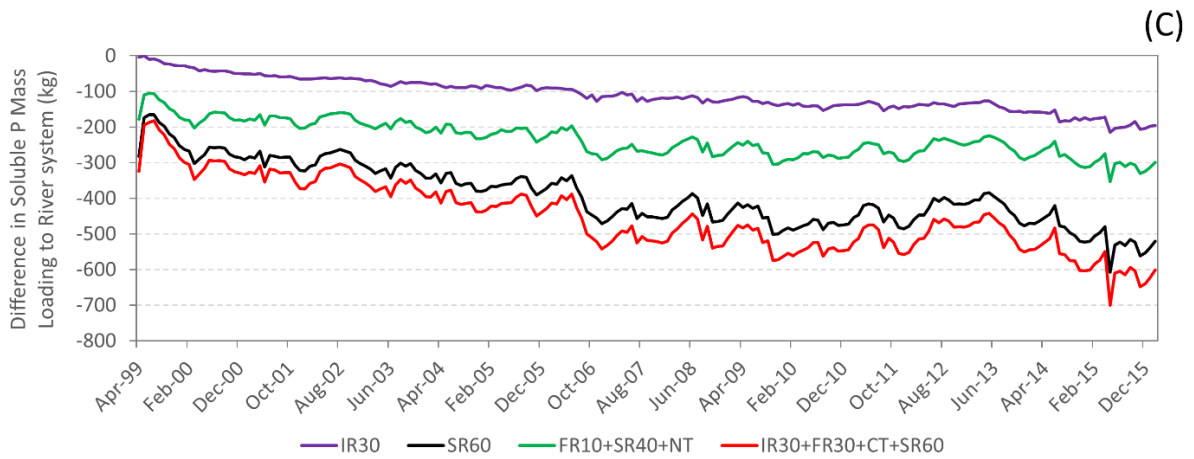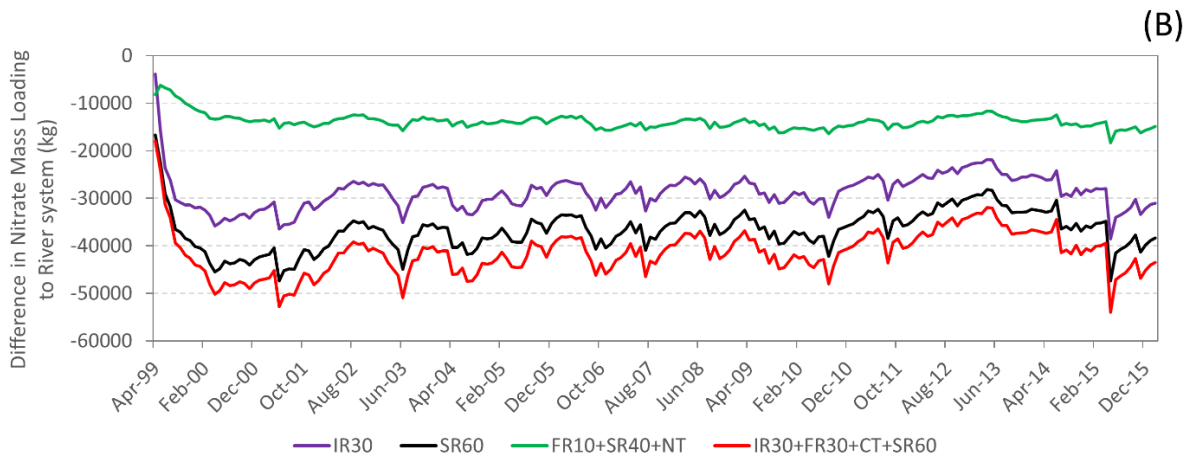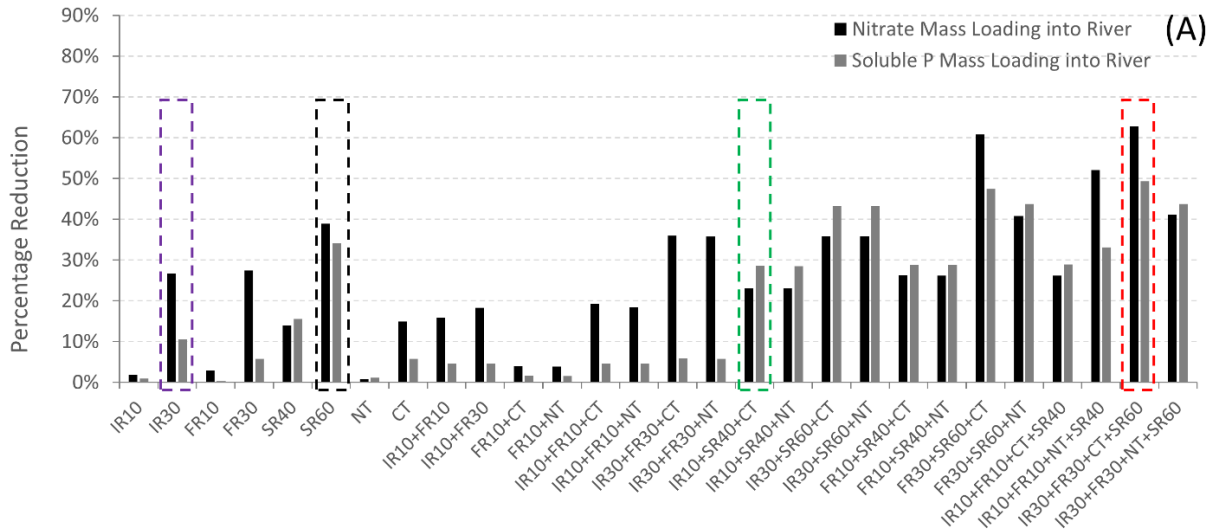
Figure 42. (A) Percent average mass loading reduction rate in NO$_3$-N and soluble P for the BMPs compared to the baseline condition; Monthly decrease from the selected BMPs' mass loading to river, as compared to baseline condition, for (B) NO$_3$-N and (C) soluble P
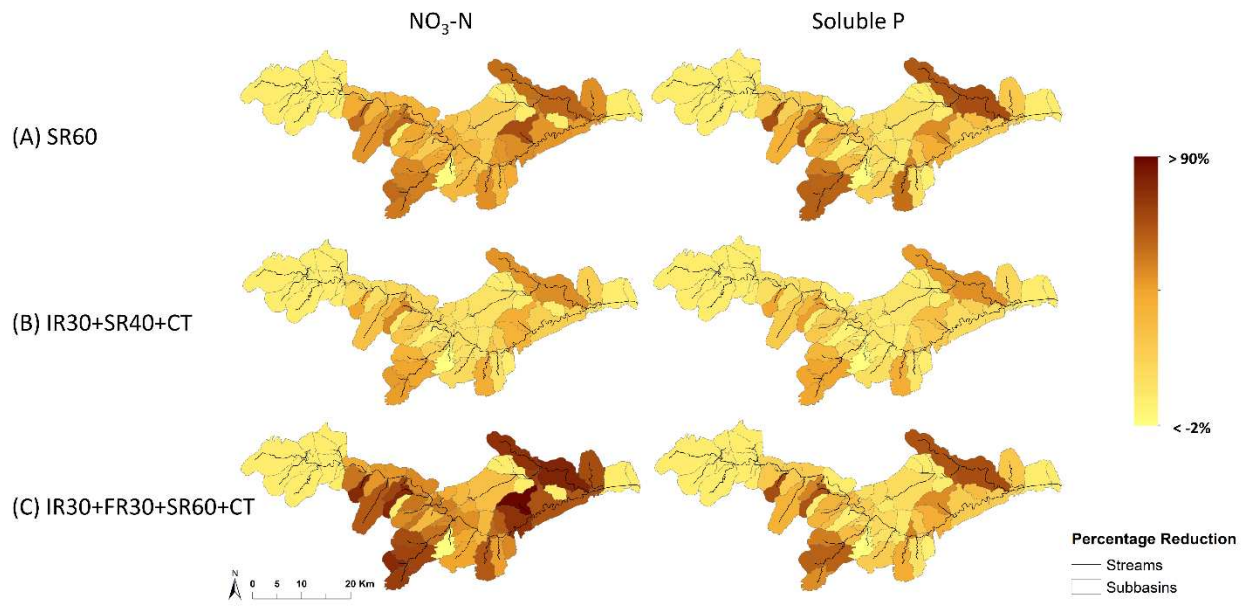
Figure 43. Average percent reduction in mass loading into subbasins from selected BMPs' mass loading to river, as compared to baseline condition, for NO$_3$-N and soluble P
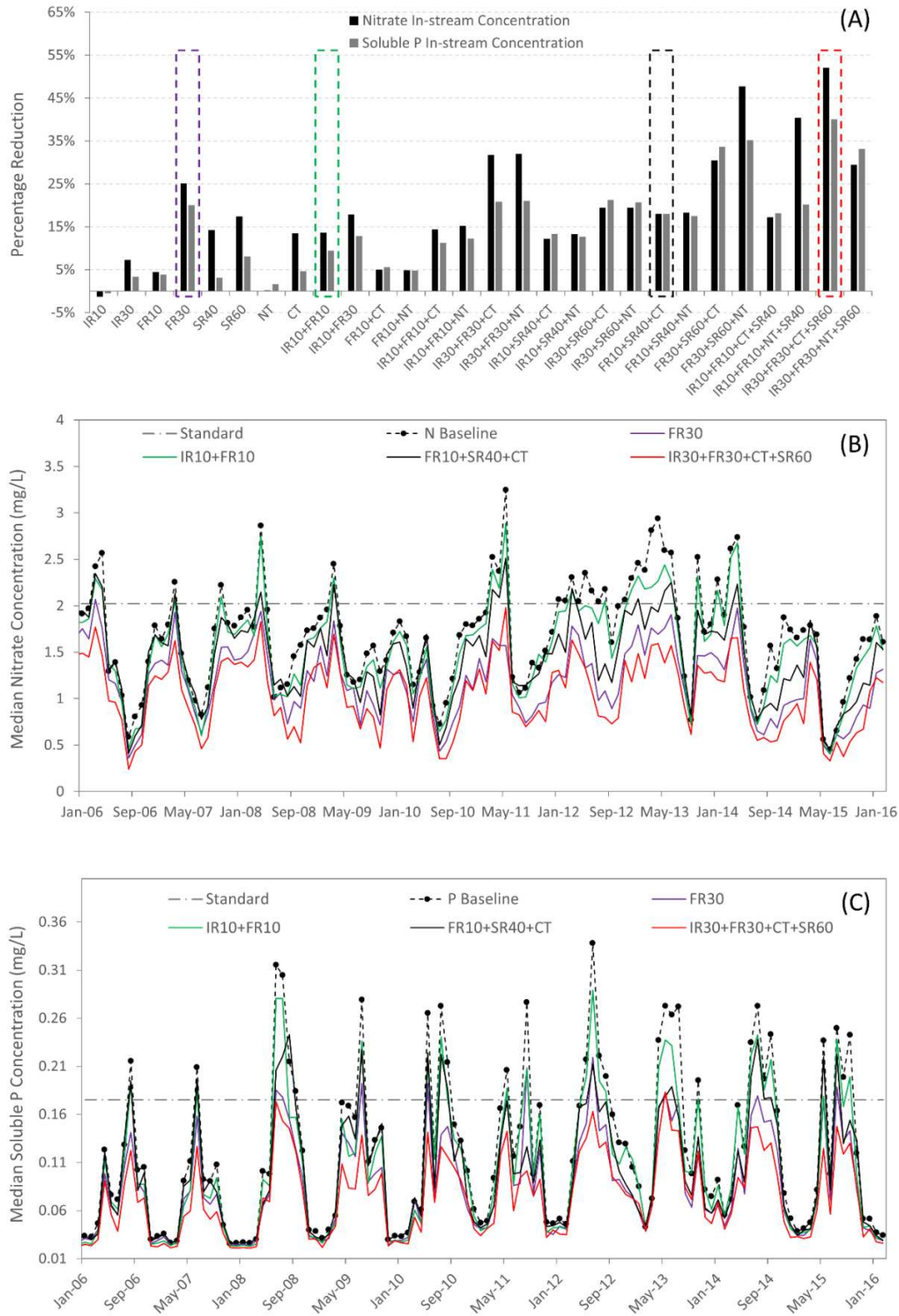
Figure 44. (A) Percent average in-stream concentration reduction rate in NO₃-N and soluble P for the BMPs compared to the baseline condition; Simulated median in-stream concentration for (B) NO₃-N and (C) soluble P over a 18 years simulation period for selected BMPs.
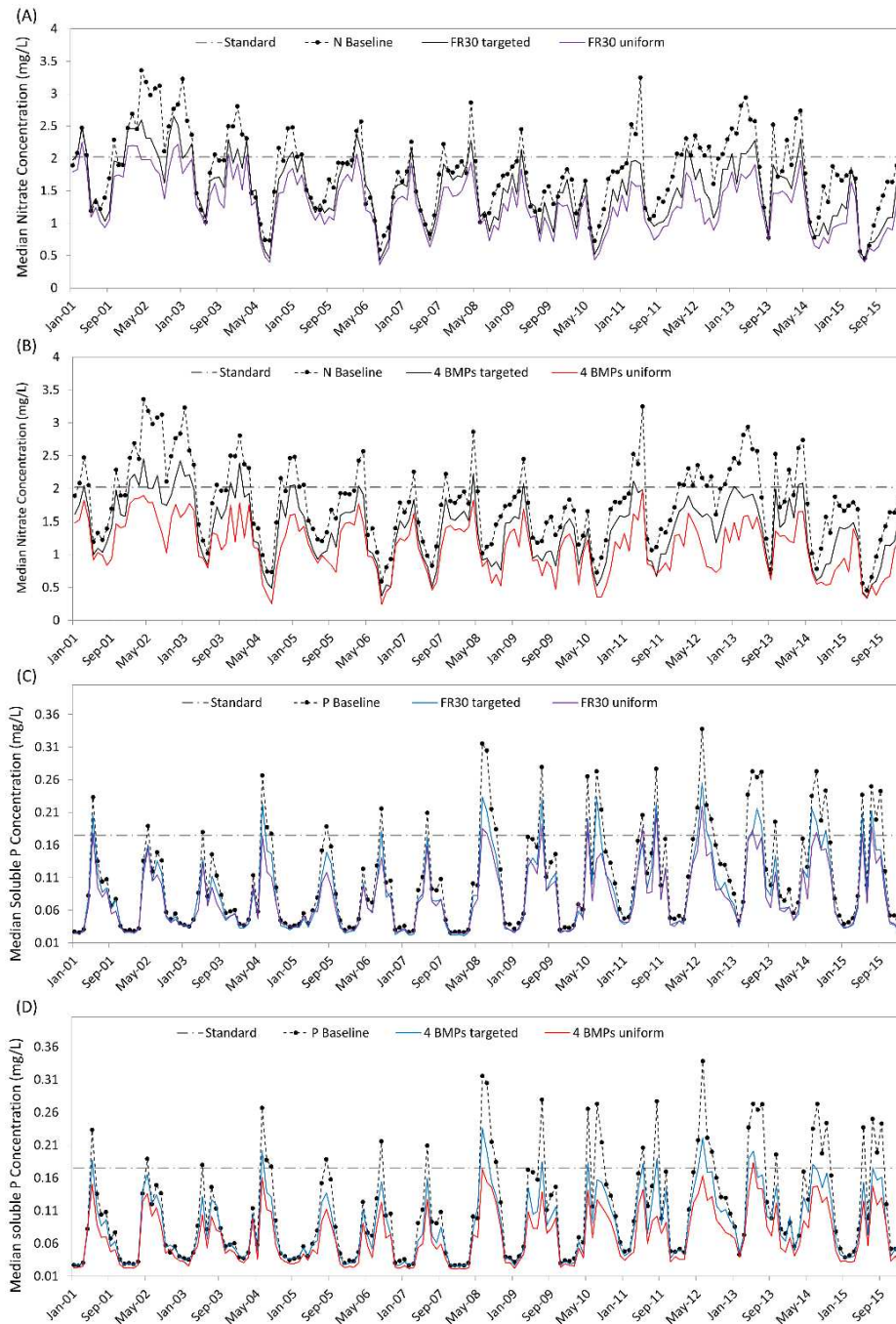
Figure 45. Simulated median in-stream concentration for (A) NO3-N of FR30 scenarios, (B) NO3-N of 4 BMPs scenarios (C) soluble P of FR30 scenarios, and (D) soluble P of 4 BMPs scenarios

Table 8. Agricultural management for the model application to the study region in the Lower Arkansas River Valley in southeastern Colorado

Category	Planting Day	First Fitilize Day	Second Fitilize Day	Harvest Date	Plow Date	F-N	F-P
Units	-	-	-	-	-	kg ha^{-1}	kg ha^{-1}
Alfalfa	1-Apr	18-Mar	13-May	30-Sep	20-Oct	22.4	112.3
Bean	20-May	6-May	1-Jul	30-Sep	20-Oct	140.0	112.3
Corn	1-May	17-Apr	12-Jun	25-Oct	14-Nov	252.0	202.2
Melon	15-May	1-May	26-Jun	10-Aug	30-Aug	112.0	112.3
Onion	20-Mar	6-Mar	1-May	15-Sep	5-Oct	140.0	112.3
Pasture	1-Apr	18-Mar	13-May	30-Sep	20-Oct	140.0	112.3
Pumpkin	1-Jun	18-May	13-Jul	30-Sep	20-Oct	140.0	112.3
Sorghum	20-May	6-May	1-Jul	15-Oct	4-Nov	112.0	112.3
Spring Grain	1-Apr	18-Mar	13-May	15-Jul	4-Aug	112.0	112.3
Squash	20-May	6-May	1-Jul	25-Jul	14-Aug	140.0	112.3
Sunflower	1-Jun	18-May	13-Jul	10-Oct	30-Oct	140.0	112.3
Vegetable	25-Apr	11-Apr	6-Jun	30-Aug	19-Sep	140.0	112.3
Winter Wheat	30-Sep	16-Sep	11-Nov	5-Jul	25-Jul	112.0	112.3

Table 9. An example of a corn-onion rotation practice

Year	Month	Day	Operation	Operation Number	Crop Type
1	January	1	Auto irrigation	10	Corn
1	April	17	First N-fertilizer	3	Corn
1	April	17	First P-fertilizer	3	Corn
1	May	1	Plant begin	1	Corn
1	June	12	Second N-fertilizer	3	Corn
1	June	12	Second P-fertilizer	3	Corn
1	October	25	Harvest and kill	5	Corn
1	November	11	Tillage	6	Corn
2	March	6	First N-fertilizer	3	Onion
2	March	6	First P-fertilizer	3	Onion
2	March	20	Plant begin	1	Onion
2	May	1	Second N-fertilizer	3	Onion
2	May	1	Second P-fertilizer	3	Onion
2	September	15	Harvest and kill	5	Onion
2	October	5	Tillage	6	Onion

Table 10. List of parameters that produced for SWAT-MODFLOW-RT3D calibration

Parameter	Model component	Definition	Calibrated values
CN2	Flow	SCS runoff curve number for moisture condition II	-3%
CH_K2	Flow	Effective hydraulic conductivity of channel	22.91
SOL_AWC	Flow	Available water capacity	-10%
SOL_K	Flow	Saturated hydraulic conductivity	-9%
USLE_K	Sediment	USLE equation soil erodibility factor	-6%
USLE_C	Sediment	Minimum value of USLE C factor for water erosion applicable to the land cover/plant	Corn: 0.08 Alfalfa: 0.05 Pasture: 0.006
CH_N2	Sediment	Manning's n value for the main Channel	0.22
CDN	N	Denitrification exponential rate coefficient	3
SDNCO	N	Denitrification threshold water content (fraction of field capacity water content above which dnitrification takes place)	0.188
NPERCO	Mineral N	Nitrate percolation coefficient	0.096
PPERCO	Mineral P	Phosphorus percolation coefficient	10
PHOSKD	Mineral P	Phosphorus soil partitioning coefficient	175
COND	Groundwater Flow	Riverbed hydraulic conductance	0.00134 - 39.55
μ_{NO_3}	Groundwater N	first-roder rate constant for denitrifitaion	0.0005
K_{NO_3}	Groundwater N	Monod half-saturation term for denitrification	10
R_P	Groundwater P	partition coefficient for Soluble P	1.5

Table 11. Values of performance calculated for comparing simulated and observed streamflow at the five gauging for different models

Gauging Stations	Statistical Comparison	SWAT model		SWAT-MODFLOW-RT3D	
		Calibration	Validation	Calibration	Validation
In-stream NO$_3$-N loading	NSE	0.36	0.58	0.51	0.72
	R^2	0.52	0.73	0.65	0.84
In-stream Soluble P loading	NSE	0.72	-	0.82	-
	R^2	0.79	-	0.85	-

Table 12. Summary of individual and combined BMP scenarios

Scenario number	Types	Variable name	Scenario abbreviated name	BMP scenarios' description
1	Irrigation management	Irrigation Efficiency (IRR_EFF)	IR10	10% irrigation reduction
2		Surface runoff ratio (IRR_ASQ)	IR30	30% irrigation redcution
3	Nutrient management	Applied Fertilizer Amount (FRT_KG)	FR10	10% fertilizer reduction
4			FR30	30% fertilizer reduction
5	Water conveyance efficiency	Riverbed Conductance (COND)	SR40	40% canal seeapge reduction
6			SR60	60% canal seepage reduction
7	Land use management	Depth of mixing (DEPTIL)	CT	conservation tillage (DEPTIL: 100, EFFMIX: 0.25)
8		Mixing effciency (EFFMIX)	NT	no tillage (DEPTIL: 25, EFFMIX: 0.05)
9	Combination BMPs		IR10+FR10	
10			IR10+FR30	
11			FR10+CT	
12			FR10+NT	
13			IR10+FR10+CT	
14			IR10+FR10+NT	
15			IR30+FR30+CT	
16			IR30+FR30+NT	
17			IR10+SR40+CT	
18			IR10+SR40+NT	
19			IR30+SR60+CT	
20			IR30+SR60+NT	
21			FR10+SR40+CT	
22			FR10+SR40+NT	
23			FR30+SR60+CT	
24			FR30+SR60+NT	
25			IR10+FR10+SR40+CT	
26			IR10+FR10+SR40+NT	
27			IR30+FR30+SR60+CT	
28			IR30+FR30+SR60+NT	

REFERENCES

Abbaspour, K.C., Rouholahnejad, E., Vaghefi, S., Srinivasan, R., Yang, H., Kløve, B., 2015. A continental-scale hydrology and water quality model for Europe: Calibration and uncertainty of a high-resolution large-scale SWAT model. Journal of Hydrology 524, 733–752. https://doi.org/10.1016/j.jhydrol.2015.03.027

Abdelraouf, R.E., Ragab, R., 2018. Applying partial root drying drip irrigation in the presence of organic mulching. Is that the best irrigation practice for arid regions? Field and modelling study using the saltmed model - Abdelraouf - 2018 - Irrigation and Drainage - Wiley Online Library. Irrig. and Drain. 34, 491–507.

Almasri, M.N., Kaluarachchi, J.J., 2007. Modeling nitrate contamination of groundwater in agricultural watersheds. Journal of Hydrology 343, 211–229. https://doi.org/10.1016/j.jhydrol.2007.06.016

Almendinger, J.E., Ulrich, J.S., 2017. Use of SWAT to Estimate Spatial Scaling of Phosphorus Export Coefficients and Load Reductions Due to Agricultural BMPS. JAWRA Journal of the American Water Resources Association 53, 547–561. https://doi.org/10.1111/1752-1688.12523

Arabi, M., Govindaraju, R.S., Hantush, M.M., 2007. A probabilistic approach for analysis of uncertainty in the evaluation of watershed management practices. Journal of Hydrology 333, 459–471. https://doi.org/10.1016/j.jhydrol.2006.09.012

Arnold, J.G., Kiniry, J.R., Srinivasan, R., Williams, J.R., Haney, E.B., Neitsch, S.L., 2013. SWAT 2012 Input/Output Documentation (Technical Report). Texas Water Resources Institute.

Arnold, J.G., Srinivasan, R., Muttiah, R.S., Williams, J.R., 1998. Large Area Hydrologic Modeling and Assessment Part I: Model Development1. JAWRA Journal of the American Water Resources Association 34, 73–89. https://doi.org/10.1111/j.1752-1688.1998.tb05961.x

Bailey, R.T., Gates, T.K., Ahmadi, M., 2014a. Simulating reactive transport of selenium coupled with nitrogen in a regional-scale irrigated groundwater system. Journal of Hydrology 515, 29–46. https://doi.org/10.1016/j.jhydrol.2014.04.039

Bailey, R.T., Gates, T.K., Ahmadi, M., 2014b. Simulating reactive transport of selenium coupled with nitrogen in a regional-scale irrigated groundwater system. Journal of Hydrology 515, 29–46. https://doi.org/10.1016/j.jhydrol.2014.04.039

Bailey, R.T., Gates, T.K., Romero, E.C., 2015a. Assessing the effectiveness of land and water management practices on nonpoint source nitrate levels in an alluvial stream–aquifer system. Journal of Contaminant Hydrology 179, 102–115. https://doi.org/10.1016/j.jconhyd.2015.05.009

Bailey, R.T., Hunter, W.J., Gates, T.K., 2012. The Influence of Nitrate on Selenium in Irrigated Agricultural Groundwater Systems. Journal of Environmental Quality 41, 783–792. https://doi.org/10.2134/jeq2011.0311

Bailey, R.T., Romero, E.C., Gates, T.K., 2015b. Assessing best management practices for remediation of selenium loading in groundwater to streams in an irrigated region. Journal of Hydrology 521, 341–359. https://doi.org/10.1016/j.jhydrol.2014.11.079

Bosch, N.S., Allan, J.D., Selegean, J.P., Scavia, D., 2013. Scenario-testing of agricultural best management practices in Lake Erie watersheds. Journal of Great Lakes Research 39, 429–436. https://doi.org/10.1016/j.jglr.2013.06.004

Brown, L.C., Barnwell, T.O., 1987. The enhanced stream water quality models QUAL2E and QUAL2E-UNCAS: Documentation and user model. Environmental Research Laboratory, Office of Research and Development, US ….

Chu, T.W., Shirmohammadi, A., 2004. Evaluation of the SWAT model's hydrology component in the piedmont physiographic region of Maryland. Transactions of the ASAE 47, 1057.

Chukalla, A.D., Krol, M.S., Hoekstra, A.Y., 2018. Grey water footprint reduction in irrigated crop production: effect of nitrogen application rate, nitrogen form, tillage practice and irrigation strategy. Hydrology and Earth System Sciences 22, 3245–3259. https://doi.org/10.5194/hess-22-3245-2018

Davis, J., Smith, D., Croissant, R., 2005. Fertilizing Alfalfa and Grasses (Colorado State University Cooperative Extension Paper No. 0.537).

Dechmi, F., Burguete, J., Skhiri, A., 2012. SWAT application in intensive irrigation systems: Model

modification, calibration and validation. Journal of Hydrology 470–471, 227–238.

https://doi.org/10.1016/j.jhydrol.2012.08.055

Dechmi, F., Skhiri, A., 2013. Evaluation of best management practices under intensive irrigation using

SWAT model. Agricultural Water Management 123, 55–64.

https://doi.org/10.1016/j.agwat.2013.03.016

Douglas-Mankin, K.R., Srinivasan, R., Arnold, J.G., 2010. Soil and Water Assessment Tool (SWAT)

Model: Current Developments and Applications. Transactions of the ASABE 53, 1423–1431.

https://doi.org/10.13031/2013.34915

Ehtiat, M., Jamshid Mousavi, S., Srinivasan, R., 2018. Groundwater Modeling Under Variable Operating

Conditions Using SWAT, MODFLOW and MT3DMS: a Catchment Scale Approach to Water

Resources Management. Water Resour Manage 32, 1631–1649. https://doi.org/10.1007/s11269-017-

1895-z

Gassman, P.W., Reyes, M.R., Green, C.H., Arnold, J.G., 2007. The soil and water assessment tool:

historical development, applications, and future research directions. Transactions of the ASABE 50,

1211–1250.

Gates, T.K., Garcia, L.A., Hemphill, R.A., Morway, E.D., Elhaddad, A., 2012. Irrigation practices, water

consumption, & return flows in Colorado's lower Arkansas River Valley: field and model

investigations (Technical Report No. No. TR12-10). Colorado Agricultural Experiment Station.

Gaynor, J.D., Findlay, W.I., 1995. Soil and Phosphorus Loss from Conservation and Conventional Tillage

in Corn Production. Journal of Environmental Quality 24, 734–741.

https://doi.org/10.2134/jeq1995.00472425002400040026x

Halvorson, A.D., Follett, R.F., Bartolo, M.E., Schweissing, F.C., 2002. Nitrogen Fertilizer Use Efficiency

of Furrow-Irrigated Onion and Corn. Agronomy Journal 94, 442–449.

https://doi.org/10.2134/agronj2002.4420

Huizenga, A., Bailey, R.T., Gates, T.K., 2017. Stream-aquifer and in-stream processes affecting nitrogen along a major river and contributing tributary. Journal of Contaminant Hydrology 199, 24–35. https://doi.org/10.1016/j.jconhyd.2017.03.003

Laattoe, T., Post, V.E.A., Werner, A.D., 2017. A Spatially Periodic Solute Boundary for MT3DMS and PHT3D. Groundwater 55, 419–427. https://doi.org/10.1111/gwat.12490

Li, J., Liu, H., Wang, H., Luo, J., Zhang, X., Liu, Z., Zhang, Y., Zhai, L., Lei, Q., Ren, T., Li, Y., Bashir, M.A., 2018. Managing irrigation and fertilization for the sustainable cultivation of greenhouse vegetables. Agricultural Water Management 210, 354–363. https://doi.org/10.1016/j.agwat.2018.08.036

Liu, Y., Wang, R., Guo, T., Engel, B.A., Flanagan, D.C., Lee, J.G., Li, S., Pijanowski, B.C., Collingsworth, P.D., Wallace, C.W., 2019. Evaluating efficiencies and cost-effectiveness of best management practices in improving agricultural water quality using integrated SWAT and cost evaluation tool. Journal of Hydrology 577, 123965. https://doi.org/10.1016/j.jhydrol.2019.123965

Martin, C.A., Gates, T.K., 2014. Uncertainty of canal seepage losses estimated using flowing water balance with acoustic Doppler devices. Journal of Hydrology 517, 746–761. https://doi.org/10.1016/j.jhydrol.2014.05.074

McMahon, P.B., Böhlke, J.K., 1996. Denitrification and mixing in a stream—aquifer system: effects on nitrate loading to surface water. Journal of Hydrology 186, 105–128. https://doi.org/10.1016/S0022-1694(96)03037-5

McMahon, P.B., Böhlke, J.K., Bruce, B.W., 1999. Denitrification in marine shales in northeastern Colorado. Water Resources Research 35, 1629–1642. https://doi.org/10.1029/1999WR900004

Monaghan, R.M., Paton, R.J., Smith, L.C., Drewry, J.J., Littlejohn, R.P., 2005. The impacts of nitrogen fertilisation and increased stocking rate on pasture yield, soil physical condition and nutrient losses in drainage from a cattle-grazed pasture. New Zealand Journal of Agricultural Research 48, 227–240. https://doi.org/10.1080/00288233.2005.9513652

Moriasi, D.N., Gitau, M.W., Pai, N., Daggupati, P., 2015. Hydrologic and water quality models: Performance measures and evaluation criteria. Transactions of the ASABE 58, 1763–1785.

Morway, E.D., Gates, T.K., Niswonger, R.G., 2013. Appraising options to reduce shallow groundwater tables and enhance flow conditions over regional scales in an irrigated alluvial aquifer system. Journal of Hydrology 495, 216–237. https://doi.org/10.1016/j.jhydrol.2013.04.047

Nash, J.E., Sutcliffe, J.V., 1970. River flow forecasting through conceptual models part I — A discussion of principles. Journal of Hydrology 10, 282–290. https://doi.org/10.1016/0022-1694(70)90255-6

Niswonger, R.G., Panday, S., Ibaraki, M., 2011. MODFLOW-NWT, a Newton formulation for MODFLOW-2005. US Geological Survey Techniques and Methods 6, 44.

Novotny, V., 2002. Water Quality: Diffuse Pollution and Watershed Management. John Wiley & Sons.

Omernik, J.M., Abernathy, A.R., Male, L.M., 1981. Stream nutrient levels and proximity of agricultural and forest land to streams: Some relationships. Journal of Soil and Water Conservation 36, 227–231.

Özcan, Z., Kentel, E., Alp, E., 2017. Evaluation of the best management practices in a semi-arid region with high agricultural activity. Agricultural Water Management 194, 160–171. https://doi.org/10.1016/j.agwat.2017.09.007

Powlson, D.S., Jenkinson, D.S., 1981. A comparison of the organic matter, biomass, adenosine triphosphate and mineralizable nitrogen contents of ploughed and direct-drilled soils. The Journal of Agricultural Science 97, 713–721. https://doi.org/10.1017/S0021859600037084

Prommer, H., Barry, D.A., Zheng, C., 2003. MODFLOW/MT3DMS-Based Reactive Multicomponent Transport Modeling. Groundwater 41, 247–257. https://doi.org/10.1111/j.1745-6584.2003.tb02588.x

Pulido-Velazquez, M., Peña-Haro, S., García-Prats, A., Mocholi-Almudever, A.F., Henriquez-Dole, L., Macian-Sorribes, H., Lopez-Nicolas, A., 2015. Integrated assessment of the impact of climate and land use changes on groundwater quantity and quality in the Mancha Oriental system (Spain). Hydrology and Earth System Sciences 19, 1677–1693. https://doi.org/10.5194/hess-19-1677-2015

Rong, Y., Xuefeng, W., 2011. Effects of nitrogen fertilizer and irrigation rate on nitrate present in the profile of a sandy farmland in Northwest China. Procedia Environmental Sciences, 2011 2nd

International Conference on Challenges in Environmental Science and Computer Engineering (CESCE 2011) 11, 726–732. https://doi.org/10.1016/j.proenv.2011.12.113

Runkel, R.L., Crawford, C.G., Cohn, T.A., 2004. Load estimator (LOADEST): a FORTRAN program for estimating constituent loads in streams and rivers (USGS Numbered Series No. 4-A5), Techniques and Methods.

Schilling, K.E., Wolter, C.F., 2009. Modeling Nitrate-Nitrogen Load Reduction Strategies for the Des Moines River, Iowa Using SWAT. Environmental Management 44, 671–682. https://doi.org/10.1007/s00267-009-9364-y

Shultz, C.D., Bailey, R.T., Gates, T.K., Heesemann, B.E., Morway, E.D., 2018. Simulating selenium and nitrogen fate and transport in coupled stream-aquifer systems of irrigated regions. Journal of Hydrology 560, 512–529. https://doi.org/10.1016/j.jhydrol.2018.02.027

Smith, V.H., 2003. Eutrophication of freshwater and coastal marine ecosystems a global problem. Environ Sci & Pollut Res 10, 126–139. https://doi.org/10.1065/espr2002.12.142

Susfalk, R., Sada, D., Martin, C., Young, M.H., Gates, T., Rosamond, C., Mihevc, T., Arrowood, T., Shanafield, M., Epstein, B., 2008. Evaluation of linear anionic polyacrylamide (LA-PAM) application to water delivery canals for seepage reduction. Desert Research Institute Las Vegas.

Tuppad, P., Kannan, N., Srinivasan, R., Rossi, C.G., Arnold, J.G., 2010a. Simulation of Agricultural Management Alternatives for Watershed Protection. Water Resour Manage 24, 3115–3144. https://doi.org/10.1007/s11269-010-9598-8

Tuppad, P., Kannan, N., Srinivasan, R., Rossi, C.G., Arnold, J.G., 2010b. Simulation of Agricultural Management Alternatives for Watershed Protection. Water Resour Manage 24, 3115–3144. https://doi.org/10.1007/s11269-010-9598-8

Volk, M., Liersch, S., Schmidt, G., 2009. Towards the implementation of the European Water Framework Directive? Lessons learned from water quality simulations in an agricultural watershed. Land Use Policy 26, 580–588.

Wei, X., Bailey, R.T., 2019. Assessment of System Responses in Intensively Irrigated Stream–Aquifer

    Systems Using SWAT-MODFLOW. Water 11, 1576. https://doi.org/10.3390/w11081576

Wei, X., Bailey, R.T., Records, R.M., Wible, T.C., Arabi, M., 2018a. Comprehensive simulation of

    nitrate transport in coupled surface-subsurface hydrologic systems using the linked SWAT-

    MODFLOW-RT3D model. Environmental Modelling & Software.

    https://doi.org/10.1016/j.envsoft.2018.06.012

Wei, X., Bailey, R.T., Tasdighi, A., 2018b. Using the SWAT Model in Intensively Managed Irrigated

    Watersheds: Model Modification and Application. Journal of Hydrologic Engineering 23, 04018044.

Zhang, Y., Hansen, N., Trout, T., Nielsen, D., Paustian, K., 2018. Modeling Deficit Irrigation of Maize

    with the DayCent Model. Agronomy Journal 110, 1754

CHAPTER 5. GLOBAL SENSITIVITY AND UNCERTAINTY ANALYSIS OF THE SWAT-MODFLOW-RT3D MODEL

5.1. INTRODUCTION

In the past decades, distributed hydrological models are important tools in watershed management practice (Beven, 2018), which have been used to investigate many practical and pressing issues that arise during planning, operation, and management of water resources within environmental systems (Gallagher and Doherty, 2007; Dabrowski, 2014; Assegid et al., 2015). Hydrological models are currently well developed and widely adopted in practice to help managers define the scope of a problem, to make assumption explicit, and to explore possible outcomes beyond the obvious one (Jakeman et al., 2006).

A typical hydrological model consists of a large number of equations representing dominant environmental processes has particular importance in regard to evaluate the rainfall-runoff generation, and fate and transport of contaminants from non-point source activities. It contains numerous input parameters and variables, making calibration of such models, particularly the parameter specification state, far more complex (Jakeman and Hornberger, 1993; van Griensven et al., 2006). During calibration, parameters with physical significance could be adjusted interactively. Over-parameterization is a well-known problem in hydrological modelling (van Griensven et al., 2006). Therefore, insensitive parameters should be fixed as a constant value to facilitate more efficient calibration during parameter estimation stage, thus simplifying the mathematical structure of the model (Muleta and Nicklow, 2005). Sensitivity analysis (SA) can be used to establish relative importance of parameters for accurate calibration and can be treated as guidelines for future data collection and experimental design, which usually varies multiple parameters simultaneously based on predefined parameter ranges and underlying probability distribution, requires intensive computational time.

The most common classifications of SA methods are local SA (LSA) and global SA (GSA), with LSA focused on impacts of uncertain inputs around a point and GSA focused more on the impacts of uncertain

inputs over the entire input space (Razavi and Gupta, 2016). In practice, GSA methods normally recommended in hydrological modelling applications due to their ability to incorporate interactions between parameters (Saltelli et al., 2000). Widely used GSA techniques include regression analysis, screening method, meta-modelling method, and variance-based method (Song et al., 2015).

Another major problem is as models become more comprehensive, uncertainty of parameter estimates obtained through the calibration processes may increase, thus result in increasing uncertainty in the model predications (e.g. investigating the impact of BMPs on watershed remediations) (Anderton et al., 2002; Benaman and Shoemaker, 2004; Pappenberger and Beven, 2006). It is difficult to have confidence of implementing management decisions without a realistic assessment of uncertainty, especially when stakeholder are affected by the decisions contingent upon model-supported analyses (Arabi et al., 2007). For management applications, uncertainty analysis (UA) should be one of the fundamental steps in the development and evaluation of a model, and ought to be considered at a level corresponding with the purpose of the model (Jakeman et al., 2006). In fundamental sense, uncertainty associated with model output may be represented as a probability distribution such as the 95th percentile result from the probability distribution (i.e. what is the monthly in-stream nitrate concentration prediction with a 95% probability?). By introducing concepts of confidence and probability, it could provide more information to stakeholders about the degree of risk associated with particular actions. Hydrological models include substantial uncertainties associated with input data, model structural, and model parameterization (Haefner, 2005). Input uncertainty is from errors of input forcing (e.g. precipitation, land use, soil properties, and hydraulic conductivities, etc.). Model structures are invariably incomplete due to lack of knowledge about specific processes, assumptions of real world processes, and ignoring some processes that are considered insignificant for pragmatic considerations. Parameterization uncertainty, in review of literature, has received the most attention; see for example Beven (1995), Aronica et al. (2002) Gallagher and Doherty (2007), Abbaspour et al. (2015), to name just a few.

Saltelli and Annoni (2010) stated that the objective of UA is to answer the question: "How uncertain is this inference" whereas that of SA is to answer: "Where does this uncertainty come from?". SA is

intended to complement of UA that SA is usually performed prior to UA to evaluate the importance of model parameters (Laloy et al., 2010; Song et al., 2015; Zhang, 2016). Several recent studies have coupled SA/UA methods for hydrological models. Ullrich and Volk (2009) investigated the influence of uncertainty in nitrate monitoring data on model calibration and evaluation in a 315 km^2 watershed in Central Germany. DeJonge et al. (2012) using the Morris and Sobol's method to evaluate the sensitivity and uncertainty of parameters affecting water balance and crop growth in Fort Collins, CO. In the 9097 km^2 Zhangye Basin, China, Wu et al. (2014) explored how process understanding, model calibration, and management can be benefited from a systematic UA framework, using an integrated groundwater-surface water model.

The SWAT-MODFLOW-RT3D model described in Chapter 4 is a complex nonlinear dynamic system that simulates outputs such as nutrients in-stream and groundwater concentrations as a function of various inputs governing surface water responses, soil hydraulic properties, and system nutrient fate and transport processes. It contains a large number of input parameters which are commonly determined according to field experiments or estimated through model calibration. Thus, it is desirable to conduct SA and UA as components to determine which model parameter requires the most certainty. The overall objectives of this chapter are twofold: first, to identify and rank the global sensitivity of SWAT-MODFLOW-RT3D (baseline scenario in Chapter 4) parameters in regards to output responses of in-stream nutrient concentrations and groundwater concentrations using Sobol's SA approach; second, use the parameter outputs from sensitivity analysis to examine the effect of modeling uncertainties on evaluation of surface and groundwater nutrient concentrations for the coupled model.

5.2. SENSITIVITY AND UNCERTAINTY ANALYSIS METHODS

Most of the GSA methods are variance-based that uses a variance ratio to estimate the importance of parameters with the foundation of variance decomposition (Saltelli et al., 2000). Among different methods, the 'Sobol' method (Sobol, 1993) used in this study is a comprehensive GSA method with a sampling design for the exploration of the parameter space (variance based method). It is able to estimate

the total sensitivity (TS_i), which is the sum of all effects (i.e. first-order and higher-order) involving in the input factor of interest. With n input factors, the decomposition of variance of the model outputs $\mathrm{var}(Y)$ can be written as:

$$\mathrm{var}(Y) = \sum_{i=1}^{n} D_i + \sum_{1 \leq i < j \leq n} D_{ij} + \cdots + D_{1 \cdots n} \tag{5-1}$$

where D_i is the the variability associated with the major effect of input parameter x_i; The rest ($D_{ij}, \ldots, D_{1 \cdots n}$) corresponds to the variability associated with the interactions between parameters.

The sensitivity indices are calculated as

$$S_i = D_i / \mathrm{var}(Y) \tag{5-2}$$

where S_i is the first order sensitivity index for factor x_i, measuring the main effect of x_i on the output (Saltelli et al., 2000; DeJonge et al., 2012).

In this study, only total order indices were presented as they account for the interactions of a parameter with all other parameters. Total order indices can be written

$$TS_i = S_i + \sum_{1 \leq i < j \leq n} S_{ij} + \cdots S_{1 \cdots n} \tag{5-3}$$

Twenty parameters were selected from the linked SWAT-MODFLOW-RT3D model for our GSA (Arabi et al., 2006; Tuppad et al., 2010; Dechmi et al., 2012; Bailey et al., 2014; Wei et al., 2018a, 2018b; Wei and Bailey, 2019), with a realistic range assigned to each parameter (Table 1). We assumed uniform distributions as the prior parameter distributions. The SimLab's sensitivity and uncertainty analysis software (Simlab, 2011) were used for sample generation and sensitivity index calculation. A total of 672 input sets were generated using the option of Sobol's method. This minimum sample size was selected in order to minimize the total simulation time. Each input set was run from 1999 to 2007 with two years warmup period specified. SWAT-MODFLOW-RT3D simulated outputs of in-stream NO_3-N and soluble P loadings, and groundwater NO_3-N and soluble P concentrations were summarized and analyzed in SimLab to generate index rankings. The simulation outputs from our sensitivity analysis were used to

generate predictive uncertainty, with 95th percentiles interval (P.I.) calculated to represent the possible ranges for each output variable.

5.3 RESULTS AND DISCUSSIONS

5.3.1 Sensitivity analysis

Figure 46A displays the sensitivity results of in-stream nutrient loadings. It shows that among all the tested parameters, flow related parameters in SWAT had relative more impact on surface nutrient results. The output response in-stream NO_3-N loading was highly sensitive to the channel hydraulic conductivity "CH_K2". The study area is a groundwater dominant region with intensive groundwater and surface interactions. High nitrate concentrations in groundwater, resulting in "CH_K2" to be the most sensitive parameter governing the in-stream NO_3-N loadings. Channel process parameter manning's n value "CH_N2" and percolation related nitrate percolation coefficient "NPERCO" was among the most sensitive parameters for in-stream NO_3-N loadings. As can be seen from the figure that curve number "CN2" was sensitive as well, because it affects surface runoff. Large amount of nutrients come from non-point sources getting into stream through surface runoff. Curve number "CN2" was the most sensitive parameter for in-stream soluble P loadings, followed by manning's n value for the main channel "CH_N2", and USLE equation soil erodibility factor "USLEK". Both in-stream NO_3-N and soluble P were sensitive to the depth from soil surface to bottom parameter "SOL_Z", which are related with the soil water storage. The high sensitive is caused by the saturation excess runoff being dominant during the simulation period.

Figure 46B shows the sensitivity results of groundwater nutrient concentrations, with the major affection coming from MODFLOW/RT3D parameters. Groundwater NO_3-N concentration was most sensitive to first-order rate constant for NO_3 " μ_{NO_3} " and the Monod half-saturation constant for NO_3 " K_{NO_3} " due to the substantial influence of these parameters to NO_3-N reactive transport in groundwater systems. Denitrification threshold water content "SDNCO" and Denitrification exponential rate

165

coefficient "CDN" directly influence soil denitrification processes, which controlled how much NO_3-N could leaching into aquifer systems. The aquifer properties specific storage "S_s", hydraulic conductivity "K", and specific yield "S_y" were among the high sensitive parameters for NO_3-N and soluble P groundwater concentrations. These parameters describe the processes of groundwater transportation, which is the major input for RT3D to solve the governing equations. "R_P", phosphorus retardation coefficient turned out to have the highest impact on groundwater soluble P concentrations since soluble P can be attached to mineral surfaces via sorption.

5.3.2 Uncertainty analysis

All of the parameters used during the SA stage (See Table 13) were considered in the UA. Figure 47 shows the lower and upper bounds of the 95% P.I. for the response variables in-stream NO_3-N and soluble P loadings (Figure 47) and in-stream soluble P concentrations (Figure 48). In general, the uncertainty band is able to follow the spatiotemporal variability and magnitude of in-stream loadings and concentrations for both species quite well. In general, the in-stream NO_3-N loadings/concentrations varying from 755 kg/1.2 mg L^{-1} to 65870 kg/20.2 mg L^{-1} for the upper bound and from 45 kg/0.2 mg L^{-1} to 51195 kg/3.4 mg L^{-1} for the low bound, while in-stream soluble P loadings ranging from 12 kg/0.03 mg L^{-1} to 40053 kg/2.6 mg L^{-1} for the upper bound and from 5 kg/0.02 mg L^{-1} to 9309kg/0.9 mg L^{-1} for the lower bound, respectively. The uncertainty band given in Figure 47 indicate that the model's in-stream nutrients loading prediction is fairly consistent, with the baseline in-stream nutrient concentrations peaks values simulated close to the upper bound. Some parameter combinations have substantial impact on reducing NO_3-N and soluble P peak loadings, resulting large uncertainty range at those peaks. Similar results can be seen in the nutrient in-stream concentrations' uncertainty band shown in Figure 48.

The predicted output uncertainty of groundwater nutrient concentrations are shown in Figure 49 for NO_3-N and Figure 50 for soluble P. As can be seen from the figures, the high concentration values of both species for upper and lower bound typically located along the river corridor. Average of predicted NO_3-N concentrations is 5.2 mg L^{-1} for upper bound and 3.2 for lower bound while mean value of predicted

soluble P concentrations is 0.13 mg L^{-1} for upper bound and 0.09 mg L^{-1} for lower bound. Figure 49A and Figure 50 A predicts the cell-wise upper bound groundwater NO$_3$-N and soluble P spatial distribution, with the NO$_3$-N ranges from 0.01 to 66.3 mg L^{-1} and soluble P ranges from 0.0003 to 2.17 mg L^{-1}, respectively. On the other hand, Figure 49B and Figure 50B displays the lower bound groundwater NO$_3$-N and soluble P spatial distribution, with the NO$_3$-N varies from 0.01 to 31.3 mg L^{-1} and soluble P ranges from 0.0002 to 1.37 mg L^{-1}, respectively. These results can be used by stakeholders to determine long-term effects of contaminant remediation strategies in stream-aquifer systems.

5.4 SUMMARY AND CONCLUSIONS

In this chapter, parameter sensitivity and predictive uncertainty were analyzed using Sobol method through Simlab for SWAT-MODFLOW-RT3D simulated in-stream and groundwater nutrient concentrations. Among the 20 parameters tested, flow related parameters (CH_K2, CH_N2, and CN2) in SWAT had the strongest control on surface nutrient loadings while groundwater nutrient concentrations were mainly affected by parameters governed processes of groundwater denitrification and groundwater flow from MODFLOW/RT3D. In the predictive UA, 95% P.I. uncertainty bands for in-stream nutrient loadings and concentrations, and variations for groundwater nutrient concentrations are generated by changing the same parameters applied in SA. The uncertainty results show the influence of model parameters on predicted result and provide possible ranges of model response to help stakeholders making decision.
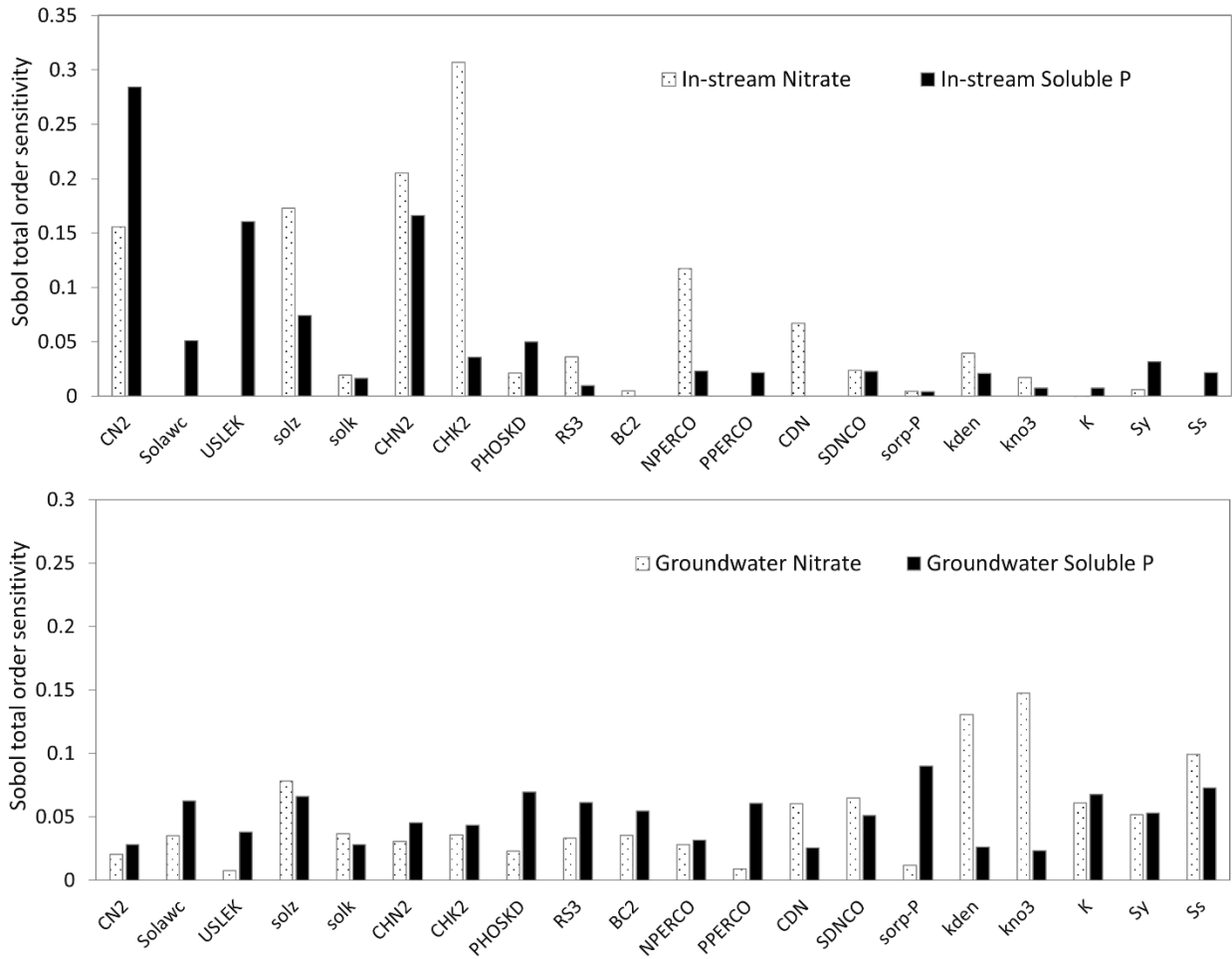
Figure 46. Model input parameters sensitivity estimated by Sobol method under in-stream NO$_3$-N and soluble P loadings.
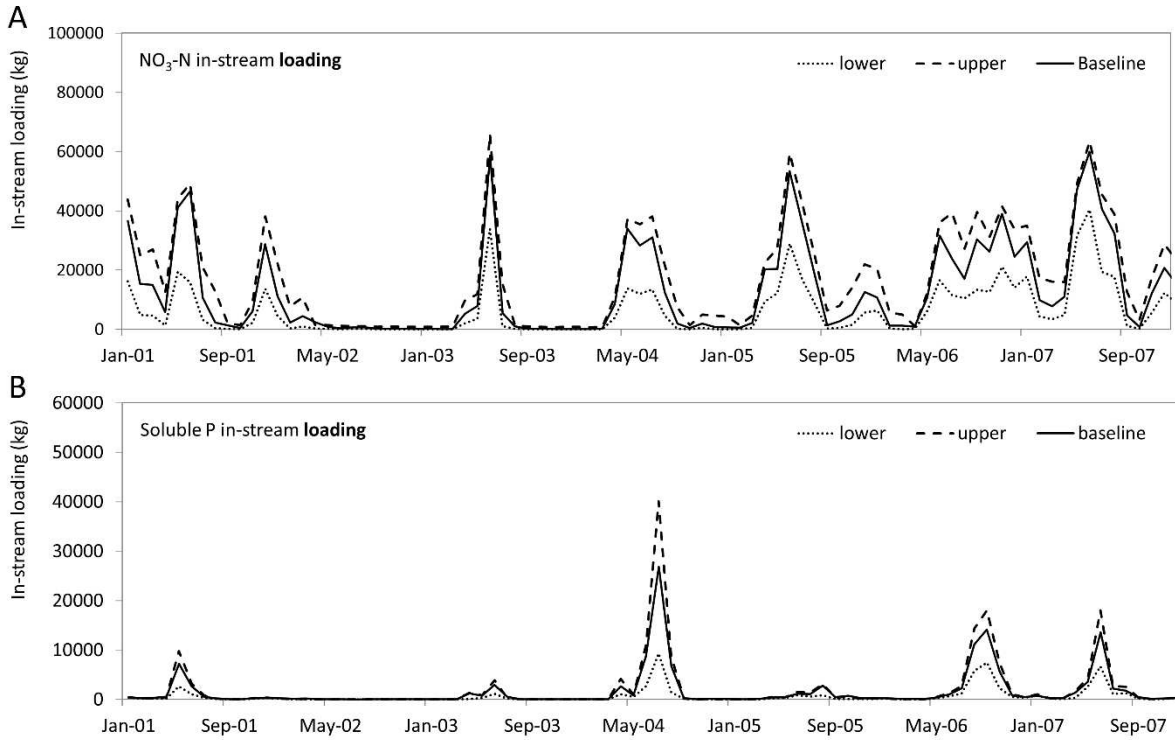
Figure 47. Effect of model parameters on nutrient in-stream loadings.
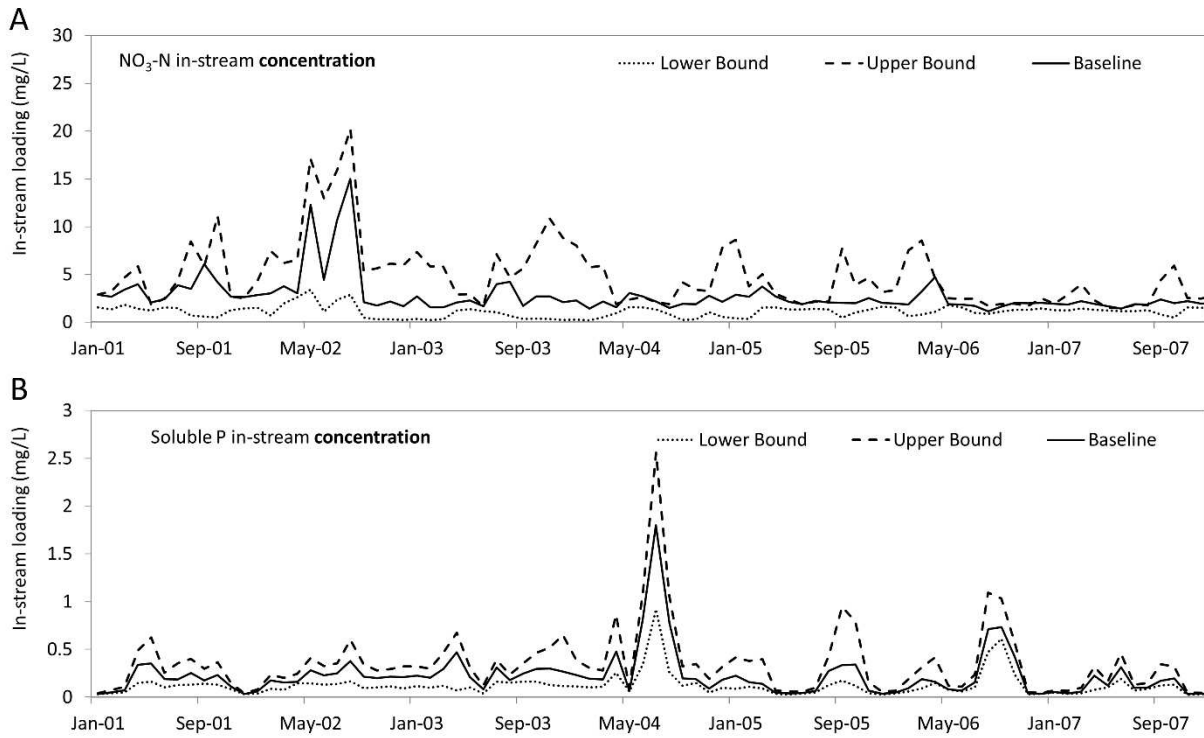
Figure 48. Effect of model parameters on nutrient in-stream concentrations
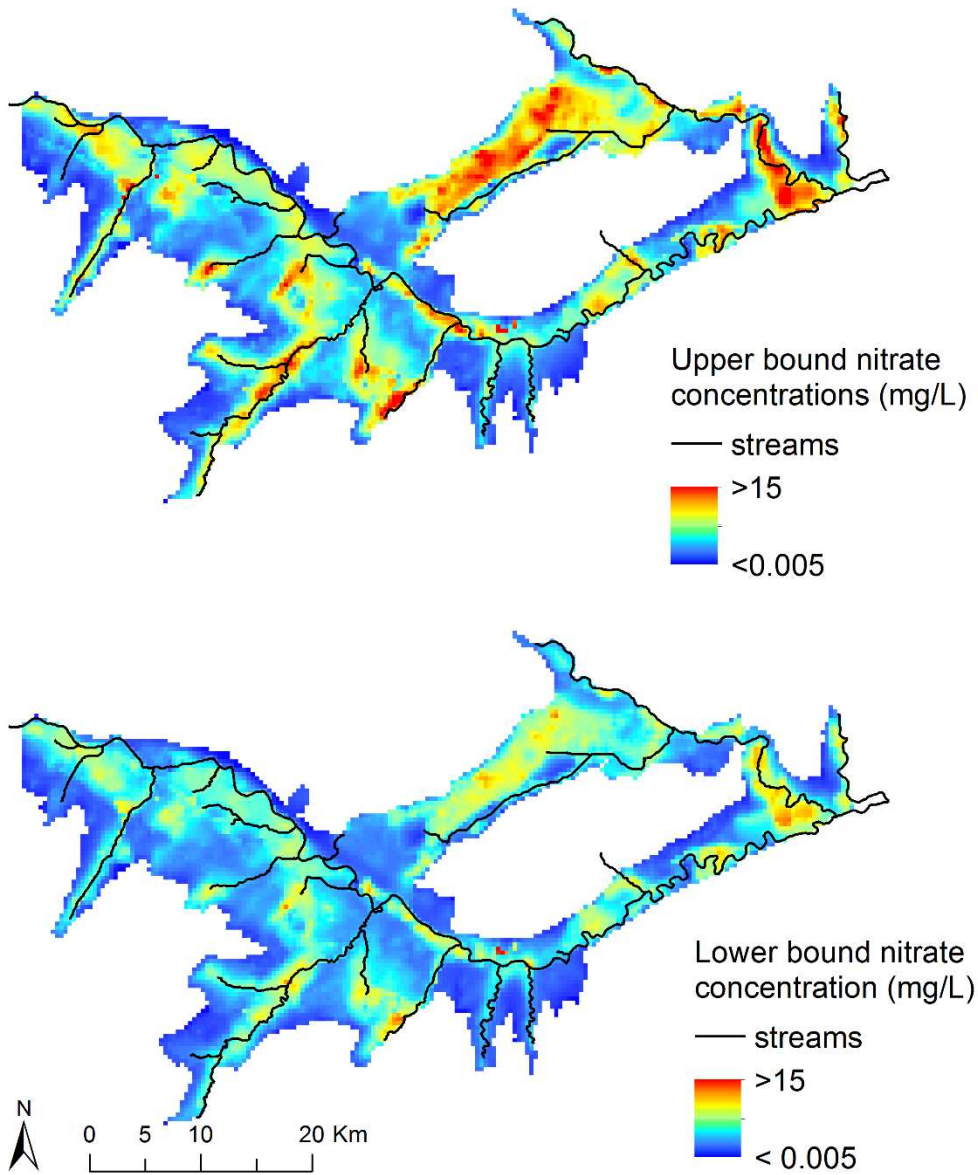
Figure 49. Groundwater NO$_3$-N predicted cell-wise distributions for upper and lower bound of uncertainty analysis.
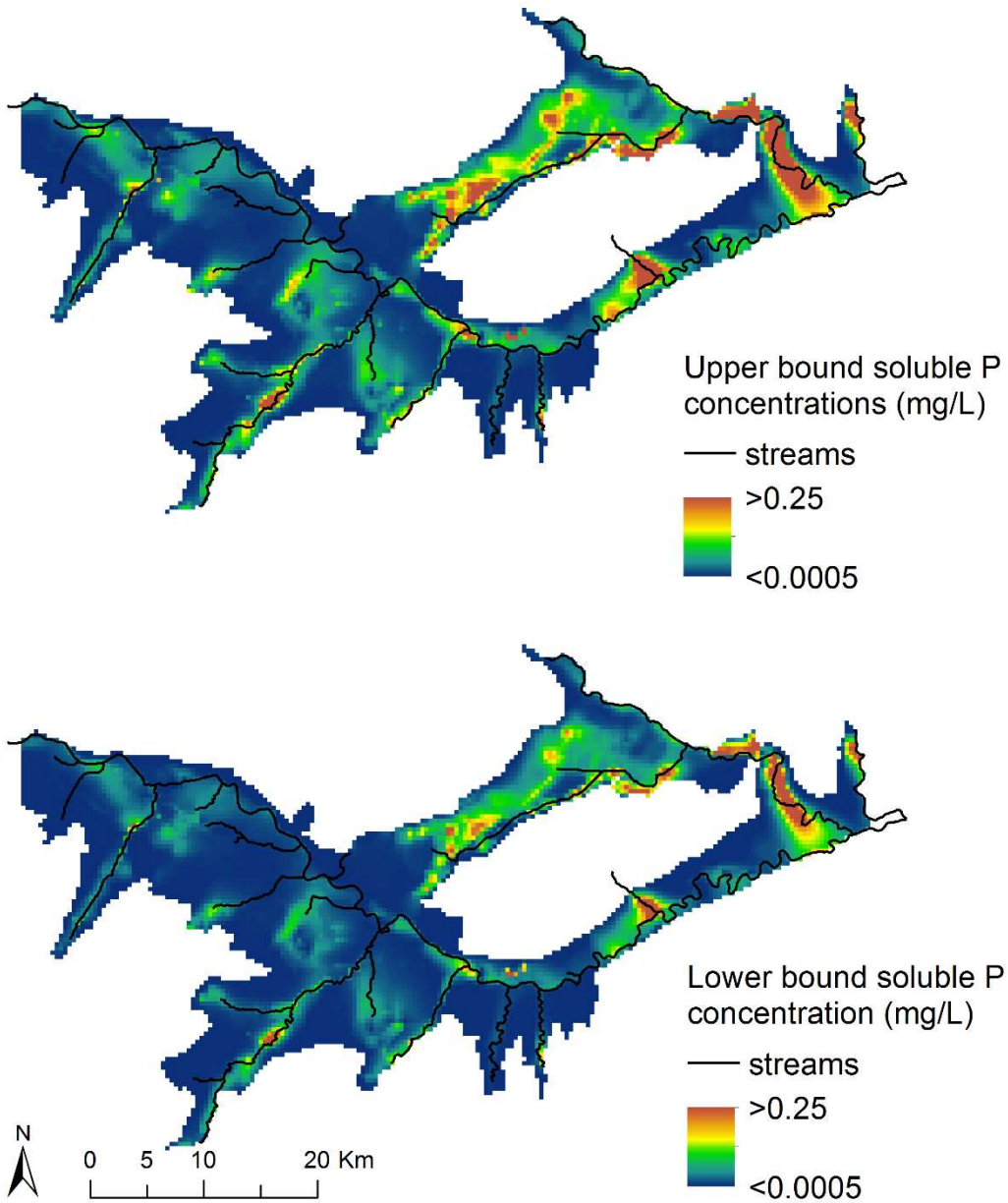
Figure 50. Groundwater soluble P predicted cell-wise distributions for upper and lower bound of uncertainty analysis.Table 1.1. The input parameters and their ranges for the sensitivity/uncertainty analysis.

Table 13. Sensitivity and Uncertainty input parameters

Name	Definition	Lower bound	Upper bound	Scalar[1]
SWAT parameters				
CN2	SCS runoff curve number for moisture condition II	0.95	1.05	Yes
SOL_AWC	Available water capacity	0.95	1.05	Yes
USLEK	USLE equation soil erodibility factor	0.95	1.05	Yes
SOL_Z	Depth of soil surface to bottom of layer	0.95	1.05	Yes
SOL_K	Saturated hydraulic conductivity	0.95	1.05	Yes
CH_N2	Manning's n value for the main Channel	0.95	1.05	Yes
CH_K2	Effective hydraulic conductivity of channel	0.95	1.05	Yes
PHOSKD	P soil partitioning coefficient	160	190	
RS3	Benthic source rate for NO_4-N in the reach	0.06	0.6	
BC2	Rate constant for biological oxidaton of NO_2 to NO_3 in the reach	0.4	1	
NPERCO	Nitrate percolation coefficient	0.1	0.5	
PPERCO	Phosphorus percolation coefficient	10	14	
CDN	Denitrification exponential rate coefficient	0.5	2.5	
SDNCO	Denitrification threshold water content (fraction of field capacity water content above which dnitrification takes place)	0.1	0.5	
RT3D parameters				
R_P	partition coefficient for Soluble P	0.1	2	
μ_{NO3}	first-roder rate constant for denitrifitaion	0.0001	0.01	
K_{NO3}	Monod half-saturation term for denitrification	0.1	10	
MODFLOW parameters				
K	Hydraulic conductivity	0.95	1.05	Yes
Sy	Specific yield	0.95	1.05	Yes
Ss	Specific storage	0.00001	0.00003	

1. If a scalar option is used, the value picked from the range served as a scalar, which means the original value of the parameter multiplied the scalar value. As each cell used different values of the same paramter, the scalar option allowed us to maintain the relative differences between the cells.

REFERENCES

Abbaspour, K.C., Rouholahnejad, E., Vaghefi, S., Srinivasan, R., Yang, H., Kløve, B., 2015. A

continental-scale hydrology and water quality model for Europe: Calibration and uncertainty of a

high-resolution large-scale SWAT model. Journal of Hydrology 524, 733–752.

https://doi.org/10.1016/j.jhydrol.2015.03.027

Anderton, S., Latron, J., Gallart, F., 2002. Sensitivity analysis and multi-response, multi-criteria

evaluation of a physically based distributed model. Hydrological Processes 16, 333–353.

https://doi.org/10.1002/hyp.336

Arabi, M., Govindaraju, R.S., Hantush, M.M., 2007. A probabilistic approach for analysis of uncertainty

in the evaluation of watershed management practices. Journal of Hydrology 333, 459–471.

https://doi.org/10.1016/j.jhydrol.2006.09.012

Arabi, M., Govindaraju, R.S., Hantush, M.M., Engel, B.A., 2006. Role of Watershed Subdivision on

Modeling the Effectiveness of Best Management Practices with Swat1. JAWRA Journal of the

American Water Resources Association 42, 513–528. https://doi.org/10.1111/j.1752-

1688.2006.tb03854.x

Aronica, G., Bates, P.D., Horritt, M.S., 2002. Assessing the uncertainty in distributed model predictions

using observed binary pattern information within GLUE. Hydrological Processes 16, 2001–2016.

https://doi.org/10.1002/hyp.398

Assegid, Y., Melesse, A.M., Naja, G.M., 2015. Spatial relationship of groundwater–phosphorus

interaction in the Kissimmee river basin, South Florida. Hydrological Processes 29, 1188–1197.

https://doi.org/10.1002/hyp.10241

Bailey, R.T., Gates, T.K., Ahmadi, M., 2014. Simulating reactive transport of selenium coupled with

nitrogen in a regional-scale irrigated groundwater system. Journal of Hydrology 515, 29–46.

https://doi.org/10.1016/j.jhydrol.2014.04.039

Benaman, J., Shoemaker, C.A., 2004. Methodology for Analyzing Ranges of Uncertain Model

    Parameters and Their Impact on Total Maximum Daily Load Process. Journal of Environmental

    Engineering 130, 648–656. https://doi.org/10.1061/(ASCE)0733-9372(2004)130:6(648)

Beven, K., 2018. Environmental Modelling : An Uncertain Future? CRC Press.

    https://doi.org/10.1201/9781482288575

Beven, K., 1995. Linking parameters across scales: Subgrid parameterizations and scale dependent

    hydrological models. Hydrological Processes 9, 507–525. https://doi.org/10.1002/hyp.3360090504

Dabrowski, J.M., 2014. Applying SWAT to predict ortho-phosphate loads and trophic status in four

    reservoirs in the upper Olifants catchment, South Africa.

Dechmi, F., Burguete, J., Skhiri, A., 2012. SWAT application in intensive irrigation systems: Model

    modification, calibration and validation. Journal of Hydrology 470–471, 227–238.

    https://doi.org/10.1016/j.jhydrol.2012.08.055

DeJonge, K.C., Ascough, J.C., Ahmadi, M., Andales, A.A., Arabi, M., 2012. Global sensitivity and

    uncertainty analysis of a dynamic agroecosystem model under different irrigation treatments.

    Ecological Modelling 231, 113–125. https://doi.org/10.1016/j.ecolmodel.2012.01.024

Gallagher, M., Doherty, J., 2007. Parameter estimation and uncertainty analysis for a watershed model.

    Environmental Modelling & Software 22, 1000–1020. https://doi.org/10.1016/j.envsoft.2006.06.007

Jakeman, A.J., Hornberger, G.M., 1993. How much complexity is warranted in a rainfall-runoff model?

    Water Resources Research 29, 2637–2649. https://doi.org/10.1029/93WR00877

Jakeman, A.J., Letcher, R.A., Norton, J.P., 2006. Ten iterative steps in development and evaluation of

    environmental models. Environmental Modelling & Software 21, 602–614.

    https://doi.org/10.1016/j.envsoft.2006.01.004

Laloy, E., Fasbender, D., Bielders, C.L., 2010. Parameter optimization and uncertainty analysis for plot-

    scale continuous modeling of runoff using a formal Bayesian approach. Journal of Hydrology 380, 82–

    93. https://doi.org/10.1016/j.jhydrol.2009.10.025

Muleta, M.K., Nicklow, J.W., 2005. Sensitivity and uncertainty analysis coupled with automatic

    calibration for a distributed watershed model. Journal of Hydrology 306, 127–145.

    https://doi.org/10.1016/j.jhydrol.2004.09.005

Pappenberger, F., Beven, K.J., 2006. Ignorance is bliss: Or seven reasons not to use uncertainty analysis.

    Water Resources Research 42. https://doi.org/10.1029/2005WR004820

Razavi, S., Gupta, H.V., 2016. A new framework for comprehensive, robust, and efficient global

    sensitivity analysis: 2. Application. Water Resources Research 52, 440–455.

    https://doi.org/10.1002/2015WR017559

Saltelli, A., Annoni, P., 2010. How to avoid a perfunctory sensitivity analysis. Environmental Modelling

    & Software 25, 1508–1517. https://doi.org/10.1016/j.envsoft.2010.04.012

Saltelli, A., Chan, K., Scott, E.M., 2000. Sensitivity Analysis: Gauging the Worth of Scientific Models.

    Vol. 134. Wiley.

Simlab, 2011. SimLab: Software package for uncertainty and sensitivity analysis. Downloadable for free

    at: http://simlab. jrc. ec. europa. eu [Last accessed 10 Dec 2012].

Sobol, I.M., 1993. Sensitivity analysis for non-linear mathematical models. Mathematical modelling and

    computational experiment 1, 407–414.

Song, X., Zhang, J., Zhan, C., Xuan, Y., Ye, M., Xu, C., 2015. Global sensitivity analysis in hydrological

    modeling: Review of concepts, methods, theoretical framework, and applications. Journal of

    Hydrology 523, 739–757. https://doi.org/10.1016/j.jhydrol.2015.02.013

Tuppad, P., Kannan, N., Srinivasan, R., Rossi, C.G., Arnold, J.G., 2010. Simulation of Agricultural

    Management Alternatives for Watershed Protection. Water Resour Manage 24, 3115–3144.

    https://doi.org/10.1007/s11269-010-9598-8

Ullrich, A., Volk, M., 2009. Application of the Soil and Water Assessment Tool (SWAT) to predict the

    impact of alternative management practices on water quality and quantity. Agricultural Water

    Management 96, 1207–1217. https://doi.org/10.1016/j.agwat.2009.03.010

van Griensven, A., Meixner, T., Grunwald, S., Bishop, T., Diluzio, M., Srinivasan, R., 2006. A global sensitivity analysis tool for the parameters of multi-variable catchment models. Journal of Hydrology 324, 10–23. https://doi.org/10.1016/j.jhydrol.2005.09.008

Wei, X., Bailey, R.T., 2019. Assessment of System Responses in Intensively Irrigated Stream–Aquifer Systems Using SWAT-MODFLOW. Water 11, 1576. https://doi.org/10.3390/w11081576

Wei, X., Bailey, R.T., Records, R.M., Wible, T.C., Arabi, M., 2018a. Comprehensive simulation of nitrate transport in coupled surface-subsurface hydrologic systems using the linked SWAT-MODFLOW-RT3D model. Environmental Modelling & Software. https://doi.org/10.1016/j.envsoft.2018.06.012

Wei, X., Bailey, R.T., Tasdighi, A., 2018b. Using the SWAT Model in Intensively Managed Irrigated Watersheds: Model Modification and Application. Journal of Hydrologic Engineering 23, 04018044.

Wu, B., Zheng, Y., Tian, Y., Wu, X., Yao, Y., Han, F., Liu, J., Zheng, C., 2014. Systematic assessment of the uncertainty in integrated surface water-groundwater modeling based on the probabilistic collocation method. Water Resources Research 50, 5848–5865. https://doi.org/10.1002/2014WR015366

Zhang, Y., 2016. Simulating canopy dynamics, productivity and water balance of annual crops from field to regional scales (Thesis). Colorado State University. Libraries.

CHAPTER 6. SUMMARY AND FUTURE WORK

The research presented in this dissertation summarizes efforts to understanding the movement, transportation, and storage of Nitrate as N (NO_3-N) and soluble P species in intensively managed irrigated systems. These effects contained first, enhancing the capacity of SWAT model within such a system, which includes designating each cultivated field as a hydrologic response unit (HRU) and including recorded crop rotations; applying scheduled irrigation according to water rights; simulating seepage from earthen irrigation canals, and account for N and P mass sources that substantially affect the nutrient transportation in the watershed; second, integrating SWAT with two widely-used models, MODFLOW, and RT3D, in order to address pressing needs for credible representation of N and P processes in irrigated agroecosystems; and third, assess viable remediation strategies for N and P contamination in highly-managed irrigation watersheds in semi-arid region. The model is applied to a 732 km^2 study area within the Lower Arkansas River Valley (LARV) in southeastern Colorado. Conditions along the Arkansas River are typical of those in many other intensively irrigated regions, the results of this dissertation can be applied to other semi-arid irrigated regions world-wide.

The major conclusions for the development and testing of the SWAT, SWAT-MODFLOW, and SWAT-MODFLOW-RT3D are contained in Chapter 2-5. Possible areas of future work can be addressed:

- Better model calibration can be performed for areas adjacent to tributaries.

- Percolation and upward flux of water and nutrient mass through the vadose zone between the root zone and the water table can be addressed by using MODFLOW-UZF package.

- Solute transport through river riparian areas can be considered, which are influenced by uptake by vegetation, volatilization, and enhanced sorption and denitrification due to large amount of organic matters.

- Adopt the coupled model to estimate future impact climate changes on hydrology behavior and processes that govern N and P fate and transportations.

- More species could be included in this model such selenium (Se), ammonium (NH_4), etc.

- Incorporating interactions between N and P with other species.

- Apply the model to investigate a larger array of BMP scenarios.

- Extension of the model to the downstream study region of the LARV.

- Uncertainty and venerability of this complex model can be further addressed.

APPENDIX A

Comprehensive Simulation of Nitrate Transport in Coupled Surface-Subsurface Hydrologic Systems using the linked SWAT-MODFLOW-RT3D model[1]

A1. SUMMARY

This paper presents SWAT-MODFLOW-RT3D, a model that couples the semi-distributed watershed model SWAT (Soil and Water Assessment Tool) with the groundwater flow model MODFLOW and the groundwater solute reactive transport model RT3D to simulate nitrate (NO_3) fate and transport in a watershed system. The model is based on a recently developed SWAT-MODFLOW model, with RT3D now called as a subroutine within the MODFLOW code to provide a single, stand-alone model code. RT3D uses NO_3 concentration of deep percolation water from SWAT and groundwater heads and flows from MODFLOW to simulate spatially-varying groundwater NO_3 concentration and NO_3 loading to/from streams, with the latter used by SWAT to route NO_3 mass through the network. Model use is demonstrated through an application to the Sprague River Watershed ($4,100$ km^2) in Oregon. Other chemical species of interest can be included in the RT3D reaction module in applications of the model to other watersheds.

A2. INTRODUCTION

Due to the requirement for increased production of food and energy, the application of fertilizers has increased augmenting nitrogen (N) pollution in the environment (Erisman et al., 2013). Nitrate (NO_3) has been one of the dominant forms of increased N loading since the 1970s (Dise and Wright, 1995; Smith et al., 1999). High concentration of NO_3 dissolved in surface water can lead to eutrophication of water bodies (Puckett, 1994; Nolan et al., 1997; Vidon et al., 2010), and also can cause health problems such as methemoglobinemia in infants and stomach cancer in adults (Carpenter et al., 1998).

The presence of NO_3 in groundwater systems also can contribute to the oxidative dissolution and inhibition of chemical reduction of other dissolved environmental pollutants, such as selenite (SeO_4) and sulfate (SO_4) (e.g. Wright, 1999; Bailey et al., 2012a). As such, the US Environmental Protection Agency (US EPA) has established a maximum contaminant level (MCL) of 10 mg/L NO_3-N (US EPA, 1995) for drinking water. NO_3 is very mobile in soil water and groundwater systems, with a low sorption capacity, but can undergo chemical reduction (denitrification) if the following conditions are met: the presence of microbial populations possessing the appropriate metabolic capacity, the presence of an electron (e^-) donor such as organic carbon, and restricted availability of dissolved oxygen (O_2), and near-saturation conditions (Korom, 1992). Under rainfall or irrigated conditions, high levels of soluble NO_3 can occur in groundwater due to leaching through the soil profile (Randall and Iragavarapu, 1995). NO_3 then is transported through the saturated zone according to advection-dispersion processes and finally delivered to streams and rivers via groundwater discharge (Duff and Triska, 2000).

Approaches to assess NO_3 contamination, fate, and reactive transport at the watershed and river-basin scale are needed to investigate remediation strategies under scenarios of changes in land use and climatic patterns. Models can be useful assessment tools for the quantification of pollution pressures by nutrients (Refsgaard et al., 1999; Conan et al., 2003). Over the last decades, several empirical, lumped models of nutrient transport, retention and loss in river basins have been developed based on the export-coefficient approach (Hetling et al., 1999), small-scale lysimeter-based processes (Wriedt et al., 2007; Kaufmann et al., 2014), GIS-based mass balance method (Pieterse et al., 2003), and statistical regressions (Seitzinger et

al., 2002). Each model was initially developed for a different region and goal, and differed from other models in its complexity, spatial and temporal resolution, and data requirements. Often, however, individual hydrological and chemical processes need to be simulated in space and time to relate plant growth and root uptake, land use and cropping patterns, and climate change to the corresponding responses. These responses include surface runoff, root-soil zone processes and nutrient cycling, soil moisture flow and chemical transport, groundwater flow and chemical transport, and groundwater/surface water interactions. Examples of models that incorporate many of these processes include the Nitrogen Modelling System (NMS) (Lunn et al., 1996), which accounts for NO_3 transport at the catchment scale; the Integrated Nitrogen model in Catchments (INCA) model (Whitehead et al., 1998), which simulates N surface and subsurface pathways undergoing reaction kinetics; and the Soil and Water Assessment Tool (SWAT) (Arnold et al., 1998; Neitsch et al., 2011), which simulates plant growth, surface and subsurface flow, and in-stream flow and nutrient transport processes.

Another subset of existing groundwater solute reactive transport models, e.g. Reactive Transport in 3 Dimensions (RT3D) (Clement, 1997) and Modular 3-D Multi-Species Transport model (MT3DMS) (Zheng and Wang, 1999), has been modified to include nitrogen chemical kinetics (Molenat and Gascuel-Odoux, 2002; Wriedt and Rode, 2006; Bailey et al., 2014) at the regional scale. These models receive groundwater head and flow output from the 3D groundwater flow model MODFLOW (Harbaugh, 2005) to simulate solute transport in a heterogeneous aquifer system. However, these studies lack the appropriate land surface and soil-plant hydrological processes to analyze NO_3 at the watershed scale and in the pathways (groundwater, runoff, in-stream) of concern.

In attempts to account for the main hydrological processes in both the land surface system and the groundwater system, several researchers in the past two decades have linked SWAT with MODFLOW at varying levels of complexity (Sophocleous and Perkins, 2000; Conan et al., 2003; Kim et al., 2008; Guzman et al., 2015). Most recently, Bailey et al (2016) provided an enhanced SWAT-MODFLOW modelling framework which uses an internal mapping scheme to pass simulated data between SWAT Hydrologic Response Units (HRUs), the i.e. unique combinations of land use, soil, and slope that

182

comprise SWAT's main computational unit, and MODFLOW finite difference grid cells on a time step defined by the model user. The modelling system also allows the SWAT and MODFLOW models to be of difference spatial extents. To incorporate nitrate fate and transport, three specific studies have linked MT3DMS to SWAT-MODFLOW modelling systems: Conan et al. (2003) for a 12 km^2 catchment in Brittany, France; Galbiati et al. (2006) for the 20 km^2 Bonello watershed in Italy; and Narula and Gosain (2013) for the 11,600 km^2 Upper Yamuna watershed in the Ganga River Basin, India. Each modelling systems, consisted of the three separate models (SWAT, MODFLOW, MT3DMS) that are loosely coupled, i.e. outputs from the SWAT are provided to MODFLOW and MT3DMS, but MODFLOW and MT3DMS outputs are not provided to SWAT on the following time step. Therefore, groundwater flow and solute transport processes are dependent on land surface processes, but land surface processes such as streamflow and stream solute transport are not dependent on groundwater processes. A direct integration is required, particularly in watersheds wherein groundwater is close to the ground surface. Each study also used month-averaged rates and loads, adequate if water tables are deep but not appropriate for watersheds wherein groundwater is a significant component of streamflow.

In this study, the recently developed SWAT-MODFLOW model (Bailey et al., 2016) that includes internal mapping of HRU data to grid cell format is modified to include RT3D to improve the assessment of reactive transport of NO_3 in both surface and groundwater systems at the watershed scale. RT3D is included as a subroutine within the MODFLOW code, thus providing a single stand-alone SWAT-MODFLOW-RT3D model executable with surface/subsurface coupling occurring on a daily time step. This integration allows spatio-temporal characterization of groundwater NO_3-N concentration, groundwater NO_3-N loading to/from the stream network, and in-stream NO_3-N loading. To demonstrate model capabilities, the SWAT-MODFLOW-RT3D model is applied to the Sprague River watershed (4100 km^2) within the Upper Klamath Basin in southern Oregon. This watershed was chosen due to observed groundwater-driven streamflow in several catchments. Model results are tested against groundwater NO_3-N concentration, groundwater NO_3-N loading to/from the stream network, and in-

stream NO_3-N loading. Observation data also are compared against a calibrated stand-alone SWAT model to demonstrate the advantages of using the coupled SWAT-MODFLOW-RT3D model.

A2. Model Overview

This section summarizes the base models that are used in the SWAT-MODFLOW-RT3D framework. Section 3 provides the details of linking the base models to provide the stand-alone fully coupled model.

A2.1 The Soil and Water Assessment Tool (SWAT)

The SWAT model (Arnold et al., 1998; Neitsch et al., 2005; Gassman et al., 2007; Neitsch et al., 2011) is a physically-based, semi-distributed parameter, basin-scale, continuous-time hydrologic model that operates on a daily time step. It is designed to predict the influence of land management practices on water, sediment, and nutrient yields at the watershed scale. The lumped model emphasizes land surface hydrologic, sediment, and nutrient processes and is computationally efficient for long-term simulation. The watershed is divided into multiple sub-basins, with each sub-basin containing one stream. Within each sub-basin, mass balance equations for water, sediment, and nutrients are computed at the level of hydrologic response units (HRUs), which are areal regions that have a unique combination of land use, soil properties, and slope. HRUs can be spatially disconnected and do not have a designated geographic location. Water, nutrient, and sediment output from each HRU are routed directly the outlet of the corresponding sub-basin, with the connectivity used to route to downstream sub-basin. In terms of groundwater flow and solute transport, SWAT employs one-dimensional analytical lagging routines to route groundwater and nutrient mass from each HRU to the sub-basin outlet through the stream network. These routines, therefore, neglect heterogeneity in aquifer parameters (e.g. hydraulic conductivity, porosity, specific yield, and specific storage) and regional flow gradients and do not consider the subsurface spatial interactions between HRUs. SWAT, therefore, is not capable of expressing the spatial distribution of groundwater levels and groundwater interactions with surface water, i.e. groundwater discharge and stream seepage.

A2.2 MODFLOW

MODFLOW (Harbaugh 2005) is a physically based, three-dimensional groundwater model used in confined, unconfined, or mixed aquifer systems. Both steady state and transient conditions can be simulated. MODFLOW solves the groundwater flow equation based on the finite difference approach that requires the aquifer to be discretized into grid cells laterally and vertically, with aquifer properties assumed to be uniform within each cell. Model output includes groundwater hydraulic head at the center of each cell and, if using boundary condition packages such as the River (RIV) package or the Streamflow Routing (SFR) package, groundwater flow rates to/from each stream segment. To obtain spatially-varying

recharge rates, MODFLOW often is linked with land surface models such as the Precipitation-Runoff Modelling System (PRMS: Markstrom et al., 2015), such as in the integrated GSFLOW model (Markstrom et al., 2008), or SWAT, as is done in the model presented in this paper.

MODFLOW simulation results (hydraulic head, groundwater flow rates, sources/sinks flow rates) can be used by groundwater solute transport models such as MT3DMS (Prommer et al., 2003; Mao et al., 2006), RT3D (Huang et al., 2008; Bailey et al., 2013a; Bailey et al., 2014), and PHT3D (Prommer et al., 2003; Appelo and Rolle, 2010). Among all these solute transport models, RT3D allows the use of predefined (e.g., sequential decay reactions, microbial growth and transport) or user-defined sets of kinetically controlled reactions with the option of Monod and dual-Monod kinetics (e.g., Lee et al., 2006; Wriedt and Rode 2006). An ordinary differential equation (ODE) solver is used to solve multiple chemical reaction rate laws simultaneously, thereby allowing species' concentrations to affect each other, e.g. limiting the chemical reduction of an electron acceptor if microbially-preferred acceptors are present in the groundwater. Due to the capability of interactive multi-species transport for any number of solutes, we therefore have selected RT3D to include in the SWAT-MODFLOW modeling framework in this study (Section 2.4).

A2.3 SWAT-MODFLOW Model

The SWAT-MODFLOW (Bailey et al., 2016) modelling code used in this study uses the MODFLOW-NWT (Niswonger et al., 2011) version of MODFLOW and employs an internal mapping scheme that passes data between SWAT computational units (HRUs, sub-basins) and MODFLOW grid cells. The hydrological processes simulated by SWAT and by MODFLOW in the coupled SWAT-MODFLOW model are shown in Figure A1, with SWAT processes labeled in green and MODFLOW processes labeled in blue. The RT3D processes are labeled in red, and will be discussed in Section 3.
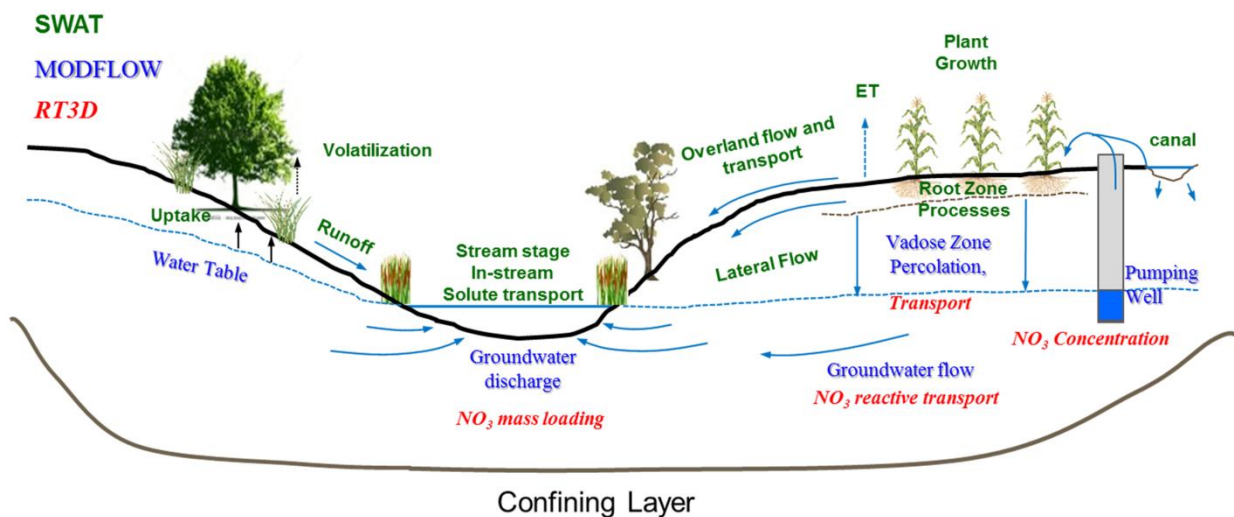

Figure A1. Schematic of the hydrologic cycle and SWAT, MODFLOW, and RT3D simulation processes.

The River package within MODFLOW is used to simulate volumetric exchange flow rates (i.e. either groundwater discharge rates or stream seepage rates) between the aquifer and the stream network using streambed hydraulic conductivity and Darcy's Law, with groundwater discharge occurring when water table elevation is higher than the stream stage. Deep percolation from the bottom of the soil profile, as calculated for each HRU in the watershed, is passed to MODFLOW grid cells as recharge, and the depth of each sub-basin stream is passed to the MODFLOW River cells. MODFLOW then solves the groundwater flow equation, and then passes water table elevation to each SWAT HRU and volumetric exchange flow rates to each SWAT sub-basin, with the latter added to the water routed through the watershed's stream network using SWAT's routing algorithms. Hence, SWAT provides surface water runoff and soil lateral flow to the stream network, where MODFLOW provides groundwater discharge and also seepage from the stream to the aquifer.

The mapping scheme between SWAT computational units and the MODFLOW finite difference grid cells is based on geo-processing routines performed during model construction. Due to the difference in the spatial discretization between the models, each HRU must be geographically located, which then can be intersected with the MODFLOW grid cells to provide connectivity between the two. The HRUs, typically constructed using ArcSWAT (Winchell et al., 2013), are first split into individual polygons to provide geographical locations to the original HRUs. These individual polygons are termed Disaggregated HRUs (DHRUs) (Bailey et al., 2016), which are used to pass HRU-based values to the MODFLOW grid cells, based on the percentage of the DHRU area that contributes to the grid cell area. According to this definition, the separated DHRUs share the same variable information with the original HRU calculation (e.g. soil deep percolation). The MODFLOW River cells are identified by intersecting the watershed stream network with the MODFLOW grid and, since the River cells in MODFLOW contribute groundwater-surface water interaction to each sub-basin stream, the group of River Cells that reside in each sub-basin must also be identified. Four SWAT-MODFLOW input text files are generated to store the mapping information for HRUs to DHRUs (*File 1*), DHRUs to MODFLOW grid cells (*File 2*), MODFLOW grid cells to DHRUs (*File 3*), and SWAT sub-basin to MODFLOW River cells (*File 4*). The information in these four text files is read at the beginning of the SWAT-MODFLOW simulation and stored in memory for use when MODFLOW is called by SWAT. These files can convert information back and forth between these models by running an executable file through a FORTRAN code. Figure A2 shows a schematic diagram of the coupling and spatial interaction between SWAT HRUs, DHRUs, river, and grid cells.
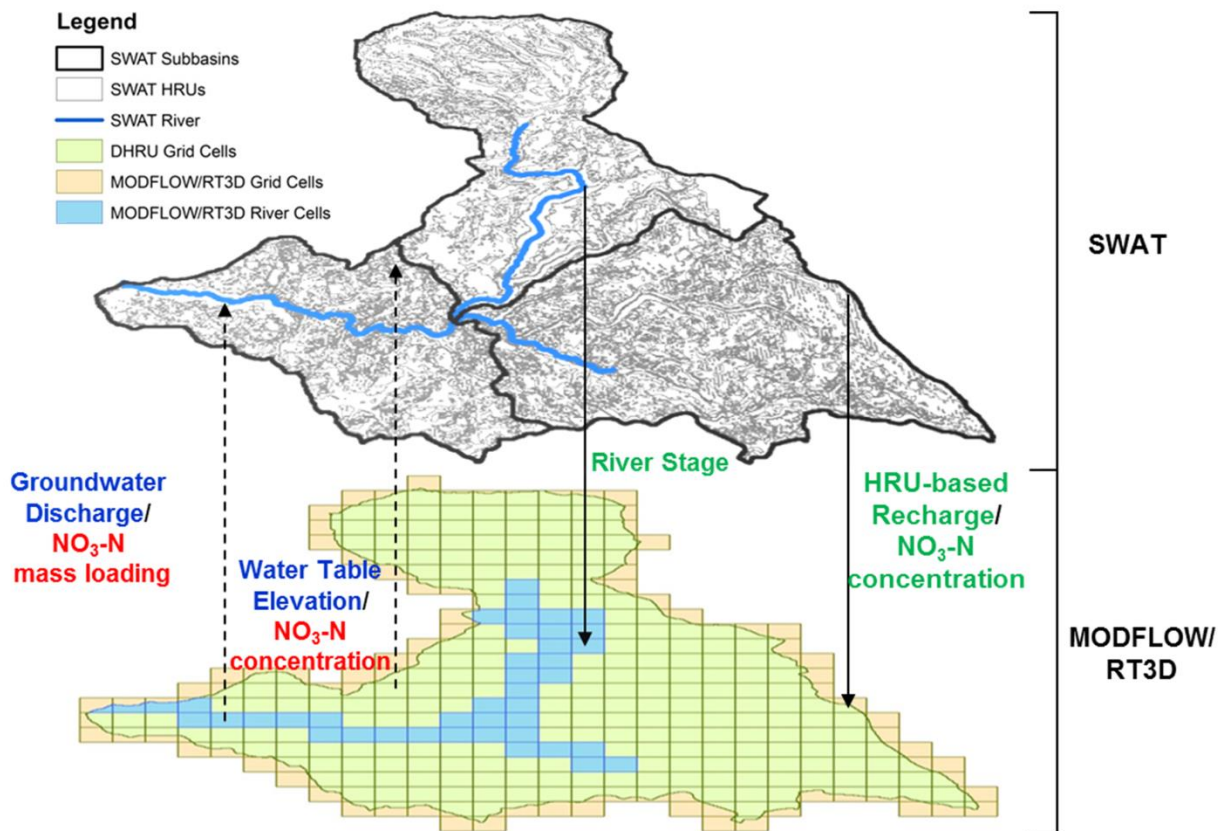
Figure A2. Schematic diagram of the SWAT-MODFLOW/RT3D coupling and spatial interactions between SWAT HRUs, DHRUs, river, and MODFLOW/RT3D grid cells. MODFLOW receives recharge values from HRU, simulates groundwater surface water interactions, and passes groundwater elevation and groundwater discharge back to SWAT. RT3D receives in-stream NO_3-N concentration from HRU, groundwater flow, source and sink from MODFLOW, and passes groundwater NO_3-N concentration and NO_3-N mass back to SWAT.

Lateral groundwater flow from adjacent subbasins, or from other parts of the regional aquifer system that is beyond the boundaries of the SWAT model, can be represented by specified head or time-varying head boundary conditions. These boundary conditions will bring groundwater into/out of the model domain based on the difference in simulated head and the boundary conditions at the boundary. Also, a larger MODFLOW model that encompasses the regional aquifer system can be used, with the SWAT model linked only for the area within the SWAT watershed boundary.

The theoretical documentation for SWAT-MODFLOW and tutorials for preparing SWAT-MODFLOW simulations are available on the main SWAT model website: http://swat.tamu.edu/software/swat-modflow/. The model has recently been applied to the Sprague River watershed (Bailey et al., 2016), the same study watershed for this study. Model results were compared

against groundwater elevation, stream discharge, and groundwater discharge to stream reaches within the watershed.

A2.4 RT3D (Reactive Transport in 3 Dimensions) Model

RT3D is a three-dimensional groundwater contaminant and solute transport model that can simulate advection, dispersion, and chemical reactions of dissolved constituents in groundwater (Clement, 1997; Clement et al., 1998). RT3D uses the groundwater hydraulic head, cell-by-cell flow data in all aquifer dimensions, and groundwater sources and sinks (e.g. groundwater pumping, recharge, groundwater-surface water exchange flow rates) outputs computed by a companion MODFLOW model to establish the groundwater flow field. RT3D was chosen due to its ability to simulate chemical kinetics of multiple interacting species. Assuming rigid porous media, linear equilibrium sorption, and saturated conditions, the system of advection-dispersion-reaction (ADR) equations describing the fate and transport of contaminants of species k can be written as follows (Clement, 1997):

$$\phi \frac{\partial C_k}{\partial t} = -\frac{\partial}{\partial x_i}\left(\phi v_i C_k\right) + \frac{\partial}{\partial x_i}\left(\phi D_{ij}\frac{\partial C_k}{\partial x_j}\right) + q_s C_{s_k} - \rho_b \frac{\partial \overline{C}_k}{\partial t} + \phi r \quad k = 1, 2, \ldots, m \qquad (1)$$

where m is the total number of aqueous-phase species, C_k is the concentration of the kth species $[M_f L_f^{-3}]$ where f denotes the fluid phase, D_{ij} is the hydrodynamic dispersion coefficient $[L^2 T^{-1}]$, v is the average seepage velocity $[L_b T^{-1}]$ where b denotes the bulk phase, ϕ is the soil porosity $[L_f^3 L_b^{-3}]$, q_s is the volumetric flux of water representing sources and sinks of the species $[L_f^3 T^{-1} L_b^{-3}]$, C_{s_k} is the concentration of the source or sink $[M_f L_f^{-3}]$, r represents the rate of all reactions that occur in the aqueous phase for the kth species $[M_f L_f^{-3} T^{-1}]$, ρ_b is the bulk density of the porous media $[M_b L_b^{-3}]$, and $\overline{C}_k$ is the concentration of the kth species sorbed on solids $[M_f M_b^{-1}]$.

The system of ADR equations, with one equation for each chemical species, is solved for the spatially-variable change in C_k using the operator-split (OS) numerical scheme (Yeh and Tripathy, 1989) using the same finite difference grid as the accompanying MODFLOW model. With the OS method, an iterative solver is used to simulate the change in concentration implicitly due to advection, dispersion, and sources and sinks, with results provided to the chemical reaction subroutine to solve for the change in concentration due to chemical reactions using an ordinary differential equation (ODE) solver. The chemical reaction subroutine within the RT3D FORTRAN can be modified to incorporate any number of interacting chemical species, and rate laws for r can describe decay or production of species according to first-order chemical kinetics with Monod terms. For example, Lee et al. (2006) developed a nitrogen

transformation module for RT3D that accounted for nitrification and denitrification, whereas Bailey et al. (2015) develop a nitrogen module that accounted for the full nitrogen cycle in the crop-soil-water system in agricultural areas. Bailey et al. (2013a) also developed a selenium cycling module for RT3D.

A3. SWAT-MODFLOW-RT3D Modelling Framework

The SWAT-MODFLOW-RT3D modelling code uses the SWAT-MODFLOW model as the base code, and incorporates RT3D as a subroutine within the MODFLOW FORTRAN code. Thus, the developed modelling code is a single model that produces a single FORTRAN executable. The chemical transport processes simulated by RT3D within the coupled model are summarized in Figure A1 (with red labels), and the data flow of the coupled model is presented in Figure A3. The current version of SWAT-MODFLOW-RT3D includes only NO_3-N reactive transport in groundwater, since it is also simulated by SWAT and thus can be routed through the stream network using the current in-stream nitrogen algorithms of SWAT. Based on user needs, other reactive chemical species could be implemented into the RT3D reaction module.

As with SWAT-MODFLOW, the computed recharge from each SWAT HRU is passed to MODFLOW grid cells, and river stage is passed to MODFLOW River cells. When MODFLOW finishes solving the groundwater flow equation, the RT3D subroutine is called, with the modified RT3D model receiving groundwater fluxes across cell interfaces in each aquifer dimension, flow rates of the various sources and sinks from the MODFLOW model, and also receives NO_3-N concentration in recharge water and NO_3-N concentration in each sub-basin stream from the SWAT model. The process of passing data between SWAT units and MODFLOW/RT3D grid cells is demonstrated in the schematic of Figure A2. RT3D simulates the change in NO_3-N concentration for each grid cell and the NO_3-N mass loading to/from to/from each stream, with the latter passed to SWAT for in-stream water quality modelling and routine through the stream network of the watershed. Model results can be tested against groundwater NO_3-N concentration, in-stream NO_3-N mass loading rates and, if available, NO_3-N groundwater mass loading rates to stream reaches. The default time step for coupling between SWAT, MODFLOW, and RT3D is one day, although the code allows users to specify the frequency of SWAT calls to MODFLOW/RT3D allowing, for example, a daily surface simulation and monthly subsurface if desired.
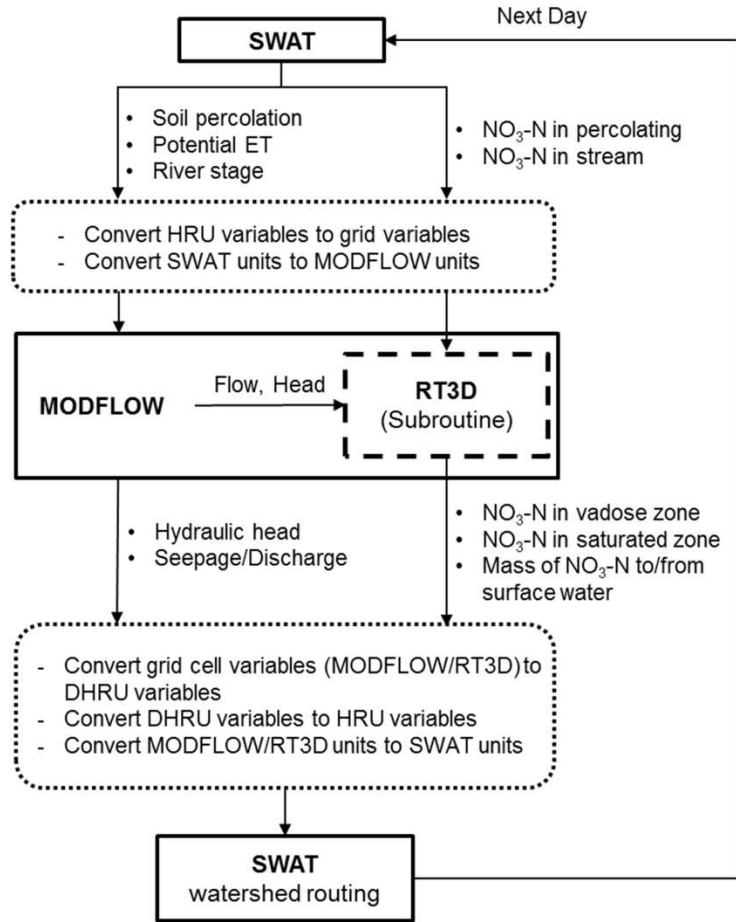
Figure A3. A conceptual modeling frame work for integrating SWAT-MODFLOW-RT3D models. Linking input files (dashed boxes) are created that contain the information necessary to convert model output from HRUs to geographically-located disaggregated HRUs (DHRUs), from DHRUs to MODFLOW/RT3D grid cells, and from SWAT sub-basin rivers to MODFLOW/RT3D river cells.

A4. Model Application: Sprague River watershed

A4.1 Study Area

The integrated SWAT-MODFLOW-RT3D framework is tested in the Sprague River watershed (4000 km^2) for the 1970 to 2003 time period. The Sprague River watershed is located in Upper Klamath River Basin (Figure A4a) of southern Oregon, USA, with the annual average precipitation ranging from 340 to

950 mm/yr and the elevation ranging from 1,270 m to 2,600 m

Figure A4. Sprague River watershed, located on the eastern end of the Upper Klamath Basin, Orgen, USA: (a) location of Klamath Basin; (b) Upper Klamath Basin showing: Water bodies, river system, MODFLOW MODEL boundary, and Sprague River watershed; (c) MODFLOW grid cells for Sprague River watershed, showing: the river grid cells, North Fork catchment, and stream gage location. Identified monitoring wells' corresponding the time series groundwater NO_3-N concentrations are plotted in Figure A7.
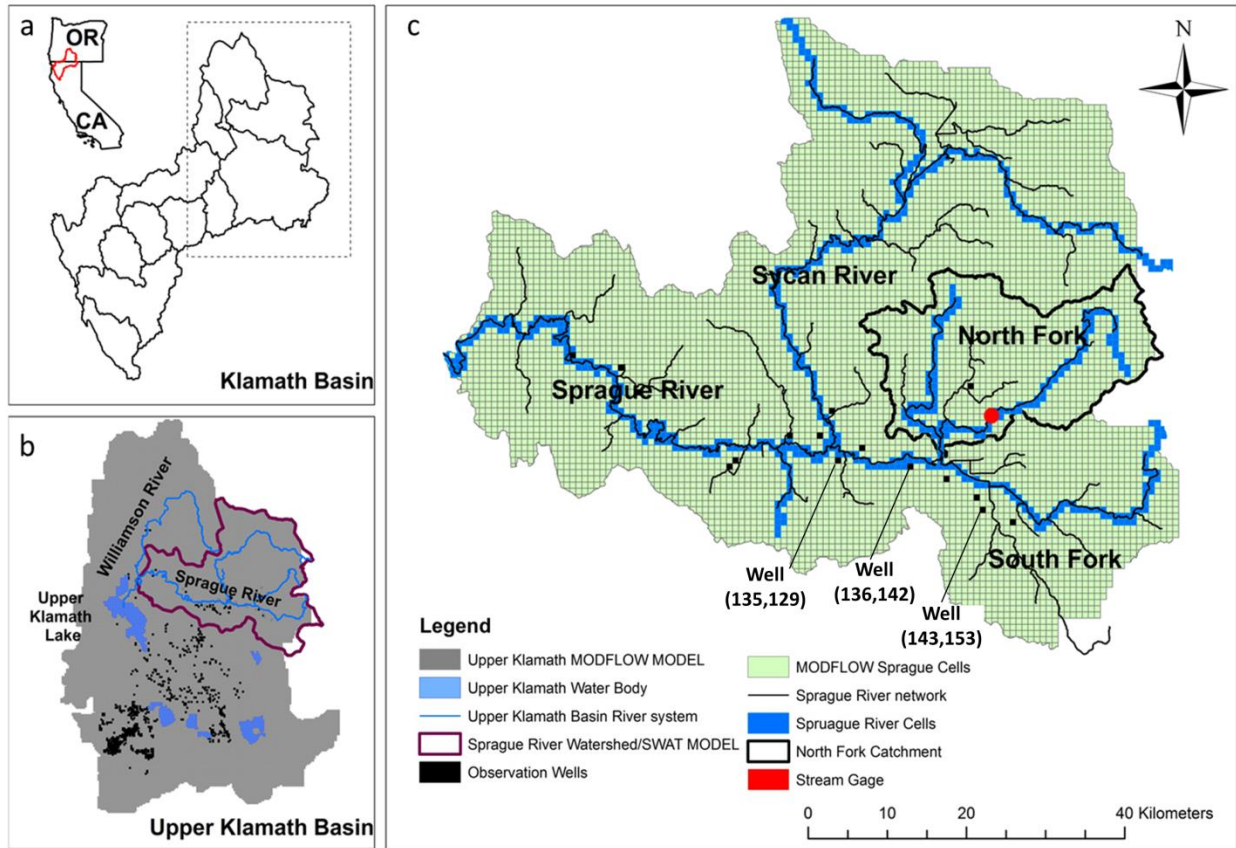
above sea level (USGS, 2009). High elevations occur in the northeast region of the Sycan and North Fork rivers, and low elevations occur in the southwest region along the Sprague River corridor (Figure A5a). The watershed is comprised mostly of coniferous forest (Rabe and Calonje, 2009), with minor land cover of herbaceous (14.7%), shrubland (14%), depressional wetlands (3.4%), and cultivated area (2.5%) (Figure A5b). The Sprague River is supplied by three major tributaries: The South and North Forks, which join to form the Sprague River main-stem, and the larger Sycan River, which reaches the main-stem about 20 km downstream of this confluence (Figure A4c). The Sprague and Williamson Rivers are two of the three largest tributaries to the large, shallow Upper Klamath Lake (see Figure A4b) and contribute over half of the lake's inflow. The third main tributary is the Wood River, which lies to the east of the Sprague and Williamson Rivers (Records et al., 2014). Outflow from Upper Klamath Lake also

supplies the U.S. Bureau of Reclamation's Klamath Irrigation Project, which provides water for more than 1,000 farms (Thorsteinson et al., 2011).
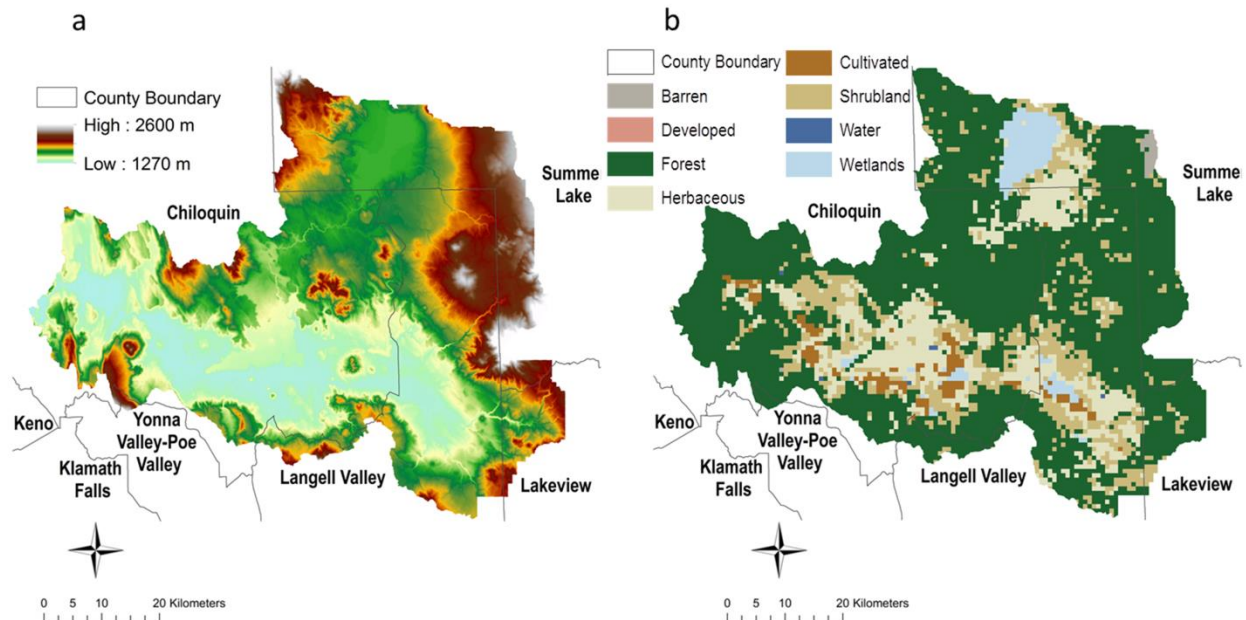

Figure A5. (a) Digital elevation model of topographic elevations for the Sprague River watershed. (b) Land use types in the Sprague River watershed.

The Sprague River watershed has complex interactions between groundwater and river network. Groundwater supplies a large percentage of annual stream in the Upper Klamath Basin, especially in the North Fork of the Sprague River, where groundwater discharges into streams are approximately 3 to 4 m^3/s. However, the groundwater influence is relatively low in the Sycan River and South Fork of the Sprague River, with only about a groundwater discharge rate of 1 m^3/s groundwater to the streams (Gannett et al., 2007).

Much of the Cascade Mountains region is highly nitrogen-limited, which means these aquifers can be recognized as sensitive to NO_3 inputs (Anderson et al., 2002). For the study area, denitrification was considered as the sole dominant chemical reaction that affects nitrate concentration in the aquifer. The low levels of dissolved oxygen along the deep groundwater flow path and the presence of nitrite in the water samples from the deep wells demonstrate that denitrification occurs in the aquifer. Available data for model testing include NO_3-N concentration in groundwater and surface water, stream flow, and water table elevation (see Section 4.2).

A4.2 Nitrate Data for Model Testing

In-Stream NO_3-N Loading: Approximately biweekly stream NO_3-N grab samples, collected by the Klamath Tribes Research Station following standard protocol (Klamath Tribes, 2008), are available at a stream gage site from March 2001 to December 2010 along the North Fork river in the Sprague

Watershed (see Figure A4c). These concentration values were combined with daily flow rates to compute monthly in-stream NO_3-N loads using the program LOAD ESTimator (LOADEST) (Runkel and Cohn, 2004). While LOADEST assumes long-term daily flow datasets are collocated with water quality samples, the flow data from the closest gage (Oregon Water Resources Department gage 11495900) were available only after September 2008, while water quality data collection began in approximately March 2001. This flow gage is located less than 0.6 km downstream of the water quality sample location, with no intervening tributaries. However, long-term daily flow data for the entire period of water quality data collection were available at US Geological Survey gage 11495800, approximately 1.7 km upstream of the water quality sample location, but with an intervening, ungaged tributary. Therefore, a scatter plot was derived using the flow data at one gage against another during the period of overlapping data availability for both gages (September 2008-September 2011). The slope of the linear regression line between the two flow points is treated as the scaling factor and is used to estimate a time series of daily flows at the downstream Oregon Water Resources Department gage for flow inputs to the LOADEST program from 2001-2010.

Groundwater NO_3-N Concentrations: Available NO_3-N groundwater data in the Sprague River watershed in recent decades are entirely from drinking water quality compliance monitoring for domestic and small commercial wells. Groundwater NO_3-N data for Klamath County was retrieved from the Oregon Public Health Drinking Water Data Online inventory (https://yourwater.oregon.gov/countyinventory.php, accessed 26 August 2015), including all agencies and well status (active and inactive). From the query results, all well logs containing the name of any towns known to occur in or near the Sprague River watershed (e.g., Beatty, Bly, Sprague River, Chiloquin) were selected. Well log locations were provided only in the Public Land System Survey Grid to quarter-quarter section or coarser spatial resolution; depending on the coarseness of the resolution, well location grids were then matched in ArcGIS from one to 16 intersecting MODFLOW grid cells. There are 16 observation wells with a total of 602 measurements of groundwater NO_3-N concentration that are available for model testing. The average groundwater NO_3-N concentration is 0.34 mg/L, with a standard deviation of 0.77 mg/L. The locations of the observation wells are shown in Figure A4c. They are situated principally along the South Fork and Sprague Rivers.

A4.3 Model Construction

The SWAT-MODFLOW model for the Sprague River Watershed was developed by Bailey et al. (2016) by linking a calibrated SWAT model for the Sprague River watershed (Records, et al., 2014), with a calibrated MODFLOW model for Upper Klamath Basin (Gannett et al., 2012). The SWAT model was developed to study the influence of climate change and wetland loss on water quality whereas the MODFLOW model was used to quantitative evaluate the regional groundwater system within the basin.

The MODFLOW model was developed by the US Geological Survey. Although the MODFLOW model included the entire Upper Klamath Basin, only the portion covered by the Sprague River Watershed was coupled with the SWAT model.

Since the main stem and tributaries have different hydrologic characteristics, the developed SWAT model was separated into four SWAT models, the Sprague River main stem, Sycan River, South Fork, and North Fork (Records et al., 2014). For more details of SWAT setup, refer to Records et al. (2013). The SWAT model was calibrated and tested using monthly stream flow during the 2001-2010 period. It was auto-calibrated with Dynamically Dimensioned Search (DDS) algorithms, employing manual calibration where necessary to fine-tune model performance using tools developed by Tolson and Shoemaker (2007). Model performance was generally acceptable for streamflow with a monthly Nash-Sutcliff Efficiency Coefficient (NSEC) greater than 0.7 at the outlet of the Sprague River (Records et al., 2014). However, monthly streamflow percent bias was 31% overestimated for the North Fork, a groundwater-driven tributary. As such, the four SWAT models were merged and the parameters for North Fork model were applied to the entire watershed. The model domain of the MODFLOW model encompasses the entire Upper Klamath Basin (see Figure A4b), which drains an area of about 20,000 km^2. This region was divided into cells, with a cell-size of 762 m. Within MODFLOW, the aquifers are represented as three variable thickness layers, discretized into a grid of 285 rows and 210 columns. The original model was set to simulate 3-month (quarterly) stress periods from 1970 through 2003, with each stress period subdivided into 5 flow time steps to evaluate the timing of the hydrologic response to changes in stresses. The model was calibrated for the 1989 and 2003 time period (Gannett et al., 2012).

For the SWAT-MODFLOW model simulation (Bailey et al., 2016), model results were compared against groundwater head data, stream discharge rates at the North Fork gage site, and groundwater discharge rates to 6 stream reaches throughout the Sprague River Watershed. For the SWAT-MODFLOW-RT3D model, the RT3D component used the same grid as the MODFLOW model, with the following ADR equation used to simulate reactive transport of NO$_3$ in the aquifer system:

$$\frac{\partial C_{NO_3}}{\partial t} R_{NO_3} = -\frac{\partial}{\partial x_i}\left(v_i C_{NO_3}\right) + \frac{\partial}{\partial x_i}\left(D_{ij}\frac{\partial C_{NO_3}}{\partial x_j}\right) + \frac{q_s}{\phi} C_{s_{NO_3}} + r \tag{2}$$

Since NO$_3$ has a very low sorption capacity, the retardation factor R_{NO_3} is set to 1.0 for each grid cell indicating no sorption. The rate law for denitrification is specified using a single-Monod expression wherein the rate of the reaction depends only on the presence of NO$_3$:

$$r_{NO_3} = -\mu_{NO_3} C_{NO_3}\left(\frac{C_{NO_3}}{K_{NO_3} + C_{NO_3}}\right) \tag{3}$$

where μ_{NO_3} is the first-order rate constant (d^{-1}) for denitrification, and K_{NO_3} is the Monod half-saturation constant [$M_f L_f^{-3}$] for NO$_3$. Since spatially-varying information on denitrification activity is not available for the watershed, constant values for both μ_{NO_3} and K_{NO_3} are provided to each grid cell. μ_{NO_3} was assigned a value of 0.07 day^{-1}, which corresponds to a half-life of 10 days. This value is approximately the average of most published denitrification first-order rates in soils and aquifers throughout the world (Heatwole and McCray, 2007; Bailey et al., 2012b), and similar to the half-life value of 11 days and 8 days found in aquifer studies presented in Conan et al. (2003) and Pauwels et al. (1998), respectively.

The coupled SWAT-MODFLOW-RT3D was simulated from 1970 to 2003 with daily time steps. Although the MODFLOW model simulates the entire Upper Klamath Basin, it is still capable of coupling with the SWAT model in only the Sprague River Watershed area. The coupled model contains 142 SWAT sub-basins and 763 river cells in the Sprague River Watershed. According to the principles described in model coupling section, 1,940 HRU polygons used in the construction of the SWAT model were spatially disaggregated to create 207,804 DHRUs.

A5. Results and Discussion

AS5.1 Groundwater NO$_3$-N Concentrations

Typical results of the SWAT-MODFLOW-RT3D simulation in regards to groundwater head and NO$_3$-N groundwater concentration are shown in Figures A6 to A11. Simulated cell-wise groundwater hydraulic head (m) at the end of the coupled model simulation (2003) is shown in Figure A6a, with the water table

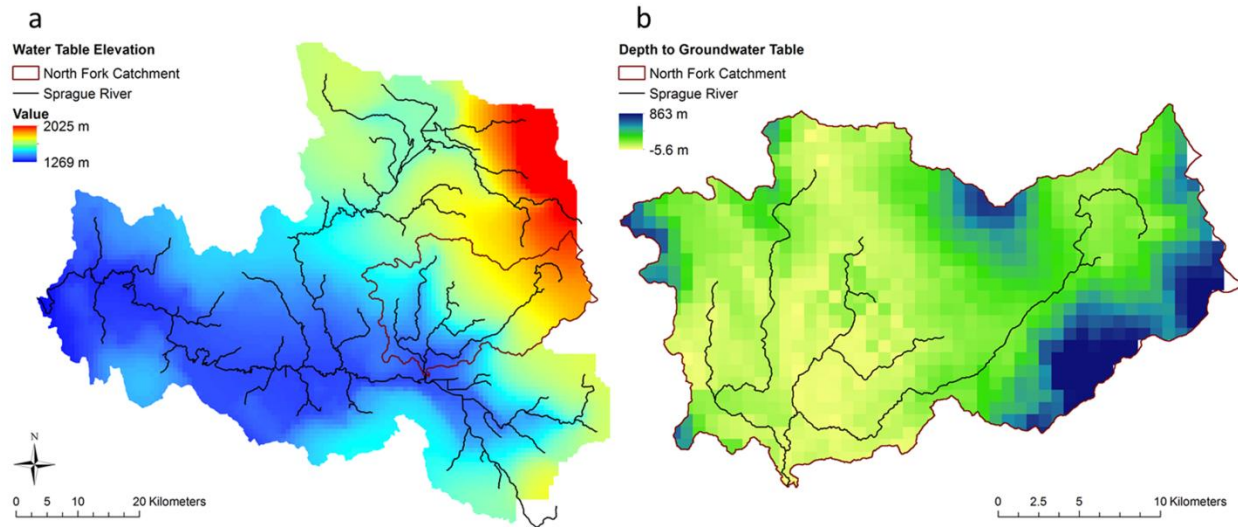elevation ranging from 1,268 m to 2,025 m above MSL. The

Figure A6. (a) Cell-wise water table elevation for MODFLOW grid in the Sprague River watershed at 12/31/2003. (b) Cell-wise depth to groundwater table in the North Fork watershed at 12/31/2003.

spatial pattern of the head field is similar to the ground surface elevation, with high head and low head occurring in regions of high and low surface elevation, respectively. The lowest water table elevation occurs along the main corridor of the Sprague River. The depth to water table for the North Fork catchment, where the stream and water quality gage is located, is shown in Figure A6b, showing the areas of high water table along the stream network.

Figure A7a shows the spatial distribution of simulated annual averaged NO_3-N concentration (mg/L) in groundwater of the Sprague River Watershed, with NO_3-N values ranging from 0 to 1.2 mg/L. The highest concentrations occur along the main Sprague River corridor and in the northwest region of the watershed. An increasing trend of concentration was found from the watershed boundary toward the stream site due to the distribution of land use types (Figure A5b). Figure A7 b, c, d, show the time series of simulated and observed NO_3-N concentration at the location of three groundwater monitoring wells for the time period 1985 to 2003, with the location of the wells shown in Figure A7a. These three wells are selected due to multiple samples available for each site. The simulated values correspond to RT3D grid cells within which the monitoring wells are located. Wells (136, 142) and (135, 129) are located in cultivated areas. In general, the model captures well the within-season and long-term trend of NO_3-N magnitude. In particular for Well (136, 142), the seasonal pattern of rapid concentration increase (due to fertilizer) and then slow concentration decrease due to denitrification during the fall and winter months is

replicated and corresponds well to observed values.
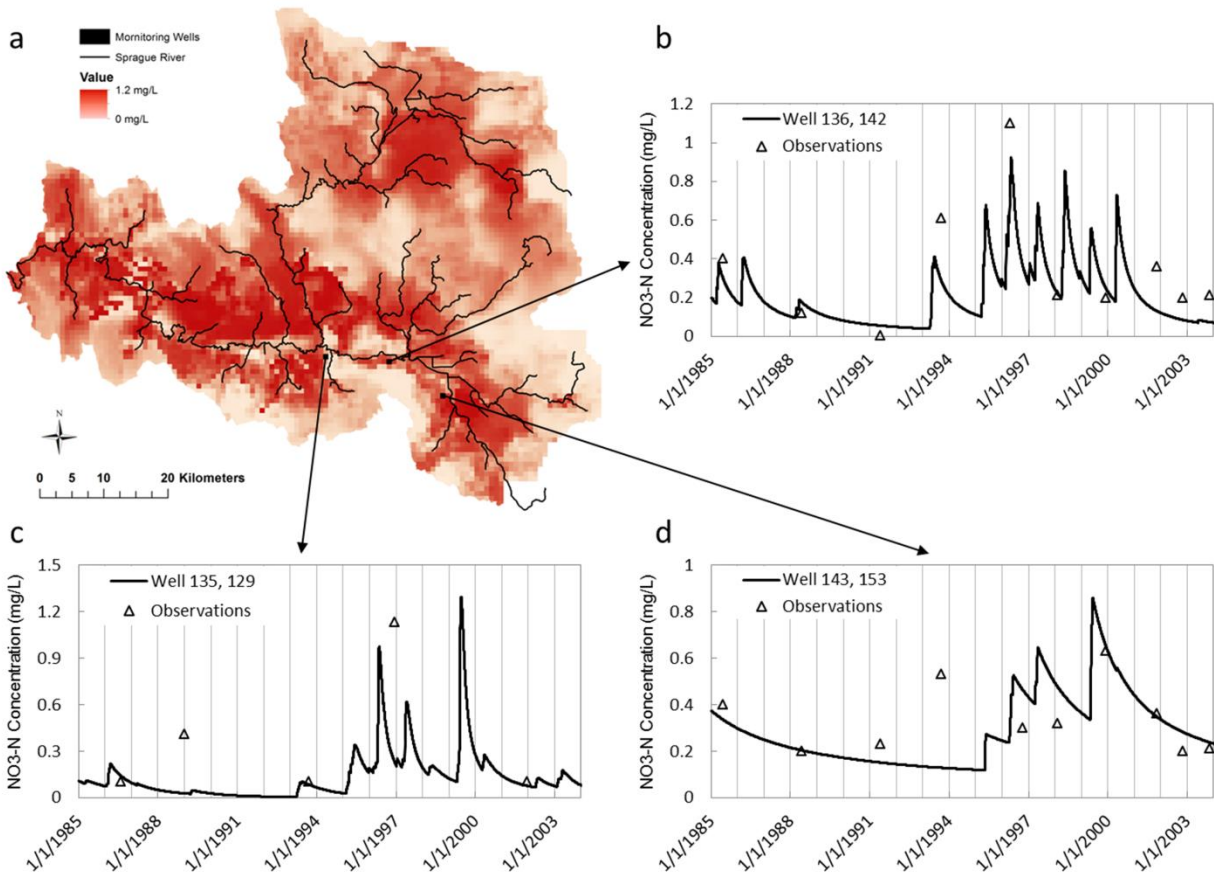
Figure A7. (a) Average annual cell-wise groundwater NO$_3$-N Concentrations in the Sprague River Watershed. (b), (c), and (d) are the model performances in predicted NO$_3$-N concentrations at Well (143, 153,), Well (136, 142), and Well (135, 129), respectively in the Sprague River watershed. Well (135,129) and Well (136,142) are located inside the cultivated field area.

Figure A8 shows boxplots of average annual simulated groundwater NO$_3$-N concentrations for different land use types. Both the spatial distribution and boxplots demonstrate that higher NO$_3$-N concentrations occur in the cultivated filed areas and herbaceous regions, with low NO$_3$-N concentrations

in the upland forested areas and along the main corridor of the South Fork catchment.

Figure A8. Boxplot of average annual groundwater NO_3-N concentrations under different land use types. Boxplot illustrates the 25th, 50th, and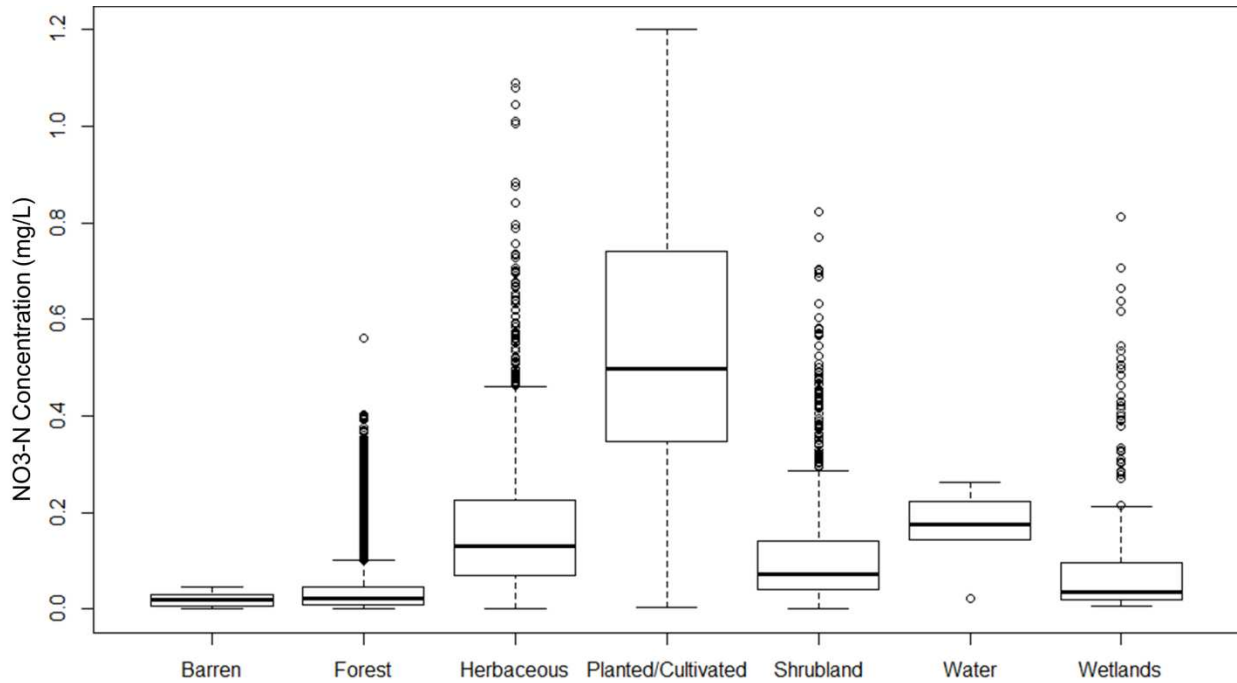 75th percentiles; whiskers indicate the 5th and 95th percentiles; and the circles represent data outliers.

When comparing the average of the measured NO_3-N values in the observation wells (0.33 mg/L) with the average simulated values from all grid cells (0.08 mg/L), the model seems to under-predict NO_3-N concentration. However, the majority of observation wells are located along the river corridors (see Figure A4c), which are cultivated fields and herbaceous land use types with higher NO_3-N concentration than natural background concentrations (Anderson, 2002; see also boxplots in Figure A8). Especially for the cultivated field area, the averaged simulated NO_3-N concentration is 0.52 mg/L. Therefore, annually averaged NO_3-N concentrations from grid cells along the rivers are selected to evaluate the model performance close to the observation wells. Four different sets of spatial analysis were performed using four different buffer zones all grid cells within a 500 m, 1,000 m, and 2,000 m buffer from the Sprague River Watershed stream network, and finally all grid cells in the Sprague River Watershed model domain. This resulted in 2,278, 3,220, 4,685, and 7,060 grid cells for the four scenarios, respectively. Frequency distributions are used to compare the 602 observed values with model results (Figure A9). Frequency distributions analyzes the ability of the coupled model to represent accurately the range of the concentration values as compared to observed values and the relative frequency of concentration values within a given concentration interval to verify if the model captures the regional spatio-temporal statistics
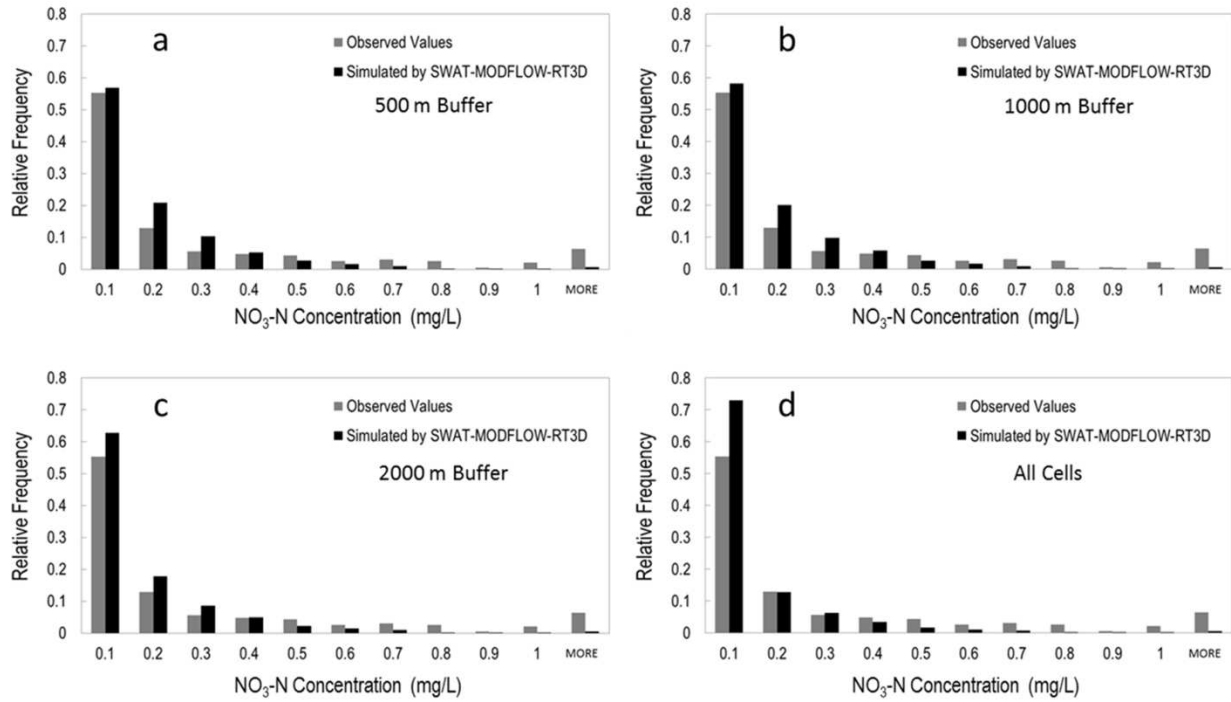
of solute concentration.

Figure A9. Frequency distribution of observed and simulated values of NO_3-N concentration for different buffer zones along the Sprague River network, (a) 500 m buffer zone, (b) 1000 m buffer zone, (c) 2000 m buffer zone, (d) all grid cells.

As can be seen from Figure A9, the shape and the magnitude of frequency for each concentration interval produced by the model is similar to the frequency from the observed data, particularly for the 500 m buffer zone as the observation wells are located close to the river network. The SWAT-MODFLOW-RT3D model slightly overestimates the low-range to mid-range concentrations (0 to 0.4 mg/L according to Figure A9 a, b, c, or 0 to 0.3 mg/L according to Figure A9d) and slightly underestimates the mid-range to high-range concentrations (> 0.4 mg/L for all buffer zones). For example, for the 500 m buffer zone, simulated relative frequencies for 0.1 to 0.2 mg/L and over 1.0 mg/L concentration ranges are 20.9% and 0.7%, whereas the observed data indicated that relative frequencies are 12.9% and 6.4% of the ranges, respectively. The large discrepancy between the simulated and observed frequency over low-range concentration values could be an artifact of not having samples in areas of low NO_3-N concentration, i.e. observation well placement is biased towards areas of probable high NO_3-N concentration due to cultivated areas and animal grazing.

A5.2 NO_3-N In-Stream Loading

Simulated and measured NO_3-N in-stream loading for the North Fork gage (see location in Figure A4c) are shown in Figure A10a. The unit for the in-stream loading is kg/ha, which is calculated by kg of

199

in-stream NO_3-N divided by the watershed area. As seen in the figure, the SWAT-MODFLOW-RT3D model is able to track the measured in-stream loading quite well, with simulated results matching measured results for peak flow periods and base flow periods, with peaks occurring after the precipitation season (shaded areas in Figure A10a). As compared to the original SWAT model (Records et al., 2013), there is a marked improvement in performance statistics (Nash-Sutcliff Efficiency Coefficient - NSEC, Root Mean Square Error - RMSE, Mean Average Error - MAE, and coefficient of determination - R^2) for the coupled SWAT-MODFLOW-RT3D model (NSEC = 0.42, RMSE = 0.001 kg/ha, MAE = 0.278 kg/ha, R^2 = 0.77 as compared to SWAT NSEC = -0.26, RMSE = 0.002 kg/ha, MAE = 0.491 kg/ha, R^2 = 0.70). The uncoupled SWAT model consistently underestimates the in-stream loading, particularly during the periods of low baseflow (i.e. groundwater discharge), likely due to the lack of physically-based groundwater and solute transport modelling.

Figure A10b shows the scatterplot of the observed versus simulated monthly NO_3-N in-stream concentration for the gage site on the North Fork River (see Figure A4c) from the SWAT model and the SWAT-MODFLOW-RT3D model, respectively. Error bounds were calculated by adding (and subtracting) the percentage of error to the simulated and observed values and then drawing the corresponding upper and lower lines that go through. As can be seen in the figure, the average measured NO_3-N in-stream concentration is 0.00359 kg/ha for 2001-2003 period and the simulated value from the SWAT and the coupled model is 0.00239 kg/ha and 0.00361 kg/ha, respectively. The RMSE and MAE from the coupled model provide low relative errors during the simulation period. Moriasi et al. (2015) summarized that model performance can be judged as "very good" if monthly $R^2 > 0.7$, indicating along with the visual inspection of the time series plots in Figure A10 that the model out-performs the SWAT model. Based on the SWAT-MODFLOW-RT3D results there are a few outliers below the error range, which demonstrates the model underestimates the loads at these receptors. Nevertheless, 80% of the simulated in-stream loading values fall within an error margin of 30% whereas the majority of the points from the SWAT model are below -30% error bound. Overall, the coupled model shows a substantial

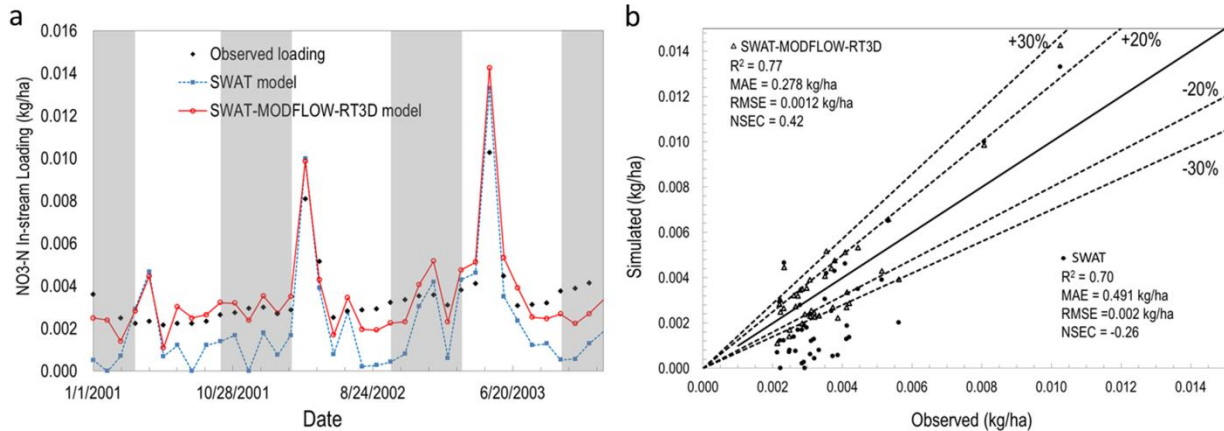improvement and yields good similarity with the observed values.

Figure A10. (a) Monthly time series NO₃-N in-stream loading (kg/ha) for the North Fork catchment of the Sprague River. Results of both SWAT-MODFLOW-RT3D simulation and the original calibrated SWAT model are shown, with the SWAT model results available starting on 1 January 2001. Shaded areas represent the precipitation season (October to March). The location of the stream gage is shown in Figure A4c. (b) Scatterplot of the observed versus simulated monthly nitrate in-stream loading for the North Fork catchment of the Sprague River from SWAT-MODFLOW-RT3D (triangles) and SWAT (points), respectively. The solid line represents the 1:1 line and the dashed lines represent the ±20% and 30% error bounds. The symbols are: coefficient of determination (R^2), mean average error (MAE), root mean squared error (RMSE), and Nash-Sutcliff Efficiency Coefficient (NSEC).

A5.3 Groundwater NO₃-N Mass loading to the Sprague River

Simulated NO₃-N mass loading (kg/year) from the aquifer to the stream network during the 1970-2003 period is shown in Figure A11a, which is important to quantify spatio-temporal patterns of groundwater and surface water interaction in the watershed. Values are plotted for average annual mass loading for each of the 763 River cells within the Sprague River Watershed. Red bars represent NO₃-N loading from the aquifer to the stream, whereas green bars indicate NO₃-N loading from the stream into the aquifer via stream seepage. As can be seen in Figure A11a, the magnitude of NO₃-N loading is highly spatially-variable based on different local hydrologic conditions and groundwater NO₃-N concentration. The main sites for groundwater mass loading are located in the North Fork catchment and the downstream portion of the Sprague River.

Average annual NO₃-N mass loading during the 1970-2003 time period for the entire Sprague River Watershed is shown in Figure A11b. Loading varies from year to year, with the estimated values changing from 4,843 kg/year (1983) to 6,318 kg/year (2001), with a standard deviation of 354 kg/year. For the entire 34 years, the average mass of NO₃-N discharge into stream was approximately 5,711 kg/year. Further analysis shows that the average NO₃-N discharge loading for each kilometer length of the stream network is approximately 14 kg/year. This rate is similar to the loading of 26 kg/year-km estimated by Morgan et al. (2007) for the La Pine, Oregon area, a region located approximately 100 km

north of the Sprague River Watershed, during the year 1999. The higher loading rate in the La Pine area likely is due to septic tank effluent being the primary source of NO_3-N (Hinkle et al., 2007), which results in higher NO_3-N groundwater concentrations than in the Sprague River Watershed.
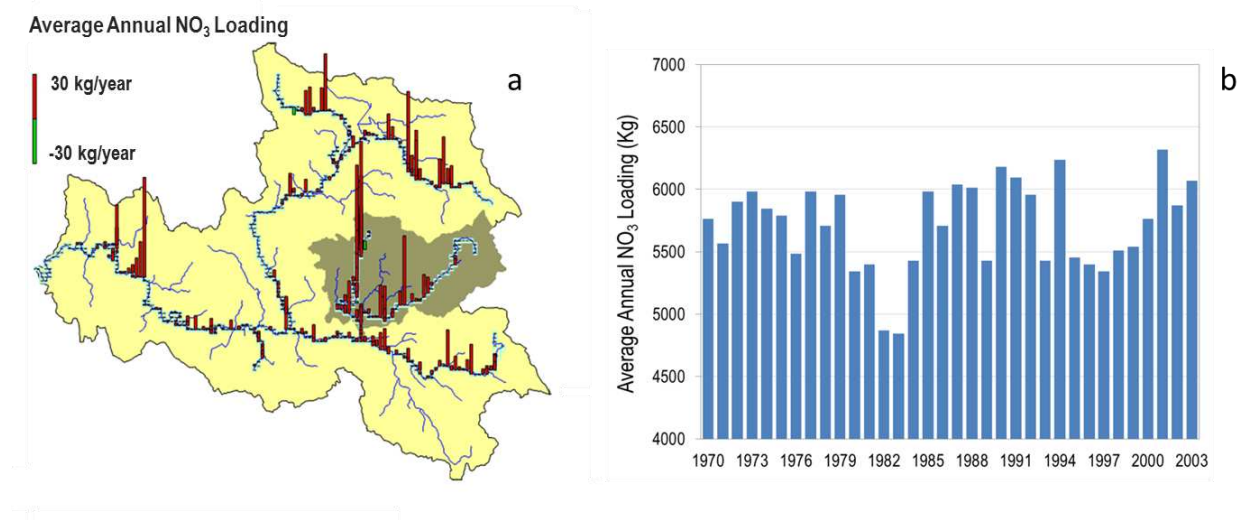

Figure A11. (a) Spatial distribution of annual-averaged simulated NO_3-N mass loading along the length of the Sprague River network. (b) Average annual NO_3-N mass loading from aquifer to the Sprague River network over the 1970 – 2003 time period.

A5.4 Model Capabilities and Limitations

The integrated SWAT-MODFLOW-RT3D model can be a useful tool to explore the fate and transport of NO_3 in coupled surface and subsurface systems, and to identify plausible best-management practices for controlling contaminant pollution in agricultural watersheds. For now only NO_3 is included, but other nitrogen species (e.g. NH_4, NO_2) could be simulated as well as other chemical species or contaminants for a given watershed. The model provides the advantage of accounting for spatial-variability in nutrient loadings and allows the realistic long-term allocation of different nutrient sources with the existing land use practices present in the watershed. The coupled model can provide maps of spatially-varying groundwater nutrient concentration and nutrient mass fluxes between surface and groundwater, which can help to assess possible hot-spot nutrient areas in the aquifer and sensitive locations of nutrient loading from the aquifer to the river network. These areas can be targeted for future remediation and fulfill the potential requirement for removal/changes of drinking water sources under a given management alternative to satisfy groundwater quality.

Currently, the model does not account for NO_3 transport in the vadose zone, between the bottom of the soil profile and the water table. However, the UZF (Unsaturated Zone Flow) package for MODFLOW (Niswonger et al., 2006) can be employed to simulate one-dimensional groundwater flow in the vadose zone, and can be coupled with a recent version of RT3D (UZF-RT3D, Bailey et al., 2013b) that can

simulate reactive solute transport in the vadose zone. This option will be included in future versions of SWAT-MODFLOW-RT3D.

A6. Summary and Conclusions

In this study the recently developed SWAT-MODFLOW model is extended to simulate the fate and transport of solute species in variably saturated subsurface systems by including the reactive transport model RT3D as a subroutine within the MODFLOW code. The resulting model is a single FORTRAN code that provides a single model executable. The framework provides a valuable simulation tool for watersheds in which groundwater processes and groundwater nutrient concentrations significantly impact stream flow and in-stream nutrient loading, or wherein groundwater sources and sinks can impact land surface hydrologic processes. Model source code and a tutorial outlining the preparation of SWAT-MODFLOW-RT3D simulations are available on the main SWAT model website: http://swat.tamu.edu/software/swat-modflow/. Applicability of this model was tested in the Sprague River Watershed (4,100 km^2) in the Upper Klamath Basin during the 1970-2003 time period. Model results are tested against spatio-temporal averages of NO_3-N groundwater concentrations and in-stream NO_3-N loading at a stream gage site. Annual average mass loadings of NO_3-N from the aquifer to the stream network also are presented to demonstrate the capabilities of the model in providing spatially-varying nutrient loading information.

The integrated model can be further applied to identify plausible best-management practices for controlling contaminant pollution in agricultural watershed. For now only NO_3 is included, but other nitrogen species (e.g. NH_4, NO_2) could be simulated as well as other chemical species or contaminants for a given watershed. Areas that need improvements include: (1) incorporating UZF-RT3D with the Unsaturated-Zone Flow (UZF) package of MODFLOW to better represent the solute transport in both the unsaturated and saturated zones; and for agricultural irrigated areas: (2) modification of SWAT HRU to better represent cultivated field for irrigation requirements; and (3) incorporation of new algorithms to simulate the impact of earthen canals on aquifer systems.

A7. Software availability

The SWAT-MODFLOW-RT3D model is a FORTRAN code developed using the Intel FORTRAN Compiler for Microsoft Visual Studio 10 (Microsoft Corporation). The program executable (SWAT-MODFLOW-RT3D.exe) was made available July 2016, and is available for download at no cost on the main webpage for the SWAT model: http://swat.tamu.edu/software/swat-modflow/. The size of the executable is 28.5 MB. The FORTRAN source code also is available (7 MB) for download from the same

webpage with instructions for compiling in the Intel Visual FORTRAN environment. The program executable can run on any personal computer. A workshop tutorial and example dataset for constructing a SWAT-MODFLOW-RT3D model for the Little River Watershed, Georgia, also is available on the webpage.

The modeling code is based on the original modeling codes of SWAT, MODFLOW, and RT3D, and was developed by Ryan Bailey and Tyler Wible. Ryan Bailey can be contacted at: Department of Civil and Environmental Engineering, Colorado State University, 1372 Campus Delivery, Fort Collins, CO, 80523-1372, United States. Telephone: 970-491-5045; Fax: 970-491-7727; E-mail: rtbailey@colostate.edu.

REFERENCES

Anderson, C.W., 2002. Ecological effects on streams from forest fertilization: literature review and conceptual framework for Future Study in the Western Cascades. U.S. Geological Survey, U.S. Department of the Interior. Water-Resources Investigations Report 01-4047.

Appelo, C.A.J., Rolle, M., 2010. PHT3D: A reactive multicomponent transport model for saturated porous media. Ground Water. 48 (5), 627-632.

Arnold, J.G., Srinivasan, R., Muttiah, R.S., Williams, J.R., 1998. Large area hydrologic modeling and assessment part I: Model development. J. Am. Water Resour. Assoc. 34 (1), 73-89.

Bailey, R.T., Hunter, W.J., Gates, T.K., 2012a. The influence of nitrate on selenium in irrigated agricultural groundwater systems. J. Environ. Qual. 41 (3), 783-792.

Bailey, R.T., Baù, D.A., Gates, T.K., 2012b. Estimating spatially-variable rate constants of denitrification in irrigated agricultural groundwater systems using an Ensemble Smoother. J. Hydrol. 468, 188-202.

Bailey, R.T., Gates, T.K., Halvorson, A.D., 2013a. Simulating variably-saturated reactive transport of selenium and nitrogen in agricultural groundwater systems. J. Contam. Hydrol. 149, 27-45.

Bailey, R.T., Morway, E.D., Niswonger, R.G., Gates, T.K., 2013b. Modeling Variably Saturated Multispecies Reactive Groundwater Solute Transport with MODFLOW-UZF and RT3D. Ground Water. 51 (5), 752-761.

Bailey, R.T., Gates, T.K., Ahmadi, M., 2014. Simulating reactive transport of selenium coupled with nitrogen in a regional-scale irrigated groundwater system. J. Hydrol. 515, 29-46.

Bailey, R.T., Ahmadi, M., Gates, T.K., Arabi, M., 2015. Spatially distributed influence of agro-environmental factors governing nitrate fate and transport in an irrigated stream-aquifer system. Hydrol. Earth Syst. Sci. 19 (12), 4859.

Bailey, R.T., Wible, T.C., Arabi, M., Records, R.M., Ditty, J., 2016. Assessing Regional-Scale Spatio-Temporal Patterns of Groundwater-Surface Water Interactions using a Coupled SWAT-MODFLOW model. Hydrol. Process. doi 10.1002/hyp.10933.

Carpenter, S., Caraco, N., Correll, D., Howarth, R., Sharpley, A., Smith, V,. 1998. Nonpoint pollution of surface waters with phosphorus and nitrogen. Ecol. Appl. 8 (3), 559–568.

Clement, T.P., 1997. A modular computer code for simulating reactive multi-species transport in 3-dimensional groundwater systems. Pacific Northwest National Laboratory, PNNL-SA-11720. Richland, Washington

Clement, T.P., Sun, Y., Hooker, B.S., Peterson, J.N., 1998. Modeling multispecies reactive transport in groundwater. Groundwater Mon. Rem. 18, 79-92.

Conan, C., Bouraoui, F., Turpin, N., de Marsily, G., Bidoglio, G., 2003. Modeling flow and nitrate fate at catchment scale in Brittany (France). J. Environ. Qual. 32 (6), 2026-2032.

Dise, N. B., Wright, R. F., 1995. Nitrogen leaching from European forests in relation to nitrogen deposition. For. Ecol. Manage. 71 (1), 153-161.

Duff, H., Triska, F., 2000. Nitrogen biogeochemistry and surface-subsurface exchange in streams, in Streams and Ground Waters, in: Jones, J.B., Mulholland, P. J. (Eds.). Academic Press, San Diego, pp. 197–220.

Erisman, J. W., Galloway, J. N., Seitzinger, S., Bleeker, A., Dise, N. B., Petrescu, A. R., Leach, A.M., de Vries, W., 2013. Consequences of human modification of the global nitrogen cycle. Phil. Trans. R. Soc. B. 368 (1621), 20130116.

Galbiati, L., Bouraoui, F., Elorza, F.J., Bidoglio, G., 2006. Modeling diffuse pollution loading into a Mediterranean lagoon: development and application of an integrated surface–subsurface model tool. Ecol. Modell. 193 (1), 4-18.

Gannett, M.W., Lite, K.E., La Marche, J.L., Fisher, B.J., Polette, D.J., 2007. Ground-water hydrology of the upper Klamath basin, Oregon and California. U.S. Geological Survey Scientific Investigations Report 2012-5062.

Gannett, M.W., Wagner, B.J., Lite, K.E., 2012. Groundwater simulation and management models for the Upper Klamath basin, Oregon and California. U.S. Geological Survey Scientific Investigations Report 2012-5062.

Gassman, P.W., Reyes, M.R., Green, C.H., Arnold, J.G., 2007. The soil and water assessment tool: historical development, applications, and future research directions. Trans. ASABE. 50 (4), 1211-1250.

Guzman, J.A., Moriasi, D.N., Gowda, P.H., Steiner, J.L., Starks, P.J., Arnold, J.G., Srinivasan, R., 2015. A model integration framework for linking SWAT and MODFLOW. Environ. Modell. Softw. 73, 103-116.

Harbaugh, A.W., 2005. MODFLOW-2005, the U.S. Geological Survey Modular Ground-Water Model: The Ground-Water Flow Process. U.S. Geological Survey Techniques and Methods, pp. 6-A16.

Heatwole, K.K., McCray, J.E., 2007. Modeling potential vadose-zone transport of nitrogen from onsite wastewater systems at the development scale. J. Contam. Hydrol. 91 (1), 184-201.

Hetling, L.J., Jaworski, N.A., Garretson, D.J., 1999. Comparison of nutrient input loading and riverine export fluxes in large watersheds. Water Sci. Technol. 39 (12), 189-196.

Hinkle, S.R., Böhlke, J.K., Duff, J.H., Morgan, D.S. Weick, R.J., 2007. Aquifer-scale controls on the distribution of nitrate and ammonium in ground water near La Pine, Oregon, USA. J. Hydrol. 333(2-4), 486-503.

Huang, J., Christ, J.A., Goltz, M.N., 2008. An Assembly Model for Simulation of Large-Scale Ground Water Flow and Transport. Ground Water. 46 (6), 882-892.

Kaufmann, V., Pinheiro, A., dos Reis Castro, N.M., 2014. Simulating transport of nitrogen and phosphorus in a Cambisol after natural and simulated intense rainfall. J. Contam. Hydrol. 160, 53-64.

Kim, N.W., Chung, I.M., Won, Y.S., Arnold, J.G., 2008. Development and application of the integrated SWAT–MODFLOW model. J. Hydrol. 356 (1), 1-16.

Klamath Tribes, 2008. Quality Assurance Project Plan (QAPP) Project: Baseline Water Quality Monitoring Project, Chiloquin, Oregon, USA.

Korom, S.F., 1992. Natural denitrification in the saturated zone: a review. Water Resour. Res. 28 (6), 1657-1668.

Lee, M.S., Lee, K.K., Hyun, Y., Clement, T.P., Hamilton, D., 2006. Nitrogen transformation and transport modeling in groundwater aquifers. Ecol. Modell. 192 (1), 143-159.

Lunn, R.J., Adams, R., Mackay, R., Dunn, S.M., 1996. Development and application of a nitrogen modelling system for large catchments. J. Hydrol. 174 (3), 285-304.

Mao, X., Prommer, H., Barry, D.A., Langevin, C.D., Panteleit, B., Li, L., 2006. Three-dimensional model for multi-component reactive transport with variable density groundwater flow. Environ. Modell. Softw. 21 (5), 615-628.

Markstrom, S.L., Niswonger, R.G., Regan, R.S., Prudic, D.E., Barlow, P.M., 2008. GSFLOW-Coupled Ground-water and Surface-water FLOW model based on the integration of the Precipitation-Runoff Modeling System (PRMS) and the Modular Ground-Water Flow Model (MODFLOW-2005). U.S. Geological Survey Techniques and Methods 6-D1.

Markstrom, S.L., Regan, R.S., Hay, L.E., Viger, R.J., Webb, R.M., Payn, R.A., LaFontaine, J.H., 2015. PRMS-IV, the precipitation-runoff modeling system, version 4. U.S. Geological Survey Techniques and Methods 6-B7.

Molenat, J., Gascuel-Odoux, C., 2002. Modelling flow and nitrate transport in groundwater for the prediction of water travel times and of consequences of land use evolution on water quality. Hydrol. Process. 16 (2), 479-492.

Morgan, D.S., Hinkle, S.R., Weick, R.J., 2007. Evaluation of approaches for managing nitrate loading from on-site wastewater systems near La Pine, Oregon. U.S. Geological Survery, U.S. Department of the Interior, Scientific Investigations Report 2007-5237.

Moriasi, D.N., Gitau, M.W., Pai, N. Daggupati, P., 2015. Hydrologic and water quality models: Performance measures and evaluation criteria. Trans. ASABE. 58(6), 1763-1785.

Narula, K.K., Gosain, A.K., 2013. Modeling hydrology, groundwater recharge and non-point nitrate loadings in the Himalayan Upper Yamuna basin. Sci. Total Environ. 468, S102-S116.

Neitsch, S.L., Arnold, J.G., Kiniry, J.R., Williams, J.R., King, K.W., 2005. Soil and water assessment tool theoretical documentation, version 2005. Temple, Tex.: USDA-ARS Grassland, Soil and Water Research Laboratory.

Neitsch, S.L., Williams, J.R., Arnold, J.G., Kiniry, J.R., 2011. Soil and water assessment tool theoretical documentation, version 2009. Temple, Tex.: Texas Water Resources Institute Technical Report No. 406.

Niswonger, R.G., Prudic, D.E., Regan, R.S., 2006. Documentation of the unsaturated-zone flow (UZF) package for modeling unsaturated flow between the land surface and the water table with MODFLOW-2005. U.S. Geological Survey Techniques and Methods 6-A19.

Niswonger, R.G., Panday, S., Ibaraki, M., 2011. MODFLOW-NWT, a Newton formulation for MODFLOW-2005. U.S. Geological Survey Techniques and Methods 6-A37.

Nolan, B.T., Ruddy, B.C., Hitt, K.J., Helsel, D.R., 1997. Risk of Nitrate in groundwaters of the United States a national perspective. Environ. Sci. Technol. 31 (8), 2229-2236.

Pauwels, H., Kloppmann, W., Foucher, J.C., Martelat, A., Fritsche, V., 1998. Field tracer test for denitrification in a pyrite-bearing schist aquifer. Appl. Geochem. 13 (6), 767-778.

Pietersen, N.M., Bleuten, W., Jørgensen, S.E., 2003. Contribution of point sources and diffuse sources to nitrogen and phosphorus loads in lowland river tributaries. J. Hydrol. 271 (1), 213-225.

Prommer, H., Barry, D.A., Zheng, C., 2003. MODFLOW/MT3DMS-Based Reactive Multicomponent Transport Modeling. Ground Water. 41 (2), 247-257.

Puckett J. 1994. Nonpoint and Point Sources of Nitrogen in Major Watersheds of the United States. Reston, Virgina: U.S. Geological Survey, Water-Resources Investigations Report 94-4001.

Rabe, A., Calonje, C., 2009. Lower Sprague-Lower Williamson watershed assessment. Klamath Falls, Oregon: Prepared for Klamath Watershed Partnership.

Randall, G.W., Iragavarapu, T.K., 1995. Impact of long-term tillage systems for continuous corn on nitrate leaching to tile drainage. J. Environ. Qual. 24 (2), 360-366.

Records, R.M., 2013. Water quality benefits of wetlands under historic and potential future climate in the Sprague River watershed, Oregon (Doctoral dissertation, Colorado State University).

Records, R.M., Arabi, M., Fassnacht, S.R., Duffy, W.G., Ahmadi, M., Hegewisch, K.C., 2014. Climate change and wetland loss impacts on a western river's water quality. Hydrol. Earth Syst. Sci.18 (11), 4509-4527.

Refsgaard, J.C., Thorsen, M., Jensen, J.B., Kleeschulte, S., Hansen, S., 1999. Large scale modelling of groundwater contamination from nitrate leaching. J. Hydrol. 221 (3), 117-140.

Runkel, R.L., Cohn, T.A., 2004. Load Estimator (LOADEST): A FORTRAN program for estimating constituent loads in streams and rivers. U.S. Geological Survey, Techniques and Methods 4-A5.

Seitzinger, S.P., Styles, R.V., Boyer, E.W., Alexander, R.B., Billen, G., Howarth, R.W., Mayer, B., Van Breemen, N., 2002. Nitrogen retention in rivers: model development and application to watersheds in the northeastern USA. Biogeochemistry. 57/58, 199-237.

Smith, V. H., Tilman, G. D., Nekola, J. C., 1999. Eutrophication: impacts of excess nutrient inputs on freshwater, marine, and terrestrial ecosystems. Environ. Pollut. 100 (1), 179-196.

Sophocleous, M., Perkins, S.P., 2000. Methodology and application of combined watershed and ground-water models in Kansas. J. Hydrol. 236 (3), 185-201.

Thorsteinson, L., VanderKooi, S., Duffy, W., 2011. Proceedings of the Klamath Basin Science Conference, Medford, Oregon, February 1-5, 2010. U.S. Geological Survey, Open-File Report 2011-1196, 312 p.

Tolson, B.A., Shoemaker, C.A., 2007. Dynamically dimensioned search algorithm for computationally efficient watershed model calibration. Water Resour. Res. 43 (1), W01413, doi:10.1029/2005WR004723.

U.S. Environmental Protection Agency, 1995. Drinking water regulations and health advisories. Washington, D.C.: Office of Water, Environmental Protection Agency 822-B-96-002.

U.S. Geological Survey, 2009. 1-Arc Second National Elevation Dataset SDE raster digital data, available at: http://seamless.usgs.gov/ (accessed 10.05.20).

Vidon, P., Allan, C., Burns, D., Duval, T.P., Gurwick, N., Inamdar, S., Lowrance, R., Okay, J., Scott, D., Sebestyen, S., 2010. Hot spots and hot moments in riparian zones: potential for improved water quality management1. J. Am. Water Resour. Assoc. 46 (2), 278-298.

Winchell, M., Srinivasan, R., Di Luzio, M., Arnold, J., 2013. ArcSWAT interface for SWAT2012: user's guide. Blackland Research and Extension Center, Texas Agrilife Research. Grassland. Soil and Water Research Laboratory, USDA Agricultural Research Service, Texas, 3.

Whitehead, P.G., Wilson, E.J., Butterfield, D., 1998. A semi-distributed Integrated Nitrogen model for multiple source assessment in Catchments (INCA): Part I—model structure and process equations. Sci. Total Environ. 210, 547-558.

Wright, W.G., 1999. Oxidation and mobilization of selenium by nitrate in irrigation drainage. J. Environ. Qual. 28 (4), 1182-1187.

Wriedt, G., Rode, M., 2006. Modelling nitrate transport and turnover in a lowland catchment system. J. Hydrol. 328, 157-176.

Wriedt, G., Spindler, J., Neef, T., Meißner, R., Rode, M., 2007. Groundwater dynamics and channel activity as major controls of in-stream nitrate concentrations in a lowland catchment system? J. Hydrol. 343 (3), 154-168.

Yeh, G.T., Tripathi, V.S., 1989. A critical evaluation of recent developments in hydrogeochemical transport models of reactive multichemical components. Water Resour. Res. 25 (1), 93-108.

Zheng, C., Wang, P.P., 1999. MT3DMS: a modular three-dimensional multispecies transport model for simulation of advection, dispersion, and chemical reactions of contaminants in groundwater systems; Documentation and user's guide. U.S. Army Engineer Research and Development Center Contract Report SERDP-99-1, Vicksburg, USA.